Geology, Geochemistry and Geochronology of the Hemlo East Property, Schreiber-Hemlo Greenstone Belt, Ontario

Adam Fage

A thesis submitted to the Faculty of Graduate Studies in partial fulfillment of the requirements for the degree of Master of Science

Geology Department
Lakehead University
Thunder Bay, Ontario
2011

Abstract

The Hemlo East property is located approximately 50 kilometres east of the town of Marathon, Ontario and is situated within the Schreiber-Hemlo greenstone belt of the Wawa-Abitibi Terrane of the Archean Superior Province. Lithologies within the Hemlo East Property are broadly divided into mafic metavolcanic, felsic metavolcanic, metasedimentary, intrusive and metaintrusive rocks. Stratigraphic continuity within the study area is demonstrated by the large number of drill holes in the area. Rock staining indicates that the K-feldspar present in felsic metavolcanic rocks in the Gouda-Thor-Carroll area of the Hemlo East Property is a product of alteration likely associated with base metal and gold mineralization.

New major and trace element, Sm-Nd isotope, and geochronology data are presented for volcanic, plutonic, and metasedimentary rocks of the Hemlo East property to investigate their origins. Positive to negative ε_{Nd} (-1.14 to 2.15) for tholeiitic basalts indicate that they were derived from depleted to moderately contaminated sources. FI rhyolites with steep trace element patterns (La/Yb_n = 16 to 44) and fractionated HREE (Gd/Yb_n = 2.1 to 7.5) are interpreted to have been derived from a deep mantle source. Metasedimentary rocks are geochemically similar to felsic metavolcanic rocks and are interpreted to be derived wholly, or in part, from a felsic source.

New U-Pb age dates include 2704.8 ±1.1 Ma and 2705.6 ±1 Ma from the Gouda and Thor metarhyolites, respectively; 2694.5 ±1 Ma from the DC Lake metadacite; 2691.6 ±1.1 Ma from the Upper Anomalous Zone volcaniclastic unit; 2693.1 ± 1 Ma from the Moose Lake Porphyry at Hemlo; 2683.4 ± 1.7 Ma from the Cedar Lake Pluton granodiorite; 2686.5 ±1.3 Ma from the White River Pluton monzogranite; and a maximum age of ~2696 Ma from the Frank Lake felsic metasedimentary unit. Results from the new and compiled U-Pb geochronological data indicate that there are two associations of felsic volcanism and two associations of plutonism, with a new association of felsic volcanism at 2705 Ma. This 2705 Ma phase represents the oldest felsic volcanic unit dated in the greenstone belt. This data points toward a northward younging of stratigraphy in the Gouda-Thor-Carroll area implying that the stratigraphy is right way up.

A long lived oceanic subduction zone produced the arc rhyolites and granitic intrusive rocks seen in the Hemlo East Property. There is no indication from this study as to what comprised the crust that the pre-tectonic plutons were intruded into. High La/Yb_n ratios for the rhyolites suggest that their source magmas were derived at depth from the melting of the subducting slab. Island arc tholeiites (metabasalts) erupted from a primitive back-arc behind the island arc. The area between the arc and back-arc would have allowed for island arc tholeiites to be deposited alongside rhyolites in conjunction with sediments coming off of the volcanic arc to produce the stratigraphic associations seen in the Gouda-Thor-Carroll area. These supracrustal units were later intruded by TTG plutons.

Acknowledgements

I would like to acknowledge the Ontario Centres of Excellence and MetalCORP Ltd. for making this study possible. MetalCORP staff are thanked for providing a great work environment, especially Charlie Greig for providing advice and direction while in the field. Lakehead faculty and staff members are thanked for their help in various aspects of this work. I would also like to thank my thesis advisor Pete Hollings for his many hours spent revising drafts and discussing ideas. I am grateful to friends and family for their continued support.

Table of Contents

Appendices

List of Figures

List of Tables

Chapter 1

Introduction

1.1 Location and Background

The Hemlo East Property, currently held by MetalCORP Ltd., is located within the Schreiber-Hemlo greenstone belt near Marathon, Ontario (Fig. 1.1). The property is located close to the Hemlo Camp, Canada's fifth largest gold mine, and situated within a greenstone belt with known VMS mineralization (Rinne, 2010). This research project was funded by MetalCORP Ltd., Lakehead University, and the Ontario Centres of Excellence.

Figure 1.1: Location Map. The Hemlo East Property is located approximately 40 km east of Marathon, Ontario.

1.2 Objectives

The key aim of this study was to use field mapping, petrography, whole-rock geochemistry, Sm-Nd isotopes, and U-Pb geochronology to investigate the geology, age and tectonic setting of the Hemlo East Property and compare it to both the Schreiber-Hemlo Greenstone Belt and the region as a whole. Geological mapping, geochronology and whole-rock geochemistry were undertaken to resolve which units correlate across the DC Lake fault.

1.3 Methodology

Samples were collected by the author from outcrops and diamond drill core, with the goal of sampling a suite of felsic and mafic metavolcanic rocks ranging from least to most altered. The author spent 20 days in the field mapping and sampling on the Hemlo East Property. Ten days were spent re-logging and sampling 19 archived Teck Exploration drill holes stored at the Hemlo mine site.

1.3.1 Petrographic Analysis

Representative core and surface samples were prepared at Lakehead University for petrographic analysis in transmitted and reflected light. The IUGS classification of igneous rocks was used where possible, with names intended to describe protolith compositions. Where not specified, crystal size classifications used were: fine-grained <1 mm, medium-grained 1-3 mm, and coarse-grained 3-10 mm. Petrographic descriptions, as well as core logs and whole-rock geochemical data, are provided in the appendices.

1.3.2 Potassium Feldspar Staining

Rock slabs were etched by submersion in concentrated HF for 15 – 20 seconds. Slabs were dipped in water to remove the acid and then immersed in saturated sodium cobaltinitrite solution for 1-2 minutes. The samples were rinsed, dried and covered with varnish to preserve the staining. The K-feldspar stains bright yellow, the plagioclase stains chalky white and the quartz stains dull grey (Hutchison, 1974).

1.3.3 Whole-Rock Geochemical Analysis

Geochemical data used in this study were compiled from many workers, and all data used are whole-rock. Geochemical analyses were mostly performed using X-ray Fluorescence (XRF), inductively coupled plasma - atomic emission spectrometry (ICP-AES), and inductively coupled plasma - mass spectrometry (ICP-MS) methods from two laboratories, as follows.

1.3.3.1 OGS Analytical Methods

Outcrop samples were crushed and pulverised in an agate mill at Lakehead University, with working surfaces cleaned with acetone between samples. Samples were analyzed for major elements by X-ray fluorescence (XRF) and for trace and rare earth elements by inductively coupled plasma mass spectrometry (ICP–MS) at the Geoscience Laboratories (Geo Labs) of the Ministry of Northern Development Mines and Forestry in Sudbury, Ontario. Selected trace elements (e.g., Zr and Y) were also analyzed by XRF using a pressed pellet to allow comparison with data generated by ICP–MS. Totals for major element oxide data were generally 100±2% and have been recalculated to a 100% volatile-free basis. Detection limits for major elements are 0.01 weight % and relative standard deviations of duplicate analyses are within 5%. Trace elements, including the REE and HFSE analyzed at the Geoscience

Laboratories were completed on a Perkin-Elmer Elan 9000 ICP–MS following a variation on the protocol described by Burnham and Schweyer (2004) and Tomlinson et al. (1998). Twenty four trace elements were determined using 200 mg aliquots of powder digested by a two stage procedure involving an initial decomposition in a closed beaker by a mixture of HF with lesser HCl and $HClO_4$ followed by a second mixture of dilute HCl and $HClO_4$ as described by Burnham et al. (2002). Detection limits for some critical elements, defined as 3σ of the procedural blank, are as follows: Th (0.032 ppm), Nb (0.044 ppm), Hf (0.085 ppm), Zr (3.2 ppm), La (0.048 ppm) and Ce (0.08 ppm) (Burnham and Schweyer, 2004).

1.3.3.2 ALS Chemex Analytical Methods

Samples used in this study were collected by the author from outcrops and diamond drill core. Standard sampling procedure was applied to avoid cross-contamination of samples and with efforts made to avoid sampling across lithological contacts. Split core samples were mostly 0.3-1.1 m long. Chemex analytical procedure codes (e.g., ME-MS61) are given for each method described.

Samples were crushed in Thunder Bay and pulverised in a low chrome steel mill. Most core samples were analysed by a standard 47 element assay package (ME-MS61) at ALS Chemex Vancouver. Following four acid (HF, HNO_3, $HClO_4$, HCl) digestion, samples were analysed by ICP-MS for Ag, Al, As, Ba, Be, Bi, Ca, Cd, Ce, Co, Cr, Cs, Cu, Fe, Ga, Ge, Hf, In, K, La, Li, Mg, Mn, Mo, Na, Nb, Ni, P, Pb, Rb, Re, S, Sb, Se, Sn, Sr, Ta, Te, Th, Ti, Tl, U, V, W, Y, Zn, and Zr, as well as for Au, Pt, and Pd. Cu and Zn contents greater than 1 wt. % were analysed by atomic absorption spectra (AA62). About one third of the assay samples were processed by a 27 element assay package (ME-ICP61) by ICP-AES for Ag, Al, As, Ba, Be, Bi, Ca, Cd, Co, Cr, Cu, Fe, K, Mg, Mn, Mo, Na, Ni, P, Pb, S, Sb, Sr, Ti, V, W, and Zn following four-acid digestion. As well as the 47 element assay package (ME-MS61) described

above, major element oxides and LOI were analysed by XRF (ME-XRF06) and trace elements (Ce, Dy, Er, Eu, Gd, Ho, La, Lu, Nd, Pr, Sm, Tb, Th, Tm, U, Y, Yb) by ICP-MS (ME-MS82) following lithium borate fusion and four acid (HF, HNO_3, $HCLO_4$, HCl) digestion .

1.3.4 Nd Isotope Analysis

Least altered samples were chosen for Sm-Nd isotope analysis in order to cover a representative suite of rocks for the sample area. Least altered samples were chosen on the basis of absence of alteration minerals and a lack of alteration signature in their whole-rock geochemistry. The samples were crushed at the Lakehead University Lapidary Facility until they were 2 to 3 mm in diameter using a tungsten carbide mallet. The crushing area and devices were thoroughly cleaned between each sample. The crushed sample was then further pulverized in an agate rotary mill, which reduces the sample to approximately 75µm in diameter. Analyses were carried out at Carleton University in Ottawa, Ontario at the Isotope Geochemistry and Geochronology Research Centre (IGGRC) using a ThermoFinnigan TRITON T1 Thermal Ionization Mass Spectrometer (TIMS).

Between 100 and 200 milligrams of powder were dissolved in 50% HF-12N HNO_3, then attacked with 8N HNO_3 and finally 6N HCl. The residue was taken up in 1N HBr for Pb/Sr/Nd, or 2.5N HCl for Sr/Nd only. Samples were dissolved in 0.26N HCl and loaded onto Eichrom Ln Resin chromatographic columns containing Teflon powder coated with HDEHP (di(2-ethylhexyl) orthophosphoric acid (Richard et al., 1976). Nd was eluted using 0.26N HCl, followed by Sm in 0.5N HCl. Total procedural blanks for Nd were < 50 picograms; < 6 picograms for Sm. Samples were spiked with a mixed ^{148}Nd-^{149}Sm spike prior to dissolution. Concentrations were precise to + 1%, but $^{147}Sm/^{144}Nd$ ratios are reproducible to 0.5%. Samples were loaded with H_3PO_4 on one side of a Re double filament, and run at temperatures of 1700-1800 °C. Isotope ratios are normalized to $^{146}Nd/^{144}Nd = 0.72190$. Analyses of the USGS standard BCR-1 yield Nd = 29.02 ppm, Sm = 6.68 ppm, and

$^{146}Nd/^{144}Nd$ = 0.512668 ± 20 (n=4). The international La Jolla standard produced: $^{143}Nd/^{144}Nd$ = 0.511847 ± 7, n = 26 (Feb 2005 – June 2007). Internal lab standard = 0.511818 ± 8, n = 28 (Feb 2005-June 2007) and 0.511819 ± 10 n = 94 (Feb 2005 – Aug 2009).

Total procedural blanks for Nd were <200 pg and concentrations were precise to ± 1%. The La Jolla standard was run by the Isotope Geochemistry and Geochronology Research Centre (IGGRC) regularly to ensure accuracy and precision of the preparation process. The ratios were then normalized to $^{146}Nd/^{144}Nd$ = 0.72190 (Cousens, 1996). The 2σ uncertainty in the $^{146}Nd/^{144}Nd$ values was ±0.000002 to 0.000008. Depleted mantle model ages were calculated assuming a modern upper mantle with $^{147}Sm/^{144}Nd$ = 0.214 and $^{143}Nd/^{144}Nd$ = 0.513115.

1.3.5 U-Pb Geochronology

Bulk rock samples were sent to the University of British Columbia and processed by Dr. Richard Friedman. The procedure for the Chemical Abrasion-Thermal Ionization Mass Spectrometer (CA-TIMS) analytical technique is as follows.

This technique has been modified from CA-TIMS procedures outlined in Mundil et al. (2004), Mattinson (2005) and Scoates and Friedman (2008). After rock samples have undergone standard mineral separation procedures zircons were handpicked in alcohol. The clearest, crack- and inclusion-free grains were selected, photographed and then annealed in quartz glass crucibles at 900˚C for 60 hours. Annealed grains were transferred into 3.5 mL PFA screwtop beakers, ultrapure HF (up to 50% strength, 500 mL) and HNO_3 (up to 14 N, 50 mL) were added and caps are closed finger tight. The beakers were placed in 125 mL PTFE liners (up to four per liner) and about 2 mL HF and 0.2 mL HNO_3 of the same strength as acid within beakers containing samples are added to the liners. The liners were then slid into stainless steel Parr™ high pressure dissolution devices, which were sealed and brought up to a maximum of 200˚C for 8-16 hours (typically 175˚C for 12 hours). Beakers were removed

from liners and zircon is separated from leachate. Zircons were rinsed with >18 MΩ.cm water and subboiled acetone. Then 2 mL of subboiled 6N HCl was added and beakers were set on a hotplate at 80˚-130˚C for 30 minutes and again rinsed with water and acetone. Masses were estimated from the dimensions (volumes) of grains. Single grains were transferred into clean 300 mL PFA microcapsules (crucibles), and 50 mL 50% HF and 5 mL 14 N HNO_3 were added. Each was spiked with a ^{233}U-^{235}U-^{205}Pb tracer solution (typically 2 mL), capped and again placed in a Parr liner (8-15 microcapsules per liner). HF and nitric acids in a 10:1 ratio, respectively, were added to the liner, which was then placed in Parr high pressure device and dissolution was achieved at 240˚C for 40 hours. The resulting solutions were dried on a hotplate at 130˚C, 50 mL 6N HCl was added to microcapsules and fluorides were dissolved in high pressure Parr devices for 12 hours at 210˚C. HCl solutions were transferred into clean 7 mL PFA beakers and dried with 2 mL of 0.5 N H_3PO_4. Samples were loaded onto degassed, zone-refined Re filaments in 2 mL of silicic acid emitter (Gerstenberger and Haase, 1997).

Isotopic ratios were measured using a modified single collector VG-54R or 354S (with Sector 54 electronics) thermal ionization mass spectrometer equipped with analogue Daly photomultipliers. Measurements were prepared in peak-switching mode on the Daly detector. Analytical blanks were 0.2 pg for U and for Pb 1-4 pg. U fractionation was determined directly on individual runs using the $^{233\text{-}235}U$ tracer, and Pb isotopic ratios were corrected for fractionation of 0.23%/amu, based on replicate analyses of the NBS-982 Pb reference material and the values recommended by Thirlwall (2000). Data reduction employed the excel based program of Schmitz and Schoene (2007). Standard concordia diagrams were constructed and regression intercepts, weighted averages calculated with Isoplot (Ludwig, 2003). Unless otherwise noted, all errors are quoted at the 2 σ or 95% level of confidence.

1.4 Organization of the Thesis

Chapter Two is a summary of the regional geology. Previous work and mineral exploration on the Hemlo East property are reviewed in Chapter Three. Chapter Four is a review of the microscopic and macroscopic igneous and sedimentary petrology of the Hemlo East Property as well as a discussion of the lithostratigraphy. Whole-rock geochemical data at Hemlo East are presented in Chapter Five focusing on major and trace elements, in conjunction with new geochronological data and are used to discuss the tectonic setting of the mafic and felsic metavolcanic rocks of the Hemlo East Property. Conclusions, implications and recommendations for future work are discussed in Chapter Six.

Chapter 2

Regional Geology

2.1 Superior Province

The Archean Superior Province, the largest Archean craton, is bounded to the west by the Trans-Hudson Orogen and to the east by the Grenville Province (Fig. 2.1). The Superior Province was assembled as the result of the amalgamation of volcanic, plutonic, volcanic-plutonic, high-grade gneissic, and metasedimentary terranes, domains, and tectonic or

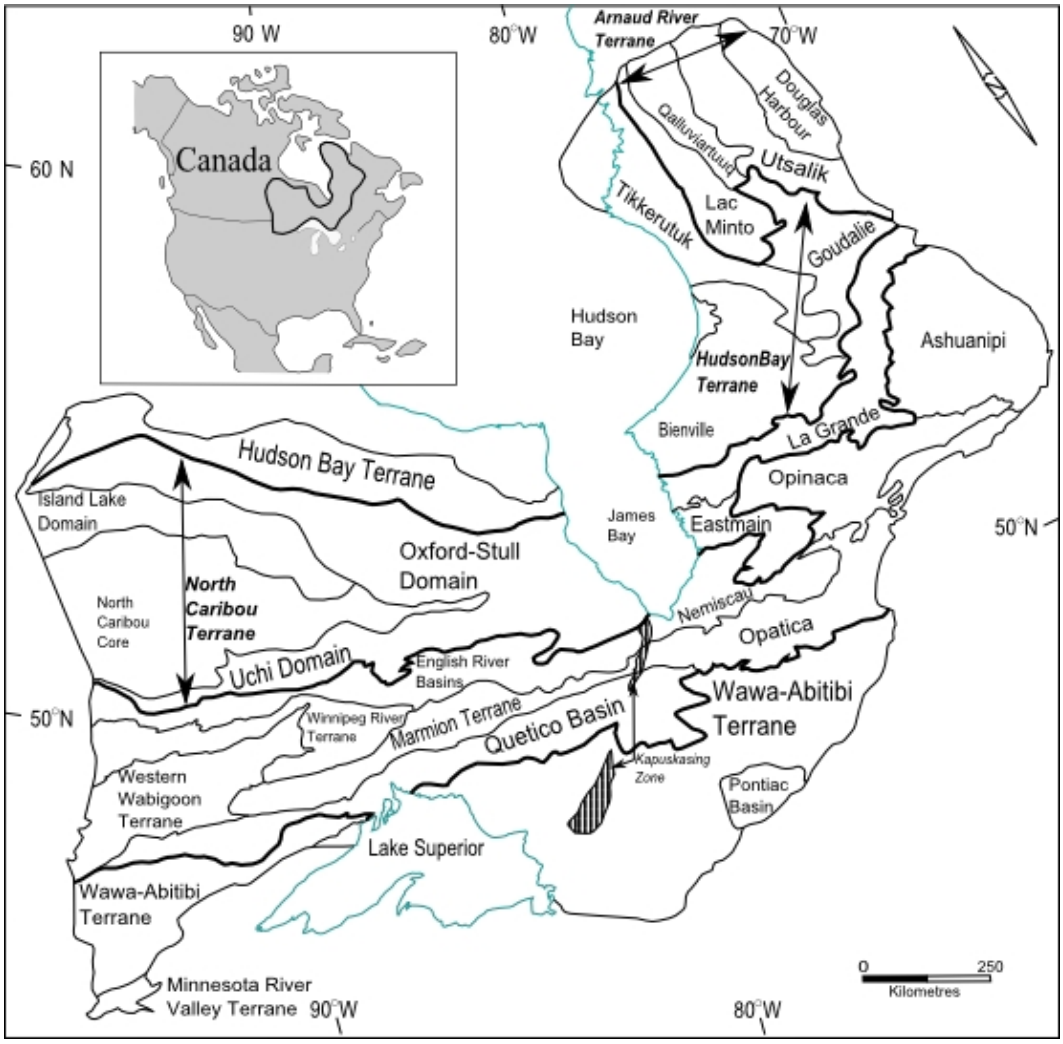

Figure 2.1 - Map of the Superior Province, divided into terranes, domains, and tectonic or tectonostratigraphic assemblages. Inset map at top left shows the location of the Superior Province within Canada. Modified after Stott et al. (2010).

tectonostratigraphic assemblages in the interval 2.74 – 2.65 Ga (Card and Ciesielski, 1986; Percival et al., 2006). A terrane is a tectonically bounded region with internal characteristics distinct from those in adjacent regions prior to Neoarchean assembly of the Superior Province (Stott et al., 2010). A domain is typically a younger, lithologically distinct part of a terrane, comprised either of juvenile crust or sharing a common basement (Stott et al., 2010). A tectonic or tectonostratigraphic assemblage is defined as being distinct in lithology, time and tectonic setting and composed of one or more stratigraphic groups or formations (Stott et al., 2010). Stott et al. (2010) have argued that there has been insufficient evidence for amalgamation of terranes prior to the Neoarchean assembly of the Superior Province to justify the designation of any large crustal block as a superterrane. Terranes and domains, containing greenstone belts and plutonic rocks, hundreds of kilometres long, can be distinguished from adjacent ones by lithology, age, isotopic character, geochemistry and bounding faults (e.g., Skulski et al., 2000; Tomlinson et al., 2004; Percival et al., 2006). These terranes and domains are generally about 100km wide and up to 1500km in length (Fig. 2.1). The age of the rocks of the Superior Province vary from between 3.7 to 2.65 Ga (Card and Ciesielski, 1986).

2.2 Wawa-Abitibi Terrane

The Wawa-Abitibi Terrane extends from the Vermillion district of Minnesota in the west into Quebec in the east, and is bounded by the Quetico basin to the north (Fig. 2.1). The terrane is a volcanic-plutonic belt composed of 2.88-2.72 Ga rocks (Percival, 2006) accreted to the southern part of the Superior Province during the 2.69 Ga Shebandowanian Orogeny (Kerrich et al., 1999). The Wawa-Abitibi Terrane is made up of several greenstone and siliciclastic metasedimentary belts separated by thrust and strike-slip faults which have been intruded by syn- to post-kinematic tonalite-trondhjemite-granodiorite (TTG) plutons (Williams et al., 1991).

The regional metamorphic grade of the Wawa-Abitibi Terrane ranges from lower greenschist to amphibolite facies, with higher metamorphic grades more common adjacent to batholiths (Pan and Fleet, 1993). At least three stages of supracrustal development took place within the Wawa-Abitibi Terrane (2.90, 2.75, and 2.70 Ga; Corfu and Muir, 1989a; Williams et al., 1991). Polat and Kerrich (1999, 2001) interpreted the northern and western Wawa-Abitibi greenstone belts as part of a ~1000km scale subduction–accretion complex that formed along an intra-oceanic convergent plate margin.

The central portion of the Wawa-Abitibi Terrane has been subdivided into a number of greenstone belts (Fig. 2.2).

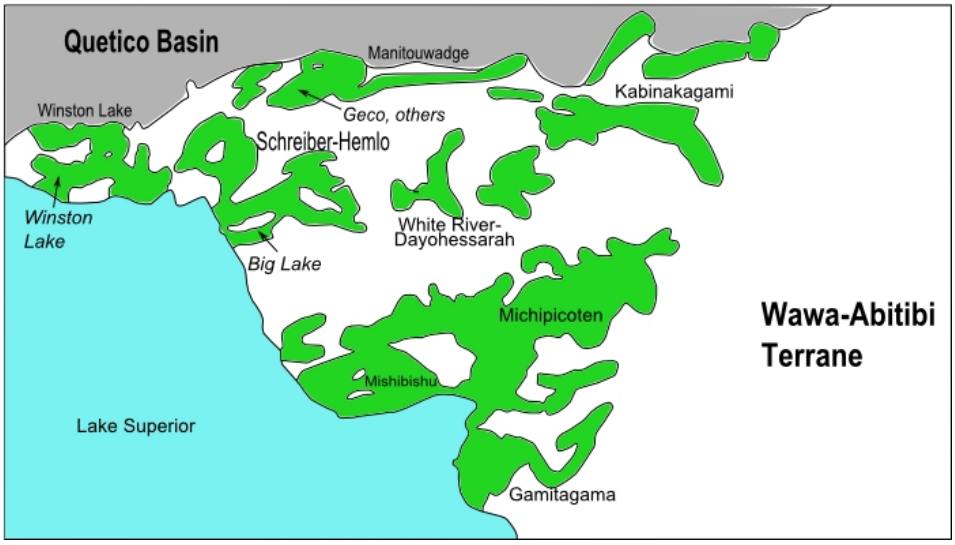

Figure 2.2: Greenstone belts of the central Wawa-Abitibi Terrane. VMS occurrences are labeled in italics. Modified after Polat and Kerrich (1999).

2.3 Schreiber-Hemlo Greenstone Belt

The Schreiber-Hemlo Greenstone Belt has been divided by Williams et al. (1991) into three assemblages: the Schreiber assemblage, west of the Proterozoic Coldwell Alkaline Complex; the Hemlo- Black River assemblage, north of the right-lateral Lake Superior-Hemlo Fault Zone (LSHFZ); and the Heron Bay-Playter Harbour assemblage, south of the LSHFZ (Fig. 2.3). These three assemblages are dominantly composed of mafic and intermediate to felsic

metavolcanic and siliciclastic metasedimentary rocks. Pan and Fleet (1989a) have shown that some of the ultramafic rocks have a komatiitic composition. The eastern side of the Hemlo-Schreiber Greenstone Belt is bounded by gneissic to foliated tonalite-granodiorite of the Black Pic Batholith to the north and the Pukaskwa Complex to the south (Fig. 2.3). Granitoid plutons and dikes intrude the supracrustal rocks. North and northwest-trending Proterozoic diabase dikes cut all rocks within the belt.

The greenstone belt is described by Polat and Kerrich (1999) as a subduction-accretion complex comprised of oceanic plateau related ultramafic to tholeiitic metabasalts, tholeiitic to calc-alkaline arc related metabasalts to metadacites, and turbiditic metasandstones interpreted as trench deposits. Although the original stratigraphic relationships have been disrupted and complicated, in several areas it is clear that komatiites and associated tholeiitic basalt flows occur at the base of volcanic sequences, whereas tholeiitic and calc-alkaline basalts, andesites, dacites, and rhyolites are most abundant at upper tectono-stratigraphic levels (Williams et al., 1991; Polat et al., 1998).

Three major deformation events have been described by Polat et al. (1998): a NNW-SSE compression during subduction-accretion with accompanying intrusion of slab-derived felsic sills and dykes; second, a NNW-SSE orogen parallel transpression with strike-slip faulting and isoclinal folding at regional scale; third, a NW-SE dextral transpression due to the collision of the Wawa and Quetico subprovinces, with strike-slip faulting and shearing, represented by the Lake Superior-Hemlo Fault Zone.

Polat et al. (1998) interpret the White River-Dayohessarah Lake greenstone belt to be the eastern continuation of the Schreiber-Hemlo greenstone belt based on geochemical and structural evidence. Out-of-sequence thrusting and orogen-parallel strike-slip faulting of the accreted oceanic plateaus, oceanic arcs and trench turbidites are interpreted to account for the analogous geological and geochemical characteristics of the two belts.

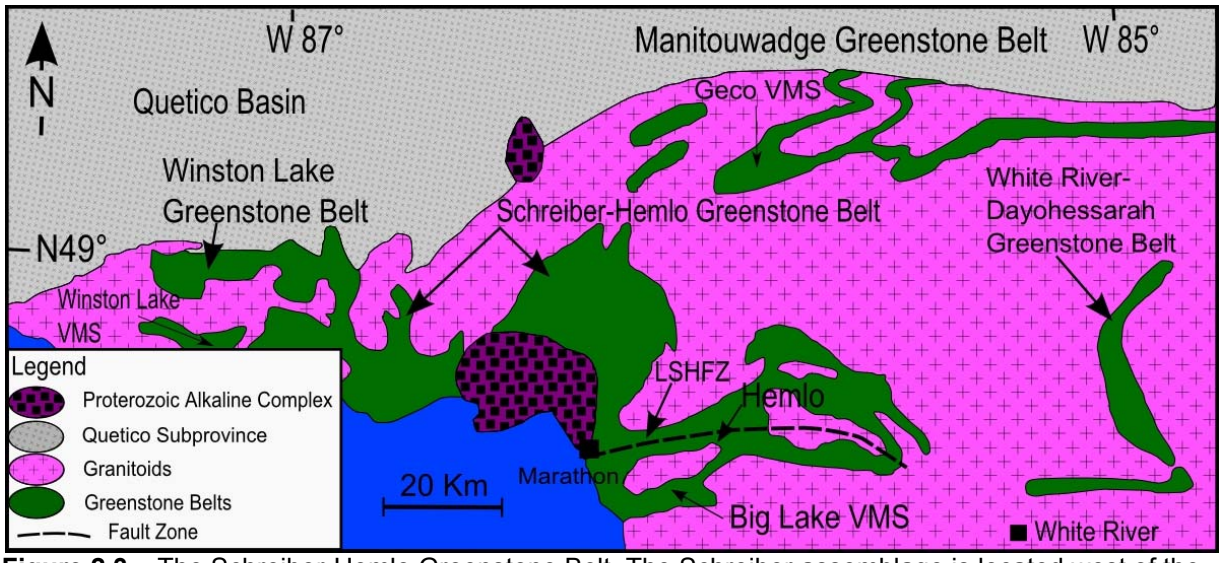

Figure 2.3 – The Schreiber-Hemlo Greenstone Belt. The Schreiber assemblage is located west of the Coldwell Complex, the Hemlo assemblage is located north of the Lake Superior-Hemlo Fault Zone (LSHFZ), and the Heron Bay assemblage is located south of the LSHFZ. Modified after Polat (2009).

2.4 Metallogeny of the Schreiber-Hemlo Greenstone Belt

Ore deposits of the Schreiber-Hemlo Greenstone Belt include the Hemlo lode gold deposit, the Winston Lake VMS deposit and the Big Lake VMS occurrence. The Geco-Willroy VMS deposits occur in the adjacent Manitouwadge Greenstone Belt (Fig. 2.3).

The Hemlo lode gold deposit contains up to 760 tonnes of contained gold in 95 million tonnes of ore averaging 8.0 g/t (based on Schnieders et al., 2000) and is stratabound within felsic metavolcanic rocks (Muir, 2002). The Hemlo deposit is located within the hangingwall of a transition zone from volcanic rocks of the Heron Bay assemblage to the south and sedimentary rocks of the Hemlo-Black River assemblage to the north (Jackson et al., 1998). The footwall is altered felsic metavolcanic rocks of the Moose Lake Volcanic Complex (Thompson et al., 1999). The deposit is spatially associated with high-strain zones (Hemlo Shear Zone), a restraining bend in the greenstone belt, and the volcanic-sedimentary contact of the Moose Lake Volcanic Complex (Lin, 2001; Muir, 2002). Emplacement controls are thought to be the restraining bend, competency contrasts at major lithological contacts and

permeability of the host fragmental unit (Muir, 2002). The potassium alteration zone associated with the gold mineralisation is 4 km long and up to 400 m wide (Muir, 2002).

The Winston Lake VMS deposit contained 4.65 million tonnes of ore at 15.4% Zn, 1% Cu, 35 g/t Ag, and 1.1 g/t Au (Mosier et al., 2009), and is hosted in highly evolved felsic volcanic (± volcaniclastic) rocks and mafic flows. The Manitouwadge deposits (Geco, Willroy, and Big Nama Creek) contained 64 million tonnes of ore grading 2% Cu, 4% Zn, 50 g/t Ag, 50 g/t Ag, and 0.3% Pb (Mosier, 2009) and are hosted in amphibolite-grade felsic metavolcanic rocks. The Big Lake VMS occurrence in the southeast part of the Schreiber-Hemlo greenstone belt and is hosted within mafic-ultramafic metavolcanic rocks (Rinne, 2010).

Chapter 3

The Hemlo East Property

3.1 Geomorphology, Access, Topography, and Vegetation

Access to the Hemlo East Property ranges from good to poor. The western and some northern areas of the property can be accessed via Highway 17 and gravel roads that degrade into skidder trails that allow ATV access. The western access road is restricted (gated) as it passes through the Hemlo tailings impoundment area. The southeastern part of the property (Gouda Lake area) can be accessed via logging roads that extend from the town of White River to the east of the property (Fig. 3.1).

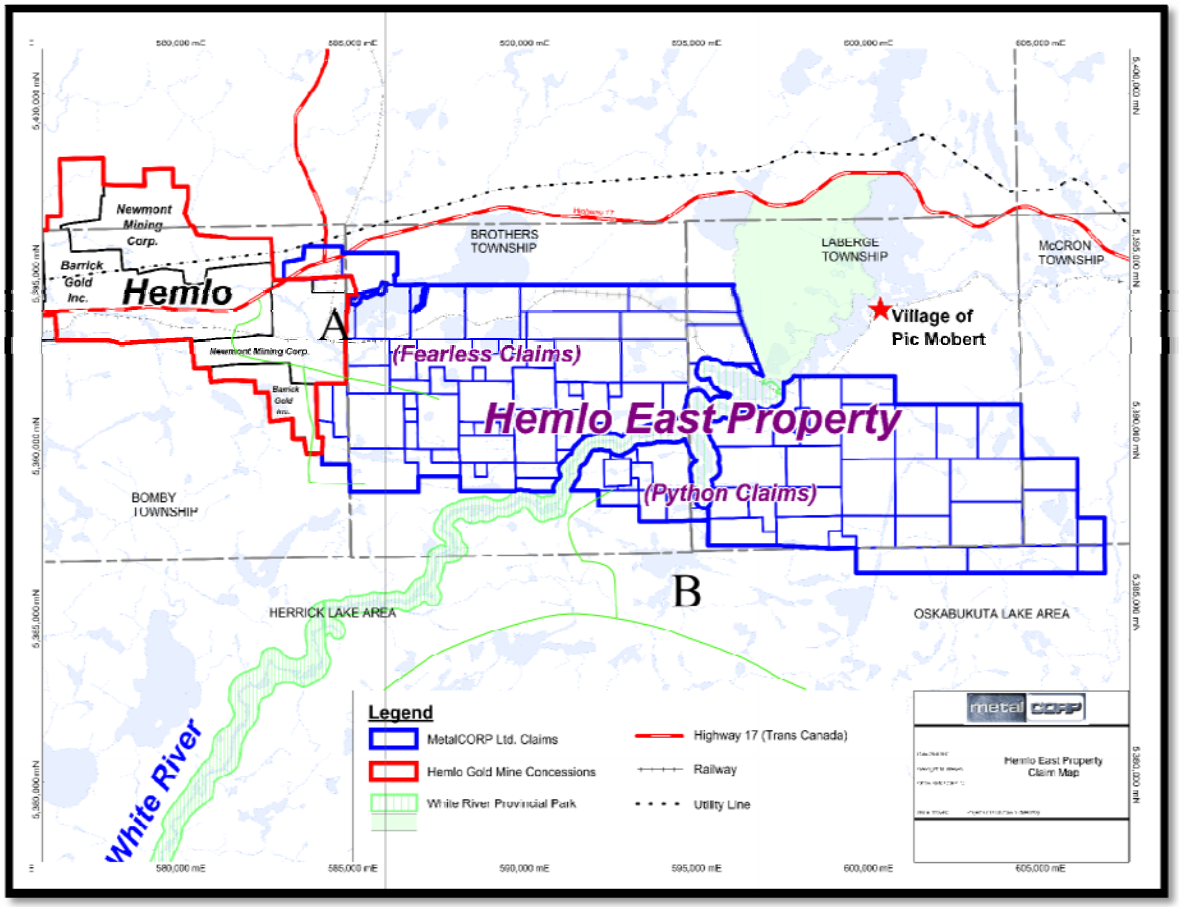

Figure 3.1: Claim map of the Hemlo East Property with access roads in green. A) Western access through the Hemlo mine tailings area. B) Southern access via logging roads from the town of White River to the East (Fage, 2010).

Topography of the Hemlo East Property is typical of most of the ground bordering Lake Superior. The northern area of the claims varies from rolling ground moraine and bedrock hills alternating with extensive spruce and alder bogs. To the south, steep rock-dominated ridges alternate with linear swamps, and lake and creek filled valleys. Elevation varies in the area but averages around 335 metres above sea level.

Vegetation is dominated by large areas of blown-down, dying and dead mixed forest, made up of over mature poplar, birch and balsam. Windstorm blow-down areas are widespread, having occurred over the last 10 to 30 years, and are overgrown with dense alders and Manitoba maple. Swampy and low-lying portions of the property are generally covered with thick tag alders with minor spruce and tamarack forest. Locally, in higher ridge areas, there are mature jack pine and spruce forest. The White River flows south through part of the eastern section of the property and along the eastern boundary.

3.2 History of the Property

The Hemlo East Property was previously named the White River Property, after being staked by Lac Minerals between 1980 and 1982 following the discovery of the Hemlo deposit. The ground was explored by Lac Minerals and other companies (Placer Dome Canada Limited, American Barrick, and TeckCominco Limited) in the years from 1982 to 2003.

The earliest documented exploration work in the White River area was in the 1950's, after discoveries in the Manitouwadge Cu-Zn-Ag district approximately 90 kilometres to the north (Thompson and Paakki, 2001). Mattagami Lake Mines completed diamond drilling and trenching programs in two localities on the White River Property; in 1968 they drilled seven holes and in 1976 they drilled two holes and dug trenches; this work was done in the area known as the Carroll Option on DC Lake (Fig. 3.2).

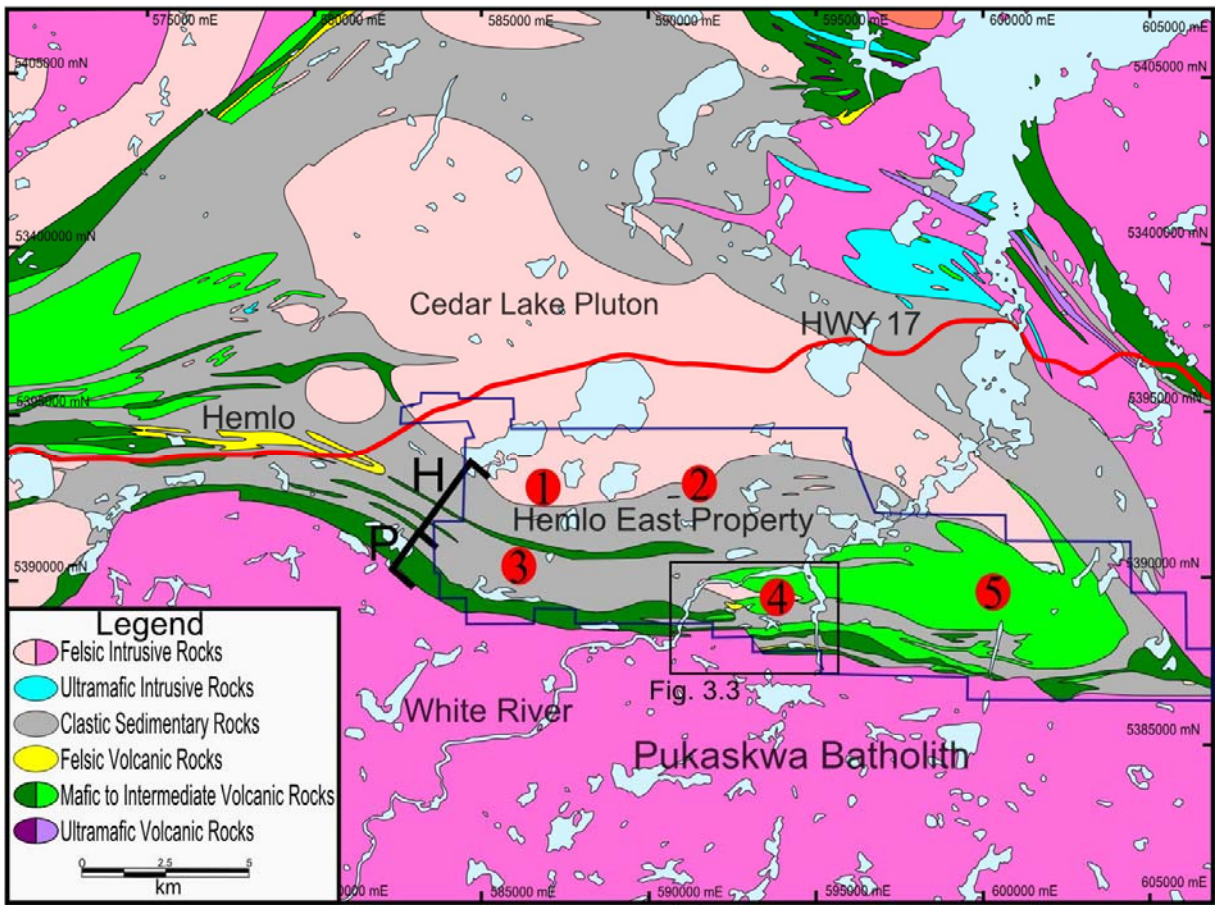

Figure 3.2: Geology of the Hemlo East Property and surrounding area. Prospects: 1) Egg Lake/Upper Anomalous Zone/ Rust Lake. 2) Yellow Birch Alteration Zone. 3) Frank Lake. 4) Gouda-Thor/ Carrol Option/ Duck Lake. 5) Python. H and P show the locations of the Heron Bay Group and Playter Harbour Group, respectively (modified after Muir, 2000)

The bulk of the work done on the property was completed by Lac Minerals from 1980 to 1992 and consisted of airborne geophysics (EM, magnetics and radiometrics), 400 line-km of grid, detailed geological mapping, soil sampling, humus sampling, ground geophysics (magnetics, VLF, EM and IP) over cut grids across the entire property. An extensive drill program of 145 BQ drillholes totalling 30,700 metres was also completed. Areas of anomalous mineralization delineated in Lac Minerals' study include the Gouda Horizon, Thor Horizon, DC Lake Horizon (originally the Carroll Option), the Duck Lake molybdenite showings, the Egg Lake and Upper Anomalous Horizons, the Frank Lake felsic horizon, and the Yellow Birch Lake alteration zone (Fig. 3.2; Thompson and Paakki, 2001).

From 1993-1996 Placer Dome Canada optioned the property and conducted an airborne radiometric survey over most of the White River Property, as well as humus geochemical surveys over the Egg Lake Horizon, Yellow Birch alteration zone and the Gouda Horizon (Shevchenko, 1995a,b; Talbot, 1997). A petrographic report on 45 thin sections sampled in 12 drill holes within the Egg Lake Area and Yellow Birch Alteration Zone was completed by Wells (1996).

Once Placer Dome's option was completed, the ownership of the White River Property was returned to Lac Minerals Ltd. (who had been acquired through a hostile takeover by American Barrick, now Barrick Gold Corporation, in August 1994). Barrick completed a limited amount of additional exploration on the property from 1996-1998. This included a prospecting program along the eastern extension of the Gouda Lake alteration zone and a revised compilation of previous work on the property plus lithogeochemical sampling program (Armstrong and Magnan, 1998).

From 1998-2003, TeckCominco Exploration Limited held the option on the White River Property. Exploration by TeckCominco Exploration Ltd. during 1999-2001 consisted of geological mapping and sampling, soil and humus sampling, and sampling of selected archived Lac diamond drill core (Page, 1999; Thompson et al., 1999; Thompson and Paakki, 2001). Thirty diamond drill holes totalling 10095.5m were completed between 2000 and 2003 focusing mainly on the eastern and western extensions of the Gouda horizon with some drill holes targeting the Egg Lake, Frank Lake, and Rust Lake areas (Fig. 3.2).

In the spring and summer of 2007, the White River claims began to lapse and MetalCORP initiated staking and acquired this open ground and renamed it the Fearless and Python properties. In the summer of 2008, the remainder of the claims became open for staking and MetalCORP staked these as well, renaming the entire property Hemlo East.

3.3 Previous Work

In conjunction with the extensive reports filed by company geologists there have been numerous reports completed by the Ontario Geological Survey on the property itself: Pan and Fleet (1988; 1989a; 1990b), and Fleet and Pan (1991) discuss the metamorphic petrology and geochemistry of the western end of the property. Pan and Fleet (1989b, 1990a) discovered Cr-rich silicates and halogen-bearing allanite within the calc-silicate-altered Cadi Fracture Zone in the western end of the property. Wells (1996) prepared a petrographic and interpretive report on the alteration mineralogy within the Egg Lake and Yellow Birch zones which concluded that the potassically altered rocks in this area display recrystallization, foliation and clearly predate peak metamorphism, similar to the Hemlo gold deposits.

Regionally, geological mapping and sampling of the Schreiber-Hemlo greenstone belt east of the Coldwell Complex was carried out in 1977-78 by T. Muir of the Ontario Geological Survey, with results published in Muir (1982). Geochronological studies within the eastern portion of the Schreiber-Hemlo Greenstone Belt have been carried out by Davis and Lin (2003), Davis et al. (1998), Beakhouse and Davis (2005), and Corfu and Muir (1989 a,b). Thompson (2006) has presented a comprehensive document outlining the metamorphic evolution and P-T conditions within the Schreiber-Hemlo Greenstone Belt and the surrounding granitoid intrusions.

3.4 Field Geology

The Hemlo East Property is sandwiched between the Cedar Lake Pluton to the north and the Pukaskwa Batholith to the south (Fig. 3.2). The property is subdivided into the Hemlo-Heron Bay Sequence in the northern and central area and the Playter Harbour Sequence in the south (Fig. 3.2). The geology is dominated by generally east trending and north dipping metasedimentary rocks with mafic to intermediate metavolcanic rocks and minor felsic

metavolcanic rocks. Proterozoic diabase dykes crosscut all lithologies. The entire Schreiber-Hemlo Greenstone belt has been affected by lower to mid amphibolite facies metamorphism which is a relatively high metamorphic grade compared to adjacent greenstone belts (Fleet and Pan, 1991). The geologic mapping and sampling for this thesis was focused on the Gouda-Thor-Carroll area of the Hemlo East property, outlined in Figure 3.3, as it has been the most prospective area of the property. Detailed macro and microscopic descriptions of collected samples are presented in Chapter 4. Seventy-four samples were collected during field mapping and submitted for whole-rock geochemistry (Chapter 5).

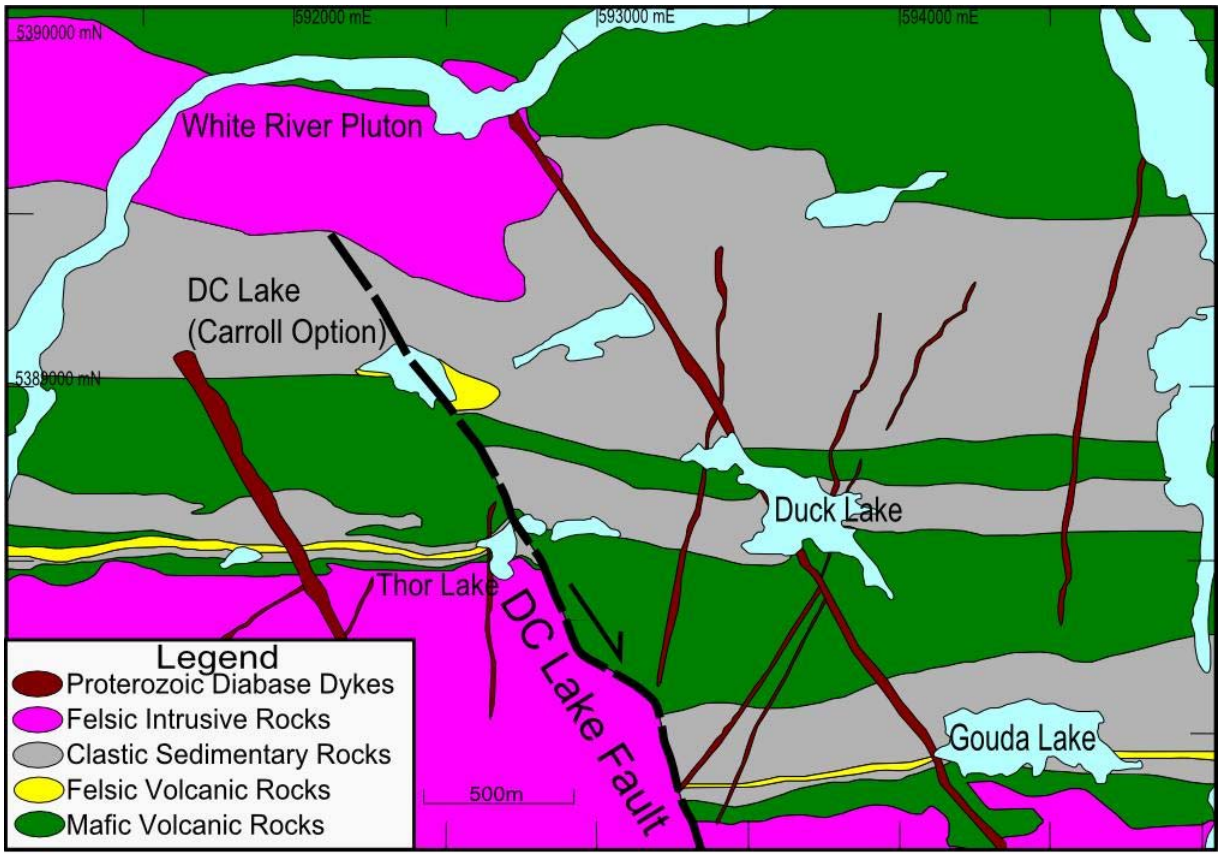

Figure 3.3: Geological map of the Gouda-Thor-Carroll area of the Hemlo East Property. Compiled from Guthrie (1985), Kent (1984), McIlveen and Stanley (1985) and the author's field work.

3.4.1 Intrusive Lithologies

The Pukaskwa Batholith, also referred to as the Pukaskwa Gneissic Complex is a tonalite to granodiorite intrusion which forms the southern boundary of the greenstone belt and extends ~60km to the south to the Mishibishu greenstone belt (Fig 2.2). The Cedar Lake pluton, a biotite-honblende granodiorite, lies along the northern border of the property (see section 4.4) and its satellite body, the Cedar Creek stock lies immediately to the west. The White River Pluton, located at the north end of the Gouda-Thor-Carroll area at the White River is a biotite hornblende monzogranite (see section 4.4).

All units have been intruded by Neoarchean pegmatite, aplite and fine-grained granitic and quartz-feldspar porphyry dikes, the latter are host to molybdenite mineralization. Proterozoic diabase dikes, trending north and northwest, crosscut all lithologies. Based on work by Osmani (1991), there are possibly five generations of diabase dike swarms in the map area. Although crosscutting relationships were observed locally during the field work, the delineation of the various swarms is not conclusive from this project (Fig. 3.3).

3.4.2 Metavolcanic Lithologies

Tholeiitic mafic metavolcanic rocks are variably recrystallized, include amphibolite and amphibolitic gneiss and have locally retained primary volcanic features (consisting of pillowed, massive and foliated flows). Outcrops where primary features are visible are mainly located near Hemlo, whereas in the Gouda-Thor-Carroll area, the mafic metavolcanic rocks are amphibolites. A plagioclase-porphyritic amphibolite unit which has been referred to as ‘the poker chip horizon’, containing flattened lenses of plagioclase within mafic flows is found to the south of the area.

Felsic to intermediate metavolcanic rocks are composed of quartz plagioclase-phyric units. The primary felsic metavolcanic rock type in the Gouda-Thor-Carroll area is a sericite schist (±quartz-eyes) where quartz eyes are interpreted to be primary volcanic features.

3.4.3 Metasedimentary Lithologies

The metasedimentary rocks at Hemlo East consist of two main varieties: dark grey-brown mafic metawackes and light grey, intermediate to felsic recrystallised feldspathic metasedimentary rocks. These siliciclastic sedimentary rocks are interpreted to be volcanic derived turbiditic greywacke sandstones and shales that are either tectonically juxtaposed against, or unconformably overlie volcanic rocks. There is no clear indication of graded bedding in any metasedimentary rocks observed in the field. Metasedimentary rocks are the most abundant unit within the Hemlo East Property.

3.5 Structural Geology

All metavolcanic and metasedimentary lithologies dip moderately to the north and have undergone at least two folding events, resulting in isoclinal folds (Talbot, 1997). The major structural trends (foliation, shear zones) within the belt are subparallel to the contacts with the adjacent batholiths.

The deformation history of the greenstone belt is multiphase and complex. This is indicated by multiple fabrics, considerable shortening and extension, tight to isoclinal folding including intrafolial folds, ductile shearing, and layer-parallel faulting in conjunction with primary layering (Muir, 1997). The style of deformation in the map area varies considerably from place to place, reflecting the different mechanical properties of the rocks; and the diversity of local deformation processes and events (Muir, 1997). At least four generations of brittle and ductile deformation have been documented by Muir (1997).

The Hemlo fault zone is the predominant fault structure in the map area and possibly in the greenstone belt as a whole. It has been interpreted as forming the boundary between the Hemlo–Black River assemblage to the north and the Heron Bay-Playter Harbour assemblage to the south (Williams et al., 1991). The dextral (from geophysical, geochemical, and field evidence) DC Lake Fault is located within the Gouda-Thor-Carroll area of the property, offsetting the boundary between the Gouda and Thor felsic metavolcanic units, extending into the Pukaskwa Batholith.

Two major shear zones on the property, the Gouda Lake and Hemlo Shear Zones, both host gold mineralization (Thompson et al., 1999). Several smaller high-strain zones also exist on the property (Thompson and Paakki, 2001). The Gouda Lake shear zone (GLSZ) extends along most of the southern claims and is separated into a northern and southern section at the DC Lake fault (Fig. 3.4). It exhibits complex structure, altered lithologies and anomalous bedrock geochemistry similar to the Hemlo deposit area (Gouda and Thor Horizons, Frank Lake felsic horizon). The Hemlo Shear Zone (HSZ), along the Hemlo Fault, has been well studied (Lin, 2001). It contains thin, discontinuous anomalous gold zones. The eastern extension of the HSZ on the Hemlo East property is interpreted to splay into the Hemlo North Shear zone and the Hemlo South Shear zone at the western end of the property (Fig. 3.4; Thompson et al., 1999). The Hemlo North splay off of the HSZ contains the Egg Lake zone and is known to contain anomalous gold mineralization; the Hemlo South splay contains the upper anomalous horizon which is also anomalous for gold (Fig. 3.4).

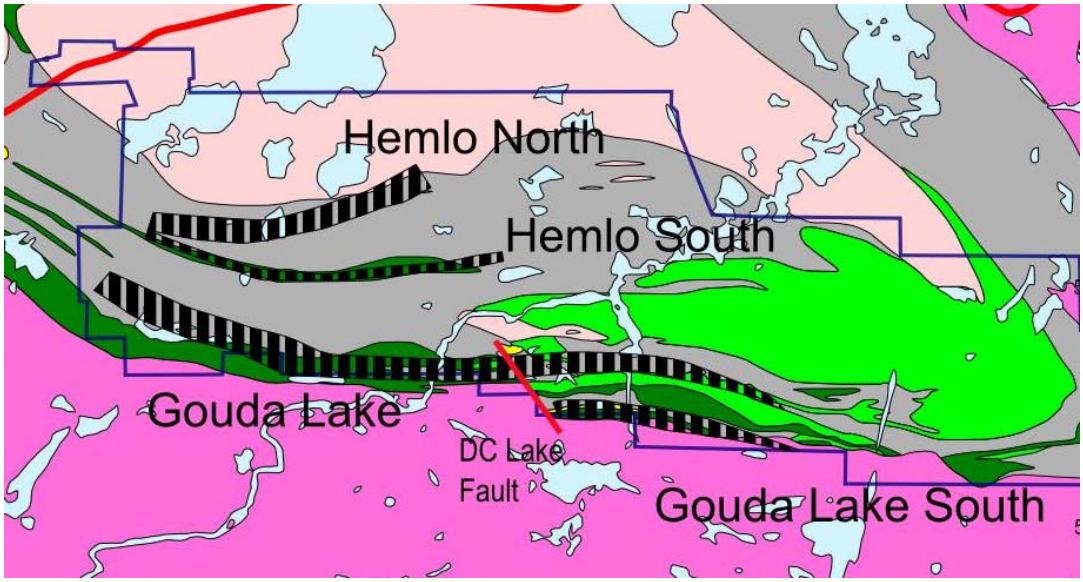

Figure 3.4: Location of the four main shear zones on the Hemlo East Property (after Thompson et al., 1999).

3.6 Metamorphic Grade

Thompson (2006) has presented a comprehensive account of the metamorphic evolution and P-T conditions within the Schreiber-Hemlo Greenstone Belt and the surrounding granitoid intrusions. The rocks of the Hemlo East property have been subjected to lower to mid-amphibolite facies metamorphism, followed tens of millions years later by a subgreenschist/-lower greenschist facies metamorphism (Fig. 3.5; Thompson, 2006). The abundant granitoids within and around the greenstone belt are either too old, too young, or of insufficient volume to be the source of heat for the primary regional metamorphism (Thompson, 2006). The regional pattern cuts across major structural trends whereas, at kilometre scale there is evidence of structural control of metamorphic grade (Thompson, 2006). Thompson (2006) has determined that the maximum metamorphic pressures were in the range of four to five kilobars.

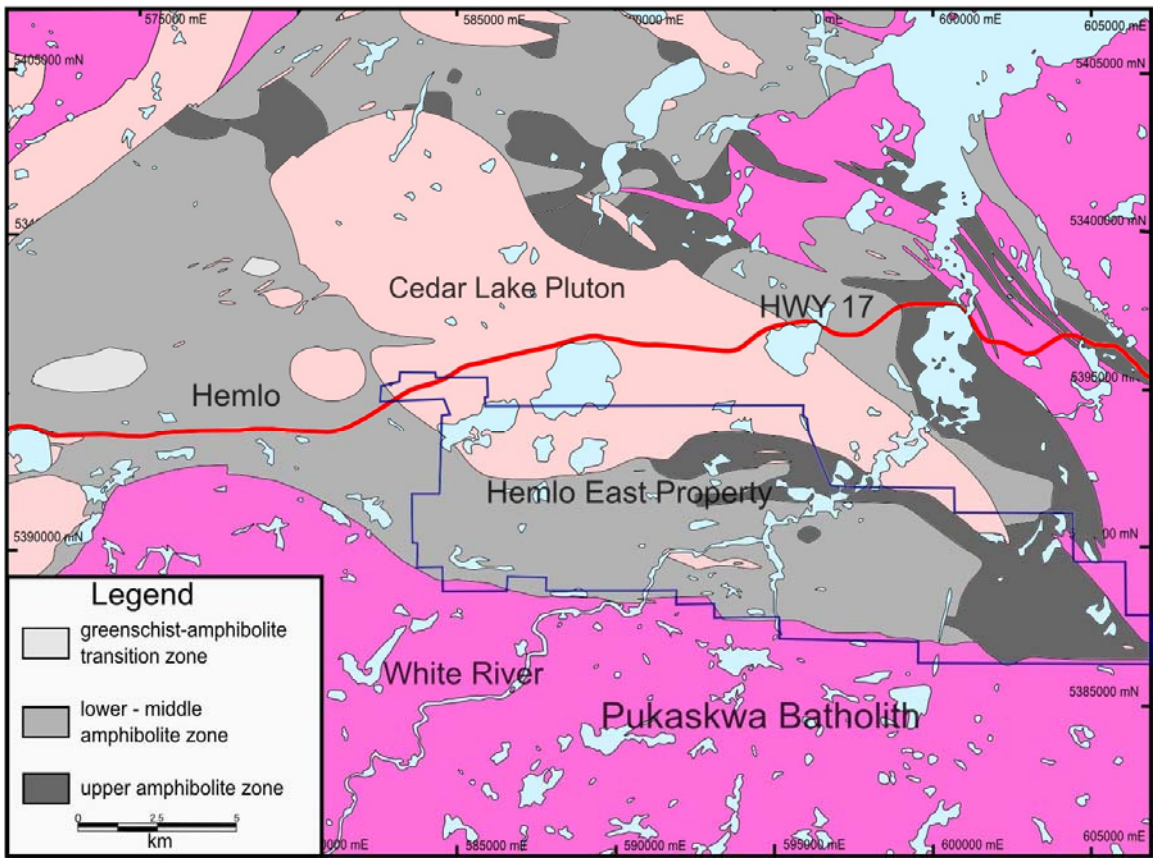

Figure 3.5: Metamorphic map of the eastern Schreiber-Hemlo greenstone belt. Metamorphic zones after Thompson (2006).

3.7 Geophysics

A report prepared by Sterritt and Rudd (2009) detailed the findings of the most recent airborne geophysical survey flown over the Hemlo East Property. An AeroTEM III helicopter-borne time-domain electromagnetic survey was flown over the Hemlo East Property in Late 2007.

3.7.1 Magnetic data

The strongest magnetic responses are associated with thin Paleoproterozoic and Mesoproterozoic mafic intrusive (diabase) dykes predominantly oriented in two sets, northwest-trending and north-trending (Sterritt and Rudd, 2009; Fig. 3.6). The Cedar Creek Stock, composed of biotite-hornblende granodiorite, appears as a strongly magnetic ovoid in

the northwest.This stock has a much stronger magnetic response than the microcline-megacrystic biotite-hornblende granodiorite Cedar Lake pluton to the northeast, suggesting that the magnetite content of the stock is much higher. Felsic-intermediate volcanic rocks and clastic metasedimentary rocks have low magnetic signatures. The Pukaskwa Batholith in the east and south of the survey area is distinguishable from the felsic-intermediate volcanic and metasedimentary rocks by a slightly higher magnetic response. Thin, folded belts of mafic metavolcanic rocks are readily mapped from their relatively strong magnetic responses. These vary from tens of meters wide to almost 1 km wide. Northwest-trending shear zones appear as both magnetic highs and lows. Structural features such as shear zones and faults are visible as discontinuities and offsets in magnetic features (Sterritt and Rudd, 2009).

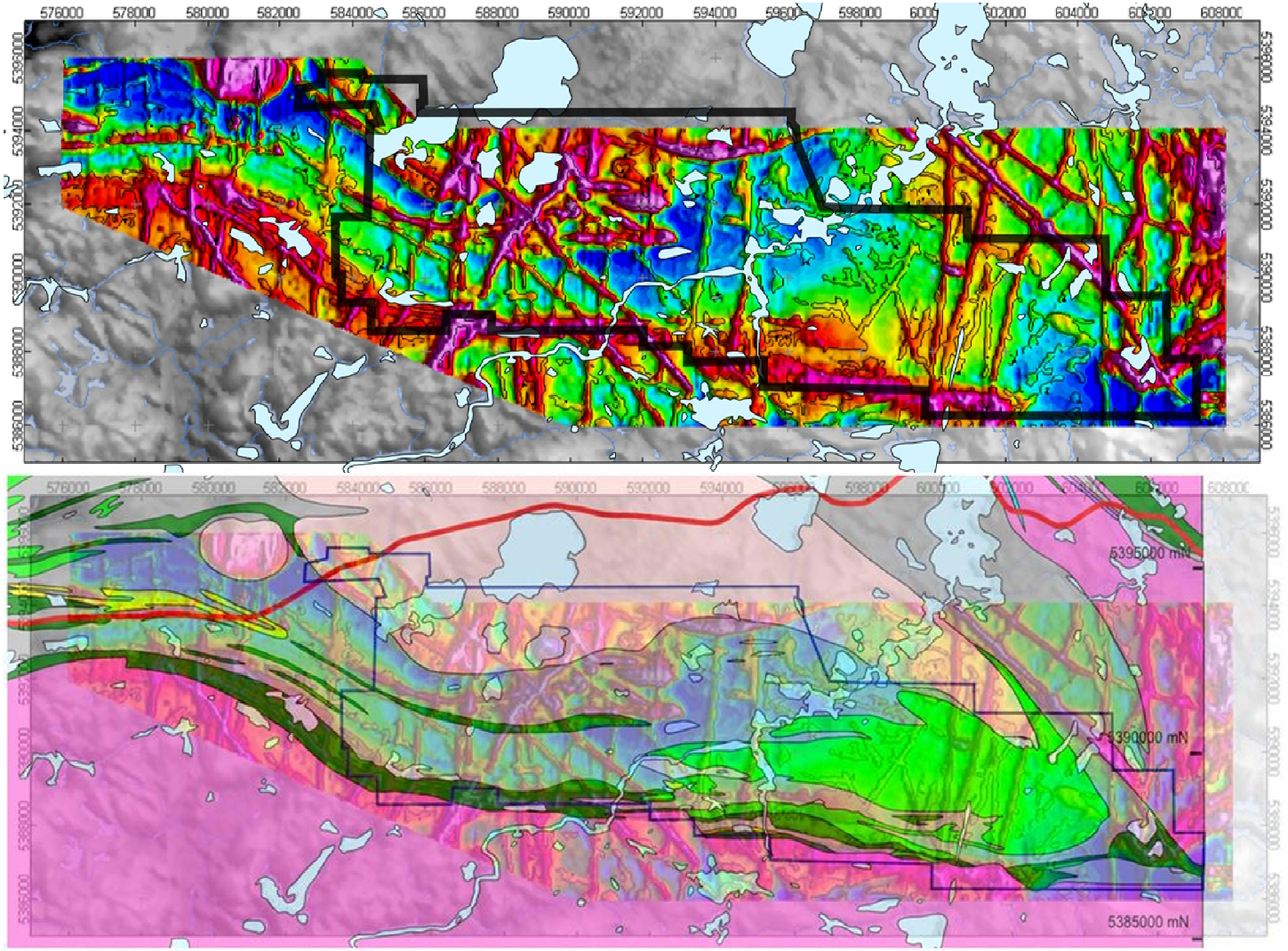

Figure 3.6: Magnetic data (A) and the same magnetic map overlain on regional geology to illustrate where lithological contacts are outlined (B). Proterozoic diabase dikes are not shown on the regional geological map (From Sterritt and Rudd, 2009).

3.7.2 Electromagnetic data

Gridded electromagnetic data are dominated by cultural effects, namely mine facilities, power lines, roads, railway tracks, and a tailings pond. EM conductors that can be clearly attributed to these features have been removed as they have no bearing on this interpretation. The remaining discrete zones of high conductance may represent areas of conductive sulphide mineralization (Fig. 3.7, Sterritt and Rudd, 2009). The electromagnetic data outlines several east-west trending conductors including the Gouda-Thor units.

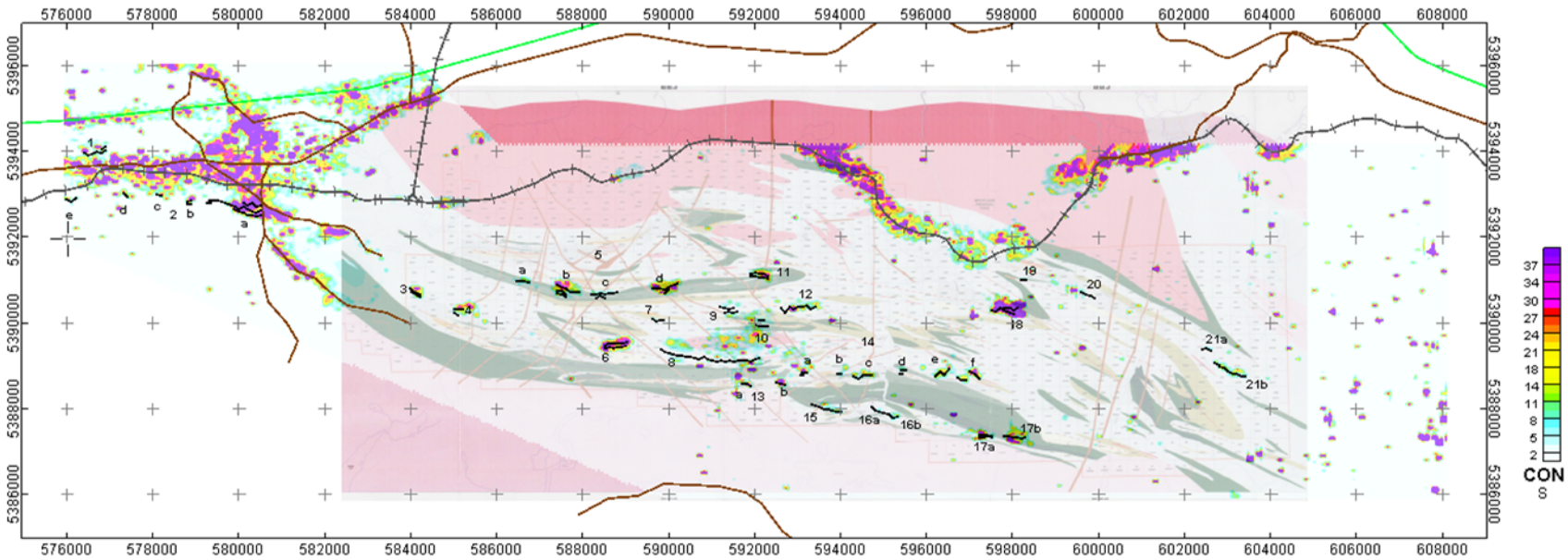

Figure 3.7: Apparent conductivity calculated from the AeroTEM data overlain on geology. EM targets are indicated by numbers and letters and the black lines indicate the conductor strike. Brown lines outline roads, grey lines show the location of the railway and the green line represents a power transmission line (From Sterritt and Rudd, 2009).

3.8 Core Logs

Logs of the 30 archived TeckCominco Exploration drill holes which were re-logged by the author are presented in Appendix A. Sixteen of these holes were drilled into the Gouda-Thor-Carroll area and five holes were drilled into the Gouda Lake Shear Zone extending east (Fig. 3.8). 122 samples were collected from this archived drill core and submitted for whole-rock geochemistry (Chapter 5).

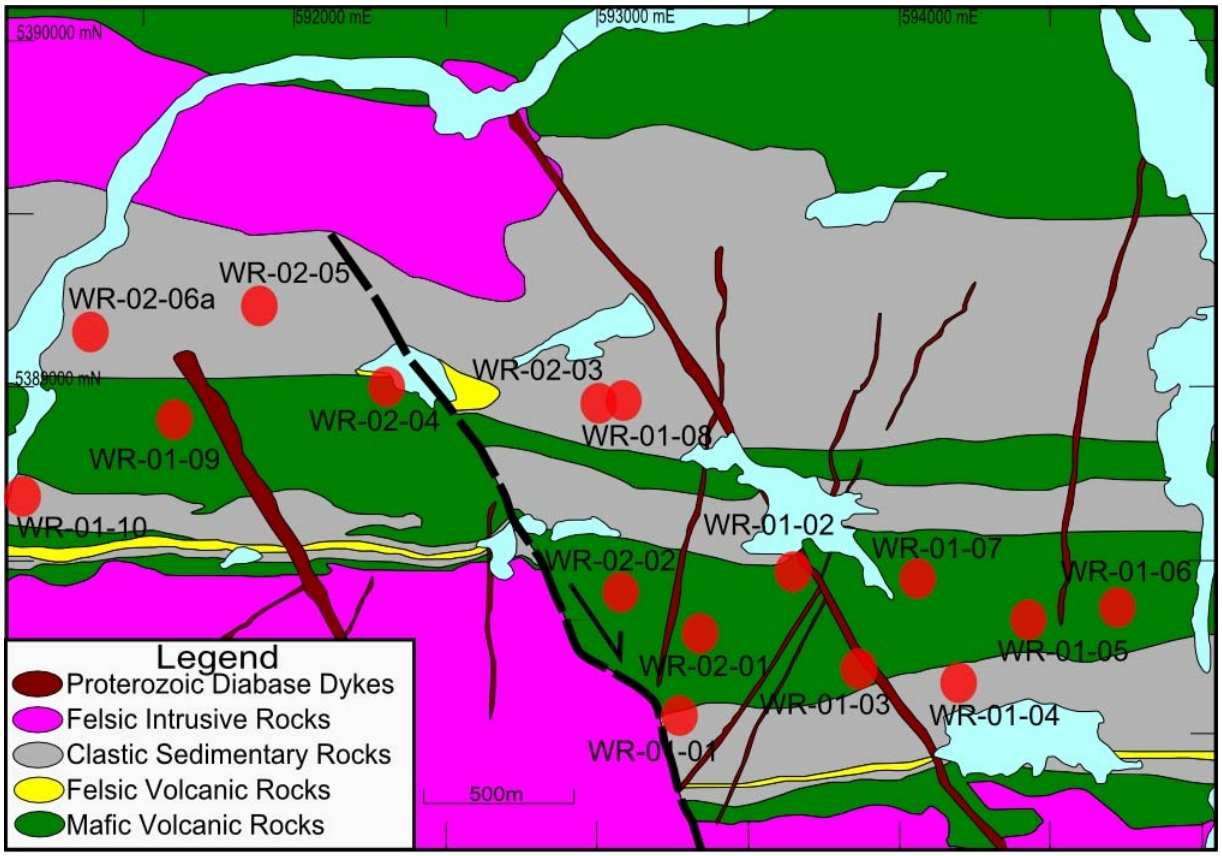

Figure 3.8: Location of Teck Exploration 2000-2003 drill holes in the immediate vicinity of the Gouda-Thor-Carroll Area.

Diamond Drill Holes WR-01-01, WR-01-02, WR-01-03, WR-01-04, WR-01-05, WR-01-06, WR-01-07, and WR-01-08 were drilled on the eastern side on the DC Lake fault into the Gouda Horizon. Holes WR-01-09, WR-01-10, WR-02-04, WR-02-04, WR-02-05, and WR-

02-06a were drilled on the western side on the DC Lake fault into the Thor Horizon. Holes WR-00-01, WR-00-02, WR-00-04, and WR-02-09 were drilled into the western extension of the Thor horizon (off of the map on Fig. 3.7) and encountered identical stratigraphy to the holes in the east. Holes WR-00-03, WR-00-07, and WR-00-08 were drilled into the Frank Lake felsic horizon. No significant gold values were returned in the assay data.

The drill holes were re-logged in order to give a better understanding of the stratigraphy in the Gouda-Thor-Carroll area. A 3D model of these drill holes is presented in Figure 3.9 to visualise the well-defined stratigraphy in this area. This diagram is a cross section of drill holes, looking west; the units are dipping north-northeast, so that in the drill holes closest to the view (eastern side), the contacts are at an apparent deeper depth. The diagram is divided into drill holes located east or west of the DC lake fault, and the regular trend of stratigraphic continuity between these holes is readily observed (Fig 3.9).

3.9 Mineralisation

Mineralisation within the Gouda-Thor horizons is restricted to the (±quartz)-sericite schist unit. The Gouda Lake deposit has been calculated to contain 253000 tonnes of ore at 4.1g/t by Lac minerals (Armstrong and Magnan, 1998). Mineralization consists of fine-grained to massive pyrite (1-50%) with interstitial sphalerite and galena (up to 5% combined; Armstrong and Magnan, 1998). Maximum gold and silver values appear to correlate with anomalous concentrations of galena, and to a lesser extent, sphalerite (Armstrong and Magnan, 1998). Thin section studies of gold-bearing intersections did not locate any gold; however electron microprobe work noted gold as inclusions in allargentum, a Ag, Sb, S mineral (Armstrong and Magnan, 1998). Drilling along strike to the east and west for 6.5 kilometres does recognize the Gouda Lake horizon with anomalous Pb and Zn values, however, there is no gold associated with it (Armstrong and Magnan, 1998).

Work done by Mattagami Lake Mines on the DC Lake felsic volcanic unit (Carroll Option) in 1967-1970 describe the mineralised units as dacitic tuffs, altered dacites, rhyolitic tuffs, brecciated rhyolites, and banded rhyolites from diamond drill hole logs with Zn values as high as 4% (Harvey, 1968). This horizon was found to contain up to 0.80% Zn over 29 metres in 1968 (Thompson and Paakki, 2001).

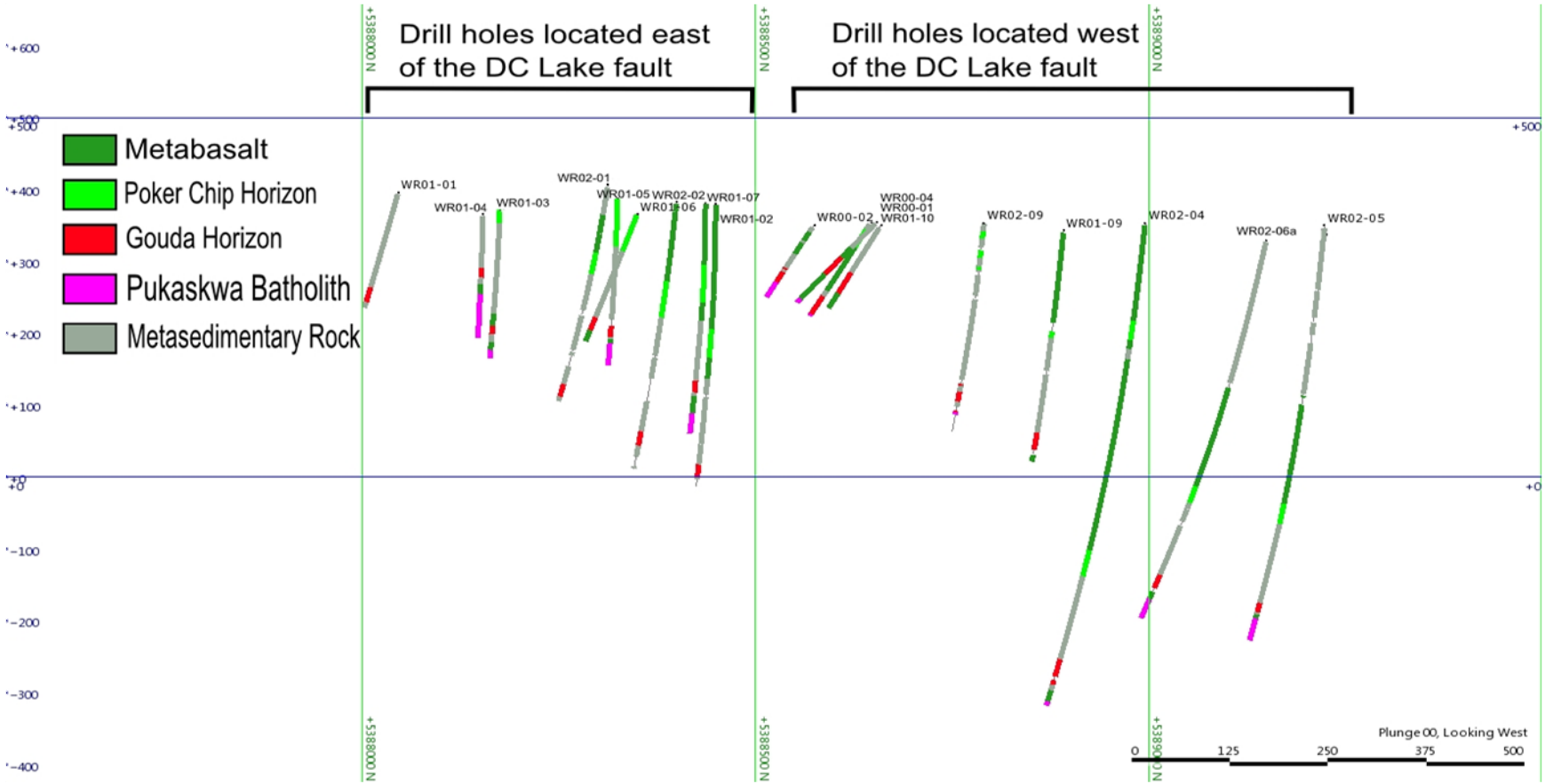

Figure 3.9: 3D image of re-logged drillholes, looking west. All units dip north-northeast. Image generated using Leapfrog 3D.

Chapter 4

Igneous and Metamorphic Petrology of the Hemlo East Property

4.1 Lithostratigraphy

Lithologies within the Gouda-Thor-Carroll area of the Hemlo East Property have been divided into mafic metavolcanic rocks, felsic metavolcanic rocks, metasedimentary rocks, intrusive and metaintrusive rocks on the basis of data collected during the 2009 field season. In the south of the study area near the contact with the Pukaskwa Batholith, the large number of drill holes means that the stratigraphy is relatively well understood and all units dip to the north at 35-50° (Fig. 4.1). On either side of the DC Lake Fault, the Pukaskwa Batholith is in contact with mafic metavolcanic rocks, overlain by metasedimentary rocks (Fig. 4.1). These metasedimentary rocks form the footwall to the Gouda/Thor gold/VMS horizons with another metasedimentary unit forming the hangingwall. Overlying the metasedimentary rocks is a distinctive thick mafic metavolcanic unit which contains the 'poker chip horizon'. On the Thor (west) side of the fault, the 'poker chip horizon' occurs near the bottom of the mafic unit, and on the Gouda side it occurs in the middle of the mafic unit. To the north, alternating units of mafic metavolcanic and metasedimentary rocks continue to the White River Pluton in the northwest of the Gouda-Thor Carroll area (Fig. 4.1). The DC Lake Fault was determined to be dextral based on the offset of stratigraphy, geochemistry, and geochronological evidence presented in Chapter 5.

4.2 Petrography

Textural and mineralogical characteristics of the lithologies presented in Section 4.1 are summarised in the following sections, with detailed petrographic descriptions provided in Appendix B. Where omitted, the prefix "meta" should be assumed for all rocks discussed.

Crystal size classifications used are: fine-grained <1 mm, medium-grained 1-3 mm, and coarse-grained 3-10 mm.

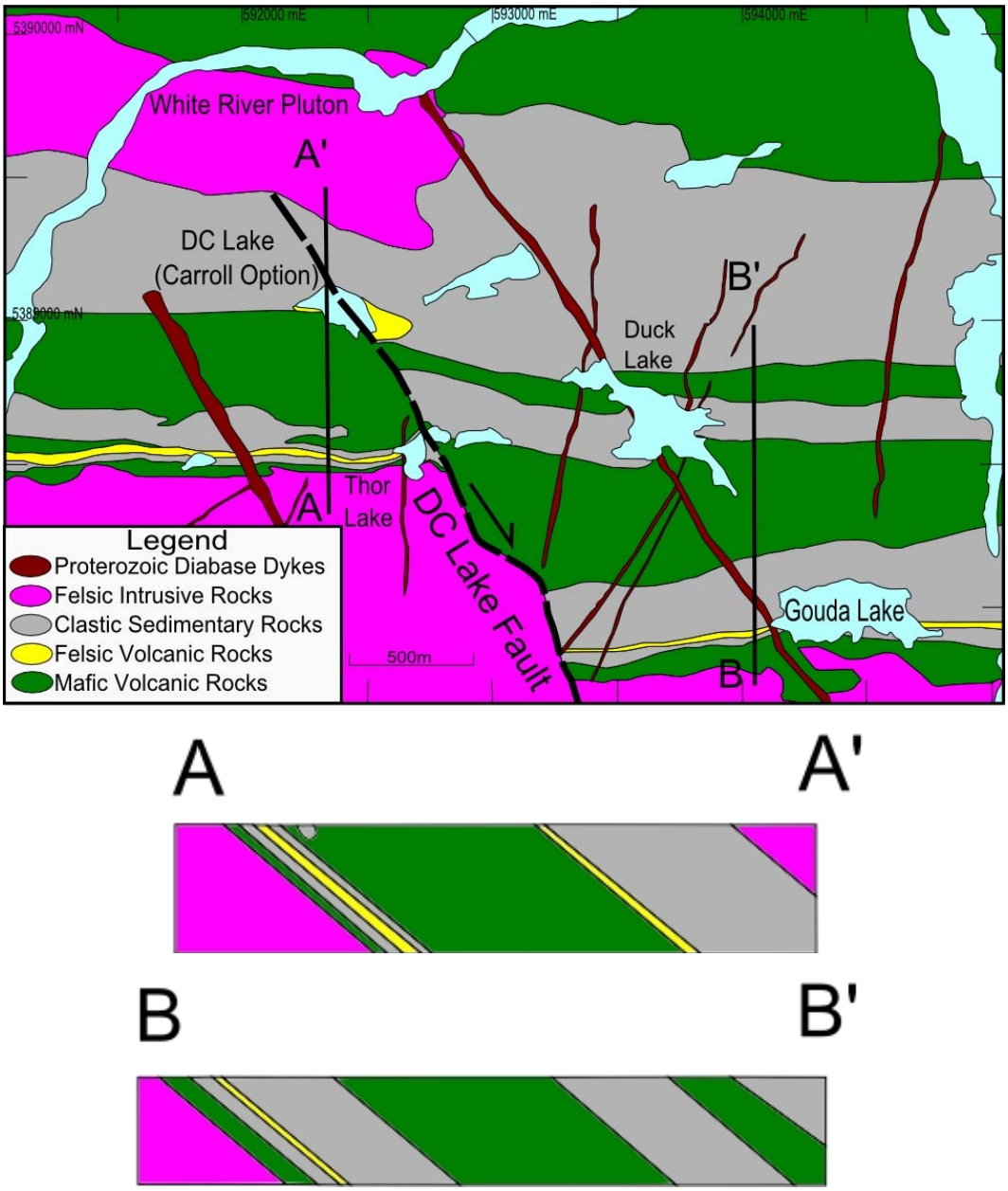

Figure 4.1: Location map and cross sections within the Gouda-Thor-Carroll area on either side of the DC Lake Fault.

4.2.1 Mafic Metavolcanic Rocks

Least altered samples of mafic metavolcanic rocks of the Gouda-Thor-Carroll area are metabasalts. They range from massive flows to foliated units, with the foliation defined by the alignment of hornblende and mica. A strong foliation or schistosity is most pronounced in the area of the Gouda Shear Zone. The mineralogy of the basalts consists of hornblende (85%), plagioclase (10%), biotite (5%); (Fig. 4.2). Figure 4.2B shows an example of a metabasalt where the foliation is defined by compositional layering; the upper right hand half of the photomicrograph contains dominantly medium-grained hornblende, whereas the lower left half of the photomicrograph contains fine-grained hornblende plus plagioclase. Metabasalts are found in east-trending belts throughout the property.

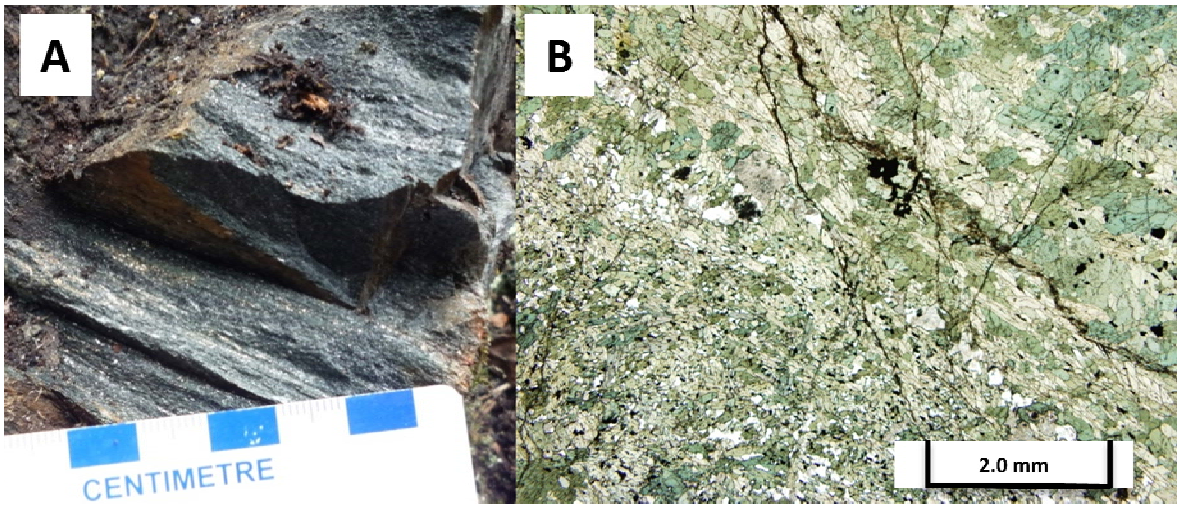

Figure 4.2: Representative photos of mafic metavolcanic rocks of the Gouda-Thor-Carroll area. A) Outcrop photo of foliated metabasalt B) Foliated metabasalt (Sample FR-01; ppl)

4.2.1.1 Mafic Lapilli Tuff

Mafic lapilli tuffs are foliated to strongly foliated and medium-grained (Fig. 4.3). Plagioclase and potassium feldspar-rich lapilli (up to 30-40%) occur flattened parallel to foliation within a hornblende-rich matrix. Lapilli often have pointed ends, measure up to 3-4cm long, and up to

1cm wide. The rock consists of lapilli fragments (extremely fine-grained hornblende, and plagioclase) (35%), hornblende (35%) plagioclase (25%), and biotite (5%). The mafic lapilli tuff is only found in the stratigraphic unit known as the 'poker chip horizon' (Fig. 4.1). The mafic lapilli tuff is confined to the lower to mid- sections of the mafic volcanic unit stratigraphically above the Gouda/Thor horizons.

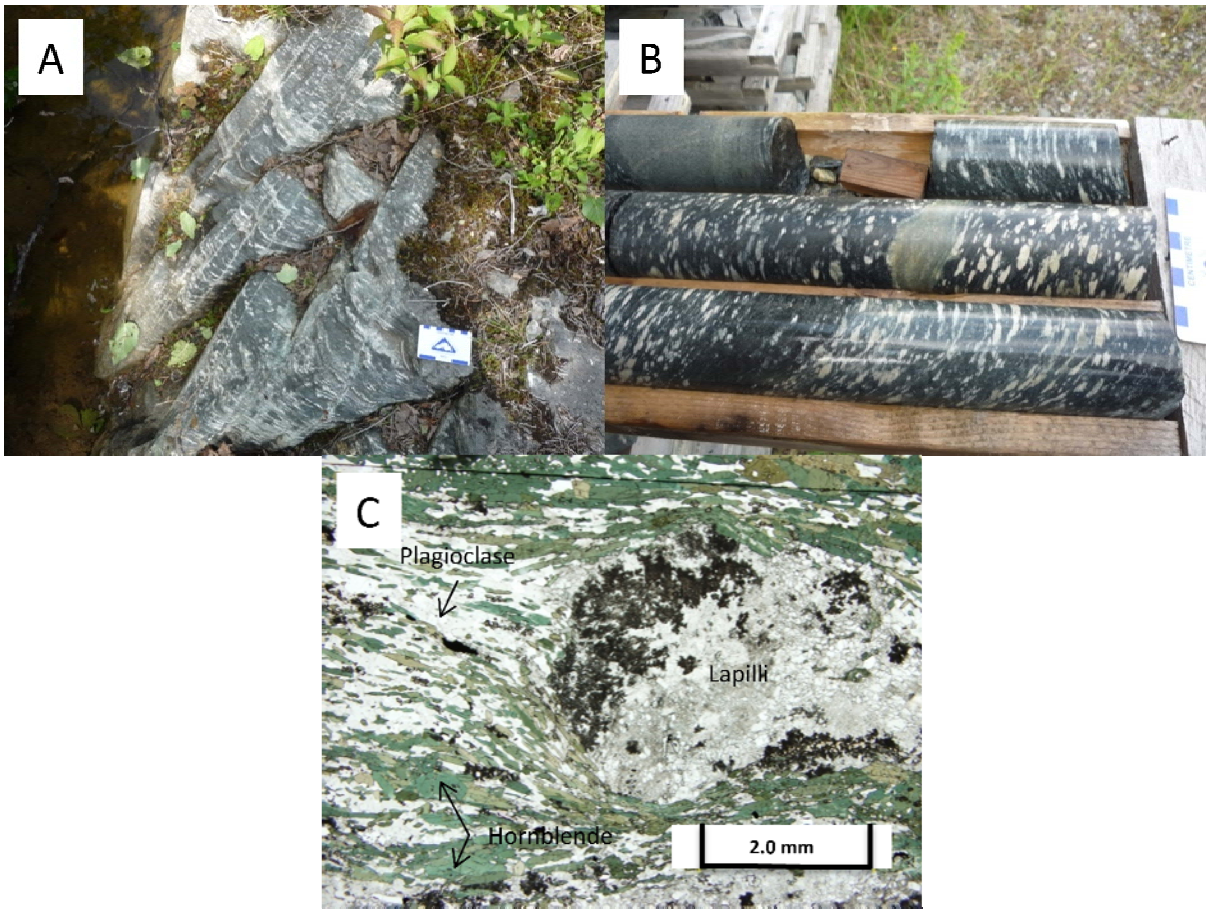

Figure 4.3: Representative photographs of 'the poker chip horizon' A) In outcrop B) In drill core (hole WR01-02, 190m) C) One of the lapilli in thin section (Sample WR06; ppl)

4.2.2 Felsic Metavolcanic Rocks

Felsic metavolcanic rocks of the Gouda-Thor-Carroll area (Fig. 4.4) are comprised of quartz sericite schists (interpreted to be meta-rhyolites based on the presence of primary quartz eyes), sericite schists (located in the same stratigraphic unit as the quartz-sericite schist: the Gouda/Thor Unit), and a metadacite (located at DC Lake; Fig. 4.1). Sericite schists with or without quartz eyes are strongly foliated, with the foliation defined by alignment of sericite, and are composed of fine-grained quartz (40%), K-feldspar (30%), plagioclase (15%), sericite (10%) and medium-grained quartz eyes (5%); the only primary minerals remaining are the quartz eyes (Fig. 4.4C). The metadacite is very fine-grained, massive to weakly foliated and heavily fractured.

A sample of the felsic volcanic unit, the 'Moose Lake quartz porphyry volcanic complex' (Davis and Lin, 2003) from an outcrop located on Highway 17 adjacent to the Hemlo mine was also collected to compare with the Hemlo east felsic volcanic rocks. This sample was collected from the unit named the 'barren sulphide zone' by previous workers as the rock contains sulphide but no gold mineralisation. The sample is a strongly foliated sericite schist composed of fine-grained quartz (40%), plagioclase (30%), K-feldspar (15%), sericite (15%). This unit has metasedimentary rocks stratigraphically underlaying and overlying it (Muir, 2002).

4.2.3 Metasedimentary Rocks

Metasedimentary rocks range from metasandstones, metasiltstones and metawackes to feldspar-quartz±biotite±amphibole paragneiss (Fig. 4.5). The metasedimentary rocks are generally banded, and in strongly metamorphosed rocks the banding defines a gneissosity, however, in weakly to moderately metamorphosed rocks the banding represents relict bedding structures. The mineralogy is extremely variable with equigranular fine-grained quartz (30-60%), plagioclase (20-60%), K-feldspar (<5%), and fine to very fine-grained

hornblende and biotite (<5-20%). In the Gouda-Thor-Carroll area, Metasedimentary rocks are confined to the horizons adjacent to the Gouda and Thor horizons, Duck Lake, and the northern ends of the property shown in Figure 4.1.

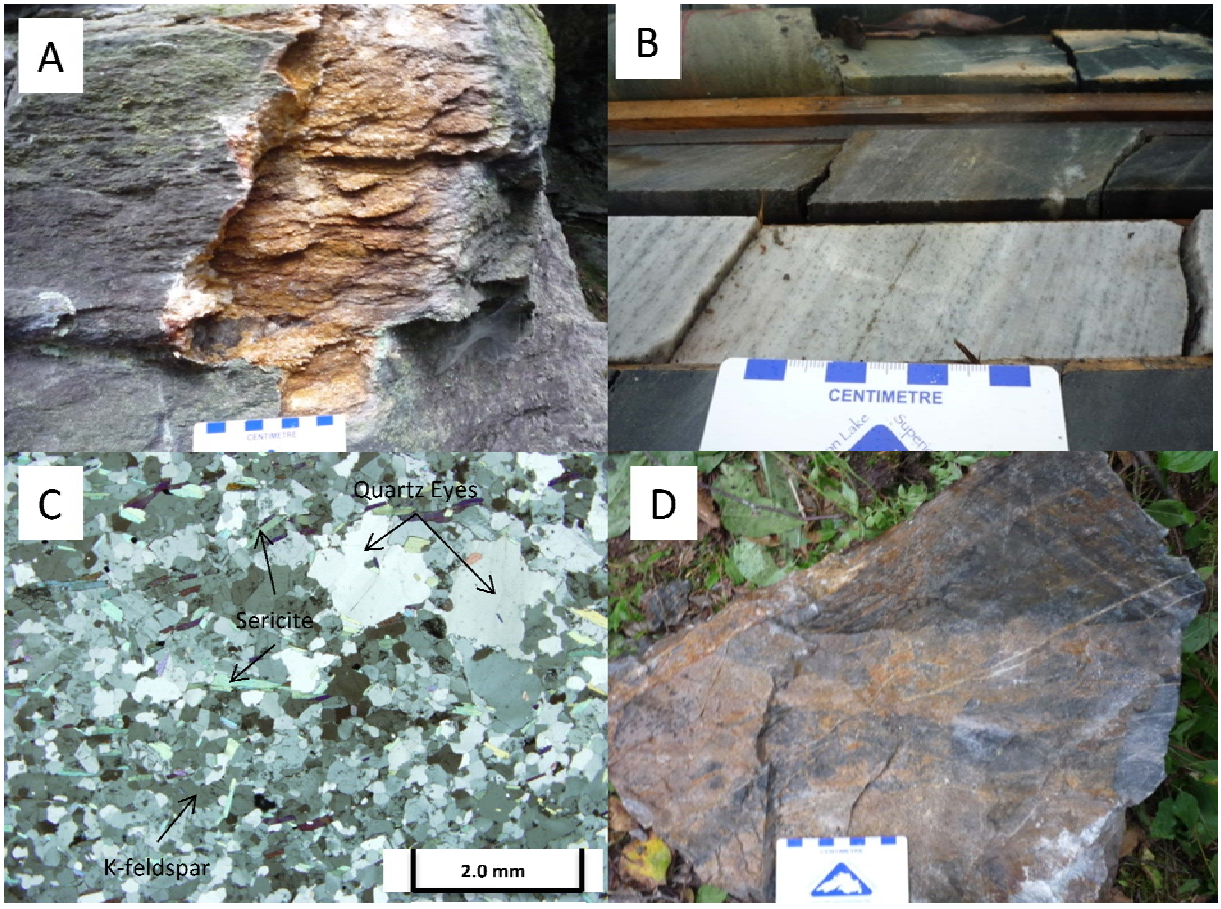

Figure 4.4: Representative photographs of felsic metavolcanic rocks of the Gouda-Thor-Carroll area. A) Quartz-sericite schist in outcrop B) Quartz-sericite schist in drill core (hole WR02-06a; 487m) C) Thin section sample HE026; xp D) DC Lake dacite (Sample HEZ02).

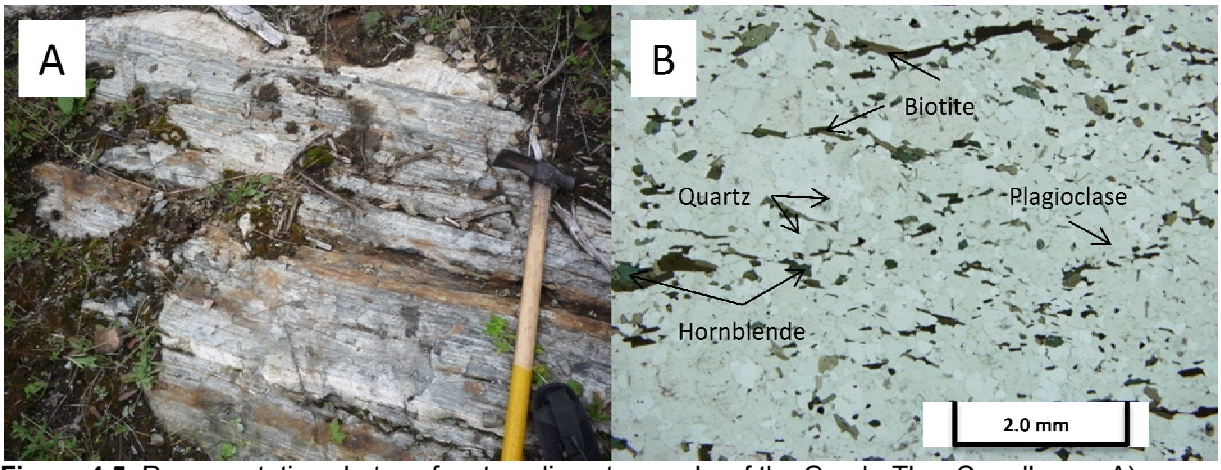

Figure 4.5: Representative photos of metasedimentary rocks of the Gouda-Thor-Carroll area. A) Layered metawacke in outcrop B) Thin section for sample HE021 (ppl).

The felsic metasedimentary rocks of the Frank Lake horizon located to the west of the Gouda-Thor-Carroll area (Fig. 4.1) are silicified feldspathic schists composed of plagioclase (65%), quartz (25%), K-feldspar (9%), and biotite (1%). Medium quartz grains in a fine-grained plagioclase-K-feldspar-biotite matrix have been observed in some samples (Fig. 4.6).

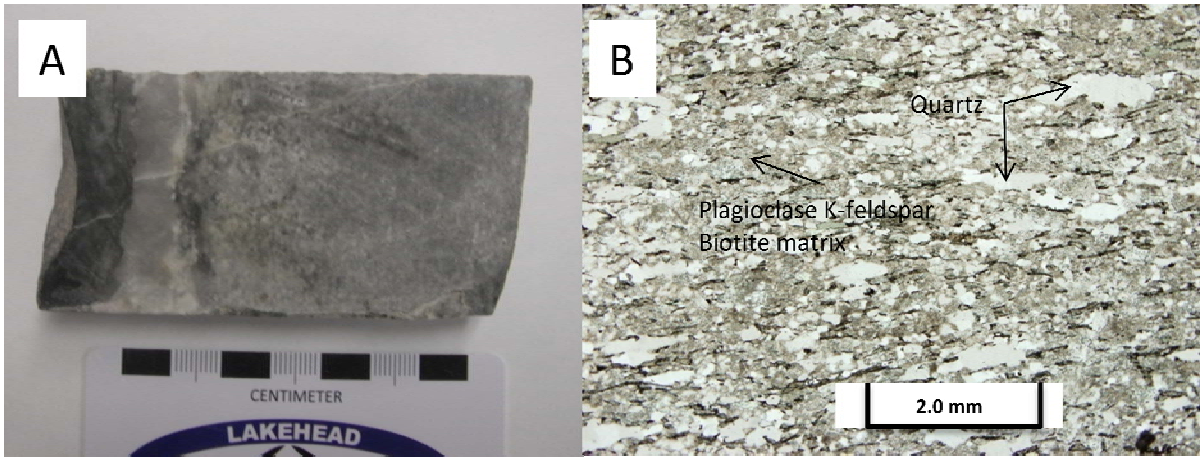

Figure 4.6: Representative photos of metasedimentary rocks of the Frank Lake area. A) Core Sample WR122. B) Thin section sample FRL (ppl, Hole WR-00-08; 155m)

4.2.4 Intrusive and Metaintrusive Rocks

Mafic metaintrusive rocks (metagabbro) are medium-coarse-grained porphyroblastic rocks showing replacement textures of hornblende after pyroxene. They are weakly to moderately foliated and are composed of amphibole after pyroxene (75%), plagioclase (20%), biotite

(5%). These rocks are found as dikes and make up a very small portion of the rocks in the study area (Fig. 4.7).

The Pukaskwa Batholith which forms the southern boundary of the greenstone belt is a medium-coarse-grained hornblende-biotite tonalite/granodiorite (Fig. 4.8). The contact between the Pukaskwa and the southern mafic metavolcanic rocks within the Hemlo East Property imparts a crenulation within the metabasalts in this area, but no other structural information could be determined. Numerous felsic dikes ranging from aplite to quartz-feldspar porphyry to pegmatite are found across the property; the quartz-feldspar porphyry dikes in the vicinity of Duck Lake contain molybdenite mineralisation (Fig. 4.8).

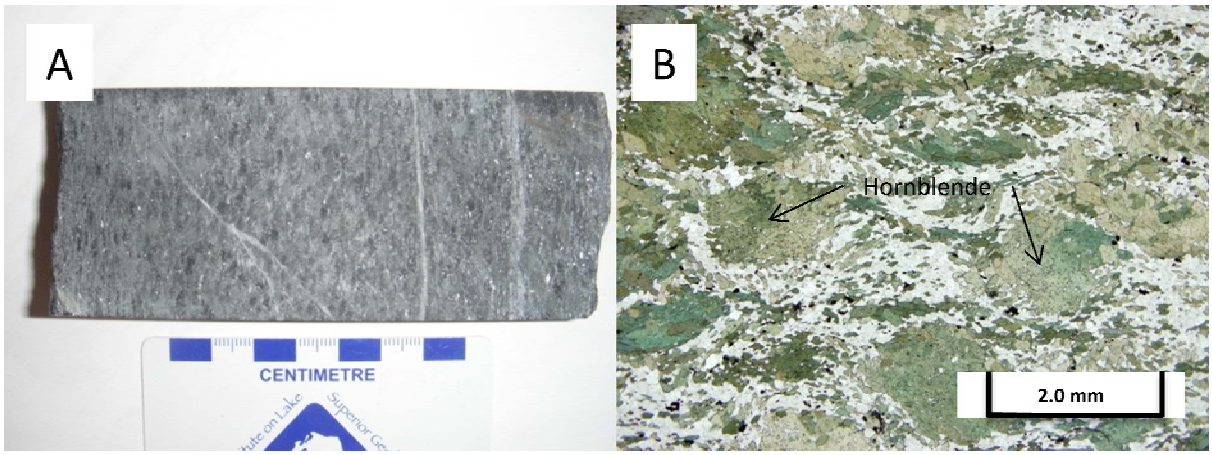

Figure 4.7: Representative photographs of mafic metaintrusive rocks of the Gouda-Thor-Carroll area. A) Core photo [Sample WR-049] of a foliated metagabbro B) Sample HE20 photomicrograph; ppl

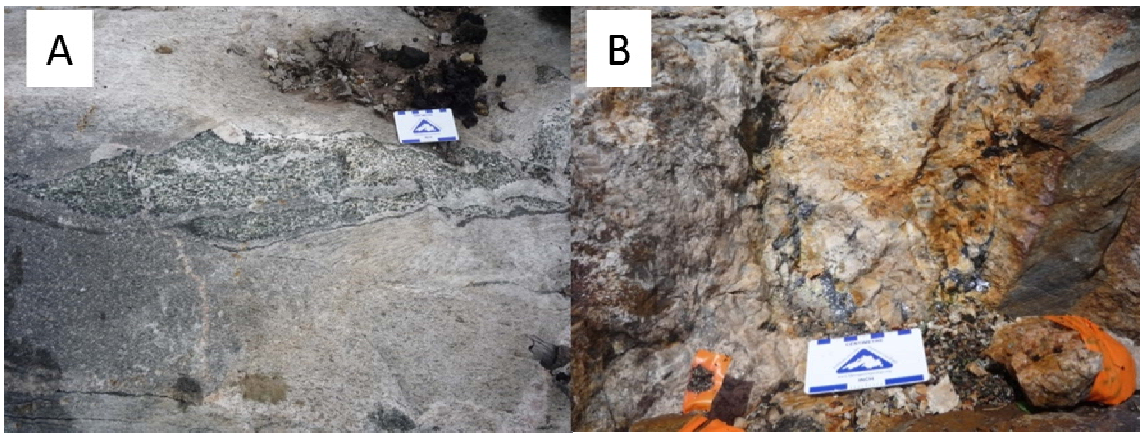

Figure 4.8: Representative photos of intrusive rocks of the Gouda-Thor-Carroll area. A) Pukaskwa Batholith granodiorite with a gabbroic xenolith B) Quartz feldspar porphyry dike with molybdenite

The White River Pluton, located in the northwest corner of the study area (Fig. 4.1), is a medium-coarse-grained monzogranite consisting of ~50% plagioclase, ~25% quartz ~20% K-feldspar and ~5% hornblende/biotite. The Cedar Lake Pluton at the north end of the Hemlo East property (Fig. 3.2) is an equigranular medium-grained granodiorite consisting of ~65% plagioclase, ~25% quartz ~5% K-feldspar and ~5% hornblende ±biotite (Fig. 4.9).

Diabase dykes within the study area are 10 to 30m thick, dark grey, holocrystalline, equigranular, fine to medium-grained, massive and magnetic. They consist of approximately equal proportions of plagioclase and pyroxene ± pyrite/pyrrhotite.

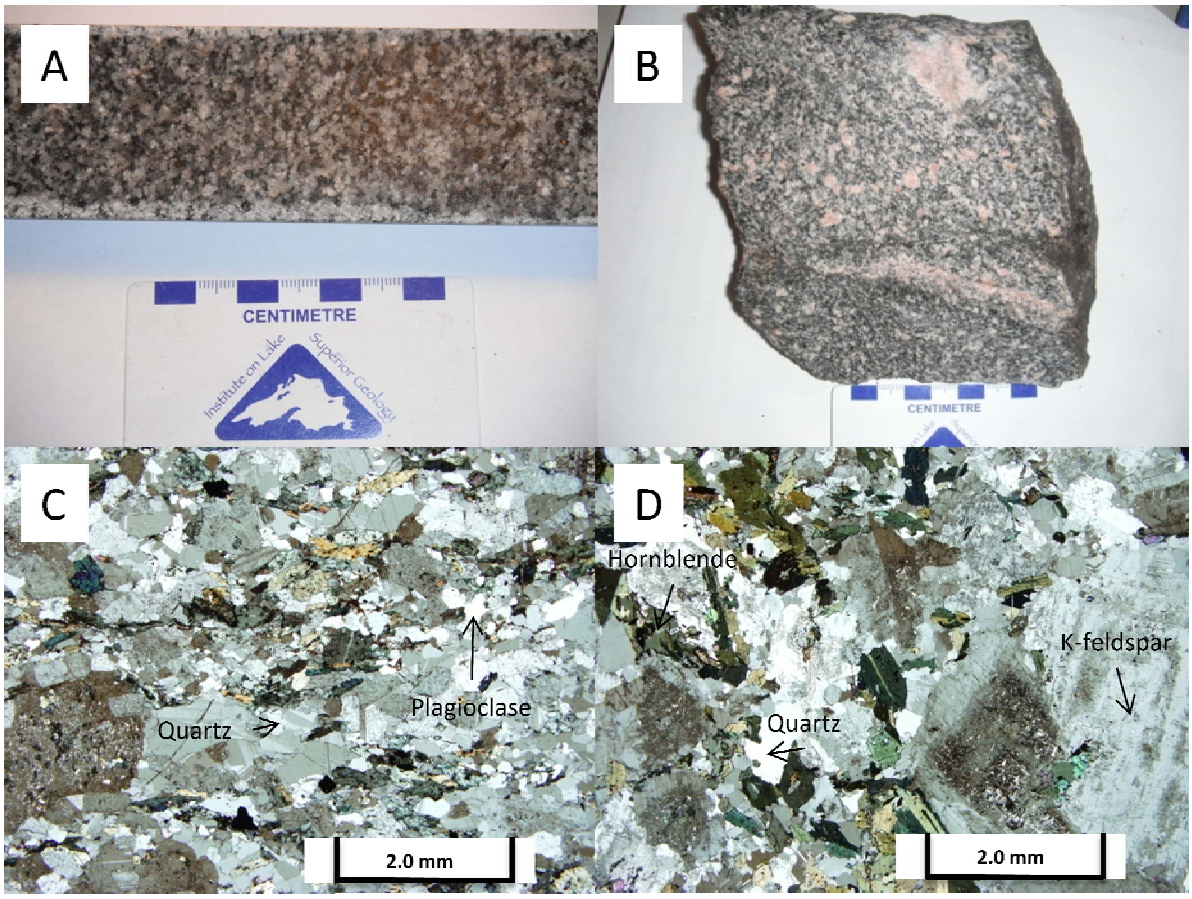

Figure 4.9: Plutons of the Hemlo East Property A) Core Sample of the Cedar Lake Pluton B) Hand Sample of the White River Pluton (Sample WRP) C) White River Pluton (Sample FR25; xp) D) White River Pluton (Sample FR26; xp).

4.2.5 Mineralisation

One sample of massive sulphides was collected from a trench on the western shore of Thor Lake which consisted of euhedral pyrite (92%) rimmed by minor anhedral sphalerite (5%) and trace galena (5%) and chalcopyrite (<1%; Fig. 4.10) and is hosted within a quartz eye sericite schist (Thor horizon). This was the only sample containing mineralisation from the Gouda/Thor horizons seen in this study but is consistent with previous worker's findings who state that gold mineralization is associated with zinc, lead, silver, mercury and molybdenum and is hosted within a well developed quartz-eye sericite schist (Thompson and Paakki, 2001).

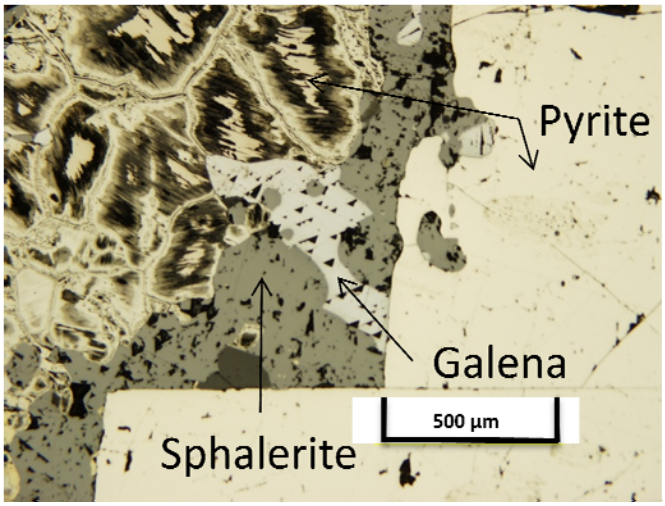

Figure 4.10: Polished thin section of massive sulphides from the Thor trench (reflected light).

The DC Lake horizon, which overlies the Gouda and Thor horizons to the north, contains galena along fracture surfaces and minor disseminated pyrite within a metadacite. This horizon was found to contain up to 0.80% Zn over 29 metres in 1968 (Thompson and Paakki, 2001).

4.3 Sodium Cobaltinitirite Staining Results

All samples collected in the 2009 field season were stained with sodium cobaltinitrite in order to quantify potassic alteration. Intensity of staining is quantified as 0 (none) to 4 (Intense), and is presented with sample descriptions and geochemistry in Appendix C. A yellow stain on rocks indicates the presence of K-feldspar which may or may not be the product of alteration. Examples of the staining are shown in Figure 4.11. Determining whether potassic alteration exists within the Hemlo East Property is important because it also occurs within the Hemlo deposit (Muir, 2002).

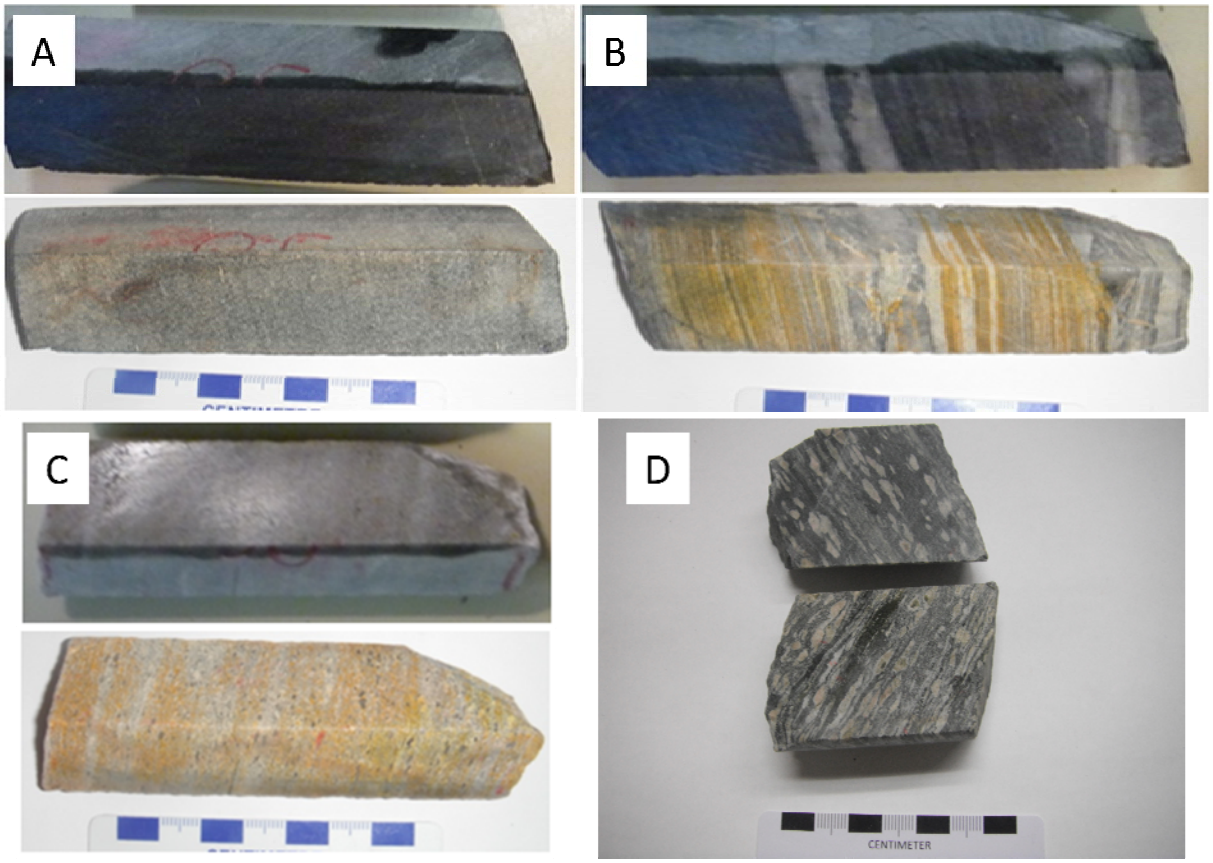

Figure 4.11: Before and after photos of stained rock samples. A) Mafic metavolcanic (Sample WR111) B) Metasedimentary (Sample WR121) C) Metarhyolite (Sample WR107) D) Mafic lapilli tuff (Sample WR065)

4.4 Discussion

Lithologies within the Gouda-Thor-Carroll area are divided into mafic metavolcanic rocks, felsic metavolcanic rocks, metasedimentary rocks, intrusive and metaintrusive rocks. The stratigraphic continuity is demonstrated by the large number of drill holes in the area. All stratigraphic units dip to the north at 35-50°. The DC Lake Fault is dextral based on the stratigraphy of the area.

Figure 4.12 shows a drill core sample of metawacke (drill hole WR02-01, 278.5m) which has been interpreted to give a way-up direction for the stratigraphy. Provided that the layering in this sample represents primary sedimentary structures, this is an example of crossbedding which has been overturned (the truncation surface displays a crosscutting

relationship with the overlying beds). This suggests that the stratigraphy in the Gouda area may be upside-down. However, this was only observed in one location, and evidence presented in Section 5.6.4 shows that the geochronology supports the stratigraphy in this area being right way up. A possible explanation for this core could be reverse-graded bedding.

Figure 4.12: Core sample (Drill hole WR02-01, 278.5m) of metawacke with possible overturned cross bedding.

Sample staining results are summarized in Table 4.1 with an outline of the intensities and whether the K-feldspar detected (if any) is interpreted to be primary or secondary. Samples were interpreted to contain primary K-feldspar if only individual grains or primary crystals responded to the stain; and interpreted to contain secondary K-feldspar if the response to the stain was pervasive, indicating an overprint of K-feldspar throughout the sample. Mafic metavolcanic rocks in general did not respond to the staining method with the exception of some minor (1-2) staining on six samples collected from the vicinity of the Gouda shear zone. The lapilli in the mafic lapilli tuff also did not stain, indicating that they are

composed primarily of plagioclase ± quartz. Eight metasedimentary rocks contained K-feldspar grains which did stain; two metasedimentary rock samples proximal to the Gouda unit showed a pervasive response to the staining method. Four samples from the Frank Lake felsic metasedimentary horizon also responded to the staining.

Table 4.1: Table showing the number of samples stained for each lithology and how each lithology reacted to the staining method proportionally.

Lithology	# of Samples Responded/Stained	Primary Intensity				Secondary Intensity			
		1	2	3	4	1	2	3	4
Mafic Metavolcanic	6/96					4	2		
Felsic Metavolcanic	33/46					6	2	16	9
Metasedimentary	8/21	3	2	1			1	1	
Frank Lake Felsic Horizon	4/6					2		2	

Felsic metavolcanic rocks in the vicinity of the Gouda and Thor areas, as well as the rocks from the DC lake area (i.e. areas of known mineralization) all responded to the staining method (Fig. 4.11), whereas felsic metavolcanic samples from drillholes into the Gouda/Thor horizon to the west ~2.5km across the White River (where there is no evidence of mineralization) did not respond. This suggests that the response to staining (presence of K-feldspar) on the felsic metavolcanic rocks in the Gouda/Thor area is due to alteration because samples 2.5km west within the same stratigraphic unit did not respond to the staining method (are not altered). If the presence of K-feldspar in this unit were primary, all rocks within the unit would have responded to the staining method. All of the units with potassic alteration within the Gouda-Thor-Carroll area are in proximity to the DC Lake fault (Thor/Gouda unit, DC Lake unit; Fig. 4.1). These samples are all also within 1km of areas with reported mineralisation (Thor trench, Gouda prospect, and DC Lake prospect; Thompson and Paakki, 2001). Potassic alteration has also been reported in the Egg Lake and Yellow birch zones of the Hemlo East property by Wells (1996). All of the potassic alteration encountered is within shear zones. It is unclear whether the source of the alteration is due to regional metamorphism or hydrothermal alteration.

Chapter 5

Geochemistry and Geochronology

This chapter examines the major and trace element geochemistry of the metavolcanic and metasedimentary rocks of the Gouda-Thor-Carrol area. This data has been used to classify the rocks and evaluate the genesis and tectonic environment in which the rocks formed. A total of 185 were samples collected by the author from the study area. Analytical procedures are described in Chapter 1. All data used in this chapter are provided in Appendix C. Samples are grouped according to the petrographic scheme outlined in Chapter 4.

5.1 Whole-rock Geochemistry

5.1.1 Major and Trace Element Geochemistry

Trace elements are sensitive to igneous processes not recorded by major element variations (Albarède, 2003), and are thus better suited to igneous rock classifications and determining tectonic setting and as demonstrated in the previous section are generally immobile in the Gouda-Thor-Carroll area.

Using the volcanic rock classification scheme of Winchester and Floyd (1977), the samples show a bimodal distribution with all rocks defined as mafic metavolcanic rocks in Chapter 4 plotting within the andesite/basalt field and felsic metavolcanic rocks plotting across the rhyodacite/dacite, trachyandesite and trachyte fields (Fig. 5.1).

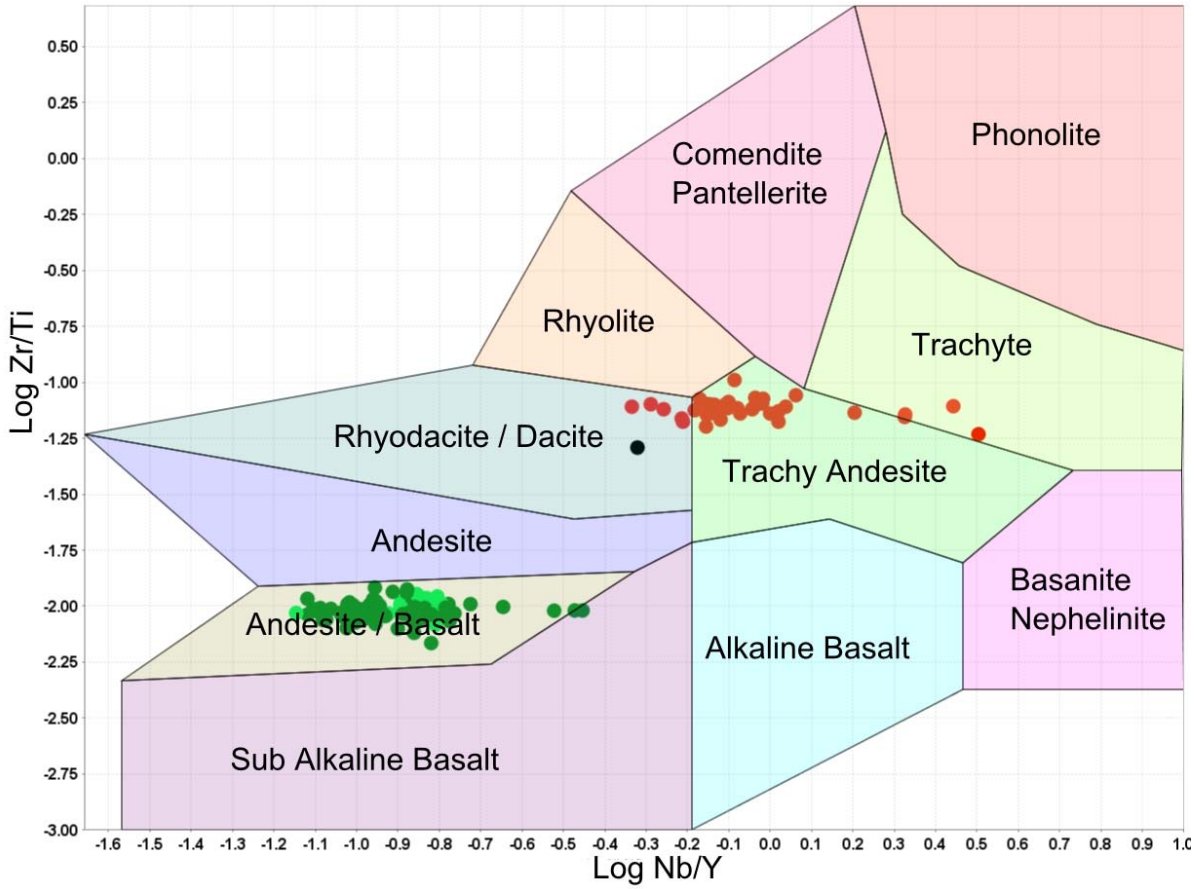

Figure 5.1: Volcanic rocks classification scheme after Winchester and Floyd (1977). Red: Felsic metavolcanic rocks. Dark green: metabasalts. Light Green: Mafic lapilli tuffs. Black: Sericite schist from Highway 17 near Hemlo.

Metabasalts range in SiO_2 and MgO contents from 45 to 53 and 3 to 9 wt.% respectively. Cr and Ni contents range from 20 to 360 and 23 to 256 ppm respectively over a range of Mg# from 22 to 48. Nb/Nb* values range from 0.13 to 0.66 with two outliers at 1.14 and 1.15 (Appendix C). All metabasalts plot in the tholeiiitic field of Miyashiro (1974; Fig. 5.2). Metabasalts exhibit negative Nb anomalies and do not exhibit Ti anomalies (Fig. 5.3). La/Sm_n ratios are 0.8-2.0 and Gd/Yb_n ratios are 0.9-1.3. In general, metabasalts do not exhibit Eu anomalies except for a few outliers. Two outlying samples (WR018 which occurs in the middle of the southernmost metabasalt unit, and WR022 which occurs at the top of the second metabasalt unit in the south) have MgO of 9.4, 11.7 wt%; Mg# of 0.43, 0.46; Ni of

468, 521 ppm; and Cr of 1400, 1340 ppm respectively and overall have more mafic compositions than the rest of the basalts.

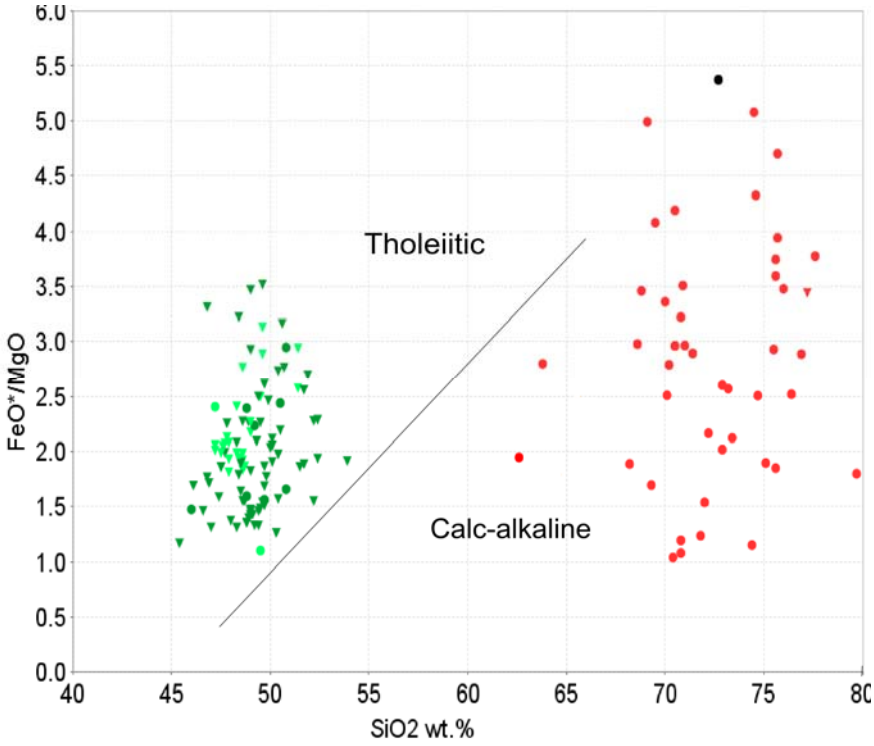

Figure 5.2: Discrimination diagram for tholeiitic vs. calc-alkaline magma series. Fields from Miyashiro (1974). Red: Felsic metavolcanic rocks. Dark green: metabasalts. Light Green: Mafic lapilli tuffs. Black: Sericite schist from Highway 17 near Hemlo.

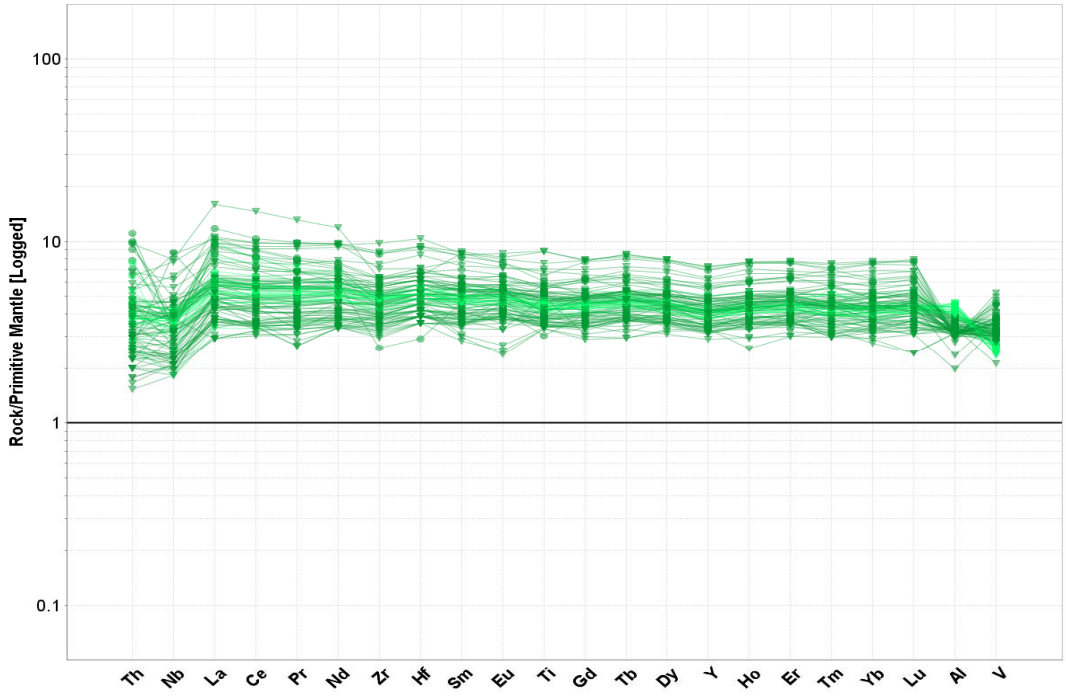

Figure 5.3: Primitive mantle normalised plot for metabasalt samples from the Gouda-Thor-Carroll Area. Dark green: metabasalts. Light Green: Mafic lapilli tuffs (normalising values from Sun and McDonough, 1989).

Felsic metavolcanic rocks range in SiO_2 contents from 64 to 80 wt.% and plot in the calc-alkaline field of Miyashiro (1974; Fig. 5.4). Nb/Nb* values range from 0.02 to 0.25 with one outlier at 0.65. Felsic metavolcanic rocks exhibit negative Nb, Eu, and Ti anomalies and are characterized by LREE enrichment as well as weakly fractionated to fractionated HREE (Fig. 5.4). La/Sm_n ratios are 3.1-6.4 and Gd/Yb_n ratios are 2.0-7.5. One sample collected from Highway 17 near Hemlo from the unit known as ‘the barren sulphide zone’ within the Moose Lake porphyry volcanic complex shares the same geochemical characteristics as the Hemlo East felsic metavolcanic rocks.

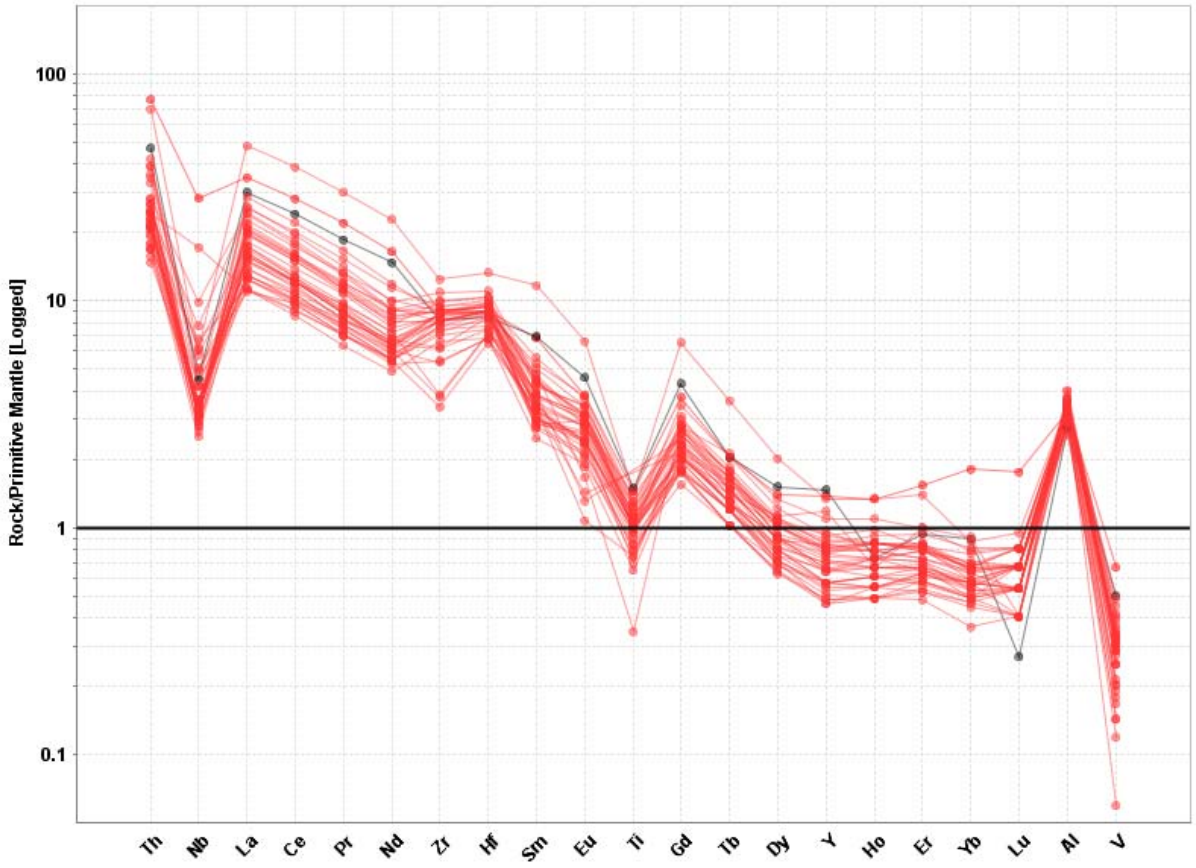

Figure 5.4: Primitive mantle normalised plot for felsic metavolcanic samples from the Gouda-Thor-Carroll Area (normalising values from Sun and McDonough, 1989). Black: Sericite schist from highway 17 near Hemlo.

Metasedimentary rocks of the Gouda-Thor-Carroll and Frank Lake areas share similarities with felsic metavolcanic rocks (Fig. 5.5). Metasedimentary rocks exhibit negative Nb, Eu, and Ti anomalies and are characterized by LREE enrichment as well as HREE depletion. Several samples share the extreme HREE fractionation seen in felsic metavolcanic rocks. The similarities between the metasedimentary rocks and the felsic metavolcanic rocks suggests that the metasedimentary rocks may have been derived from a felsic source.

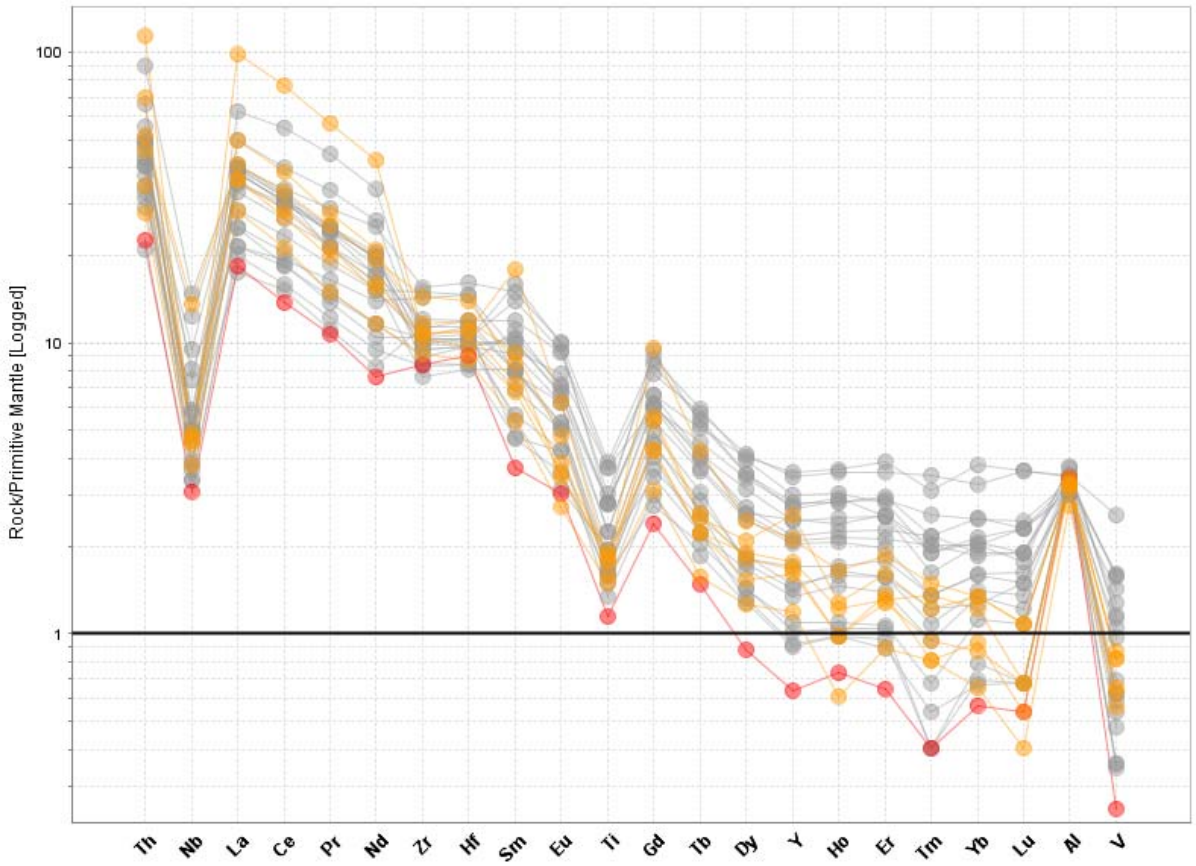

Figure 5.5: Primitive mantle normalised plot for metasedimentary rock samples from the Gouda-Thor-Carroll Area (normalising values from Sun and McDonough, 1989). Grey: Gouda area metasedimentary rocks. Orange: Frank Lake area metasedimentary rocks. Red: Felsic metavolcanic for comparison.

The two samples collected from the White River Pluton have SiO_2 contents of 61 and 62 wt.%, Nb/Nb* values are 0.05 and 0.06. White River Pluton Samples exhibit negative Ti anomalies and are characterized by LREE enrichment and flat HREE with La/Sm_n ratios of 3.2-3.7 and Gd/Yb_n ratios of 2.0-2.1 (Fig. 5.6).

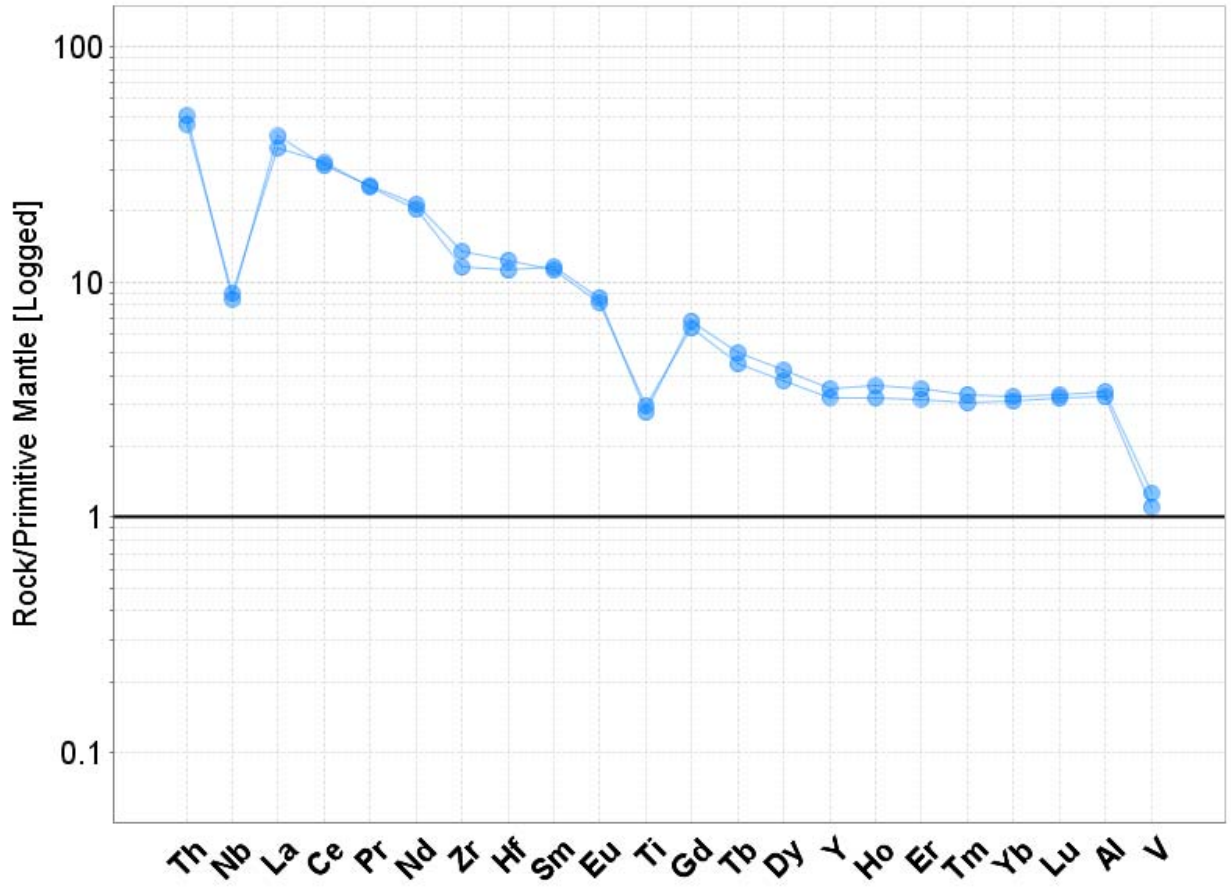

Figure 5.6: Primitive mantle normalised plot for samples from the White River Pluton (normalising values from Sun and McDonough, 1989).

5.1.2 Element Mobility

To determine whether elements are mobile, a given element can be plotted against an element known to be generally immmobile, such as Zr, Nb, or TiO_2 (Jenner, 1996). A linear trend (co-variance) of a comagmatic suite of samples suggests immobility of both elements. Lower- to mid-amphibolite facies metamorphism throughout the Schreiber-Hemlo Greenstone Belt could have resulted in the mobility of elements even in least altered samples. To test this, variation diagrams for rocks of the Gouda-Thor-Carrol area are shown in Figures 5.7 and 5.8.

The scatter of data for all samples suggests that Na_2O, and K_2O are mobile for all metavolcanic and metasedimentary rocks (Fig. 5.7). In contrast SiO_2, MgO, Fe_2O_3, TiO_2, Zr, Th, and Y display well defined trends on Figures 5.7 and 5.8 and are interpreted to be effectively immobile. Because of the evidence for mobility, geochemical classifications that utilise the elements Na_2O or K_2O will not be used for the rocks of the Gouda-Thor-Carrol area. The different rocks types form distinct trends on Figures 5.7 and 5.8 which implies that each rock type shares a common source and has undergone similar geologic processes within each rock type (multiple trends within a rock type would denote multiple sources). Outliers on these plots within the felsic volcanic and metasedimentary units are located near the Gouda shear zone and can be explained via alteration or the variable amounts of metasomatism in the vicinity of the shear zone. Thompson (2006) showed that there is evidence for increased metamorphic grade in the vicinity of shear zones within the Hemlo area. Most trace elements, Y and the rare earth elements in particular, are effectively insoluble in aqueous solutions (Albarède, 2003) and immobile up to lower amphibolite facies metamorphism (Pearce, 2007) and have been shown to be immobile for samples in this study.

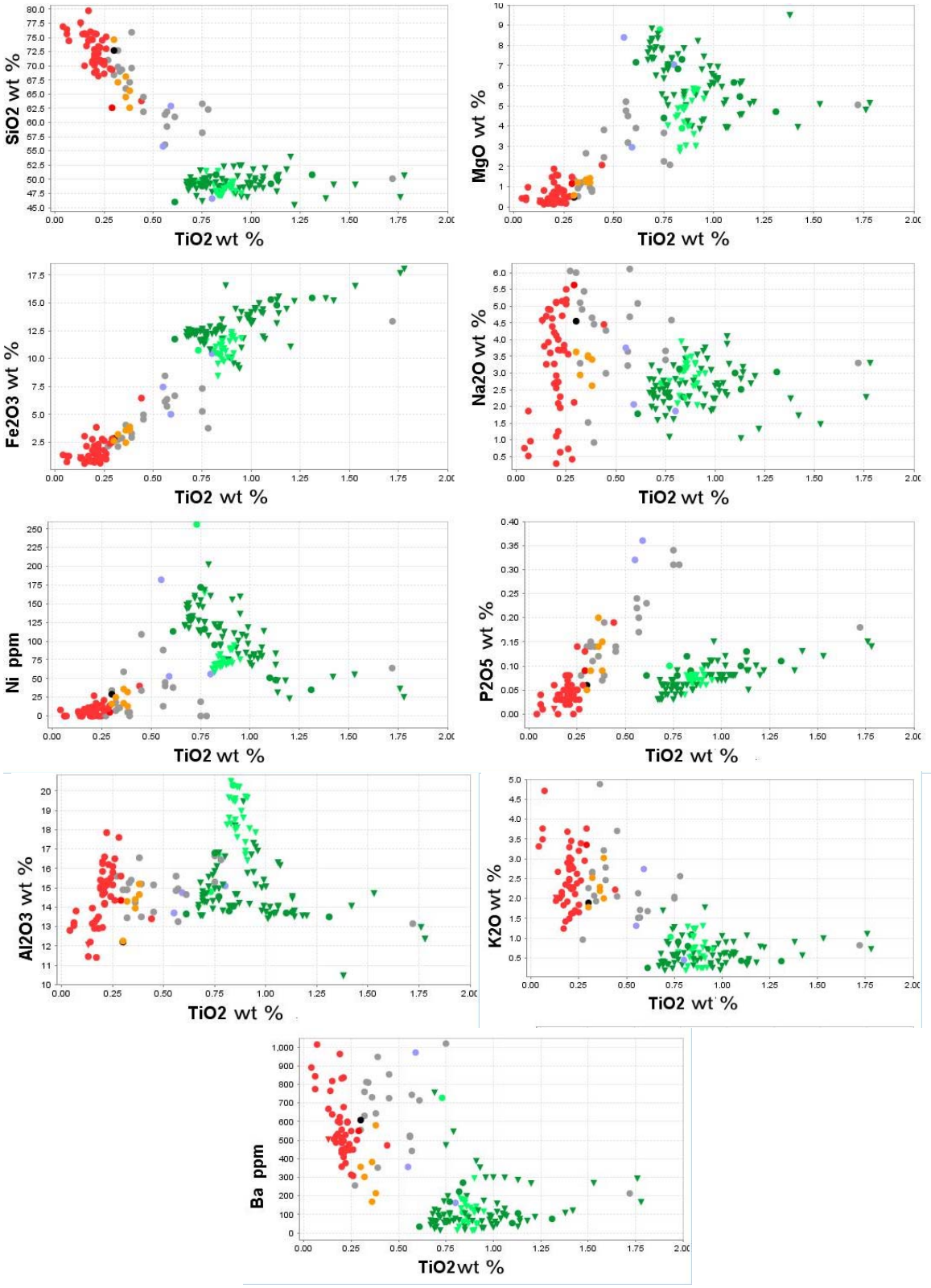

Figure 5.7: Variation diagrams of major element oxides vs. TiO_2. Red: Felsic metavolcanic rocks. Dark green: metabasalts. Light Green: Mafic lapilli tuffs. Orange: Frank Lake area metasedimentary rocks. Grey: Gouda area metasedimentary rocks. Black: Sericite schist from Highway 17 near Hemlo.

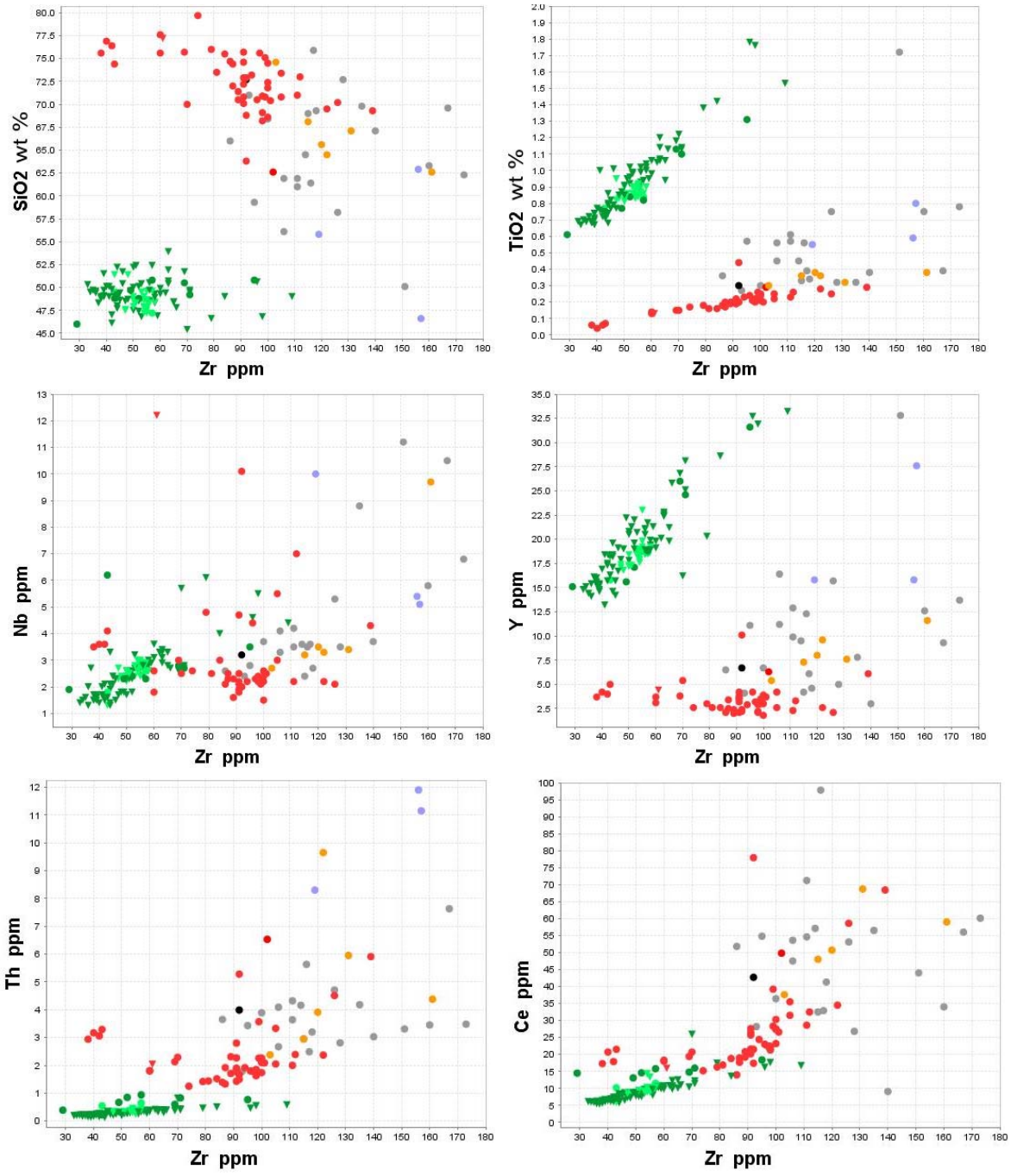

Figure 5.8: Variation diagrams of major element oxides (in wt. %) and trace elements (in ppm) with Nb. Red: Felsic metavolcanic rocks. Dark green: metabasalts. Light Green: Mafic lapilli tuffs. Orange: Frank Lake area metasedimentary rocks. Grey: Gouda area Metasedimentary rocks. Black: Sericite schist from Highway 17 near Hemlo.

5.3 Geochronology

Eight samples from the Hemlo East Property were selected for U-Pb age dating. These samples were selected to better understand the volcanic and plutonic stratigraphy in relation to both the greenstone belt, and the host rocks of the adjacent Hemlo gold deposit. Samples were limited to felsic metavolcanic, felsic volcanic-derived metasedimentary and felsic intrusive rocks to ensure the presence of primary zircons.

Three felsic metavolcanic rocks were collected from the Gouda-Thor-Carrol area of the Hemlo East property (Gouda Lake, Thor Lake, DC Lake) to investigate the relationship between these units and to determine if they could be correlated across the DC Lake Fault (Fig. 4.1). One felsic volcanic-derived metasedimentary sample from the Frank Lake area was collected to determine if it was the western extension of the Gouda-Thor stratigraphic unit. Felsic metasedimentary rocks from the Upper Anomalous Zone were collected to investigate if they were the western extension of the Moose Lake Porphyry unit at Hemlo. A sample of the Moose Lake Porphyry at Hemlo was provided by Rob Reukl, Barrick Gold Corp. Two samples from granite plutons within the Hemlo East property were also collected (Cedar Lake Pluton and White River Pluton) to compare with other intrusive rocks in the area. Sample locations are shown in Figure 5.9 and all results are presented in Table 5.1. U-Pb data is presented in Appendix D.

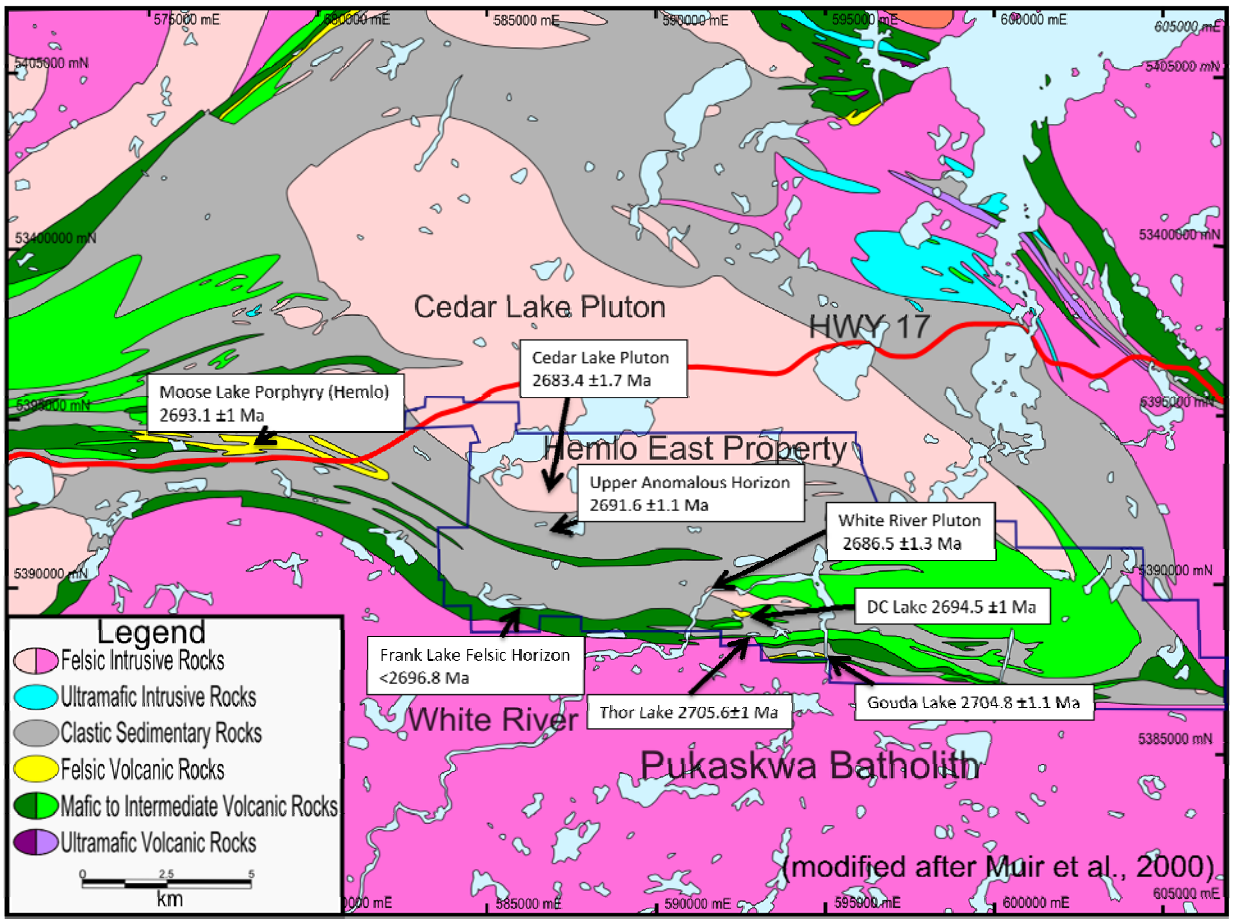

Figure 5.9: U-Pb geochronology sample location map (modified after Muir, 2000).

Table 5.1: Age and location of samples dated in this study.

Sample	Location (unit)	Rock Type	UTM_E	UTM_N	Age (Ma)	Error (Ma)
FRL	Frank Lake Felsic Horizon	Metasedimentary	587700	5389490	<2690	
HEZ01	Gouda Lake	Volcanic	593540	5387887	2704.8	1.1
HEZ03	Thor Lake	Volcanic	592629	5388535	2705.6	1
HEZ02	DC Lake	Volcanic	592553	5388990	2694.5	1
UAZ	Upper Anomalous Zone	Volcaniclastic	586774	5391632	2691.6	1.1
MooseLake ET	Moose Lake Porphyry (Hemlo)	Volcanic	579370	5394609	2693.1	1
CLP	Cedar Lake Pluton	Intrusive	586563	5398027	2683.4	1.7
WRS	White River Stock	Intrusive	591505	5389744	2686.5	1.3

From the eight samples, four distinct age associations are evident (Table 5.1). The sample from the Frank Lake Felsic Horizon located at the southwest of the Hemlo East Property is a metasedimentary rock described in Chapter 4. Zircons recovered from the Frank Lake sample are brown and range from prismatic crystals to rounded, broken grains and measure ~100µm (Fig. 5.10A) The sample returned a range of dates with the majority clustered around 2720 Ma, but because the sample is metasedimentary, it can only be interpreted as being younger then the youngest age returned which is approximately 2690 Ma (Fig. 5.11A).

Figure 5.10: Photomicrographs of picked zircon grains prior to treatment. A) Sample FRL from the Frank Lake Felsic Horizon. B) Sample UAZ from the Upper Anomalous Zone.

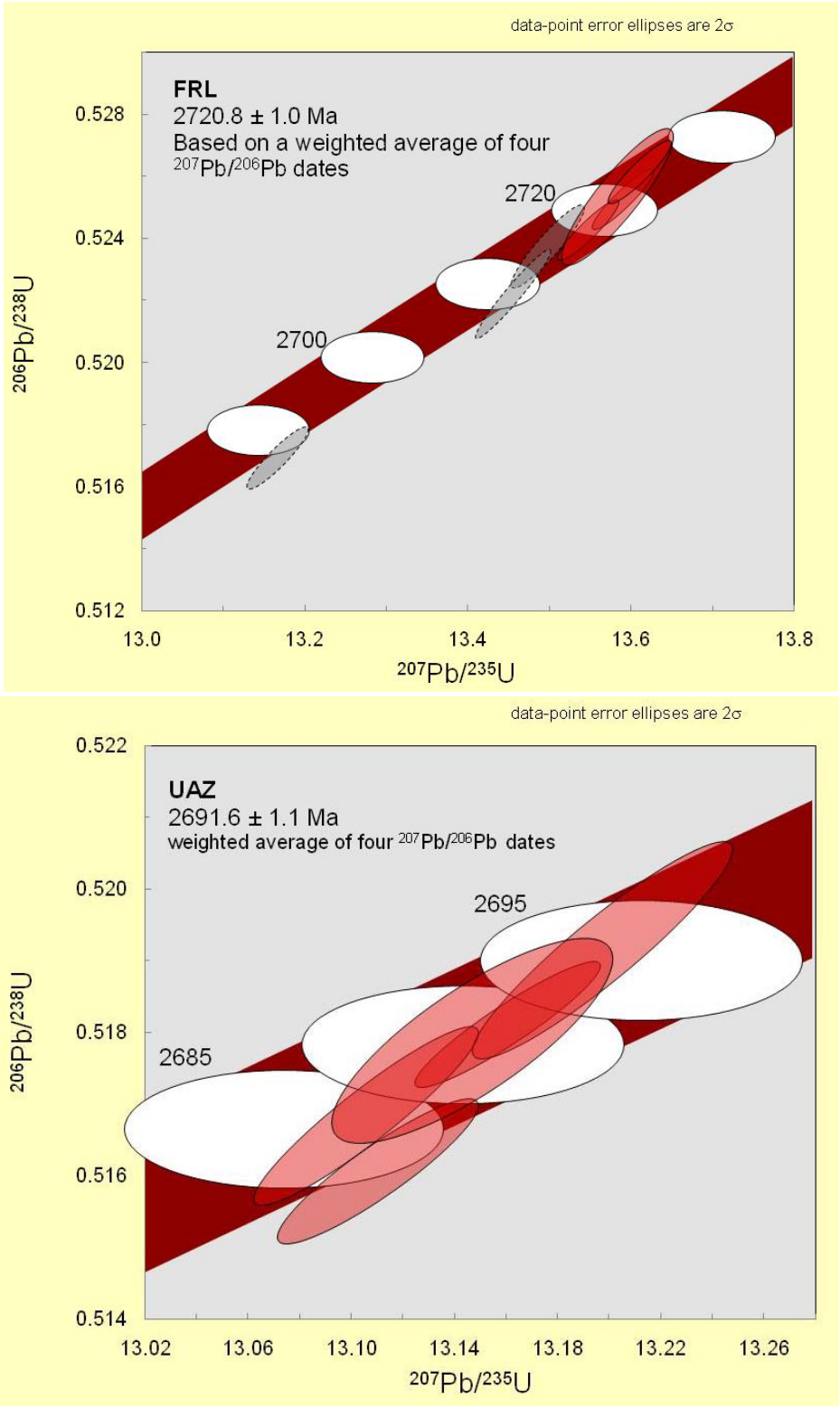

Figure 5.11: Concordia plot for metasedimentary-volcaniclastic samples. A) Sample FRL from the Frank Lake Felsic Horizon. B) Sample UAZ from the Upper Anomalous Zone

Zircons recovered from the Upper Anomalous Zone sample are clear to orange and are prismatic crystals, sometimes fractured and measure ~200µm (Fig. 5.10B). The sample from the Upper Anomalous zone was composed of an unconsolidated, variably silicified schist which is interpreted to be volcaniclastic in origin (this interpretation relies on the observations from core logs of previous workers due to the unconsolidated nature of the outcrop sampled by the author). This unit is interpreted to be the stratigraphic equivalent of the 'Moose Lake quartz porphyry volcanic complex' (a coeval felsic extrusive/intrusive volcanic–subvolcanic interpretation for this unit was presented by Muir, 2002) unit at Hemlo and the date determined (2691.6 ±1.1 Ma) agrees within error to the age of the MLP (Fig. 5.11B).

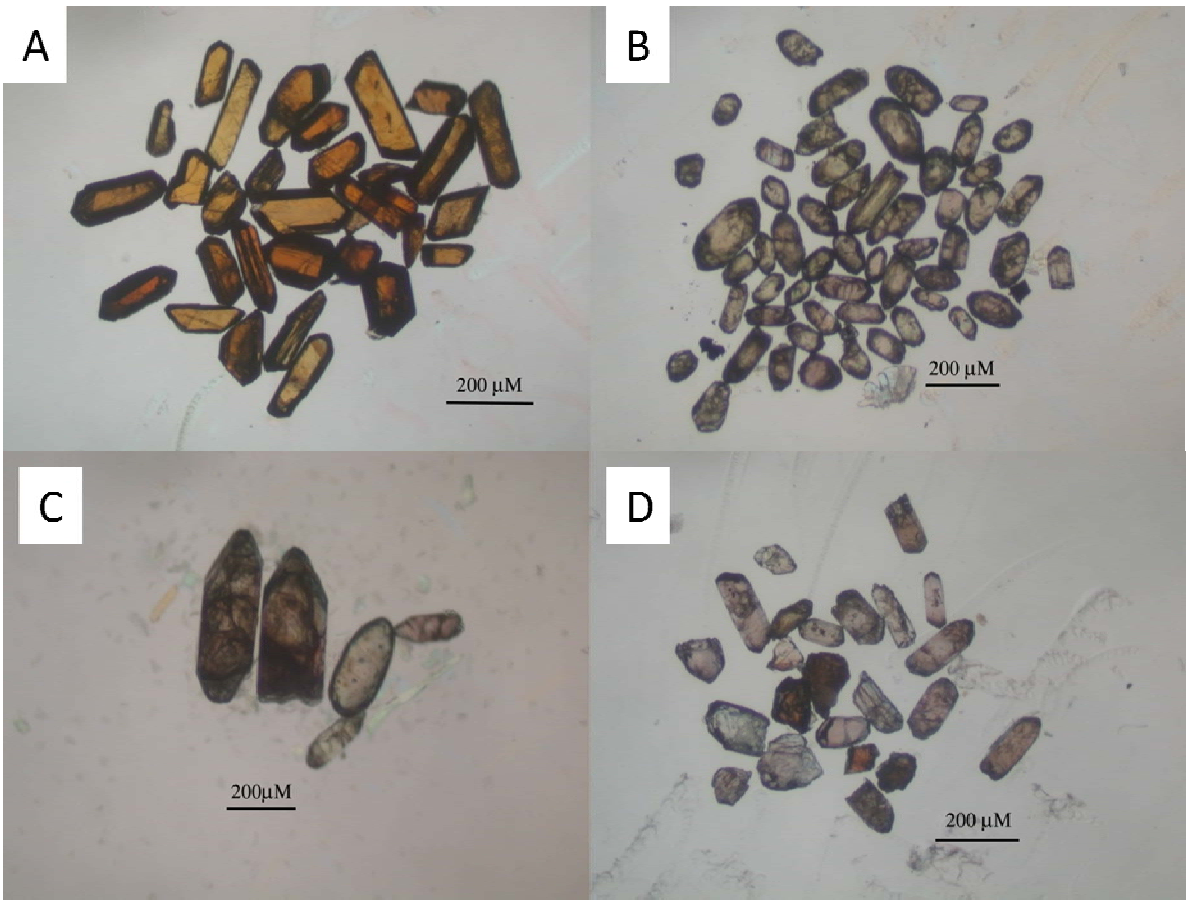

Figure 5.12: Photomicrographs of picked zircon grains prior to treatment. A) Sample HEZ01 from the Gouda Horizon. B) Sample HEZ02 from the DC Lake Unit. C) Sample HEZ03 from the Thor Horizon. D) Moose Lake Porphyry Sample from Hemlo.

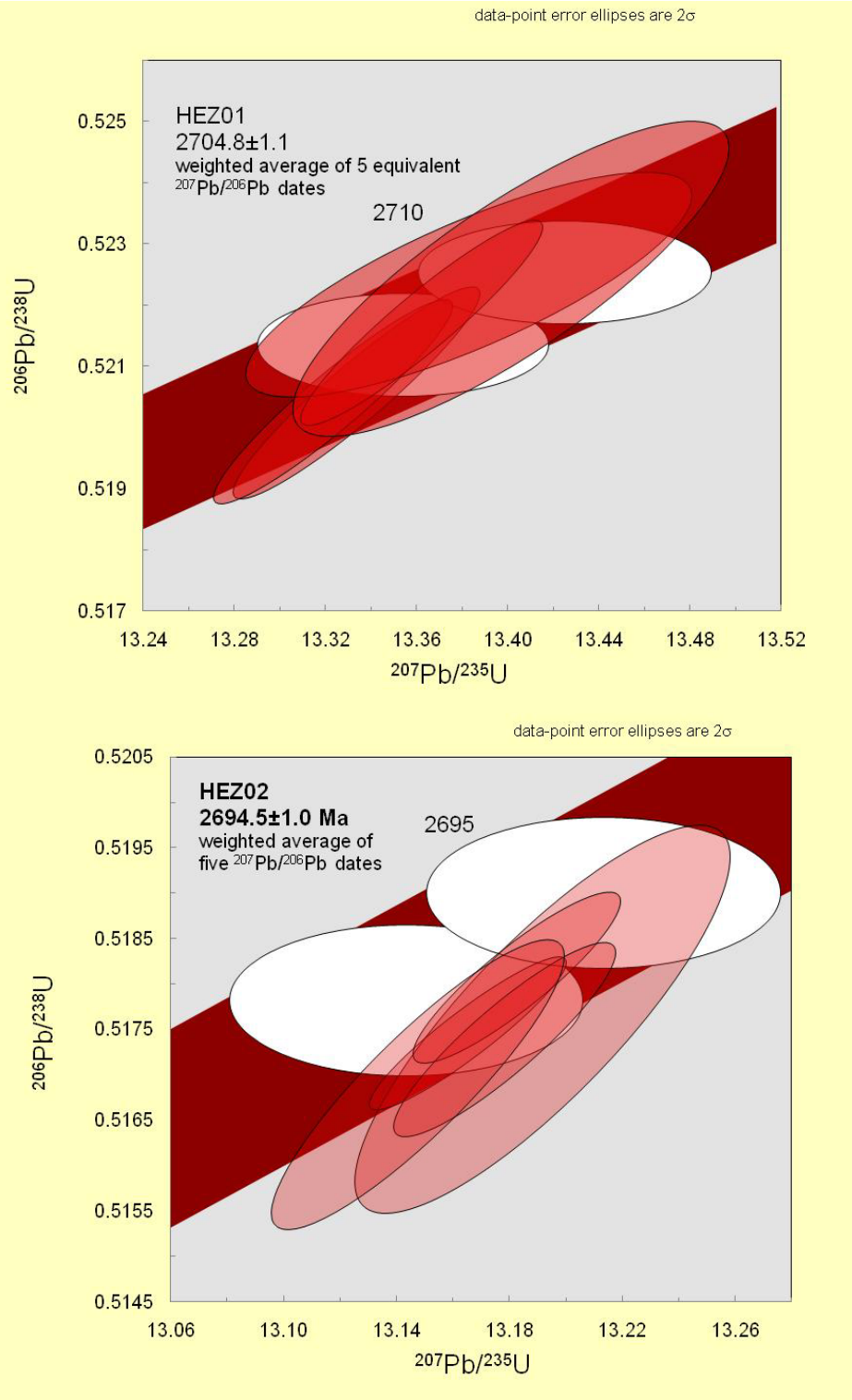

Figure 5.13: Concordia plot for felsic metavolcanic samples. A) Sample HEZ01 from the Gouda Horizon. B) Sample HEZ02 from the DC Lake Unit.

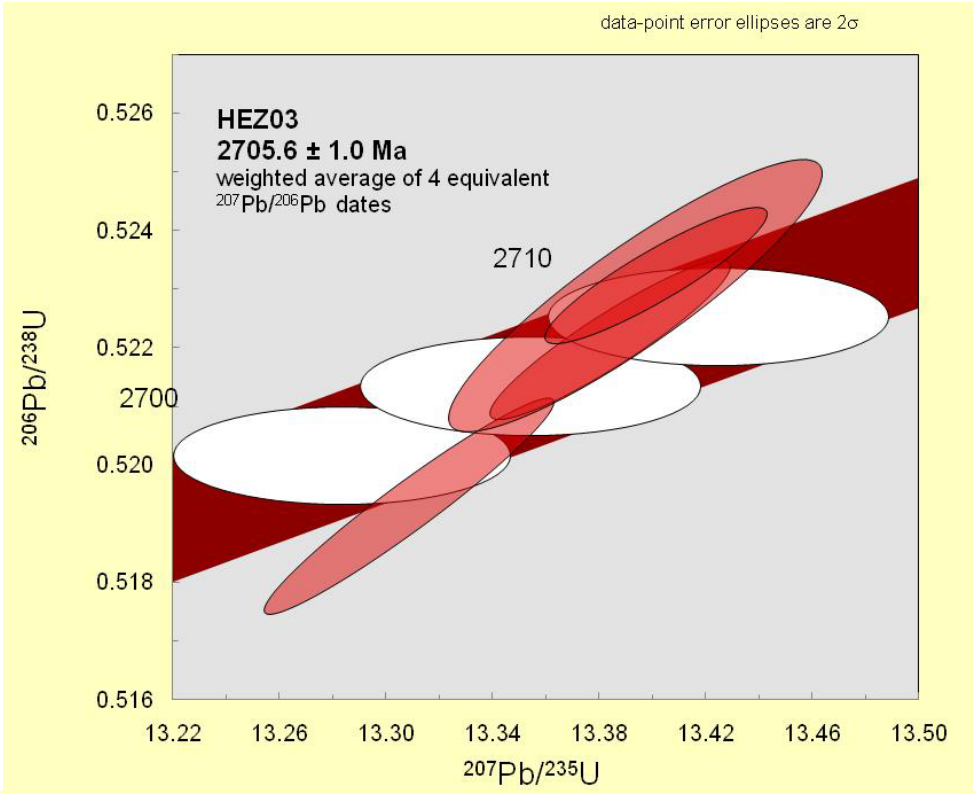

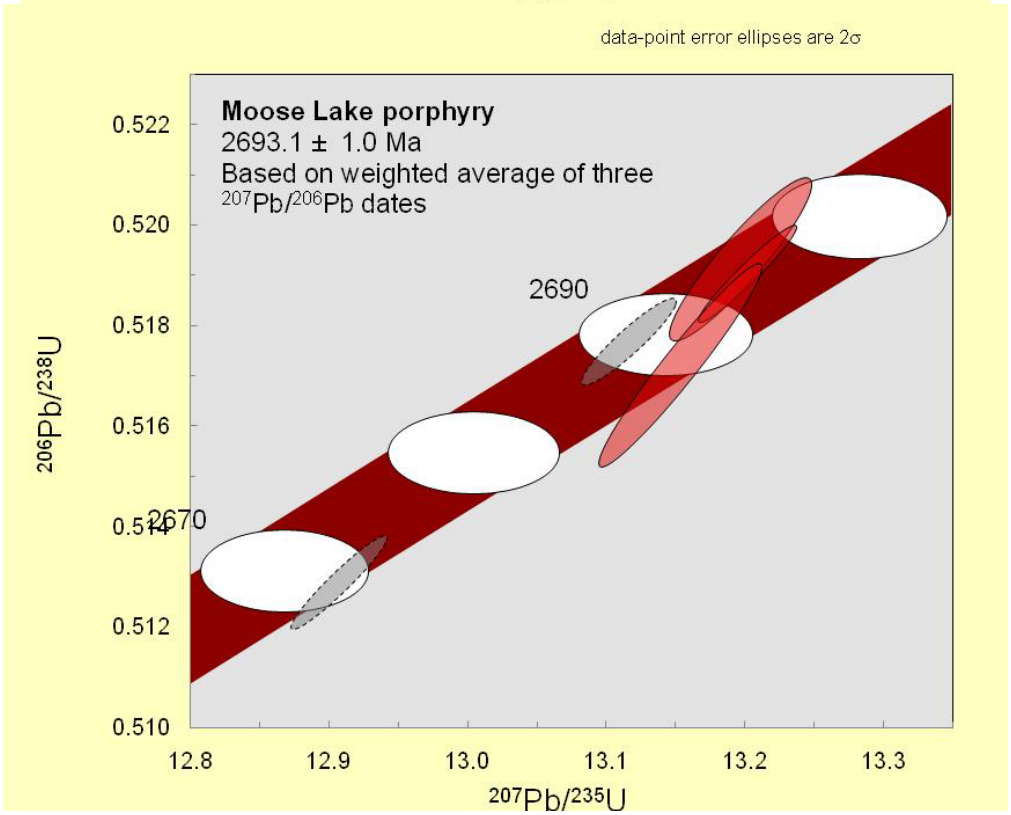

Figure 5.13: Concordia plot for felsic metavolcanic samples. C) Sample HEZ03 from the Thor Horizon. D) Moose Lake Porphyry Sample from Hemlo.

Zircons recovered from the Gouda sample are brown, prismatic and euhedral and measure ~200μm (Fig 5.12A), whereas zircons recovered from the Thor sample are dark brown, prismatic and measure ~400μm (Fig 5.12C). The Gouda Lake and Thor Lake units are both felsic volcanic protolith- ±quartz-eye sericite schists which are interpreted to be a continuous unit offset by the DC Lake fault. These samples yielded the same age (within error) at 2704.8±1.1 and 2705.6±1.0 Ma respectively which supports the syngenetic interpretation (Fig. 5.13A,C). These rocks also represent an age association not previously documented within the Schreiber-Hemlo Greenstone Belt.

Zircons recovered from the DC Lake sample are pale green, prismatic to rounded, and measure 100-200μm (Fig 5.12B). Zircons recovered from the Moose Lake Porphyry sample are pale green, dark brown and rose, are prismatic and fractured, and measure 100-200μm (Fig. 5.12D). Samples taken from DC Lake area fine-grained metadacite unit (2694.5 ±1 Ma) and the Moose Lake Porphyry at Hemlo (2693.1 ±1 Ma) have the same age within error.

Two granite units were also dated. Zircons recovered from the Cedar Lake Pluton sample are pale brown, are prismatic to rounded, and measure 150-200μm (Fig. 5.14A). Zircons recovered from the White River Pluton sample are pale green, dark brown and pale orange, are prismatic, and measure ~200μm (Fig. 5.14B). The Cedar Lake Pluton (2683.4 ±1.7 Ma), an equigranular medium-grained granodiorite, and the White River Pluton (2686.5 ±1.3 Ma; Fig. 5.15), a medium-coarse-grained monzogranite, are broadly contemporaneous and were intruded into the older sedimentary and volcanic rocks.

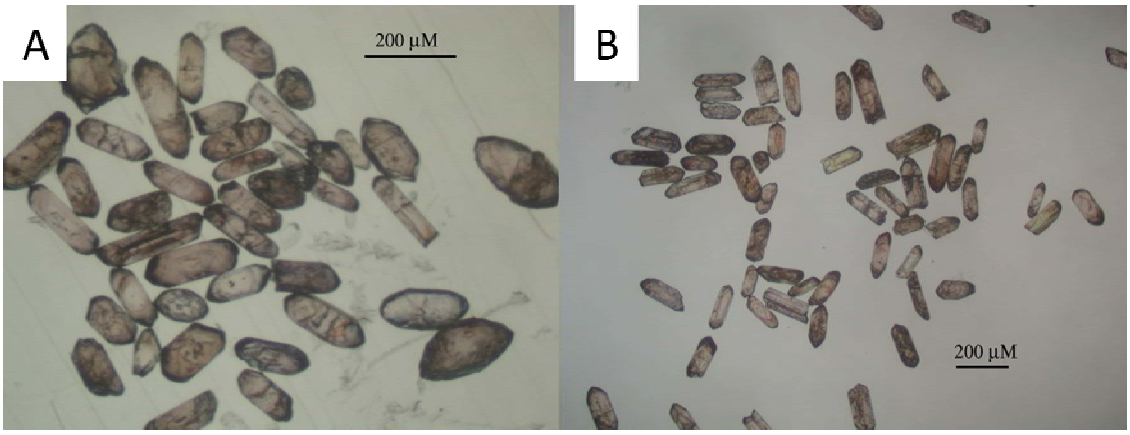

Figure 5.14: Photomicrographs of picked zircon grains prior to treatment. A) Sample CLP from the Cedar Lake Pluton. B) Sample WRS from the White River Pluton.

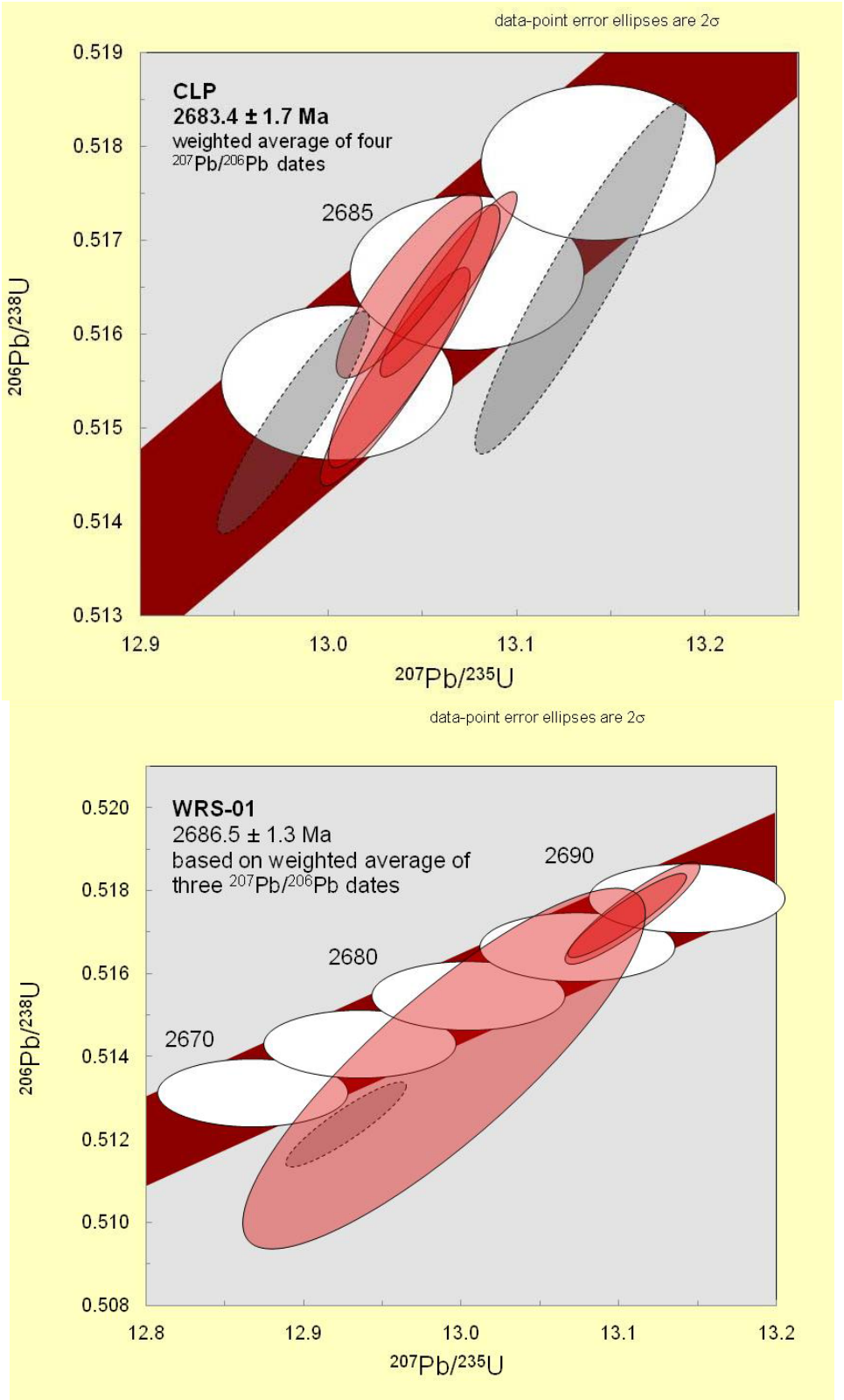

Figure 5.15: Concordia plot for intrusive samples. A) Sample CLP from the Cedar Lake Pluton. B) Sample WRS from the White River Pluton.

5.4 Sm-Nd Data

Four samples of tholeiitic ocean plateau basalts were collected for Sm-Nd isotope analysis. Nd values range from 4.93-8.42 ppm, Sm values range from 1.834-2.791 ppm, $^{147}Sm/^{144}Nd$ ratios range from 0.19333-0.22493, $^{143}Nd/^{144}Nd$ ratios range from 0.512667-0.513082. ε_{Nd} values calculated using an age of 2700 Ma for the four tholeiitic ocean plateau basalts yielded three positive values and one negative ε_{Nd} value (Table 5.2). The ε_{Nd} values were calculated using an age of 2700 Ma. The sample with negative ε_{Nd} shares the same near flat primitive mantle pattern as the other samples but has a larger negative Nb anomaly (Fig. 5.16).

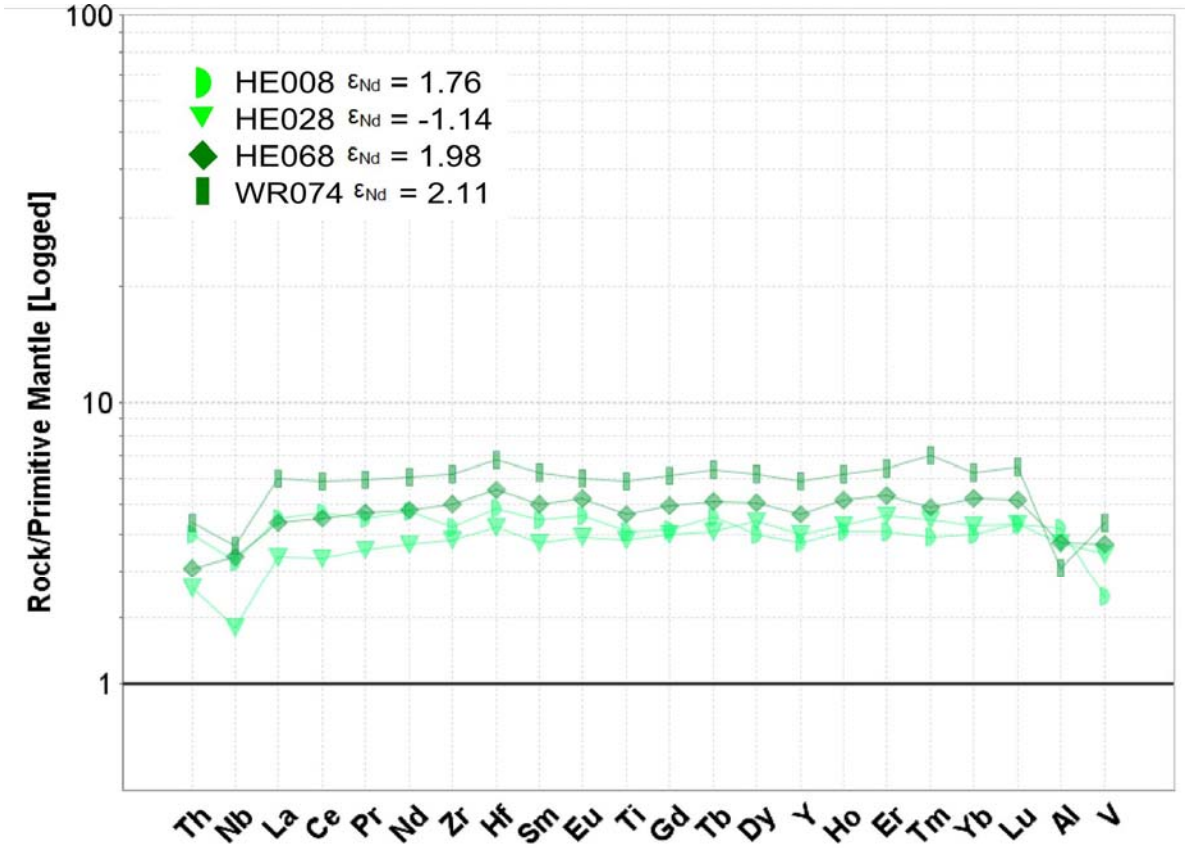

Figure 5.16: Primitive mantle normalised plot for samples with Sm-Nd data (normalising values from Sun and McDonough, 1989).

Table 5.2: Sm-Nd data for rocks from the Hemlo East Property

Sample	Nd (ppm)	Sm (ppm)	$^{147}Sm/^{144}Nd$	$^{143}Nd/^{144}Nd$	$\varepsilon_{Nd\ 2700\ Ma}$
HE008	6.66	2.131	0.19333	0.512667	1.76
HE028	4.93	1.834	0.22493	0.513082	-1.14
HE068	6.57	2.174	0.20029	0.512801	1.98
WR074	8.42	2.791	0.20057	0.512812	2.11

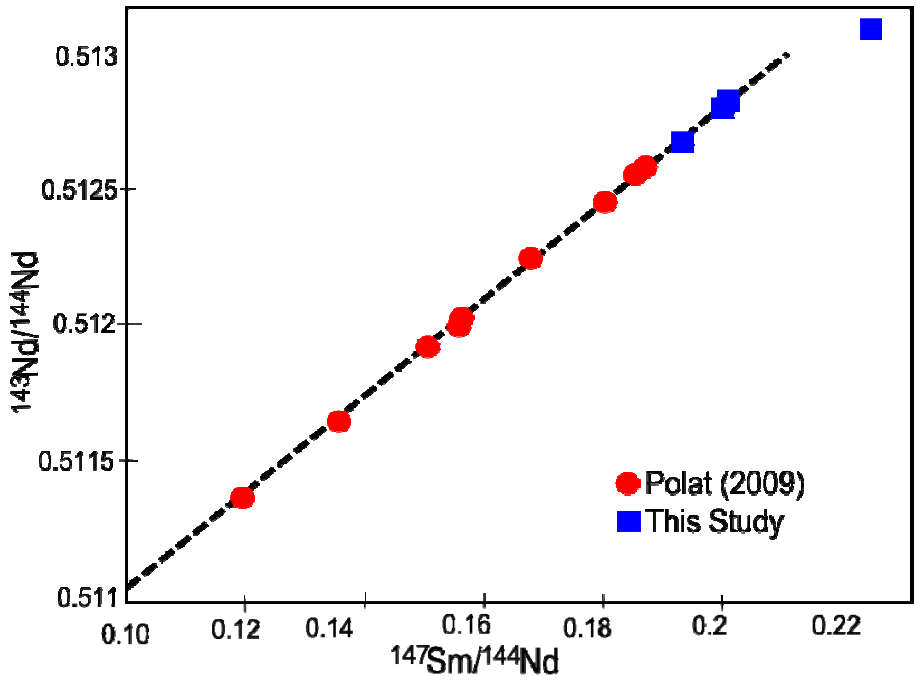

Figure 5.17: $^{147}Sm/^{144}Nd$ versus $^{143}Nd/^{144}Nd$ variation diagram for metabasalts from this study and from Polat (2009).

An isochron could not be calculated with the Sm-Nd data from this study as the data points, when plotted on a $^{147}Sm/^{144}Nd$ versus $^{143}Nd/^{144}Nd$ variation diagram are too closely spaced; however, the three samples which yielded positive ε_{Nd} values are concordant with the data presented by Polat (2009) who calculated a 2678 ± 48 isochron age which is in good agreement with the spatially associated felsic volcanic rocks (Fig. 5.17).

5.5 Discussion

5.5.1 Metabasaltic Rocks

Mg- to Fe-tholeiitic metabasalts are the prevalent volcanic rock type in the study area. These rocks are characterized by near flat patterns on a primitive mantle normalized plot (Fig. 5.3). Metabasalts plot on the low Ce–Yb trend of Hawkesworth et al. (1993) comparable to intraoceanic arc basalts such as the South Sandwich Islands and Tonga–Kermadec arcs (Fig. 5.18). Consequently, the metabasalts of the Gouda-Thor-Carroll area are interpreted to have erupted in a similar intraoceanic environment. Positive ε_{Nd} values (1.76-2.11) are comparable to values reported by Polat (2009) for metabasalts within the Schreiber-Hemlo Greenstone Belt (1.68-2.15). These values are close to the Nd isotopic composition of depleted mantle at ~2.7 Ga (+3.0, Tomlinson et al., 2004), suggesting that the metabasalts have not assimilated significant volumes of older crustal material, consistent with them having formed in an intraoceanic setting. The single negative ε_{Nd} value (-1.14) from the metabasalt sample suggests either crustal contamination or an enriched-mantle input into the magma. Polat (2009) argued for a heterogeneous mantle plume source for Schreiber-Hemlo theoleiitic metabasalts based on an association with komatiites. No komatiites were encountered in this study but La/Sm_n ratios (0.8-2.0) of metabasalts are consistent with a heterogeneous source. Hemlo East metabasalts are comparable to Phanerozoic and Recent arc basalts in having Nb abundances of ~1-3 ppm (the range of values is 1.3 - 6.2 ppm while the mean is 2.6). Niobium contents are mostly <1 and <2 ppm in the Eastern and Central Lau basin basalts, respectively (Pearce et al., 1995); <1 ppm in the Mariana arc (Elliott et al., 1997; Pearce et al., 1999); <2 ppm in basalts of the Lau–Tonga arc (Ewart et al., 1994); and Izu-Bonin forearc basalts possess <0.5 ppm Nb (Taylor et al., 1992). Hemlo East metabasalts are similar to most modern arc basalts in having negative anomalies, except for rare Nb enriched basalts (Pearce and Peate, 1995; Sajona et al., 1996). A primitive mantle normalised plot of

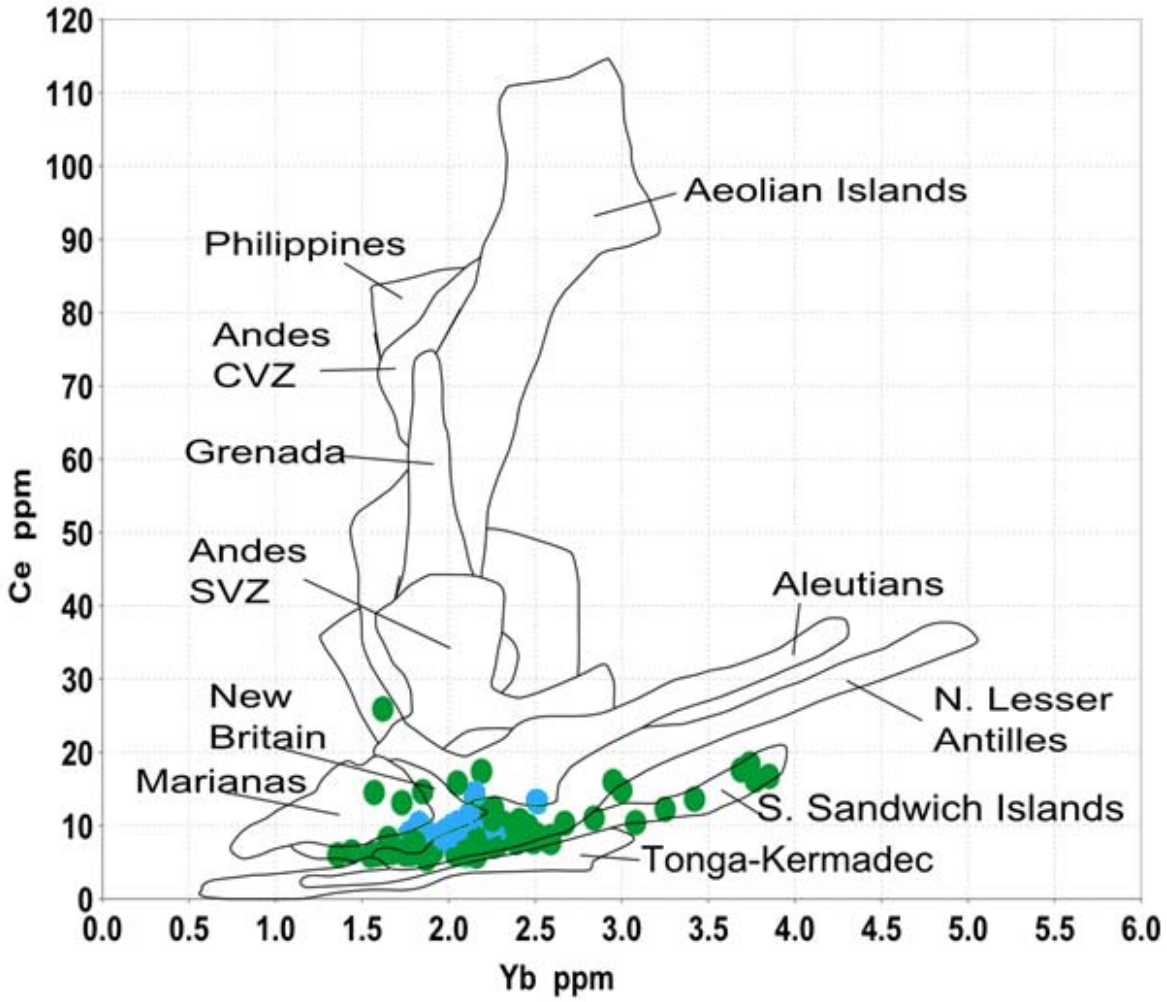

Figure 5.18: Plot of Ce vs. Yb for metabasalts of the Gouda-Thor-Carrol area which plot on the intraoceanic arc basalt trend. Dark green represents metabasalts; Light blue represents mafic lapilli tuffs. Oceanic and continental margin arc basalt fields from Hawkesworth et al. (1993).

basalt environments is shown in Figure 5.19; Hemlo East metabasalts (Fig 5.5) most closely resemble protoarc and early arc basalts in having a negative Nb anomaly and a relatively flat pattern.

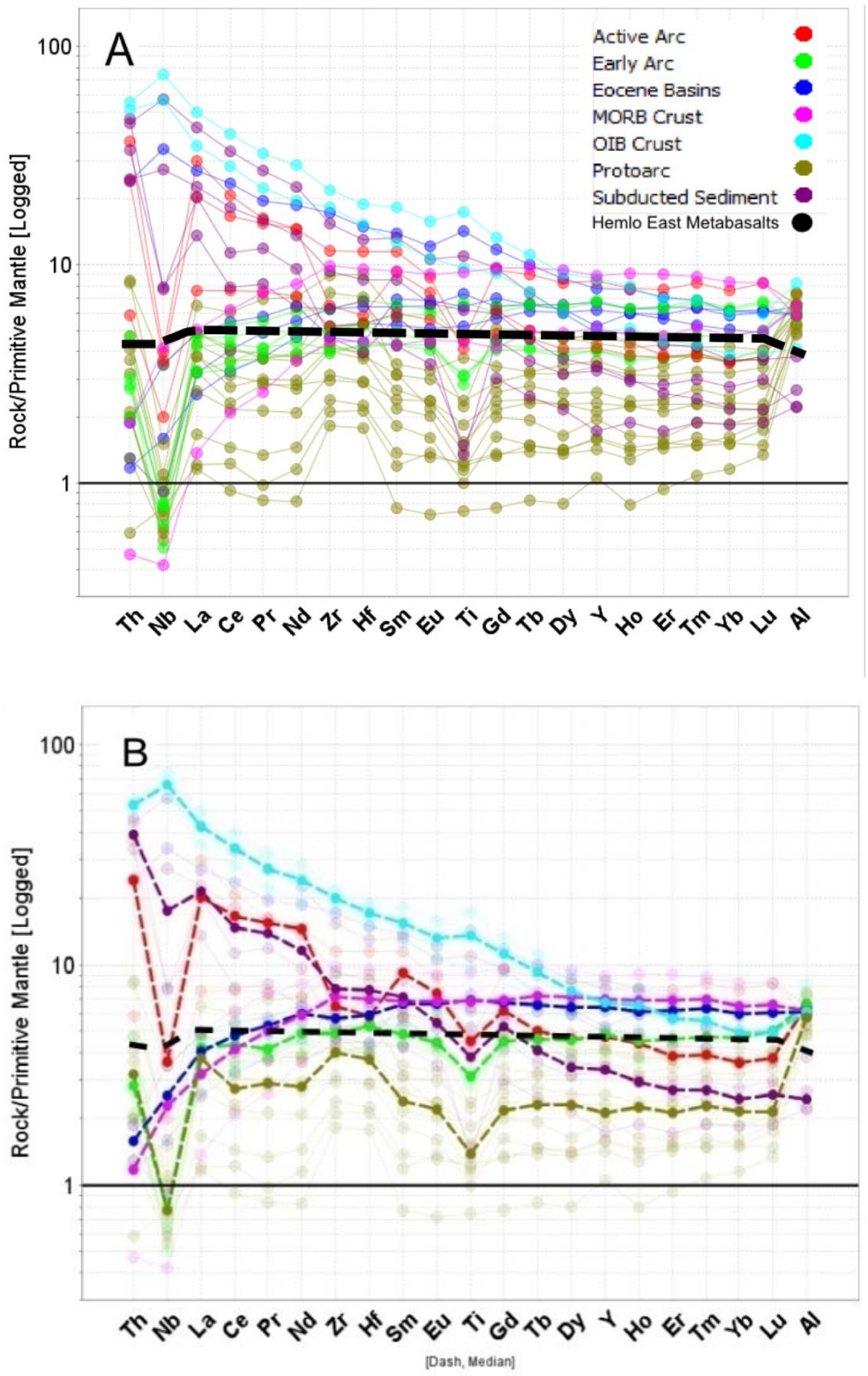

Figure 5.19: Primitive mantle normalised plot for basalts from different environments (normalising values from Sun and McDonough, 1989). A) All data points. B) Mean of the data for clarity. Data from Pearce et al. (1999).

HFSE ratios of arc basalts generally plot within the MORB array as defined by Pearce and Peate (1995; Fig. 5.20), whereas crustally contaminated samples would typically plot outside this array. However, the total range of Zr/Nb in primitive arcs is 9–87, versus 11–39 for MORB (average 32), signifying variably enriched to depleted mantle sources compared to MORB for the primitive arcs (Davidson, 1996; Macdonald et al., 2000). In the Mariana arc, lavas have Zr/Nb ratios as high as 87, in conjunction with high Ta/Nb, indicative of a mantle source extremely depleted by previous melt extraction events. Basalts of the Gouda-Thor area have Zr/Nb of 6–35, consistent with derivation from a primitive subarc mantle varying from enriched to depleted, relative to MORB, whereas Ta/Nb ratios (0.03-0.16) are close to MORB (Fig. 5.21). From this evidence, the Hemlo East basalts are interpreted to be primitive arc basalts.

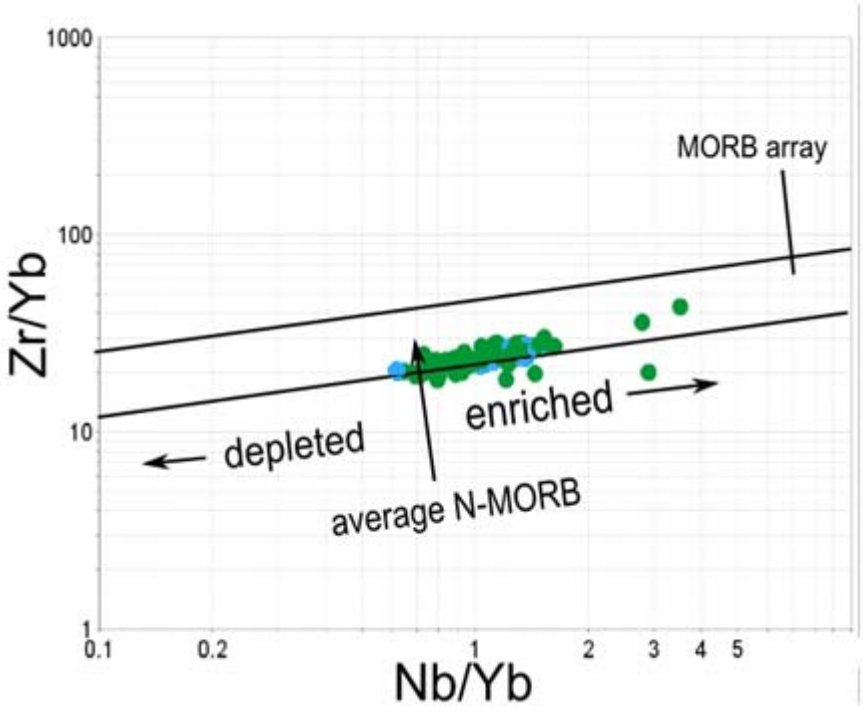

Figure 5.20: MORB array as defined by Pearce and Peate (1995).

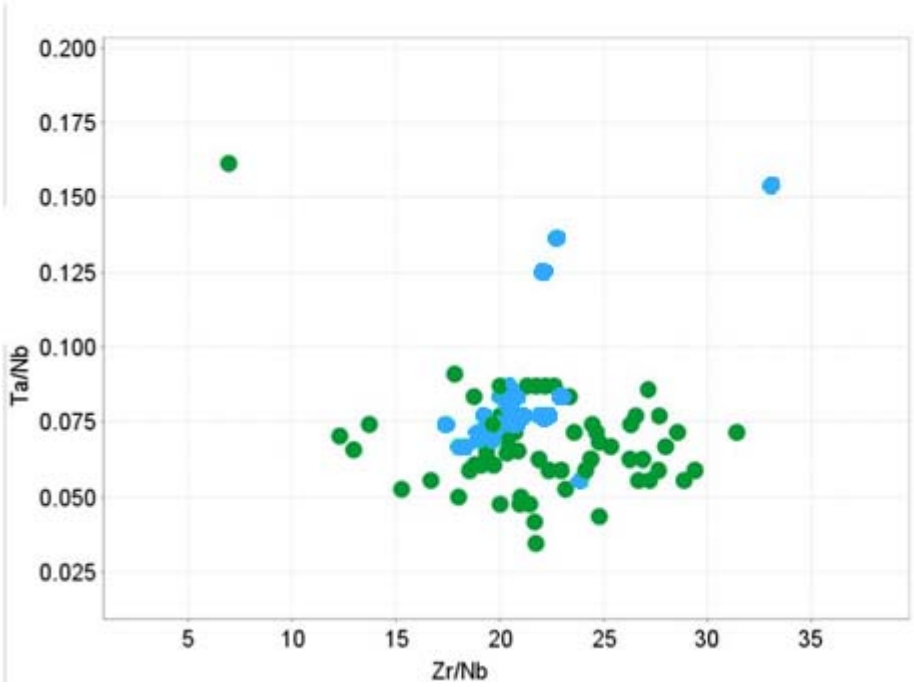

Figure 5.21: Plot of Zr/Nb vs Ta/Nb for the metabasalts of the Gouda-Thor-Carroll area. Light green represents mafic lapilli tuffs.

Polat et al. (1998) and Polat (2009) presented data on metabasalts from the Schreiber-Hemlo, Winston Lake, Manitouwadge, and White River-Dayohessarah greenstone belts. They recognise three associations of metabasalts: tholeiitic basalts, calc-alkaline basalts, and transitional to alkaline basalts (Fig. 5.22). Tholeiitic basalts closely resemble the primitive arc basalts from this study in having a flat pattern on a primitive mantle normalized plot (Fig. 5.22A) and are described as mantle plume-related oceanic plateau basalts by Polat (2009). Calc-alkaline basalts exhibit negative Nb and Ti anomalies and are characterized by LREE enrichment as well as flat to moderate HREE depletion and share geochemical similarities with felsic metavolcanic and metasedimentary rocks of this study (Fig 5.22B). Transitional to alkaline basalts are characterized by positive Nb anomalies and a gently sloping pattern on a primitive mantle normalized plot (Fig. 5.22C). The transitional to alkaline samples could be considered Nb-enriched basalts (NEB), which have been described by Wyman et al. (2000) as having primitive mantle-normalized Nb/La (Nb/La_{MN}) between 0.5 and

1.4 and Nb contents greater than 6 ppm; all of these samples meet this criteria (there were no NEB sampled from the Hemlo East Property in this study). The presence of NEB in other parts of the greenstone belt and adjacent greenstone belts could point towards an evolution from primitive arc basalts in the Hemlo East area to NEB in other, younger parts of the greenstone belt(s).

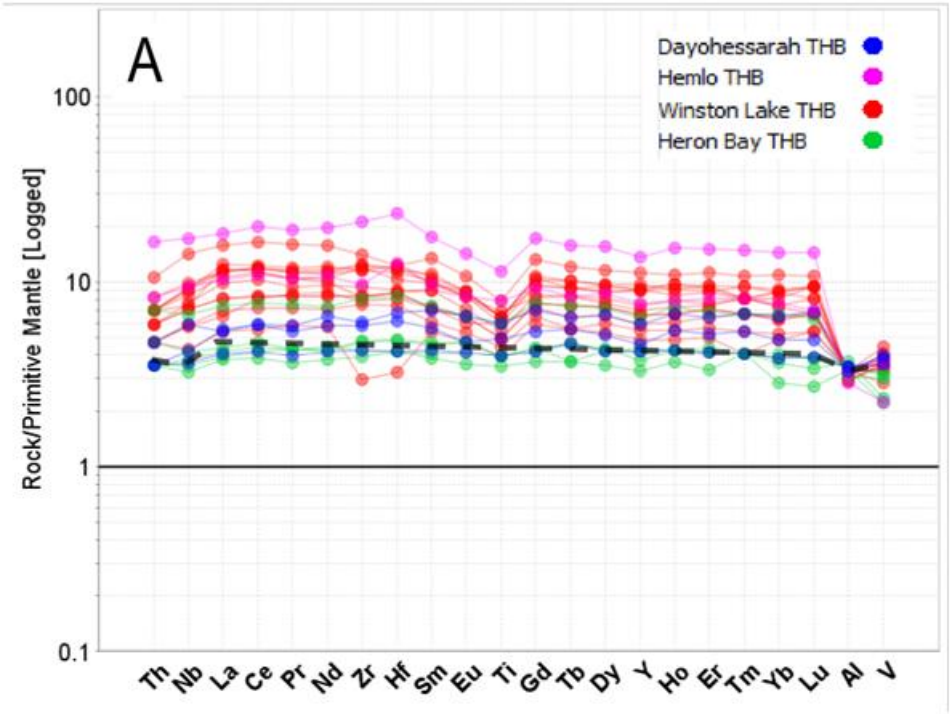

Figure 5.22: Primitive mantle normalised plot for metabasalts from the Schreiber-Hemlo, Winston Lake, Manitouwadge, and White River-Dayohessarah greenstone belts. THB = tholeiitic basalt. Mean Hemlo East metabasalts are shown by a black dotted line (data from Polat et al., 1998 and Polat, 2009; normalising values from Sun and McDonough, 1989).

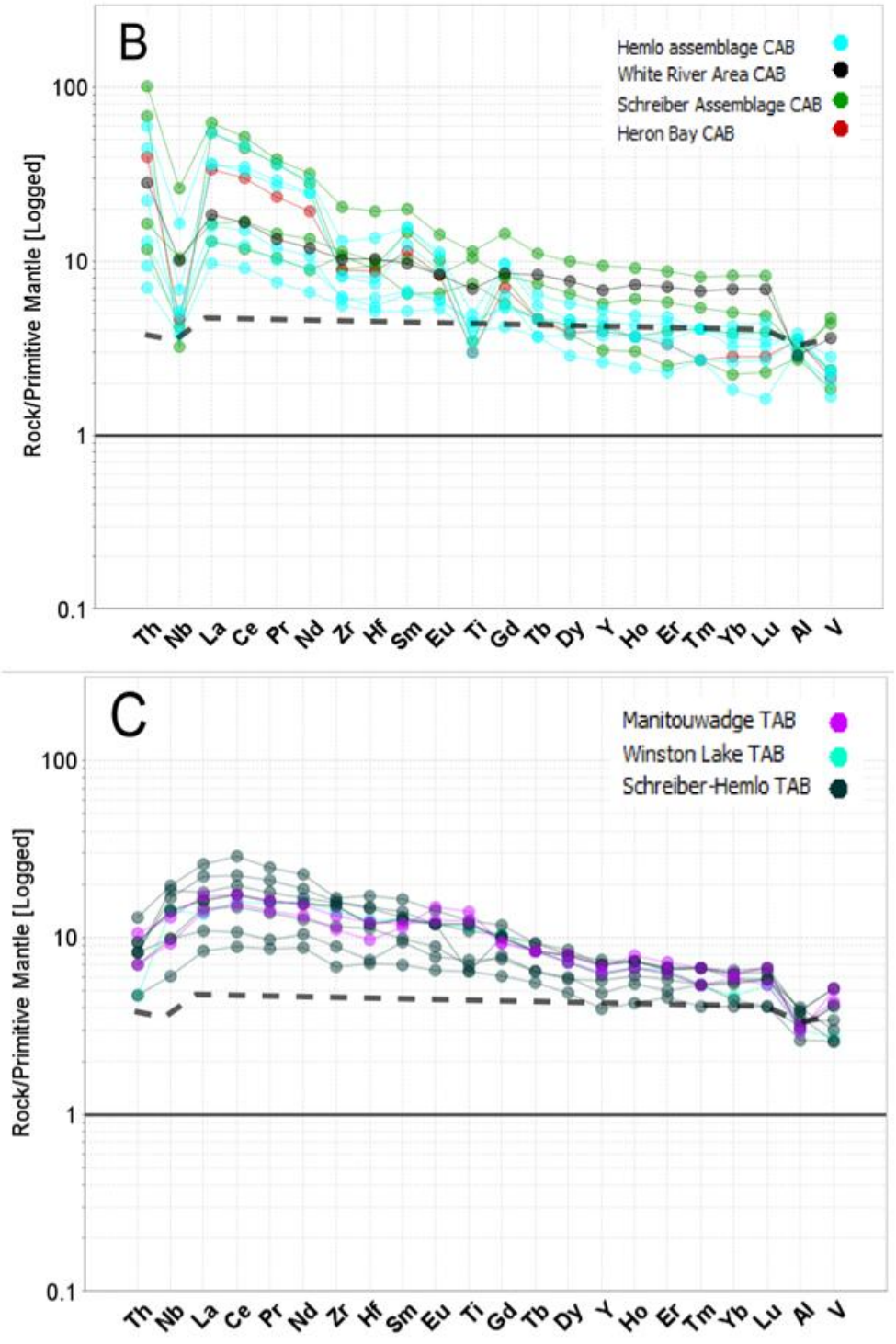

Figure 5.22: Primitive mantle normalised plot for metabasalts from the Schreiber-Hemlo, Winston Lake, Manitouwadge, and White River-Dayohessarah greenstone belts. CAB = calc-alkaline basalt. TAB = transitional to alkaline basalt. Mean Hemlo East metabasalts are shown by a black dotted line (data from Polat et al., 1998 and Polat, 2009; normalising values from Sun and McDonough, 1989).

5.5.2 Felsic Metavolcanic Rocks

Felsic metavolcanic rocks from the Gouda-Thor-Carrol area are FI rhyolites with trace element characteristics of a suprasubduction zone environment (Figs. 5.4 and 5.23). Felsic metavolcanic rocks have steep trace element patterns (La/Yb_n = 16-44) and fractionated HREE (Gd/Yb_n = 2.1-7.5), typical of rocks derived at depth from within the garnet stability zone within the mantle (Martin, 1986).

Lesher et al. (1985) have subdivided Archaean felsic metavolcanic rocks based on trace-element abundances and ratios. Rhyolites were divided into FI, FII, and FIII(a&b) on the basis of trace element abundances and ratios to give an indication of fertility for base metal sulphide mineralization. FI felsic metavolcanic rocks are described by Lesher et al. (1985) as having steep REE patterns with weakly negative to moderately positive Eu anomalies, high Zr/Y, low abundances of HFSE and high abundances of Sr. FII felsic metavolcanic rocks are described as having gently sloping REE patterns with variable Eu anomalies, moderate Zr/Y, and intermediate abundances of HFSE and Sr. FIII felsic metavolcanic rocks are described as having relatively flat REE patterns, which may be subdivided into two types. FIIIa felsic metavolcanic rocks exhibit variable negative Eu anomalies, low Zr/Y, and intermediate abundances of HFS elements and Sr; FIIIb felsic metavolcanic rocks exhibit pronounced negative Eu anomalies, low Zr/Y, high abundances of HFS elements, and low abundances of Sr. Gouda-Thor-Carroll felsic metavolcanic rocks most closely resemble FI rhyolites which are interpreted by Lesher et al. (1986) to have been derived from deep sourced magma chambers (Fig. 5.23).

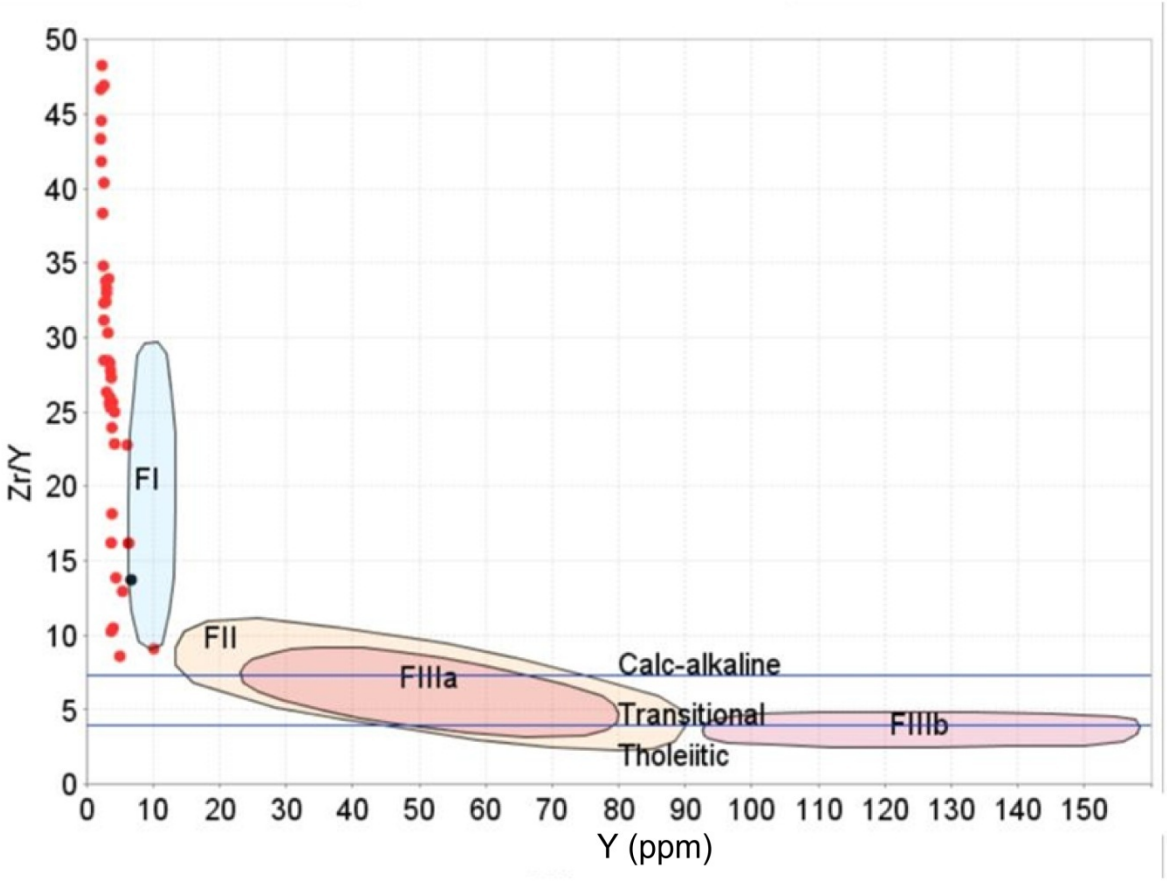

Figure 5.23: Rhyolite fertility classification using Zr/Y vs Y plot to distinguish rhyolite type (Lentz, 1998 after Lesher et al., 1986).

5.5.3 Metasedimentary Rocks

Metasedimentary rocks from the Gouda-Thor-Carrol area are geochemically similar to felsic metavolcanic rocks and are interpreted to be derived wholly, or in part, from a felsic source. When one sample with typical composition from each of three areas of the property (Gouda, Duck Lake north of Gouda, and Frank Lake) are plotted on immobile ratio plots and compared with regional data from Fralick et al. (2006; locations on Fig. 5.24) on Figure 5.25, they lie close to each other and also share some similarities to samples from Hemlo, Amwri Lake, and Pukaskwa.

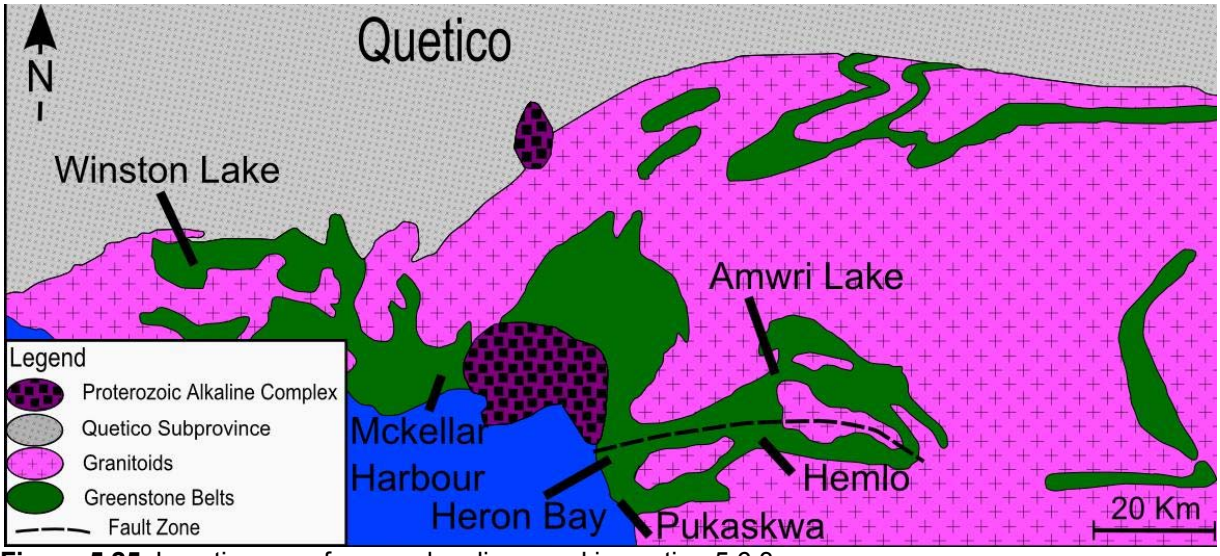

Figure 5.25: Location map for samples discussed in section 5.6.3.

This same data is plotted on extended ratio plots in Figure 5.26. On these plots, a set of samples are normalised against another sample to give a sense of similarity; a rock of similar composition would plot on a line close to one. It can be seen that the Hemlo East samples are not similar to any of the regional samples from Fralick et al. (2006). The Gouda, Duck Lake, and Frank Lake samples are similar to each other (Fig. 5.26D), with the major variations occurring in the mobile elements Ba, Sr, and CaO. Fralick et al. (2006) concluded that sedimentary rocks in the McKellar Harbour and Schreiber areas located in the western end of the Schreiber-Hemlo Greenstone Belt shared geochemical similarities with rocks of the Quetico Terrane and were transported from the north and deposited in the Wawa Terrane. The metasedimentary rocks of the Hemlo East Property are not geochemically

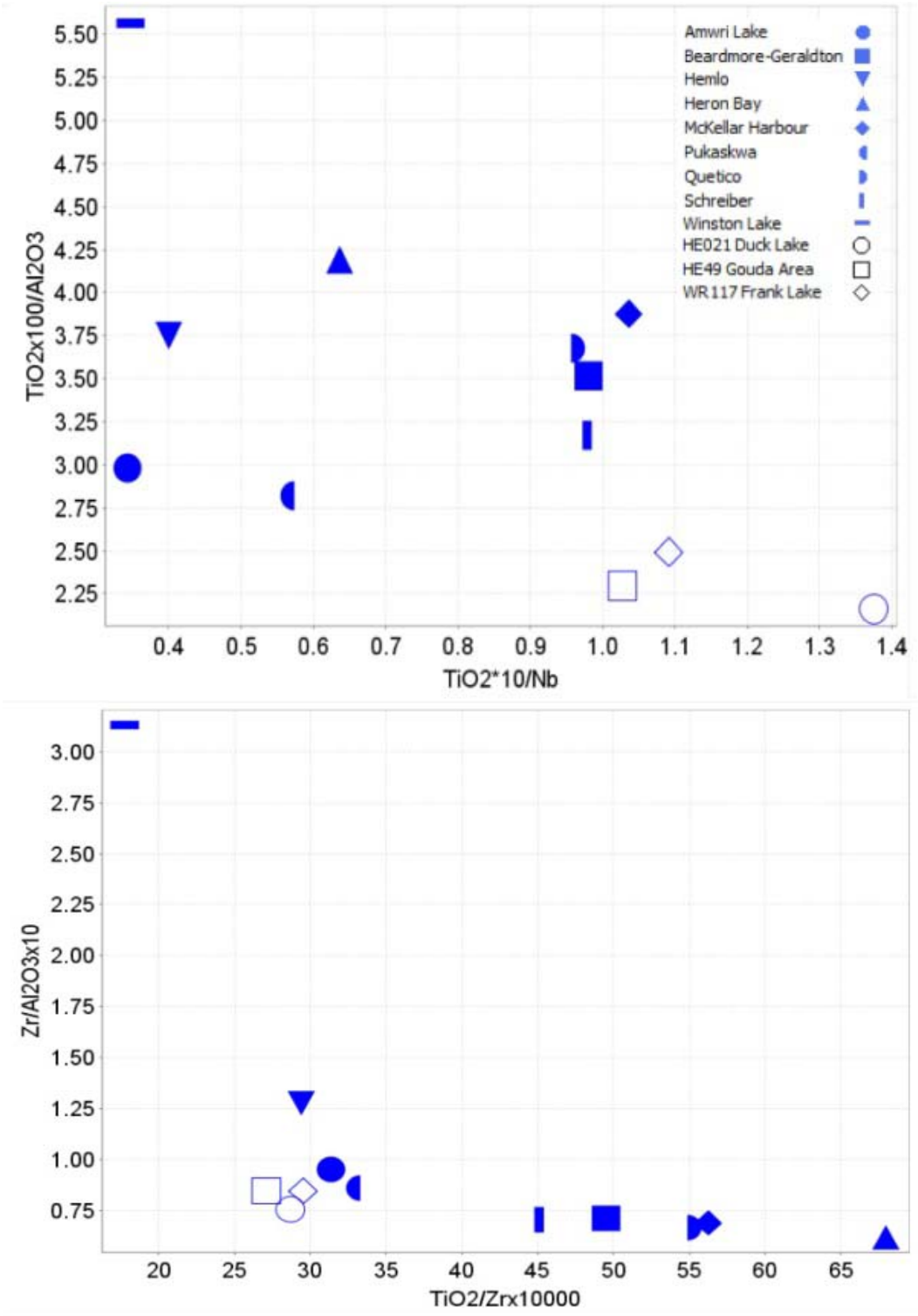

Figure 5.25: Immobile element ratio plots for Hemlo East and regional sedimentary units (regional data from Fralick et al., 2006).

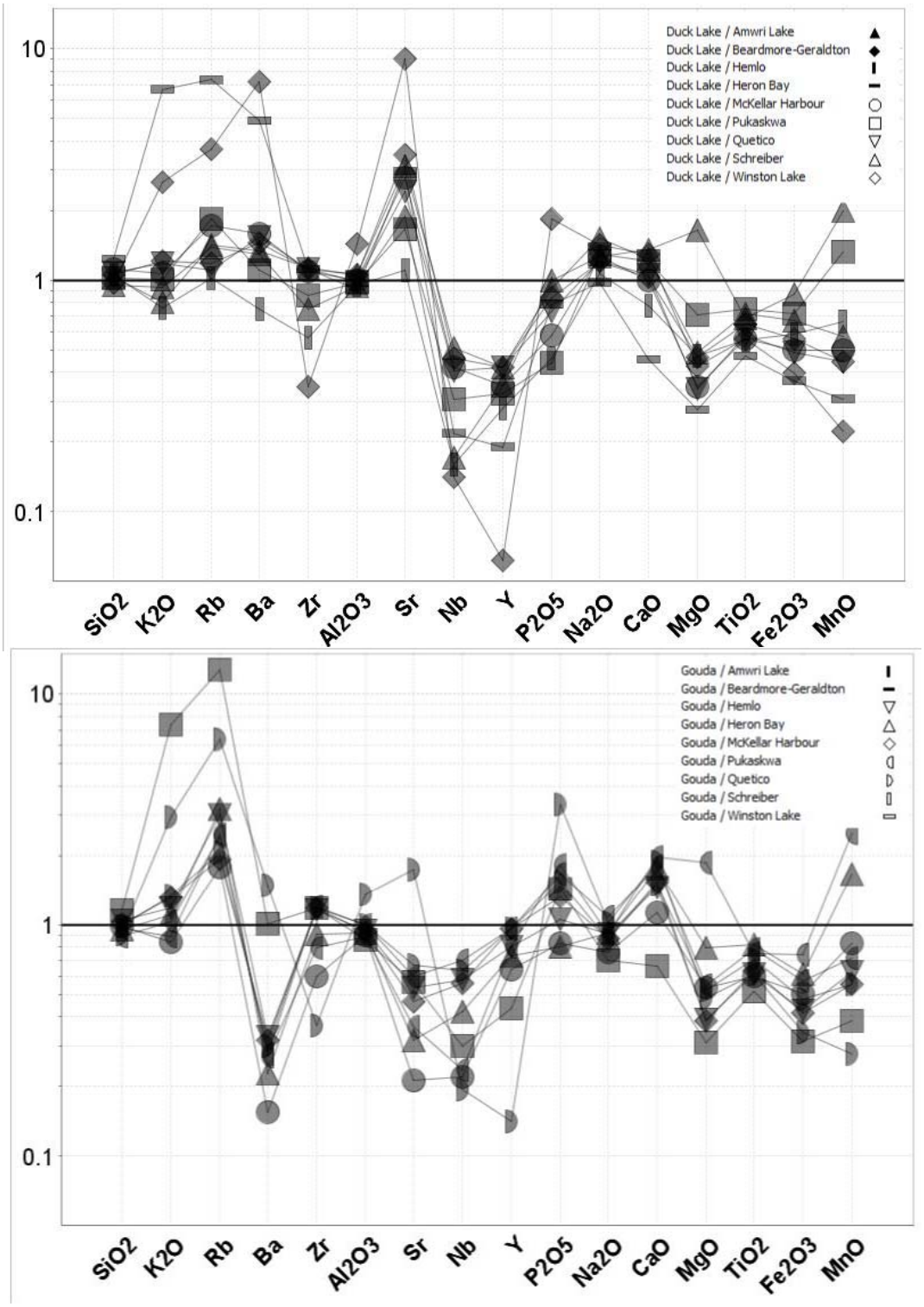

Figure 5.26: Normalized extended ratio plots comparing the geochemistry of the Hemlo East sedimentary units with regional data (regional data from Fralick et al., 2006). A) Regional data plotted against Duck Lake Unit. B) Regional data plotted against Gouda Unit.

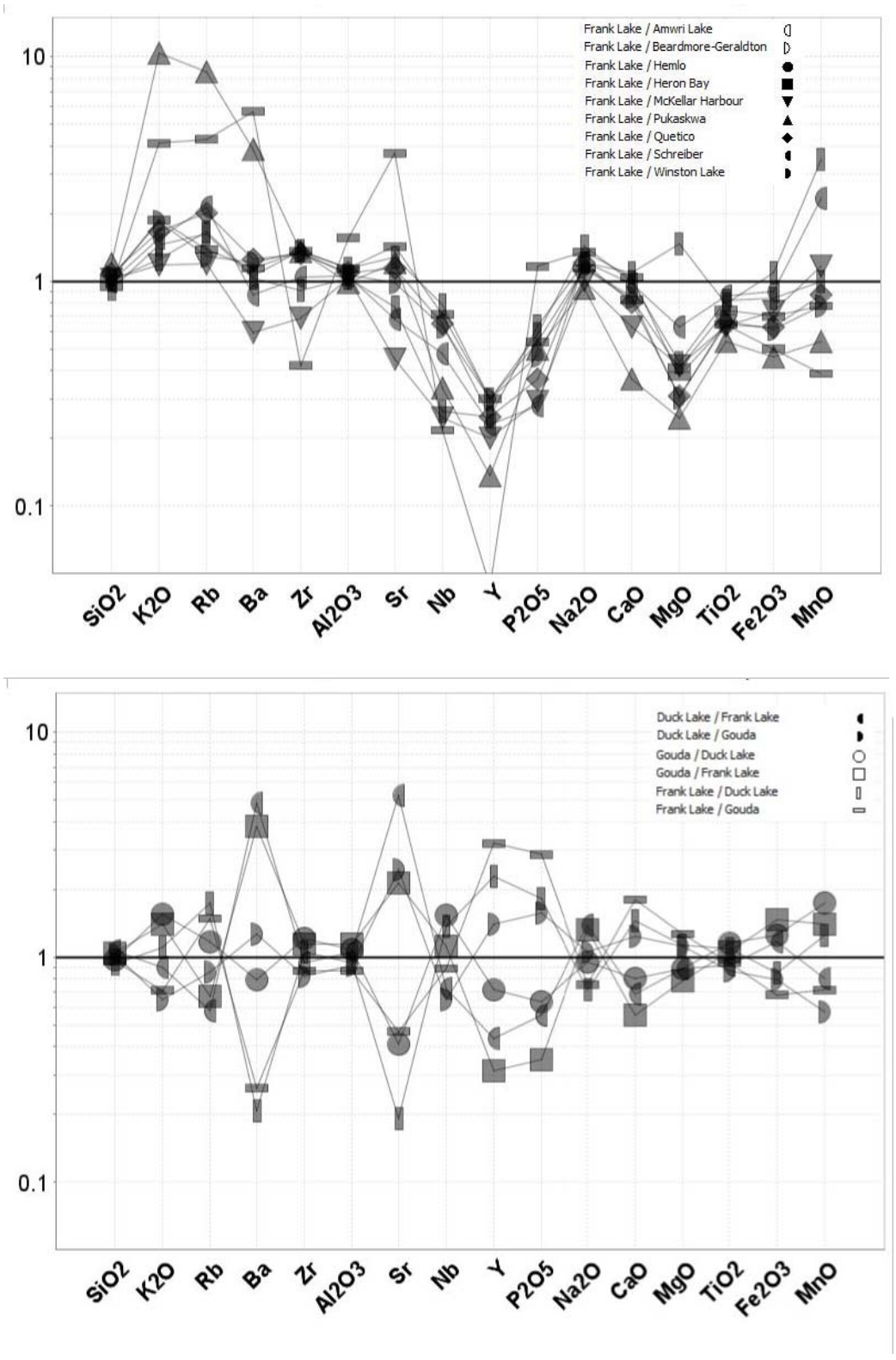

Figure 5.26: Normalized extended ratio plots comparing the geochemistry of the Hemlo East sedimentary units with regional data (regional data from Fralick et al., 2006). C) Regional data plotted against Frank Lake Unit. D) Hemlo East Units plotted against each other.

similar to these rocks and therefore were not derived from the same area and appear to be derived from a more felsic source. This may be because they were formed in a different environment and are associated with the oldest felsic volcanic rocks dated in the greenstone belt (section 5.5.4). The Hemlo East metasedimentary rocks may represent volcaniclastic sediments deposited from the volcanic arc to the back arc basin; derived from the 2704 Ma felsic metavolcanic rocks dated in this study (section 5.5.4). The geochemistry of the metasedimentary rocks of the Schreiber-Hemlo Greenstone Belt changed over time with the change of tectonic setting from volcanic arc associated metasedimentary rocks from this study to the accretionary complex of the Quetico basin to the north.

Polat et al. (1998) and Polat (2009) presented data on metasedimentary rocks from the Schreiber-Hemlo, Winston Lake, Manitouwadge, and White River-Dayohessarah greenstone belts. These metasedimentary rocks exhibit negative Nb and Ti anomalies and are characterized by LREE enrichment as well as flat to moderate HREE which is consistent with the metasedimentary rocks from Hemlo East.

5.5.4 Geochronology

A compilation of geochronology within the Hemlo Greenstone Belt from previous authors is presented in Appendix D. From the compilation of previous geochronological work in conjunction with new data, five distinct events can be recognised in the vicinity of the Hemlo East Property (Fig. 5.27).

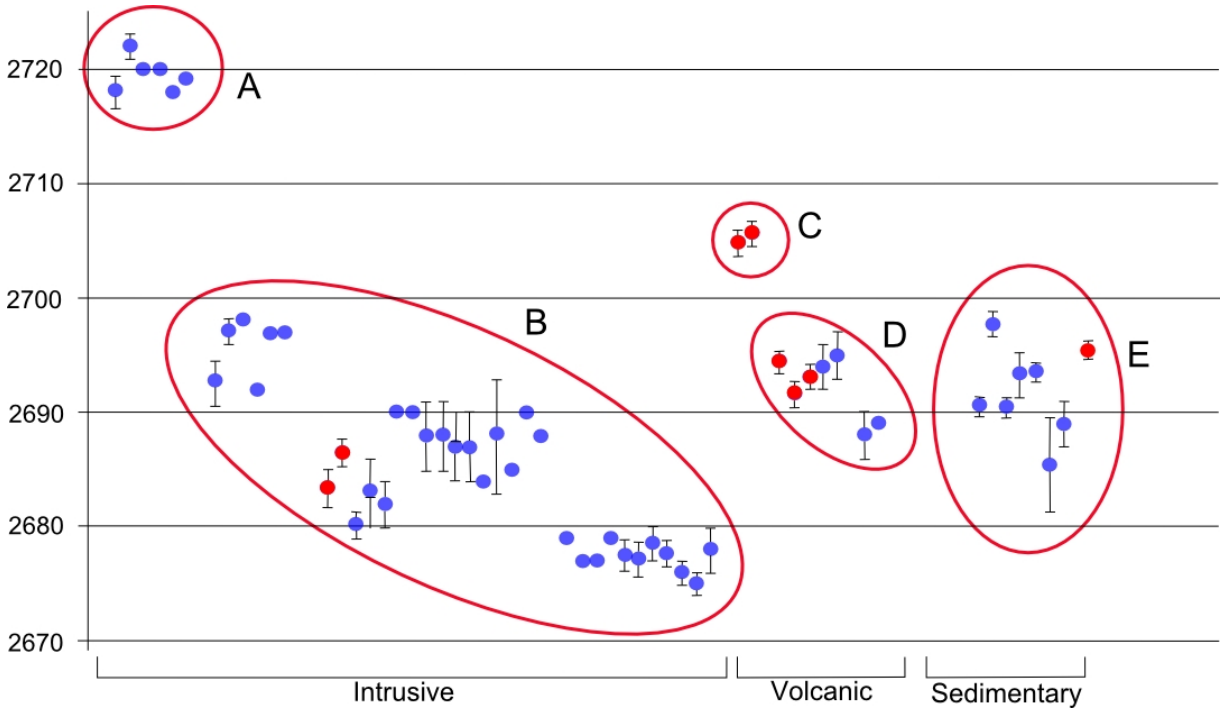

Figure 5.27: Graph of compiled geochronology for the eastern half of the Schreiber-Hemlo Greenstone Belt. Data is compiled from Corfu and Muir (1989 a,b), Davis et al (1998), Davis and Lin (2003), Beakhouse and Davis (2005). Data from this study in red. A) 2718-2722 Ma intrusive rocks e.g. Pukaskwa Batholith Margin B) 2675-2698 Ma intrusive rocks e.g. Regional Plutons, dikes, Cedar Lake Pluton, White River Pluton, Pukaskwa Batholith Interior C) 2704-2706 Ma felsic metavolcanic rocks e.g. Gouda, Thor Horizons D) 2692-2695 Ma felsic metavolcanic rocks e.g. Moose Lake Porphyry, Upper Anomalous Zone, DC Lake Metadacite, Barren Sulphide zone at Hemlo E) 2685-2698 Ma metasedimentary rocks e.g. Frank Lake Felsic Horizon.

From the new and compiled U-Pb geochronological data, it can be shown that there are two associations of felsic volcanism and two associations of plutonism. The Gouda/Thor units represent a new association at 2705 Ma which is the oldest felsic volcanic unit dated in the greenstone belt. The Moose Lake Porphyry at Hemlo (with a comparable age to that reported by Davis and Lin, 2003), DC Lake volcanic rocks, and volcaniclastic rocks of the Upper Anomalous Horizon form a second volcanic age association spanning 2688-2695 Ma. The barren sulphide unit at Hemlo (dated by Davis and Lin, 2003) has the youngest felsic volcanic age date in the area at 2688 Ma. The dates for separate groups of felsic volcanic rocks show that volcanic centres lasted for 2 to 7 million years each.

The margin of the Pukaskwa Batholith has been dated by Beakhouse and Davis (2005) as older than the oldest felsic volcanic rock at its margin (2718 ±1.4 Ma), whereas its interior has been dated at 2688 ±3 Ma which indicates that the Pukaskwa Batholith is a multiphase part of a long-lived arc system. The contact between the Pukaskwa Batholith and the greenstone belt in the Gouda-Thor-Carroll area is not a thrust contact, so the Pukaskwa Batholith may have been the basement for the deposition of the Gouda volcanic unit as part of a pre-existing arc, but further work is needed to investigate this relationship. The Cedar Lake Pluton and the White River Stock are the youngest units dated and would have intruded into the volcanic-sedimentary stratigraphy. The Frank Lake metasedimentary unit is younger than the felsic volcanic stratigraphy.

This data points toward a northward younging of stratigraphy in the Gouda-Thor-Carrol area which would mean that the stratigraphy is right way up. This does not agree with the observations made in Section 4.4. A complex history of folding throughout the greenstone belt means that the way up interpretation cannot be extrapolated beyond the immediate Gouda-Thor-Carroll area.

5.5.5 Intrusive Rocks

In section 5.5.4 it was shown that there are two age associations of plutonism in the Schreiber-Hemlo Greenstone Belt. Beakhouse and Davis (2005) have presented geochemical data on the regional plutons which will be discussed here. Group A from Figure 5.27 comprises the ‘pre-tectonic’ plutons (Pukaskwa and Black-Pic Batholiths; Beakhouse and Davis, 2005) which are characterised by negative Nb and Ti anomalies, LREE enrichment and HREE depletion. Intermediate age (Syntectonic; Beakhouse and Davis, 2005) plutons (Group B in Fig. 5.27) have two associations: the Botham Lake Stock, Cedar Creek Stock and Heron Bay Pluton are characterised by negative Nb anomalies, LREE enrichment and HREE depletion while the Cedar Lake Pluton and White River Pluton are

characterised by negative Nb anomalies and LREE enrichment. Post-tectonic plutons (Gowan Lake, Fourbay Lake and Musher Lake Plutons; Beakhouse and Davis, 2005; Group B in Fig. 5.27) are characterised by negative Nb anomalies and LREE enrichment. Intrusive units are plotted on a primitive mantle normalised plot in Figure 5.28; all units are characterised by negative niobium anomalies and LREE enrichment except for the Dotted Lake Batholith which was proposed to have a sanukitoid affinity by Beakhouse and Davis (2005). The HREE patterns have three distinct trends: a flat pattern (White River Pluton, Gowan Lake Pluton, and the Fourbay Lake Pluton), a weakly depleted HREE pattern (Cedar Lake Pluton, Musher Lake Pluton, and the Terrace Bay Pluton), and a depleted HREE pattern (Pukaskwa Batholith, Black Pic Batholith, Heron Bay Pluton, Cedar Creek Stock, and the Botham Stock); the latter is comparable to the felsic volcanic rocks seen in the Hemlo East Property. This may either represent several sources of magma or a secular evolution of composition over time (or a combination of the two, which is more likely).

The Pukaskwa Batholith has been dated by Beakhouse and Davis (2005) at 2718.1 ± 1.4 and 2688 ± 3 Ma which suggests that there has been a long history of active plutonism in the arc. The felsic metavolcanic rocks of the Gouda-Thor Carroll area most closely resemble the LREE enriched and HREE depleted character of the Group A intrusive rocks (e.g. the Pukaskwa Batholith) and therefore may have been derived from a magma of similar composition (Fig. 5.28). Intrusive rocks from group B in Figure 5.27 are contemporaneous with group D volcanic rocks.

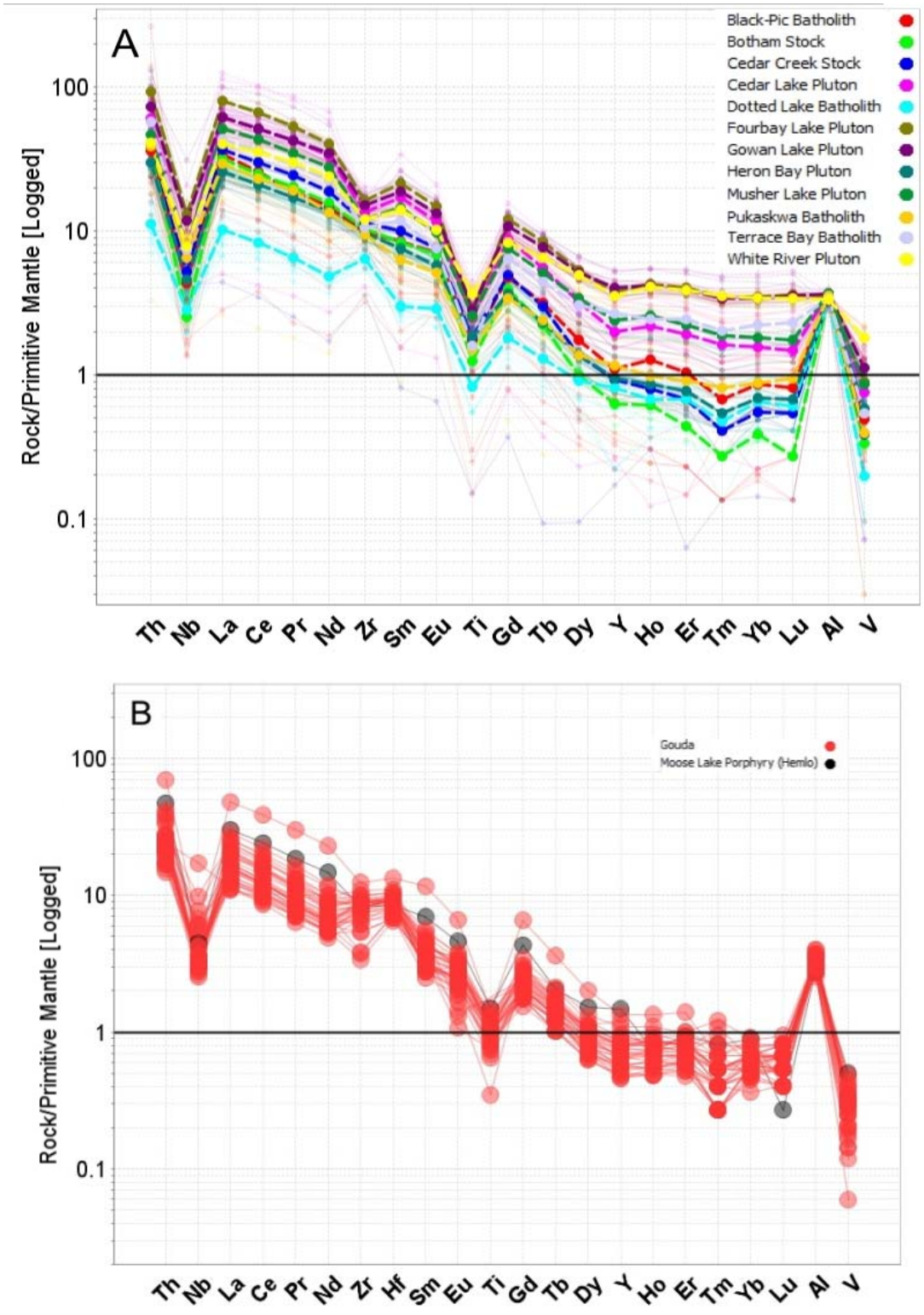

Figure 5.28: A) Primitive mantle normalised plot for intrusive rocks from the Schreiber-Hemlo greenstone belt, median values shown for clarity, compared to B) the felsic volcanic rocks of the Gouda Horizon (normalising values from Sun and McDonough, 1989; data from Beakhouse, 2001).

5.6 Tectonic Models

5.6.1 Previous Model

Polat et al. (1998) and Polat (2009) proposed a tectonic model which encompasses the Schreiber Hemlo and White River-Dayohessarah Greenstone Belts. They suggested that these belts represented collages of oceanic plateaus, juvenile oceanic island arcs, and subduction-accretion complexes accreted along a SSE-facing convergent plate margin through compressional and transpressional collisions. The supracrustal assemblages of these greenstone belts were later intruded by slab-derived TTG plutons. Polat et al. (1998) and Polat (2009) further argued that the structural, tectonostratigraphic, magmatic, and sedimentary characteristics of accreted material in the greenstone belts are analagous to certain Phanerozoic collisional belts, namely the Altaid-type (Turkic-type) collisional belts which possess very large sutures (up to several hundred km wide) characterized by subduction-accretion complexes and arc-derived granitoid intrusions- similar to the Circum-Pacific accreted terranes.

Polat et al. (1998) described three geochemical associations in their model, plume-derived oceanic plateaus, oceanic arcs and orogenic trench turbidities. They showed that crustally uncontaminated ocean plateau Fe- to Mg-tholeiites are overlain by arc-derived bi-modal, calc-alkaline volcanic rocks in the vicinity of Hemlo, although the original stratigraphic relationships have been disrupted by strike-slip faulting, thrusting, folding, and ductile deformation. These relationships suggest an intra-oceanic arc geodynamic setting formed through the initiation of a subduction zone at the margins of ocean plateau(s) (Polat et al., 1998). Out of order thrust and normal faulting resulted in the juxtaposition of plateau basalts, arc volcanic rocks and trench sediments to result in the observed stratigraphic relationships in the greenstone belt. This model is shown in Figure 5.29.

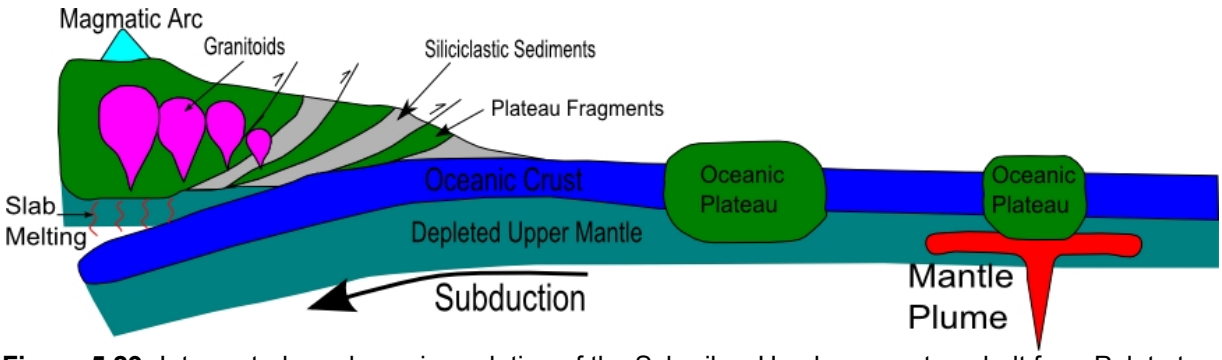

Figure 5.29: Interpreted geodynamic evolution of the Schreiber-Hemlo greenstone belt from Polat et al. (1998). Tholeiitic basalts found in the Schreiber-Hemlo Greenstone Belt erupted from a mantle plume, forming an oceanic plateau. The initiation of a subduction zone at the edge of the oceanic plateau created a magmatic island arc. Accretion of the oceanic plateau basalts, and siliciclastic sedimentary rocks with arc volcanic rocks and associated granitic plutonic rocks led to the juxtaposition of these units in the greenstone belt. Modified after Polat et al. (1998).

5.6.2 A New Model for Hemlo East

The geochemistry and geochronology presented in this study demonstrate that a long lived oceanic subduction zone produced the arc rhyolites and granitic intrusive rocks seen in the Hemlo East Property. Plutonism in the Pukaskwa Batholith spans 31 m.y. and there has been volcanism over 18 m.y. within the Hemlo East Property. There is no indication from this study as to what crust the pre-tectonic plutons would have intruded into, however, Beakhouse and Davis (2005) presented evidence of pillow basalts as xenoliths within the Pukaskwa and Black Pic Batholiths which could represent older oceanic crust from an early arc. High La/Yb_n ratios for the rhyolites at Hemlo East suggest that their source magmas were derived at depth possibly from the melting of the subducting slab, in a mechanism similar to that invoked for moden adakites. Primitive island arc tholeiites (metabasalts) are interpreted to have erupted from a spreading back-arc behind the island arc. The ε_{Nd} of metabasalts suggests that they are largely uncontaminated but some crustal contamination has taken place, possibly from the adjacent protocontinent, as the Wawa-Abitibi Terrane had begun to collide with the Wabigoon Terrane of the composite Superior province at 2695 Ma (Percival et al., 2006). The area between the arc and back-arc would have allowed for island arc tholeiites to be

deposited alongside rhyolites and sediments coming off the volcanic arc. These supracrustal units were later intruded by TTG plutons. This model is shown in Figure 5.30.

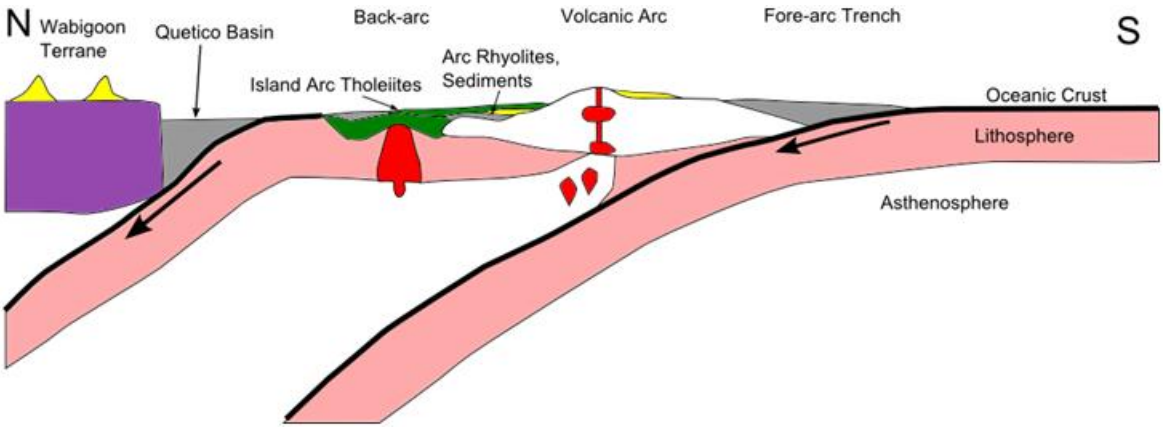

Figure 5.30: Interpreted geodynamic evolution of the Schreiber-Hemlo greenstone belt.

The Gouda felsic volcanic unit is the oldest volcanic unit dated in the greenstone belt, and it has been demonstrated that, at least in the Gouda-Thor-Carroll area, stratigraphy is right way up and younging towards the north. This means that the Hemlo East stratigraphy may represent the oldest stratigraphy preserved in the greenstone belt. The results from this study represent an earlier stage in the development of the volcanic arc compared to the results discussed in Polat et al. (1998) and Polat (2009) who reported the presence of transitional to alkaline basalts (NEB) and calc-alkaline basalts which may represent a more mature phase of the arc.

5.6.2 Discussion

Polat et al. (1998) and Polat (2009) state that the Schreiber-Hemlo Greenstone Belt resembles certain Phanerozoic collisional belts, however, Phanerozoic subduction-accretion complexes and continental suture zones typically have ophiolitic fragments and high-pressure metamorphic rocks such as blueschists and eclogites indicative of high-pressure low to hish temperature conditions in the subduction zone, and slab dehydration wedge-melting low-La/Yb_n granitoids (Martin, 1986). Archean greenstone terranes are devoid of these

associations, but are characterized by abundant, typically high La/Yb_n and Sr/Y, granitoids (Martin, 1986). The angle of subduction may be an important control on the existence of blueschists and eclogites in the Archean. The melting of a hotter Archean mantle would result in the subduction of, on average, younger oceanic lithosphere. This could be achieved either by subduction of hotter, faster, and hence shallower-subducting oceanic plates, promoting high-temperature metamorphism and slab melting (cf. Burke et al., 1976; Dewey and Windley, 1981; Abbott et al., 1994). In general, larger, colder, Phanerozoic plates subduct at steeper angles, generating high-pressure low-temperature conditions for blueschists. This may explain the secular distribution of both the high-pressure metamorphic rocks and slab-derived granitoids. Consequently, it is likely that the Schreiber-Hemlo Greenstone Belt represents horizontal tectonic processes similar but not identical to those of the Phanerzoic.

Polat et al. (1998) state that crustally uncontaminated ocean plateau Fe- to Mg-tholeiites are overlain by arc-derived bimodal, calc-alkaline volcanic rocks in the vicinity of Hemlo and use this relationship to make the conclusion that the tectonic environment was a subduction zone at the margin of an oceanic plateau (Polat et al., 1998). But it is clear from observations made within the Hemlo East Property that basalts, rhyolites, and sediments were deposited at the same time in stratigraphic continuity and these relationships are not the result of tectonic juxtaposition. It has been shown that the metabasalts of the Hemlo East Property with similar geochemical characteristics to the crustally uncontaminated mantle plume related oceanic plateau basalts reported by Polat (2009) are best interpreted as primitive island arc tholeiites. VMS mineralisation in the Gouda and DC Lake horizons is also consistent with a primitive island arc environment.

The model developed in this study and Polat's (2009) model could work in conjunction if, the entirety of units sampled in this study were shown to be part of one out of place block bounded by thrust faults. The volcanic rocks within the south end of the Hemlo East Property

have been shown to be the oldest within the greenstone belt, and consequently may fit into Polat's (2009) model as an earlier phase of development of the volcanic arc.

Chapter 6

Conclusions

6.1 Summary of Previous Chapters

Lithologies within the Hemlo East Property are broadly divided into mafic metavolcanic rocks, felsic metavolcanic rocks, metasedimentary rocks, intrusive and metaintrusive rocks. Stratigraphic continuity within the study area is demonstrated by the large number of drill holes in the area. All stratigraphic units dip to the north at 35-50°. The DC Lake Fault is dextral and separates identical offset stratigraphy on either side. Cobaltinitrite rock staining indicates that the distribution of K-feldspar in felsic metavolcanic rocks in the Gouda-Thor-Carroll area is a product of alteration associated with base metal and gold mineralization.

The geochemistry of metabasalts in the Hemlo East Property is consistent with generation within a primitive arc setting comparable to the South Sandwich Islands and Tonga–Kermadec arcs (Hawkesworth et al., 1993). Felsic metavolcanic rocks have an arc signature and most closely resemble FI rhyolites which are interpreted by Lesher et al. (1985) to have been derived from deep sourced magma chambers. Metasedimentary rocks are geochemically similar to felsic metavolcanic rocks and are interpreted to be derived wholly, or in part, from a felsic source.

Results from the new and compiled U-Pb geochronological data, indicate that there are two associations of felsic volcanism and two associations of plutonism. This data points toward a northward younging of stratigraphy in the Gouda-Thor-Carroll area which would mean that the stratigraphy is right way up. Volcanic centres have been short-lived (2 to 7 m.y.), and plutonism has been long-lived (up to 30 m.y.) in this arc.

A long-lived oceanic subduction zone is interpreted to have produced the arc rhyolites and granitic intrusive rocks seen in the Hemlo East Property. There is no indication from this study as to what comprised the crust that the pre-tectonic plutons were intruded into. High

La/Yb_n ratios for the rhyolites suggest that their source magmas were derived at depth from the subducting slab. Island arc tholeiites (metabasalts) erupted in a primitive back-arc setting behind the main island arc. The area between the arc and back-arc would have allowed for island arc tholeiites to be deposited alongside rhyolites in conjunction with sediments coming off of the volcanic arc consistent with the stratigraphic associations seen in the Gouda-Thor-Carroll area. These supracrustal units were later intruded by TTG plutons.

6.2 Exploration Implications

The felsic volcanic rocks of the Hemlo East property have been demonstrated to be FI rhyolites which are typically barren for base metal VMS mineralisation unless associated with FII or FIII type felsic volcanic rocks (Lesher et al., 1985). FI-type rhyolites appear to be particularly associated with gold-rich VMS deposits, such as the world-class Laronde deposit (Gaboury and Pearson, 2008), so the Gouda/Thor horizon may be prospective for this deposit type. The association of base metal sulphides with gold mineralisation within the Gouda deposit (Armstrong and Magnan, 1998) in conjunction with base metal mineralisation at DC Lake in an island arc environment would suggest a VMS origin for the mineralisation. There have been two models proposed for Au-rich VMS deposits by Dubé et al. (2008): A) a synvolcanic model where the VMS deposit would differ from the conventional massive sulphide deposits by an anomalous fluid chemistry and/or deposition within a shallow-water to subaerial volcanic setting which could allow for high-grade gold mineralisation to be deposited alongside base metal mineralisation; B) a conventional syngenetic volcanic-hosted Au-poor VMS mineralization overprinted by a lode-gold deposit. The world-class Hemlo lode gold deposit (Muir, 2002) is located adjacent to the Hemlo East Property. Because of the proximity of both lode gold (Hemlo) and gold-poor base metal (Big Lake, DC Lake) mineralisation to the Gouda deposit, it is possible that the gold mineralisation within the Gouda deposit is not a product of synvolcanic VMS formation, but a later overprint of an

Archean lode gold deposit over base metal VMS mineralisation. However, the lack of FII and FII rhyolites associated with the Gouda horizon argues against typical VMS mineralization in the first place, therefore it is proposed that the Gouda horizon is an example of a rare gold-rich VMS occurence.

6.3 Implications and Suggestions for Future Work

This study has generated eight new ages for the Hemlo East area and demonstrated the presence of a previously unrecognised volcanic event at 2704-2706 Ma. Geological mapping and drill core logging has given a better understanding of stratigraphy within the Gouda-Thor-Carroll area. Trace element geochemistry of 198 intrusive, metavolcanic and metasedimentary samples has allowed for interpretations of the tectonic environment in which they were formed. The combination of lithostratigraphy, geochemistry and geochronology had led to the generation of a new tectonic model for the Hemlo East Property incorporating horizontal plate tectonic theory.

The Pukaskwa Batholith was determined to be long-lived and multiphase (dated at 2718± 1.4 and 2688± 3 Ma); it would be helpful to collect geochronological samples from multiple locations within the Pukaskwa Batholith to assess its multiphase character. This would help assess whether there are multiple ages of emplacement within the batholith or if there are only the two dated phases present; if there are syn-metamorphism ages present within the batholith, it could be identified as the metamorphic heat source as none has been yet identified (Thompson, 2006). Polat's (2009) geodynamic model for the Schreiber-Hemlo greenstone belt could be tested by mapping out thrust faults within the greenstone belt. A systematic lithogeochemical sampling of mafic metavolcanic rocks within the greenstone belt could help determine whether there is a secular evolution from primitive arc basalts in the south of the greenstone belt to alkaline basalts in the north.

The tectonic model generated for the Hemlo East Property supports active horizontal plate tectonics for greenstone belt during the Archean. Beakhouse and Lin (2006) have proposed a synchronous vertical and horizontal tectonic model where the Schreiber-Hemlo Greenstone Belt formed as a result of processes similar to modern horizontal plate tectonics, whereas the Pukaskwa Batholith formed as a buoyant dome rising through the crust as in the vertical tectonic model proposed by Bédard et al. (2003) for the Archean Minto Block. Although there are no tectonic implications for the Pukaskwa batholith in this study it does support the argument for horizontal tectonism within the Schreiber-Hemlo greenstone belt of the Beakhouse and Lin (2006) model.

References

Abbott, D.H., Drury, R., and Smith. W.H.F.1994. Flat to steep transition in subduction style. Geology, 22, 937-940.

Albarède F. 2003. Geochemistry, An Introduction. University Press, Cambridge, 250p.

Armstrong, T., and Magnan, M. 1998.Compilation and lithogeochemical sampling program, White River Property, Hemlo Camp, Ontario. Lac Exploration Inc. Report No. 42C12NE200.

Beakhouse, G.P. 2001. Nature, timing and significance of intermediate to felsic intrusive rocks associated with the hemlo greenstone belt and implications for the regional geological setting of the hemlo gold deposit. Ontario Geological Survey, Open File Report 6020, 248p.

Beakhouse, G.P. and Davis, D.W. 2005. Evolution and tectonic significance of intermediate to felsic plutonism associated with the Hemlo greenstone belt, Superior Province, Canada. Precambrian Research, 137, 61-92.

Beakhouse, G.P., and Lin, S. 2006. Tectonic significance of the Pukaskwa Batholith and its contact relationships with the Hemlo and Mishibishu Greenstone Belts. Ontario Geological Survey Open File Report 6192, 7-1 to 7-7.

Bédard, J.H., Brouillette, P., Madore, L., Berclaz, A. 2003. Archean cratonization and deformation in the northern Superior Province, Canada: an evaluation of plate tectonic versus vertical tectonic models. Precambrian Research, 127, 61-87.

Burke, K., Dewey, J.F., and Kidd, W.F.1976. Dominance of horizontal movements, arc and microcontinental collisions during the later permobile regime. *In* The Early History of the Earth. *Edited by* B.F. Windley. Wiley, New York. 113-129.

Burnham, O.M., Hechler, J.H., Semenyna, L., and Schweyer, J. 2002. Mineralogical controls on the determination of trace elements following mixed acid dissolution. *In* Summary of Field Work and Other Activities 2002. Ontario Geological Survey Open File Report 6100, 36-1 to 36-12.

Burnham, O.M., and Schweyer, J. 2004. Trace Element Analysis of Geological Samples by ICP-MS at the Geoscience Laboratories: Revised Capabilities Due to Improvements to Instrumentation. *In* Summary of Field Work and Other Activities 2004. Ontario Geological Survey Open File Report 6145, 54-1 to 54-20.

Card, K., and Ciesielski, A. 1986. Subdivisions of the Superior Province of the Canadian Shield. Geoscience Canada, 13, 5-13.

Corfu, F., and Muir, T.L.1989a. The Hemlo-Heron Bay greenstone belt and Hemlo Au-Mo deposit, Superior Province, Ontario, Canada. I: Sequence of igneous activity determined by zircon U-Pb geochronology. Chemical Geology, 79, 183-200.

Corfu, F., and Muir, T.L., 1989b. The Hemlo–Heron Bay greenstone belt and Hemlo Au–Mo deposit, Superior Province, Ont., Canada. Part 2. Timing of metamorphism, alteration and Au mineralization from titanite, rutile and monazite geochronology.Chemical Geology, 79, 201–223.

Cousens, B.L., 1996. Magmatic evolution of Quaternary mafic magmas at Long Valley Caldera and the Devils Postpile, California: Effects of crustal contamination on lithospheric mantle-derived magmas. Journal of Geophysical Research, 101, 27673-27689.

Davidson, J.P., 1996. Deciphering mantle and crustal signatures in subduction zone magmatism. Subduction Top to Bottom. Geophysical Monograph, 96, 251-262.

Davis, D.W., Beakhouse, G.P., and Jackson, S.L. 1998. U–Pb zircon and titanite geochronology, Part 3 In: Regional Setting of the Hemlo Gold Deposit: An Interim Progress Report. Ontario Geological Survey, Open File Report 5977, pp. 151.

Davis, D.W. and Lin, S. 2003. Unraveling the Geologic History of the Hemlo Archean Gold Deposit, Superior Province, Canada: A U-Pb Geochronological Study. Economic Geology, 98, 51-67.

Dubé, B., Gosselin, P. Mercier-Langevin, P., Hannington, M., and Galley, A., 2007, Gold-rich volcanogenic massive sulphide deposits, in Goodfellow, W.D., ed., Mineral Deposits of Canada: A Synthesis of Major Deposit-Types, District Metallogeny, the Evolution of Geological Provinces, and Exploration Methods: Geological Association of Canada, Mineral Deposits Division, Special Publication No. 5, p. 75-94.

Dewey. J.F., and Windley, B.F., 1981. Growth and differentiation of continental crust. Philos. Trans. R. Soc. London, A30I, 189-206.

Elliott, T., Planck, T., Zindler, A., White, W., Bourdon, B., 1997. Element transport from slab to volcanic front at the Mariana arc. Journal of Geophysical Research, 102, 14,991–15,019.

Ewart, A., Hergt, J.M., Hawkins, J.W., 1994. Major element, trace element, and isotope (Pb, Sr, and Nd) geochemistry of site 839 basalts and basaltic andesites: Implications for arc volcanism. Proceedings of the Ocean Drilling Program. Scientific Result,s 135, 519-531.

Fage, A. 2010. Assessment Report on the Hemlo East Property. Metalcorp Limited, Unpublished Report, 44p.

Fleet, M.E. and Pan, Y. 1991.Metamorphic Petrology of the White River Gold Prospect, Hemlo Area.Ontario Geological Survey, Grant 305, Final Report, 47 pp.

Fralick, P., Purdon, R.H., Davis, D.W. 2006. Neoarchean trans-subprovince sediment transport in southwestern Superior Province: sedimentological, geochemical, and geochronological evidence. Canadian Journal of Earth Science, 43, 1055-1070.

Gaboury, D. and Pearson, V. 2008. Rhyolite Geochemical Signatures and Association with Volcanogenic Massive Sulphide Deposits: Examples from the Abitibi Belt, Canada. Economic Geology, 103, 1531-1562.

Gerstenberger, H., and Haase, G. 1997. A highly effective emitter substance for mass spectrometric Pb isotope ratio determinations. Chemical Geology, 136, 309–312.

Guthrie, A.E., 1985; Geological Report for Sub-Property M12; Lac Minerals Ltd. 54p. Report No. 42C12NW0164.

Harvey, J.D. 1968. Diamond drill logs, Area of White Lake (So. Part). Mattagami Lake Mines (Carroll Option). Report No. 10.

Hawkesworth, C.J., Gallagher, K., Hergt, J.M., McDermott, F. 1993. Mantle and slab contributions in arc magmas. Annual Review of Earth and Planetary Sciences, 21, 175-204.

Hutchison,C. S. 1974. Laboratory Handbook of Petrographic Techniques, A Wiley-Interscience Publication, 527 pp.

Jackson, S.L., Beakhouse, G.P., and Davis, D.W. 1998: Regional Geological Setting of the Hemlo Gold Deposit; An Interim Progress Report; Ontario Geological Survey, Open File Report 5977, 151 p.

Jenner, G., 1996. Trace element geochemistry of igneous rocks: geochemical nomenclature and analytical geochemistry. In: Wyman, D. (Ed.). Trace Element Geochemistry of Volcanic Rocks: Applications for Massive Sulphide Exploration. Geological Association of Canada Short Course Notes, 12, 51-77.

Kent, J. A. 1984; Geology Report for Sub-Property M12; Lac Minerals Ltd. p. 29. Report No. 42C12NE0019.

Kerrich, R., Polat, A., Wyman D., and Hollings, P. 1999. Trace element systematic of Mg-, to Fe-tholeiitic basalt suites of the Superior Province: implications for Archean mantle reservoirs and greenstone belt genesis. Lithos, 46, 163-187.

Lentz, D.R. 1998. Petrogenetic evolution of felsic volcanic sequences associated with Phanerozoic volcanic-hosted massive sulphide systems: the role of extensional geodynamics. Ore Geology Reviews, 12, pp. 289-327

Lesher, C.M., Goodwin, A.M., Campbell, I.H. and Gorton, M.P. 1985. Trace-element geochemistry of ore-associated and barren, felsic metavolcanic rocks in the Superior Province, Canada. Canadian Journal of Earth Sciences, 23, 222-237.

Lin, S., 2001. Stratigraphic and structural setting of the Hemlo gold deposit, Ontario, Canada. Economic Geology, 96, 477– 507.

Ludwig K.R. 2003. Isoplot 3.00, A Geochronological Toolkit for Microsoft Excel.University of California at Berkely, kludwig@bgc.org.

MacDonald, R., Hawkesworth, C.J., Heath, E., 2000. The Lesser Antilles volcanic chain; a study in arc magmatism. Earth Science Reviews, 49, 1-76.

Martin, H. 1986. Effect of steeper Archean geothermal gradient on geochemistry of subduction zone magmas. Geology, 14, 753-756

Mattinson, J.M. 2005. Zircon U–Pb chemical abrasion (CA-TIMS) method:Combined annealing and multi-step partial dissolution analysis for improved precision and accuracy of zircon ages, Chemical Geology, v. 220, pp. 47-66.

McIlveen, D.G., Stanley, M.C., 1985; Geology of the North Carroll Grid Properties L12, L113, White River Claim Group. Lac Minerals Ltd. p.43. Report No. 42C12NE0059.

Miyashiro A.1974. Volcanic rock series in island arcs and active continental margins. American Journal of Science, 274, 317-327.

Mosier, D.L., Berger, V.I., and Singer, D.A., 2009, Volcanogenic massive sulfide deposits of the world; database and grade and tonnage models: U.S. Geological Survey Open-File Report 2009-1034.

Muir, T.L. 1982.Geology of the Hemlo Area, district of Thunder Bay. Ontario Geological Survey Report 217, 65p.

Muir, T.L. 1997. Precambrian geology, Hemlo Gold Deposit Area; Ontario Geological Survey, Report 289, 219pp.

Muir, T.L. 2000 Geological compilation of the eastern half of the Schreiber-Hemlo greenstone belt; Ontario Geological Survey, Map 2614, scale 1:50000.

Muir, T.L. 2002. The Hemlo gold deposit, Ontario, Canada: principal deposit characteristics and constraints on mineralization. Ore Geology Reviews, 21, 1-66.

Mundil, R. Ludwig, K. R., Metcalfe, I, and Renne, P.R. 2004. Age and Timing of the Permian Mass Extinctions: U/Pb Dating of Closed-System Zircons. Science, 305, 1760-1763.

Osmani, I.A. 1991. Proterozoic mafic dike swarms in the Superior Province of Ontario. *in* Geology of Ontario, Ontario Geological Survey, Special Volume 4, Part 1, pp. 661–681.

Paakki, J. and Thompson, M. 2001.Teck Exploration Limited, MNDM Assessment File, Assessment Report on the 2000 Exploration Program on the White River Property.

Page, R. 1999. Teck Exploration Limited, MNDM Assessment File, Lithogeochemical Sampling of Archived Drill Core, White River Property (Bomby, Brothers, and Laberge Townships), Northern Ontario.

Pan, Y. and Fleet, M.E. 1988. Metamorphic petrology of the White River gold prospect, Hemlo area. Ontario Geological Survey, Miscellaneous Paper 140, 164-176.

Pan, Y. and Fleet, M.E. 1989a. Metamorphic petrology and gold mineralization of the White River gold prospect, Hemlo area.Ontario Geological Survey, MiscellaneousPaper 143, 42-52.

Pan, Y. and Fleet, M.E. 1989b.Cr-rich calc-silicates from the Hemlo area, Ontario. Canadian Mineralogist, 27, 565-577.

Pan, Y. and Fleet, M.E. 1990a Halogen-bearing allanite from a White River gold occurrence, Hemlo area, Ontario. Canadian Mineralogist, 28, 67-75.

Pan, Y. and Fleet, M.E. 1990b. Metamorphic petrology, geochemistry and gold mineralization of the White River gold prospect, Hemlo area.Ontario Geological Survey.

Pan, Y. and Fleet, M.E. 1993. Polymetamorphism in the Archean Hemlo - Heron Bay greenstone belt, Superior Province: P–T variations and implications for tectonic evolution. Canadian Journal of Earth Sciences, 30, 985–996.

Pearce, J., 2007. Geochemical fingerprinting of oceanic basalts with applications to ophiolite classification and the search for Archean oceanic crust. Lithos, 100, 14- 48.

Pearce, J.A., Peate, D.W., 1995. Tectonic implications of the composition of volcanic arc magmas. Annual Review of Earth and Planetary Science Letters, 23, 252-285.

Pearce, J.A., Baker, P.E., Harvey, P.K., Luff, I., 1995. Geochemical evidence for subduction fluxes, mantle melting and fractional crystallization beneath the South Sandwich island arc. Journal of Petrology, 36, 1073–1109.

Pearce, J.A., Kempton, P.D., Nowell, G.M., Noble, S.R., 1999. Hf–Nd element and isotope perspective on the nature and provenance of mantle and subduction components in Western Pacific arc-basin systems. Journal of Petrology, 40, 1579-1611.

Percival J., 2006. Geology and metallogeny of the Superior province, Canada. Geological Survey of Canada: http://gsc.nrcan.gc.ca/mindep/synth_prov/superior/pdf/ regional_synthesis.superior.percival.pdf

Percival, J., Sanborn-Barrie, M., Skulski, T., Stott, G., Helmstaedt, H., and White, D. 2006. Tectonic evolution of the western Superior Province from NATMAP and Lithoprobe studies. Canadian Journal of Earth Sciences, 43, 1085-1117.

Polat, A. 2009. The geochemistry of the Neoarchean (ca. 2700Ma) tholeiitic basalts, transitional to alkaline basalts, and gabbros, Wawa Subprovince, Canada: Implications for petrogenetic processes. Precambrian Research, 168, 83-105.

Polat, A., Kerrich, R., Wyman, D.A. 1998. The late Archean Schreiber-Hemlo and White River-Dayohessarah greenstone belts, Superior Province: collages of oceanic plateaus, oceanic arcs, and subduction-accretion complexes. Tectonophysics, 289, 295-326.

Polat, A., and Kerrich, R., 1999. Formation of an Archean tectonic melange in the Schreiber-Hemlo greenstone belt, Superior Province, Canada: implications for Archean subduction-accretion processes. Tectonics, 18, 732-753.

Polat, A. and Kerrich, R., 2001. Magnesian andesites, Nb-enriched basalts-andesites, and adakites from late Archean 2.7 Ga Wawa greenstone belts, Superior province, Canada: implications for late Archean subduction zone petrogenetic processes. Contributions to Mineralogy and Petrology, 141, 36-52.

Rinne, M.L. 2010. Seafloor Deposit Models, Geochemistry, and Petrology of the Mafic-Ultramafic Hosted Big Lake VMS Occurrence, Marathon, Ontario. Unpublished MSc Thesis, Lakehead University, Thunder Bay, Ontario. 167 p.

Richard, P., N. Shimizu, C. J. Allègre, 1976. $^{143}Nd/^{146}Nd$, a natural tracer: an application to oceanic basalts. Earth and Planetary Science Letters, 31, 269-278.

Sajona, F.G., Maury, R.C., Bellon, H., Cotten, J., Defant, M., 1996. High field strength element enrichment of Pliocene–Pleistocene island arc basalts, Zamboanga Peninsula, Western Mindanao (Philippines). Journal of Petrology 37, 693-726.

Schmitz, M. D., and Schoene, B. 2007, Derivation of isotope ratios, errors, and error correlations for U-Pb geochronology using 205Pb-235U-(233U)-spiked isotope dilution thermal ionization mass spectrometric data. Geochemistry, Geophysics, Geosystems, 8. Q08006, doi:10.1029/2006GC001492.

Schnieders, B.R., Scott, J.F., Smyk, M.C., O'Brien, M.S., 2000. Report of activities, 1999 Resident Geologists Program: Thunder Bay South District Regional Resident Geologist Report. Ontario Geological Survey, Open File Report 6005, 51 pp.

Scoates, J.S. and Friedman, R.M. 2008. Precise age of the platiniferous Merensky Reef, Bushveld Complex, South Africa, by the U-Pb zircon chemical abrasion ID-TIMS technique. Economic Geology, 103, 465-471.

Shevchenko, G. 1995a. Geological Mapping Surveys, White River Property "Main Block",Thunder Bay Mining Division, Ontario; Placer Dome Canada Limited Assessment Report, 36 pp.

Shevchenko, G. 1995b.Diamond Drilling Surveys, White River Property, Thunder Bay Mining Division, Ontario; Placer Dome Canada Limited Assessment Report, 36 pp.

Skulski, T., Corkery, M., Stone, D., Whalen J., and Stern, R., 2000. Geological and geochronological investigations in the Stull Lake-Edmund Lake greenstone belt and granitoid rocks of the northwestern Superior Province. Report of Activities, Manitoba Geological Survey (2000): 117-128.

Sterritt V. and Rudd, J. 2009. Interpretation of Helicopter-Borne AeroTEM Electromagnetic & Magnetic Data. Fearless Python Property, Marathon area, Ontario. Aeroquest Job # 08031i

Stott, G.M., Corkery, M.T., Percival, J.A., Simard, M. and Goutier, J. 2010. A revised terrane subdivision of the Superior Province; *in* Summary of Field Work and Other Activities 2010, Ontario Geological Survey, Open File Report 6260, 20-1 to 20-10.

Sun, S.-s., and McDonough, W.F. 1989. Chemical and isotopic systematics of oceanic basalts: implications for mantle composition and processes. In Magmatism in the ocean basins. Geological Society, Special Publication No.42, 313-345.

Talbot, D. A. 1997: Diamond Drilling Program, White River Property, Thunder Bay Mining Division, Northern Ontario; Placer Dome Canada Limited Assessment Report, 29 p.

Taylor, R.N., Lapierre, H., Vidal, P., Nesbitt, R.W., Croudace, I.W., 1992. Igneous geochemistry and petrogenesis of the Izu–Bonin forearc basin. In: Maddox, E.M. (Ed.), Proceedings of the Ocean Drilling Program, Bonin Arc-Trench System. Scientific Results, 405-430.

Thirlwall, M.F. 2000. Inter-laboratory and other errors in Pb isotope analyses investigated using a 207Pb–204Pb double spike. Chemical Geology, 163: 299–322.

Thompson, P.H. 2006. A new metamorphic framework for the Hemlo greenstone belt: Implications for deformation, plutonism, alteration and gold mineralization; Ontario Geological Survey, Open File Report 6190, 80pp.

Thompson, M., Galway, C., and Page, R. 1999: Geological Report on the 1999 Exploration Program, White River Property, Bomby, Brothers, Laberge Townships: Teck Exploration Ltd. Report No. 1328NB, 31 p.

Thompson, M., and Paakki, J. 2001. Assessment report on the 2000 exploration program on the White River Property. Bomby, Brothers and Laberge Townships, Ontario. Teck Exploration Ltd. Marathon, Ontario. Report No. 1340

Tomlinson, K.Y., Bowins, R., and Heshler, J. 1998. Refinement of Hafnium (Hf) and Zirconium (Zr) analysis by improvement in the sample digestion procedure. Ontario Geological Survey, Miscellaneous Paper 169, 189-192.

Tomlinson, K.Y., Stott, G.M., Percival, J.A. Stone D. 2004. Basement terrane correlations and crustal recycling in the western Superior Province: Nd isotopic character of granitoid and felsic volcanic rocks in the Wabigoon subprovince, N. Ontario, Canada. Precambrian Research, 132, 245–274.

Wells, R.C. 1996. Petrographic and interpretive reports for the White River Option (Project 505) Hemlo Greenstone Belt Ontario, Canada. Placer Dome Canada Ltd.

Williams, R.H., Stott, G.M., Heather, K., Muir, T.L., Sage, R.P. 1991. Wawa Subprovince. In:Thurston, P.C., Williams, H.R., Sutclife, H.R., Stott,G.M. (Eds.), Geology of Ontario, Ontario Geological Survey, spec. vol.4, Part1, 485–539.

Winchester J.A. and Floyd P.A., 1977. Geochemical discrimination of different magma series and their differentiation products using immobile elements. Chemical Geology, 20, 325-343.

Wyman, D.A., Ayer, J.A., Devaney, J.R., 2000. Niobium-enriched basalts from the Wabigoon subprovince, Canada: evidence for adakitic metasomatism above an Archean subduction zone. Earth and Planetary Science Letters 179, 21-30.

Appendix A

Core Logs

Appendix A-1: Drill Hole Locations. UTM zone 16U, Nad83.

Hole	Length	Easting	Northing	Elevation (m)	Azimuth	Dip
WR00-01	152.2	590225	5388647	355	180	-60
WR00-02	117.8	590500	5388575	351	180	-60
WR00-03	368	590225	5389360	350	180	-50
WR00-04	134	589615	5388660	351	185	-60
WR00-07	294	587700	5389490	351	180	-50
WR00-08	326	587700	5389490	351	180	-50
WR01-01	157	593275	5388046	396	160	-75
WR01-02	393.5	593650	5388450	380	187	-90
WR01-03	209	593847	5388175	374	190	-90
WR01-04	173	594183	5388154	366	180	-90
WR01-05	233	594400	5388325	388	180	-90
WR01-06	189	594695	5388350	366	180	-70
WR01-07	321	594050	5388437	381	180	-90
WR01-08	300	593010	5388964	374	190	-55
WR01-09	324	591607	5388892	343	180	-85
WR01-10	150	591125	5388655	355	190	-47
WR02-01	308	593337	5388313	407	180	-80
WR02-02	377	593075	5388400	383	180	-85
WR02-03	416	593075	5388956	372	180	-65
WR02-04	686	592300	5388996	354	180	-85
WR02-05	586	591885	5389224	350	180	-85
WR02-06a	551	591330	5389150	330	180	-80
WR02-09	295	590881	5388791	354	190	-85

Appendix A-2: Core Logs

Hole	From (m)	To (m)	Lithology
WR00-01	3	11.8	Biotite Metawacke
WR00-01	11.8	40.1	Lapilli Metabasalt Tuff
WR00-01	40.1	111	Metabasalt
WR00-01	111	119.8	Metasiltstone
WR00-01	119.8	149	Sericite Schist (Gouda)
WR00-01	149	152.2	Pukaskwa Gneiss
WR00-02	4	8.2	Biotite Metawacke
WR00-02	8.2	11.6	Banded Metasiltstone
WR00-02	11.6	25.4	Metabasalt
WR00-02	25.4	29.4	Banded Metasiltstone
WR00-02	29.4	47.2	Metabasalt
WR00-02	47.2	70.2	Banded Metasiltstone
WR00-02	70.2	72.7	Quartz Eye Sericite Schist (Gouda)
WR00-02	72.7	76.6	Banded Metasiltstone
WR00-02	76.6	92.8	Quartz Eye Sericite Schist (Gouda)
WR00-02	92.8	117.8	Biotite Amphibole Metawackes/ Pukaskwa Dykes
WR00-03	5.5	26.9	Biotite Feldspathic Metawacke
WR00-03	26.9	30.8	Biotite Feldspathic Graphitic Metawacke
WR00-03	30.8	121.7	Biotite Feldspathic Metawacke
WR00-03	121.7	129.6	Feldspathic Metawacke
WR00-03	129.6	211.8	Biotite Feldspathic Metawacke
WR00-03	211.8	250.3	Feldspathic Metawacke
WR00-03	250.3	321.6	Feldspathic Metawacke With Minor Sericite Schist
WR00-03	321.6	331.6	Granodiorite dike
WR00-03	331.6	334.7	Feldspathic Metawacke With Minor Sericite Schist
WR00-03	334.7	347.5	Metabasalt
WR00-03	347.5	351.1	Feldspathic Metawacke
WR00-03	351.1	368	Metabasalt
WR00-04	5	76.6	Metasiltstone
WR00-04	76.6	109.7	Sericite Schist (Gouda)
WR00-04	109.7	134	Amphibolite Gneiss
WR00-05	6.5	80.8	Biotite Metawacke
WR00-05	80.8	100.9	Biotite Metawacke, Feldspar Porphyry dikes
WR00-05	100.9	152.2	Biotite-Chlorite Metawacke
WR00-05	152.2	174.5	Diabase Dike
WR00-05	174.5	222.5	Biotite-Chlorite Metawacke
WR00-05	222.5	266	Biotite Metawacke
WR00-07	4	96	Biotite Metawacke
WR00-07	96	153.5	Silicified Felsic Schist (Frank Lake)
WR00-07	153.5	177.5	Metabasalt
WR00-07	177.5	180.5	Granodiorite Porphyry Dike, Faulted
WR00-07	180.5	243.5	Silicified Felsic Schist (Frank Lake)
WR00-07	243.5	295	Metawacke

Hole	From (m)	To (m)	Lithology
WR00-08	2	61.6	Metawacke
WR00-08	61.6	63	Gabbro Dike
WR00-08	63	96.5	Mixed Sediments
WR00-08	96.5	107.8	Silicified Felsic Schist (Frank Lake)
WR00-08	107.8	117	Feldspar Quartz Porphyry dike
WR00-08	117	171	Silicified Felsic Schist (Frank Lake)
WR00-08	171	209.5	Biotite And Feldspathic Metawacke
WR00-08	209.5	223.5	Felspar Porphyry dikes in Metawacke
WR00-08	223.5	326	Biotite And Feldspathic Metawacke
WR01-01	2	137	Banded Metasiltstone
WR01-01	137	158.3	Sericite Schist (Gouda)
WR01-01	158.3	167	Banded Metasiltstone
WR01-02	1	174.4	Metabasalt
WR01-02	174.4	214.2	Lapilli Metabasalt Tuff
WR01-02	214.2	243.3	Metabasalt
WR01-02	243.3	265.5	Banded Metasiltstone
WR01-02	265.5	268.8	Granodiorite dike
WR01-02	268.8	363.4	Feldspathic Metawacke
WR01-02	363.4	380.1	Sericite Schist (Gouda)
WR01-02	380.1	384.1	Feldspathic Metawacke
WR01-02	384.1	393.5	Diabase Dike
WR01-03	1	20.2	Lapilli Metabasalt Tuff
WR01-03	20.2	147.1	Hornblende Metawacke
WR01-03	147.1	163.9	Metabasalt
WR01-03	163.9	175.3	Quartz Eye Sericite Schist (Gouda)
WR01-03	175.3	186.6	Metasiltstone
WR01-03	186.6	197.3	Metabasalt
WR01-03	197.3	209	Pukaskwa dikes within Metabasalt
WR01-04	3	75.2	Hornblende Metawacke
WR01-04	75.2	88.2	Quartz Eye Sericite Schist (Gouda)
WR01-04	88.2	97.1	Metasiltstone
WR01-04	97.1	111	Metabasalt
WR01-04	111	173	Pukaskwa, Pegmatite dikes
WR01-05	1	66.6	Lapilli Metabasalt Tuff
WR01-05	66.6	168.6	Hornblende Metawacke
WR01-05	168.6	177.5	Fault Zone
WR01-05	177.5	193.7	Quartz Eye Sericite Schist (Gouda)
WR01-05	193.7	195.8	Metasiltstone
WR01-05	195.8	201.3	Metabasalt
WR01-05	201.3	233	Pukaskwa Gneiss
WR01-06	1	54.6	Lapilli Metabasalt Tuff
WR01-06	54.6	152.9	Hornblende Metawacke
WR01-06	152.9	172.1	Quartz Eye Sericite Schist (Gouda)
WR01-06	172.1	189	Metabasalt

Hole	From (m)	To (m)	Lithology
WR01-07	1	86.2	Metabasalt
WR01-07	86.2	138.3	Lapilli Metabasalt Tuff
WR01-07	138.3	163	Metabasalt
WR01-07	163	247.1	Hornblende Metawacke
WR01-07	247.1	263.7	Quartz Eye Sericite Schist (Gouda)
WR01-07	263.7	268.7	Hornblende Feldspathic Metawacke
WR01-07	268.7	292.5	Metabasalt
WR01-07	292.5	321	Pukaskwa, Pegmatite Dikes
WR01-08	3	36	Metabasalt
WR01-08	36	74.5	Biotite Metawacke
WR01-08	74.5	87	Metawacke
WR01-08	87	126.7	Metabasalt (altered)
WR01-08	126.7	178.1	Feldspathic Metawacke
WR01-08	178.1	300	Diabase Dike
WR01-09	3	129	Metabasalt
WR01-09	129	140.9	Granodiorite, Pegmatite dikes
WR01-09	140.9	149.8	Lapilli Metabasalt Tuff
WR01-09	149.8	196.4	Metawacke With Pegmatite dikes
WR01-09	196.4	201.6	Granodiorite dike
WR01-09	201.6	283.3	Hornblende Metawacke
WR01-09	283.3	307.6	Biotite Quartz Eye Sericite Schist (Gouda)
WR01-09	307.6	314.4	Granodiorite
WR01-09	314.4	324	Metabasalt
WR01-10	3	49.5	Metasiltstone
WR01-10	49.5	67.6	Metabasalt
WR01-10	67.8	99	Quartz Eye Sericite Schist (Gouda)
WR01-10	99	145.7	Metabasalt
WR01-10	145.7	153	Pukaskwa Gneiss
WR02-01	3.42	42.59	Metasandstone
WR02-01	42.59	95.71	Metabasalt
WR02-01	95.71	126.09	Lapilli Metabasalt Tuff
WR02-01	126.09	177.49	Hornblende Metawacke
WR02-01	177.49	185.19	Feldpar Porphyry Dike
WR02-01	185.19	234.3	Hornblende Metawacke
WR02-01	234.3	237.32	Pukaskwa Granite Dike
WR02-01	237.32	242.38	Hornblende Metawacke
WR02-01	242.38	248.43	Pukaskwa Granite Dike
WR02-01	258.2	283.45	Hornblende Metawacke And Metasiltstone
WR02-01	283.45	301.23	Quartz Eye Sericite Schist (Gouda)
WR02-01	301.23	308	Hornblende Metawacke

Hole	From (m)	To (m)	Lithology
WR02-02	3.1	111.3	Metabasalt
WR02-02	111.3	161.6	Lapilli Metabasalt Tuff
WR02-02	161.6	216.1	Hornblende Metawacke
WR02-02	216.1	218.5	Feldspar Porphyry Dike
WR02-02	218.5	248.43	Hornblende Metawacke
WR02-02	248.43	250.5	Pegmatite Dike
WR02-02	279.8	281.5	Hornblende Metawacke
WR02-02	281.5	322.45	Hornblende Metawacke And Metasiltstone
WR02-02	322.45	342.35	Sericite Schist (Gouda)
WR02-02	342.35	358.36	Metasiltstone
WR02-02	358.36	367.4	Feldspar Porphyry Dike
WR02-02	367.4	371.66	Pegmatite Dike
WR02-02	371.66	374.97	Metasiltstone
WR02-02	374.97	377	Pegmatite Dike
WR02-03	3.35	94.4	Biotite Metawacke
WR02-03	94.4	112.5	Hornblende Metawacke
WR02-03	112.5	157.1	Biotite Metawacke
WR02-03	157.1	228.3	Feldspathic Metawacke
WR02-03	228.3	240.26	Biotitic To Hornblende Metawacke
WR02-03	240.26	244.55	Pegmatite Dike
WR02-03	244.55	260.8	Biotitic To Hornblende Metawacke
WR02-03	260.8	263.22	Feldpar Porphyry Dike
WR02-03	263.22	268.31	Pegmatite Dike
WR02-03	268.31	271.23	Feldspar Porphyry Dike
WR02-03	271.23	397	Metabasalt
WR02-03	397	416	Hornblende Metawacke
WR02-04	3.2	130	Metabasalt
WR02-04	130	137	Layered Metabasalt
WR02-04	137	164.2	Lapilli Metabasalt Tuff
WR02-04	164.2	176.6	Metabasalt
WR02-04	176.6	191.1	Hornblende Metawacke
WR02-04	191.1	461.7	Metabasalt
WR02-04	461.7	498.8	Lapilli Metabasalt Tuff
WR02-04	498.8	509.5	Hornblende Metawacke
WR02-04	509.5	618.1	Metasiltstone
WR02-04	618.1	643.1	Quartz Eye Sericite Schist (Gouda)
WR02-04	643.1	647.9	Pukaskwa Granite Dike
WR02-04	647.9	654.8	Sericite Schist (Gouda)
WR02-04	654.8	663	Metasiltstone
WR02-04	663	678.9	Metabasalt
WR02-04	678.9	685	Pukaskwa Gneissic Complex

Hole	From (m)	To (m)	Lithology
WR02-05	4	89.7	Biotite Metawacke
WR02-05	89.7	91.3	Pegmatite Dike
WR02-05	91.3	129.3	Biotite Metawacke
WR02-05	129.3	135.5	Pegmatite Dike
WR02-05	135.5	153.5	Biotite Metawacke
WR02-05	153.5	164.8	Pegmatite Dike
WR02-05	164.8	236.1	Biotite Metawacke
WR02-05	238.1	241.1	Metabasalt
WR02-05	241.1	250.8	Feldspar Porphyritic dike
WR02-05	250.8	390.8	Metabasalt
WR02-05	390.8	419	Lapilli Metabasalt Tuff
WR02-05	419	531.9	Hornblende Metawacke
WR02-05	531.9	545.3	Quartz Eye Sericite Schist (Gouda)
WR02-05	545.3	548.6	Metasiltstone
WR02-05	548.6	554.05	Metabasalt
WR02-05	554.05	586	Pukaskwa Gneissic Complex
WR02-06a	2.9	123.2	Biotite Metawacke
WR02-06a	123.2	204.1	Feldspathic Metawacke
WR02-06a	204.1	211.1	Granitic Dike
WR02-06a	211.1	354.44	Metabasalt
WR02-06a	354.4	379	Lapilli Metabasalt Tuff
WR02-06a	379	406.5	Biotite To Hornblende Metawacke
WR02-06a	406.5	412.5	Felspar Porphyry Dyke
WR02-06a	412.5	486	Biotitic To Hornblende Metawacke
WR02-06a	486	505.8	Sericite Schist (Gouda)
WR02-06a	505.8	510.9	Pukaskwa Complex Dike
WR02-06a	510.9	521.33	Metabasalt
WR02-06a	521.3	535.8	Pukaskwa Complex Dike
WR02-06a	535.8	540.5	Pegmatite Dike
WR02-06a	540.5	551	Pukaskwa Complex Dike

Hole	From (m)	To (m)	Lithology
WR02-09	1.1	12.3	Biotite To Hornblende Metawacke
WR02-09	12.3	22	Lapilli Metabasalt Tuff
WR02-09	22	34.9	Hornblende Metawacke
WR02-09	34.9	38.4	Pegmatite Dike
WR02-09	38.4	49.5	Lapilli Metabasalt Tuff
WR02-09	49.5	61.8	Feldspathic Metawacke
WR02-09	61.8	65.5	Lapilli Metabasalt Tuff
WR02-09	65.5	68.9	Feldspathic Metawacke
WR02-09	68.9	73	Pegmatite Dike
WR02-09	73	96.2	Hornblende Metawacke
WR02-09	96.2	102.5	Feldspathic Metawacke
WR02-09	102.5	106.8	Feldspar Porphyry Dike
WR02-09	106.8	110.3	Hornblende Metawacke
WR02-09	110.3	124.06	Feldspathic Metawacke
WR02-09	124.06	156.6	Hornblende Metawacke
WR02-09	156.6	165.8	Metasiltstone
WR02-09	165.8	173.6	Hornblende Metawacke
WR02-09	173.6	220.5	Metasiltstone
WR02-09	220.5	224.8	Pegmatite Dike
WR02-09	224.8	226.8	Hornblende Metawacke
WR02-09	226.8	229.1	Sericite Schist (Gouda)
WR02-09	229.1	237.3	Hornblende Metawacke
WR02-09	237.3	251.4	Sericite Schist (Gouda)
WR02-09	251.4	258.6	Hornblende Metawacke
WR02-09	258.6	264	Granodiorite Dike
WR02-09	264	266.35	Sericite Schist (Gouda)
WR02-09	266.35	270	Pegmatite Dike
WR02-09	270	295	Diabase

Appendix B

Thin Section Descriptions

*Modal abundances are approximate

FR01: Metabasalt

Consisting of:

Hornblende 80%

Biotite 13%

Plagioclase 5%

Quartz 1%

Pyrite 1%

The sample is made up of weakly foliated anhedral porphyroblasts of hornblende, biotite and plagioclase with trace pyrite and quartz. A compositional banding is defined by separate zones of indentical mineralogy with equigranulare grain sizes of ~0.5mm and ~0.1mm respectively.

FR02: Metasandstone

Consisting of:

Quartz 60%

K-feldspar 20%

Plagioclase 10%

Muscovite 10%

The sample is made up of equigranular very fine-grained (<0.1mm) quartz, K-feldspar and plagioclase with <0.1mm muscovite porphyroblasts defining a foliation.

FR05: Metasandstone

Consisting of:

Quartz 60%

K-feldspar 20%

Plagioclase 10%

Biotite 5%

Muscovite 5%

The sample is made up of equigranular very fine-grained (~0.2mm) quartz, K-feldspar and plagioclase with 0.5mm biotite porphyroblasts defining a foliation. Three larger (~3mm) K-feldspar grains exhibiting perthitic texture are also present in this sample.

FR08: Metabasalt

Consisting of:

Hornblende 80%

Plagioclase 15%

Biotite 5%

Pyrite <1%

The sample is made up of weakly foliated anhedral equigranular (~0.1mm) porphyroblasts of hornblende, plagioclase and biotite.

FR09: Foliated Metabasalt

Consisting of:

Hornblende 90%

Plagioclase 5%

Biotite 4%

Pyrite 1%

The sample is made up of 3-5mm hornblende porphyroblasts within a <1mm hornblende, plagioclase with minor biotite and pyrite matrix.

FR10: Hornblende Plagioclase Schist (Amphibolite)

Consisting of:

Hornblende 40%

Plagioclase 40%

Biotite 10%

Quartz 9%

Pyrite 1%

The sample is made up of 3-5mm euhedral porphyroblasts of hornblende and biotite within a matrix of <1mm plagioclase, quartz, and biotite. 3-4mm blebs of pyrite are found throughout the sample. Schistosity is defined by alignment of biotite grains.

FR12: Metawacke

Consisting of:

Plagioclase 40%

Quartz 20%

Hornblende 15%

Biotite 15%

K-Feldspar 10%

Pyrite 1%

The sample is separated into two zones whose contact defines a foliation: 1) an equigranular (~0.2mm) porphyroblastic zone; and b) and very fine-grained (<1mm) zone of hornblende and biotite.

FR15: Metabasalt

Consisting of:

Hornblende 80%

Plagioclase 10%

Biotite 10%

Pyrite <1%

The sample is made up of moderately foliated anhedral equigranular (~0.3mm) porphyroblasts of hornblende, plagioclase and biotite.

FR18: Granodiorite adjacent to the Thor showing trench (dike)

Consisting of:

Plagioclase 60%

Quartz 23%

K-feldspar 13%

Biotite 3%

Opaque 1%

The sample is made up of 0.3-1mm plagioclase, quartz, and K-feldspar. Plagioclase is exhibiting exsolution to microcline textures.

FR20: Massive Sulphides from the Thor showing trench

Consisting of:

Pyrite 92%

Sphalerite 5%

Galena 2%

Chalcopyrite <1%

The sample is made up of dominantly euhedral pyrite rimmed by minor anhedral sphalerite with trace galena and chalcopyrite.

FR22: Feldspar Porphyritic Granitic Dike with Molybdenite

Consisting of:

Plagioclase 50%

K-feldspar 25%

Quartz 15%

Biotite 8%

Molybdenite 2%

The sample is made up of 0.5-1cm euhedral plagioclase crystals with subhedral K-feldspar (2-5mm) and quartz (1-2mm) crystals. Molybdenite occurs as layered sheets 2-5mm thick and 0.5-2cm in diameter.

FR25: Quartz Syenite – White River Pluton

Consisting of:

K-feldspar 50%

Quartz 25%

Plagioclase 15%

Hornblende 5%

Biotite 5%

Apatite <1%

Epidote <1%

Opaque <1%

The sample is made up of porphyritic K-feldspar (0.2-0.6mm), quartz (0.2-0.3mm), plagioclase (0.6-1.5mm), hornblende (0.5-1mm), and biotite (0.2-0.4mm).

FR26: Monzonite – White River Pluton

Consisting of:

Plagioclase 40%

Quartz 30%

K-feldspar 20%

Hornblende 5%

Biotite 5%

Apatite <1%

Titanite <1%

Opaque <1%

The sample is made up of porphyritic plagioclase (0.2-0.4mm), quartz (0.3-0.5mm), K-feldspar (1-3mm), hornblende (0.5-1mm), and biotite (0.3-0.5mm).

FR27: Quartz Sericite Schist – Gouda Horizon

Consisting of:

Quartz 50%

Sericite 30%

Fine-grained Groundmass 20%

The sample is made up of ~0.2mm quartz crystals and ~1.5mm relict quartz eyes with a foliation defined by sericite laths ~0.5mm thick and 2-5mm long. There is a very fine-grained groundmass made up of quartz, sericite, plagioclase, and K-feldspar.

HE20: Metagabbro

Consisting of:

Hornblende after pyroxene 75%

Plagioclase 10%

Quartz 5%

Biotite 5%

Pyroxene 5%

Opaque <1%

The sample is made up of clusters of ~0.2mm hornblende porphyroblasts pseudomorphing ~2mm pyroxene crystals. The matrix between these relict crystals is made up of ~0.2mm plagioclase, hornblende, quartz, biotite, and pyroxene crystals.

HE21: Metasandstone

Consisting of:

Quartz 80%

K-feldspar 10%

Plagioclase 8%

Biotite 2%

The sample is made up of inequigranular quartz (0.1-1.5mm), K-feldspar (0.3-1.5mm) and plagioclase (0.1-0.4mm) with a foliation defined by biotite (~0.2mm thick, 0.5-2mm long).

HE24: Metasandstone

Consisting of:

Quartz 40%

Microcline 40%

Plagioclase 18%

Biotite 2%

The sample is made up of inequigranular quartz (0.2-1mm), microcline (0.2-1mm), plagioclase (0.2-0.4mm), and biotite (~0.2mm)

HE25: Metasiltstone

Consisting of:

Quartz 30%

K-feldspar 20%

Hornblende20%

Biotite 20%

Plagioclase 10%

Opaque <1%

The sample is made up of equigranular (0.2-0.3mm) quartz, K-feldspar, plagioclase, with the foliation defined by alignment of hornblende and biotite.

HE26: Quartz Sericite Schist – Gouda Horizon

Consisting of:

Quartz 50%

Plagioclase 20%

K-feldspar 15%

Sericite 15%

The sample is made up of quartz (0.2-0.4mm), quartz eyes (1.5-2.5mm), plagioclase (0.2-0.4mm), and K-feldspar (0.2-0.4mm) with a foliation defined by sericite (~0.3mm thick and 0.4-1.5mm long).

HE34: Lapilli Metabasalt Tuff

Consisting of:

Hornblende 60%

Lapilli Fragments 20%

Plagioclase 15%

Biotite 5%

Opaque <1%

The sample is made up of metabasalt (<0.1mm-0.2mm porphyroblasts of hornblende, plagioclase and biotite; foliation defined by hornblende and biotite) with enclosed lapilli fragments. Lapilli fragments measure 3-7mm in diameter and distort the adjacent foliation.

WR06: Lapilli Metabasalt Tuff

Consisting of:

Hornblende 40%

Lapilli Fragments 20%

Plagioclase 25%

Biotite 5%

Opaque <1%

The sample is made up of metabasalt (0.2mm-0.3mm porphyroblasts of hornblende, plagioclase and biotite; foliation defined by hornblende and biotite) with enclosed lapilli fragments. Lapilli fragments measure 3-7mm in diameter and distort the adjacent foliation.

Frank Lake: Silicified Metasedimentary Rock

Consisting of:

Quartz 30%

Plagioclase 20%

K-feldspar 20%

Biotite 5%

Muscovite 5%

Fine-grained Groundmass 20%

The sample is made up of 0.1-2mm quartz, plagioclase, and K-feldspar with a foliation defined by the micas. A very fine-grained groundmass is made up of quartz, k-feldspar and muscovite.

Appendix C

Geochemistry

Appendix C-1: 2008 Geochemistry

All Samples reported in this section were collected in the 2008 field season and analysed using the OGS method. UTM zone 16U, Nad83. Major elements as wt.%, trace elements as ppm.

Sample	FR01	FR04	FR05	FR06	FR12	FR15	FR19
UTM_E	591006	590937	591009	590839	591122	591325	592633
UTM_N	5391888	5392346	5392463	5392507	5391933	5392461	5388538
Description	MetaBasalt	MetaBasalt	Meta-greywacke	MetaBasalt	Meta-greywacke	MetaBasalt	Felsic Volcanic
SiO_2	47.43	56.9	68.32	51.27	58.15	52.32	68.27
TiO_2	1.62	0.7	0.32	1.6	0.55	0.92	0.16
Al_2O_3	13.76	13.57	15.25	13.28	15.9	11.85	13.8
Fe_2O_3	17.29	7.97	2.45	17.85	5.79	10.76	6.21
MnO	0.31	0.14	0.03	0.3	0.09	0.21	0.01
MgO	5.63	5.69	1.4	4.24	3.46	8.87	0.2
CaO	9.48	7.38	2.85	4.31	5.22	10.57	1.54
Na_2O	2.86	3.77	5.3	2.35	5.02	3.09	5.24
K_2O	0.59	1.94	2.99	1.38	3.86	0.32	1.87
P_2O_5	0.1	0.45	0.21	0.12	0.42	0.45	0.06
LOI	0.63	0.68	0.47	2.67	0.68	0.65	2.37
Total	99.69	99.19	99.59	99.36	99.13	100	99.72
Cr	105	186	28	71	82	578	0
Co	61	31.5	8.7	54.6	26.3	47.1	3.5
Ni	86	55	18	57	53	105	0
Rb	23.2	49.7	63.8	69	106.9	7.2	56.8
Sr	241	893	1586	126	1197	245	810
Ba	135.3	766.2	1571.8	363.8	1739	190.7	750
Ce	11.5	67	52.9	9.9	159.6	64.2	7.7
V	385	152	38	446	114	219	34
Ta	0.2	0.3	0.3	0.2	0.2	0.3	0.2
Nb	3.1	5.89	4.47	3.35	4.65	4.56	1.67
Zr	83	143	152	88	225	121	100
Hf	2.49	3.74	4.06	2.61	5.06	3.17	2.97
Th	0.37	4.54	6.24	0.4	11.42	5.06	2.22
U	0.1	1.42	2.19	0.11	2.25	1.48	0.89
Y	33.76	18.68	8.41	27.28	22.22	21.53	1.05
La	4.03	28.02	18.46	3.2	71.44	28.67	4.56
Cs	0.325	1.201	1.436	1.677	4.208	0.445	4.837
Pr	1.86	8.65	6.1	1.65	19.64	8.13	0.84
Nd	9.84	36.65	25.36	8.93	77	33.86	3.19
Sm	3.47	8.02	5.65	3.23	13.95	7.01	0.57
Eu	1.23	2.151	1.54	0.822	3.759	1.869	0.425
Gd	4.68	6.4	3.74	4.18	9.18	6.02	0.37
Tb	0.838	0.784	0.417	0.739	1.044	0.789	0.039
Dy	5.8	3.9	1.9	5.2	4.9	4.3	0.2
Ho	1.276	0.693	0.306	1.078	0.791	0.82	0.038
Er	3.84	1.75	0.75	3.32	1.98	2.27	0.11
Tm	0.57	0.24	0.096	0.494	0.259	0.314	0.017
Yb	3.729	1.519	0.582	3.253	1.607	2.007	0.137
Lu	0.572	0.218	0.087	0.487	0.234	0.307	0.025
Cu	16	16	10	50	15	3	88
Zn	188	97	73	120	105	115	69
Mo	4.1	0.15	0.15	0.47	0.27	0.16	0.13
Ga	18.65	18.21	22.41	15.57	22.21	15.28	24.37
Tl	0.096	0.209	0.436	0.293	0.756	0.036	5.12
Pb	6	11.7	23.4	0.7	18.6	5.4	>400
Sn	0.88	1.54	1.21	0.78	1.03	1.34	3.03
W	19.3	19.8	20	20	24.1	17	13.9

Sample	FR27	FR16	FR18	FR22	FR25	FR26	FR14
UTM_E	594069	591329	592633	593548	592754	592502	591102
UTM_N	5387952	5392216	5388538	5388461	5389464	5389528	5392163
Description	Quartz Sericite Schist (Gouda)	Granite	Granodiorite	Quartz Feldspar Porphyry Dike	Quartz Syenite	Quartz Syenite	Quartz Syenite
SiO2	57.22	66.26	70.14	75.07	60.19	61.7	67.74
TiO2	0.55	0.51	0.21	0.01	0.6	0.56	0.5
Al2O3	15.17	16.56	15.52	14.82	14.38	15.22	15.34
Fe2O3	7.85	3.36	2.07	0.84	6.14	6.08	2.62
MnO	0.18	0.02	0.03	0.66	0.1	0.12	0.02
MgO	5.89	0.89	0.82	0.09	3.72	3.13	0.84
CaO	5.2	3.12	2.08	0.94	4.03	4.76	2.01
Na2O	0.24	5.87	5.43	7.08	5.34	5.08	5.55
K2O	2.89	2.99	2.41	1.06	3.44	2.85	3.78
P2O5	0.44	0.21	0.08	0	0.27	0.24	0.19
LOI	4.04	0.54	0.64	0.2	1.42	0.91	0.7
Total	99.67	100.35	99.43	100.78	99.63	100.65	99.29
Cr	289	0	0	0	95	89	0
Co	30.9	9.9	10.6	6.6	46.2	23.7	12.4
Ni	39	9	13	6	35	33	7
Rb	133.2	97.9	78.5	223.2	64	74	133.4
Sr	256	972	1021	23	359	854	655
Ba	561.3	907.3	908.9	15.2	1251.2	1246.5	990.6
Ce	79.3	56.4	15.9	8.1	55.2	57	77.4
V	161	47	31	0	93	106	38
Ta	0.3	0.4	0	21	0.4	0.4	0.4
Nb	5.91	6.32	1.86	93.64	6.03	6.38	6.24
Zr	133	197	93	16	151	129	199
Hf	3.41	5.58	2.69	2.89	3.83	3.45	5.29
Th	3.97	5.56	2.57	8.33	4.32	3.99	5.46
U	1.2	1.62	1.39	9.72	3.08	1.11	1.15
Y	20.77	3.43	3.66	45.34	14.73	15.99	3.89
La	36.76	23.25	6.09	3.64	28.55	25.51	32.31
Cs	17.464	8.934	9.658	10.546	0.854	2.271	4.457
Pr	10.01	7.21	1.51	1.07	7.06	7.02	9.14
Nd	40.81	30.36	5.58	4.25	28.95	27.51	37.88
Sm	7.58	6.05	1.21	1.51	4.98	5.15	7.08
Eu	1.796	1.534	0.498	0.055	1.368	1.444	1.773
Gd	5.59	3.71	0.99	2.11	3.79	4.07	4.26
Tb	0.729	0.351	0.131	0.424	0.483	0.539	0.394
Dy	3.9	1.2	0.7	3	2.8	3.1	1.3
Ho	0.744	0.12	0.125	0.684	0.527	0.591	0.136
Er	2.09	0.21	0.34	2.48	1.53	1.68	0.24
Tm	0.29	0.023	0.046	0.48	0.226	0.247	0.025
Yb	1.908	0.136	0.307	4.072	1.533	1.607	0.142
Lu	0.285	0.018	0.046	0.683	0.236	0.245	0.02
Cu	33	4	7	14	17	27	8
Zn	197	109	61	18	60	86	66
Mo	0.17	0.16	0.09	168.28	0.31	0.12	0.15
Ga	24.47	29.35	22.32	47.5	15.99	19.84	26.49
Tl	0.793	0.568	0.913	1.353	0.321	0.405	0.744
Pb	7.3	14.6	42.3	65.7	5.9	12.8	12.4
Sn	1.58	1.77	0.87	0.72	3.72	1.37	1.68
W	25.2	22	31.3	31.7	28.4	23.2	42.6

Appendix C-2: 2009 Mapping Samples Geochemistry

All Samples reported in this section were collected in the 2009 field season during field mapping and have been stained using the cobaltinitrite method and analysed using the ALS Chemex Method. UTM zone 16U, Nad83. Major elements as wt.%, trace elements as ppm.

Sample	HE001	HE002	HE004	HE005	HE006	HE008
Easting	592532	592200	593573	593295	593295	593706
Northing	5388710	5388543	5388162	5387999	5387999	5388182
Description	Massive Metabasalt	Silicified Sericite Schist (Gouda)	Sheared Mafic Lapilli Tuff	Foliated, Thinly Laminated Metasiltstone	Laminated Metawacke	Sheared Mafic Lapilli Tuff
Staining Intensity	2	1	0	3	2	0
Staining Interpretatio	Secondary	Secondary		Secondary	Secondary	
SiO_2	50.1	75.6	51.4	66	61.9	47.6
TiO_2	1.72	0.06	0.83	0.36	0.45	0.82
Al_2O_3	13.15	13.05	18.3	14.25	13.75	18.6
Fe_2O_3	13.35	0.72	9.52	4.03	4.95	11.05
MnO	0.19	0.02	0.17	0.07	0.12	0.16
MgO	5.05	0.35	2.91	2.65	3.81	4.86
CaO	8.06	1.2	9.47	2.71	3.94	11.95
Na_2O	3.3	1.86	3.93	1.52	2.99	2.31
K_2O	0.82	3.49	0.51	4.88	3.7	0.29
P_2O_5	0.18	0.04	0.07	0.12	0.13	0.08
Cr_2O_3	0.03	0	0.03	0.02	0.02	0.03
SrO	0.04	0.02	0.04	0.03	0.05	0.02
BaO	0.02	0.1	0.01	0.09	0.1	0
LOI	2.67	1.9	2.09	1.5	2.69	0.3
Total	98.7	98.4	99.3	98.2	98.6	98.1
Cr	160	0	200	100	110	170
Co	44.9	0.7	35.9	13.4	20.8	32.3
Ni	64	0	64	59	109	58
Rb	37	106	21.5	94.8	66	2.5
Sr	341	168	317	256	379	180
Cs	1.85	4.47	1.28	6	2.32	0.35
Ba	213	844	132	731	854	33.4
V	253		200	58	88	202
Ta	0.7	0.3	0.2	0.2	0.3	0.2
Nb	11.2	3.5	2.4	2.6	3.3	2.3
Zr	151	38	48	86	106	47
Hf	4.3	2	1.5	2.5	3	1.5
Th	3.31	2.94	0.34	3.65	4.09	0.34
U	0.62	0.72	0.1	0.5	1.37	0.09
Y	32.8	3.7	16.8	6.5	11.2	17.1
La	20.5	7.5	3.3	24.2	27	3.1
Ce	44	17.3	8.8	51.8	53.6	8.3
Pr	5.53	1.93	1.29	5.9	6.68	1.24
Nd	23	7.3	6.5	21.8	24.9	6.4
Sm	5.47	1.46	2.02	3.62	4.06	1.97
Eu	1.38	0.24	0.8	0.88	1.05	0.77
Gd	6.23	1.28	2.6	2.97	3.66	2.46
Tb	1.06	0.17	0.51	0.33	0.44	0.49
Dy	6.13	0.69	3.01	1.28	1.92	2.94
Ho	1.3	0.13	0.7	0.27	0.39	0.67
Er	3.85	0.35	2.03	0.75	1.23	1.95
Tm	0.56	0.04	0.3	0.09	0.15	0.29
Yb	3.37	0.31	1.77	0.62	0.99	1.96
Lu	0.56	0.05	0.31	0.11	0.17	0.32
Cu	117	0	170	8	5	37
Zn	119	12	83	53	68	73
Mo	0	0	2	0	0	0
Ga	16.8	20.5	16.8	18.2	18.8	16.8
Ag	0	0	3	0	0	0
Tl	0	0	0	0	0	0
Pb	9	14	8	11	10	5
Sn	1	1	1	1	1	0
W	1	1	0	0	1	1
Au	0	0	0	0	0	0

Sample	HE009	HE013	HE014	HE015	HE016	HE017	HE018
Easting	593709	592528	593323	593786	593897	594203	594123
Northing	5388205	5389006	5388511	5388162	5388136	5388300	5388366
Description	Strongly Foliated Metabasalt	Meta-siltstone	Foliated Metabasalt	Sheared Mafic Lapilli Tuff	Meta-greywacke	Metagabbro	Foliated Metabasalt
Staining Intensity	0	0	0	0	0	0	0
Staining Interpretation							
SiO_2	49.4	49.2	49	49	58.2	46.8	47.7
TiO_2	0.69	2.19	0.69	0.81	0.75	0.98	0.8
Al_2O_3	14.6	12.7	14.8	18.25	15.3	15	16.6
Fe_2O_3	12.15	15.05	12.1	10.7	7.31	13.65	12.2
MnO	0.2	0.31	0.22	0.15	0.13	0.22	0.22
MgO	8.23	4.48	7.38	4.43	3.66	6.95	5.52
CaO	10.5	5.55	10.25	11.65	5.94	10.5	10.4
Na_2O	2.47	3.2	2.79	2.08	3.66	1.86	2.81
K_2O	0.39	1.34	0.31	0.18	2	0.41	0.62
P_2O_5	0.04	0.42	0.06	0.04	0.34	0.07	0.06
Cr_2O_3	0.04	0.01	0.04	0.02	0.01	0.04	0.05
SrO	0.01	0.03	0.02	0.02	0.11	0.02	0.01
BaO	0.01	0.05	0.01	0	0.12	0.01	0.01
LOI	0.5	3.56	0.4	0.7	0.7	1.6	1.09
Total	99.2	98.1	98.1	98	98.2	98.1	98.1
Cr	240	60	260	150	40	240	310
Co	48	44	48.5	33.5	19.4	49.1	54.6
Ni	144	39	150	63	19	106	160
Rb	22.4	47.9	4.6	4.4	66.1	27.9	28.7
Sr	106	261	207	136.5	905	117.5	94.4
Cs	1.71	1.68	0.55	1.2	10.05	2.69	9.3
Ba	63.8	405	124.5	14.1	1020	70.8	76.1
V	222	248	231	201	132	261	273
Ta	0.1	1.8	0.1	0.2	0.3	0.2	0.1
Nb	1.3	28.3	1.5	2.4	5.3	3.2	1.4
Zr	36	227	38	50	126	53	44
Hf	1.2	6.6	1.2	1.5	3.7	1.6	1.4
Th	0.17	4.95	0.22	0.31	4.71	0.29	0.21
U	0.06	1.01	0.08	0.09	1.24	0.07	0.08
Y	15.4	42	16	17.2	15.7	20.7	18.4
La	2.1	38.6	2	3.2	24.4	3.7	2
Ce	5.5	81.7	5.7	8.2	53.1	8.5	5.8
Pr	0.86	10.25	0.91	1.27	6.68	1.4	0.93
Nd	4.6	42.5	4.7	6.5	27	7.3	5
Sm	1.55	9.19	1.53	2.06	5.31	2.13	1.68
Eu	0.6	2.47	0.77	0.74	1.56	0.91	0.74
Gd	1.95	9.52	2.14	2.32	4.66	2.8	2.44
Tb	0.4	1.49	0.41	0.48	0.62	0.54	0.48
Dy	2.63	7.93	2.73	2.98	3.06	3.29	3.11
Ho	0.63	1.65	0.61	0.69	0.59	0.77	0.73
Er	1.81	4.66	1.95	1.99	1.73	2.23	2.11
Tm	0.3	0.67	0.29	0.29	0.26	0.34	0.34
Yb	1.87	4.38	1.87	1.87	1.61	2.09	2.16
Lu	0.29	0.72	0.31	0.31	0.27	0.34	0.35
Cu	88	32	23	102	28	17	51
Zn	80	77	76	69	94	95	91
Mo	0	2	0	0	0	0	3
Ga	14.9	21.1	15.1	17.3	20.2	16.1	17.1
Ag	0	0	0	0	0	0	0
Tl	0	0	0	0	0	0	0
Pb	0	56	5	0	14	0	0
Sn	0	1	0	0	1	1	0
W	0	2	0	0	1	0	0
Au	0	0	0	0	0	0	0

Sample	HE020	HE021	HE023	HE025	HE026	HE027	HE028
Easting	593583	593600	593537	593701	593535	593079	592916
Northing	5388367	5388511	5388210	5388014	5387883	5388201	5388374
Description	Metagabbro	Meta-sandstone	Sheared Mafic Lapilli Tuff	Meta-siltstone	Quartz-Sericite Schist (Gouda)	Sheared Mafic Lapilli Tuff	Metagabbro
Staining Intensity	0	0	0	0	1	0	0
Staining Interpretation					Secondary		
SiO_2	50.4	69	48.6	61.4	74.5	48.7	51.4
TiO_2	0.79	0.33	0.9	0.56	0.24	0.86	0.77
Al_2O_3	13.8	15.25	16.7	14.85	14.55	17.6	16.6
Fe_2O_3	12.85	2.87	12.35	6.13	1.13	11.8	11.5
MnO	0.19	0.04	0.18	0.09	0.01	0.16	0.2
MgO	7.36	1.09	5.78	4.76	0.2	5.69	4.02
CaO	10.3	2.96	9.83	5.46	1.5	10.1	10.4
Na_2O	1.61	4.9	3.25	3.22	3.83	3.15	2.75
K_2O	0.32	2.07	0.76	2.13	2.38	0.41	0.64
P_2O_5	0.05	0.11	0.09	0.22	0.03	0.08	0.06
Cr_2O_3	0.04	0	0.04	0.02	0	0.03	0.04
SrO	0.02	0.12	0.03	0.09	0.02	0.02	0.02
BaO	0.01	0.09	0.01	0.06	0.05	0.01	0.01
LOI	0.67	1.37	1.27	0.67	1.07	0.39	1.56
Total	98.4	100	99.8	99.7	99.5	99	100
Cr	250	20	240	160	10	190	280
Co	48.8	6.5	38.4	23.5	1	39.7	54.8
Ni	107	10	73	88	0	76	164
Rb	11.9	80.9	20.9	61.9	39.6	8.5	22
Sr	154.5	952	285	762	204	161	149
Cs	1.55	8.01	1.03	3.29	1.65	0.86	1.08
Ba	66	813	108.5	518	478	92.3	92.5
V	289	52	292	133	42	262	287
Ta	0.2	0.3	0.3	0.4	0.2	0.3	0.2
Nb	1.5	2.4	2.2	3.5	1.5	2.4	1.3
Zr	46	115	50	116	100	53	43
Hf	1.4	3.2	1.5	3.2	2.8	1.5	1.3
Th	0.25	2.95	0.31	5.63	2.13	0.33	0.22
U	0.08	0.94	0.11	1.07	0.39	0.07	0.05
Y	19.1	4.2	18.4	12.3	1.8	18.8	18.2
La	2.3	14.8	3.2	43	12.4	3.4	2.3
Ce	6.5	32.5	8.1	97.8	23.2	8.8	5.9
Pr	1.06	4.01	1.27	12.3	2.57	1.4	0.98
Nd	5.5	15.7	6.5	45.7	8.8	6.9	5
Sm	1.88	3.07	2.04	7.09	1.25	2.13	1.67
Eu	0.78	0.84	0.81	1.67	0.39	0.84	0.66
Gd	2.42	2.4	2.67	5.58	1.03	2.81	2.39
Tb	0.46	0.24	0.46	0.57	0.09	0.48	0.44
Dy	3.31	0.98	3.25	2.62	0.4	3.33	3.23
Ho	0.74	0.16	0.71	0.47	0.07	0.72	0.7
Er	2.22	0.43	2.13	1.39	0.21	2.17	2.21
Tm	0.34	0.04	0.33	0.19	0.01	0.34	0.33
Yb	2.15	0.33	2.05	1.22	0.2	2.08	2.1
Lu	0.35	0.05	0.3	0.18	0.03	0.33	0.32
Cu	132	0	69	29	9	75	72
Zn	103	84	94	89	19	81	105
Mo	0	0	0	0	2	0	0
Ga	15.1	22.3	16.7	19.5	19.6	16.8	14.9
Ag	0	0	0	0	0	0	0
Tl	0	0	0	0	0	0	0
Pb	5	21	8	9	31	0	0
Sn	1	1	1	1	1	0	1
W	1	1	2	2	2	1	2
Au							

Sample	HE030	HE031	HE032	HE033	HE034	HE035	HE036	HE037
Easting	591915	591613	593041	592103	592015	591831	592687	593266
Northing	5388791	5388844	5388745	5388704	5388743	5388869	5389135	5388135
Description	MetaBasalt	Foliated Metabasalt	Foliated Metabasalt	Metabasalt	Sheared Mafic Lapilli Tuff	Foliated Metabasalt	Meta-greywacke	Sheared Mafic Lapilli Tuff
Staining Intensity	0	0	0	0	0	0	1	0
Staining Interpretation							Primary	
SiO_2	49.7	48.9	53.9	52.4	47.5	48.5	59.3	48.6
TiO_2	1.13	0.68	1.2	0.94	0.91	0.77	0.57	0.9
Al_2O_3	14.45	13.55	13.55	17.3	16.4	14.95	13.25	16.9
Fe_2O_3	13.15	12.6	11.05	9.1	12	12.35	6.35	11.9
MnO	0.22	0.21	0.22	0.19	0.18	0.24	0.12	0.18
MgO	4.53	8.12	5.19	4.23	5.81	6.78	4.5	5.84
CaO	11.15	11.45	9.48	10.05	11.1	11.55	5.19	10.75
Na_2O	1.04	1.98	2.9	3.65	2.68	1.92	6.11	2.85
K_2O	1.06	0.39	0.78	0.36	0.88	0.45	1.52	0.54
P_2O_5	0.11	0.07	0.08	0.11	0.08	0.06	0.2	0.09
Cr_2O_3	0.02	0.04	0	0.03	0.03	0.03	0.02	0.03
SrO	0.02	0.02	0.04	0.02	0.04	0.02	0.04	0.04
BaO	0.03	0.01	0.03	0	0.01	0.01	0.05	0.01
LOI	1.76	1.22	-0.87	-0.29	1.16	0.88	1.55	0.2
Total	98.4	99.2	97.6	98.1	98.8	98.5	98.8	98.8
Cr	170	290	20	240	240	250	100	210
Co	49.3	57.7	32.3	44.7	43.8	59	17	47
Ni	83	143	23	82	88	125	45	90
Rb	36	25.9	54.1	4.7	35.6	44.5	38.4	26.3
Sr	151.5	196	322	170.5	310	132	297	346
Cs	2.29	3.29	1.57	0.65	2.56	4.63	0.51	3.32
Ba	285	101.5	266	26.3	141	101.5	442	123
V	370	276	398	286	273	308	120	255
Ta	0.3	0.1	0.2	0.2	0.2	0.1	0.2	0.2
Nb	2.8	1.7	3.4	2.8	2.6	1.7	2.8	2.7
Zr	71	38	63	57	55	47	95	56
Hf	2	1.2	1.9	1.7	1.6	1.4	2.6	1.7
Th	0.43	0.19	0.36	0.33	0.35	0.21	3.43	0.32
U	0.1	0.06	0.19	0.1	0.12	0.06	2.39	0.09
Y	25.1	15.6	22.8	21.7	23	17.9	11.1	21
La	4.5	2.5	3.9	3.9	5.7	3	26.2	4
Ce	11.4	6.1	10.3	9.9	13.3	7.3	54.8	10.2
Pr	1.82	0.97	1.54	1.55	1.87	1.13	6.95	1.55
Nd	9	4.9	7.7	7.7	8.7	5.7	27.7	7.7
Sm	2.78	1.64	2.48	2.45	2.54	1.86	4.91	2.43
Eu	1.04	0.64	0.98	0.89	0.92	0.72	1.18	0.91
Gd	3.58	2.12	3.03	3	3.19	2.44	3.93	2.96
Tb	0.64	0.4	0.58	0.55	0.57	0.45	0.45	0.53
Dy	4.41	2.79	4.05	3.84	3.95	3.18	2.31	3.78
Ho	0.96	0.6	0.87	0.83	0.85	0.69	0.41	0.79
Er	2.92	1.71	2.55	2.38	2.46	2.03	1.21	2.32
Tm	0.45	0.31	0.41	0.37	0.38	0.29	0.14	0.38
Yb	2.79	1.75	2.67	2.39	2.51	2.04	1.06	2.39
Lu	0.43	0.28	0.43	0.38	0.4	0.34	0.17	0.39
Cu	96	50	79	35	39	68	9	74
Zn	125	126	127	95	89	101	43	105
Mo	0	0	0	0	0	4	0	0
Ga	18.1	17	22.5	19.3	19.9	18.1	16.5	18.9
Ag	0	0	0	0	0	1	0	0
Tl	0	0	0	0	0	0	0	0
Pb	5	11	13	14	15	14	13	12
Sn	1	1	1	1	1	1	1	1
W	1	1	1	1	2	1	2	1
Au								

Sample	HE038	HE039	HE040	HE041	HE042	HE043	HE044	HE045
Easting	592710	592748	592751	592701	592701	592631	592668	592445
Northing	5388507	5388587	5388630	5388603	5388603	5388582	5388526	5388552
Description	Foliated Metabasalt	Massive Metabasalt	Foliated Metabasalt	Foliated Metabasalt	Sercitie Schist (Gouda)	Foliated Metabasalt	Foliated Metabasalt	Foliated Metabasalt
Staining Intensity	0	0	0	0	0	1	0	0
Staining Interpretation						Secondary		
SiO_2	50.1	46	50.3	52.2	70.2	47.4	51.7	50.1
TiO_2	1.02	0.61	0.69	0.86	0.25	0.92	1.01	0.77
Al_2O_3	13.55	13.65	13.55	14.65	16.1	14.15	13.4	16.8
Fe_2O_3	14.5	11.75	12.35	12.7	1.77	14.45	13.35	11.8
MnO	0.26	0.23	0.24	0.23	0.03	0.24	0.23	0.24
MgO	6.36	7.16	8.82	5.02	0.57	8.2	6.37	5.02
CaO	10.25	15.35	8.36	8.9	2.1	9.54	9.8	11.35
Na_2O	2.44	1.78	2.24	2.05	5.06	2.52	2.68	1.08
K_2O	0.62	0.25	1.69	1.23	3.2	0.72	0.6	0.59
P_2O_5	0.1	0.08	0.06	0.07	0.14	0.08	0.08	0.09
Cr_2O_3	0.01	0.03	0.04	0.04	0	0.04	0.01	0.04
SrO	0.02	0.13	0.06	0.03	0.14	0.02	0.03	0.01
BaO	0.01	0	0.09	0.02	0.17	0.01	0.01	0.01
LOI	0.1	2.49	1.98	1.97	0.49	1.72	1.08	1.97
Total	99.3	99.5	100.5	100	100	100	100.5	99.9
Cr	80	230	260	270	10	290	70	290
Co	54.3	48	55.3	53.3	3.7	55.7	45.8	55.4
Ni	82	113	131	105	0	110	67	168
Rb	26.1	5.5	76.8	47.8	61.3	19.7	21.5	20.6
Sr	173	1020	460	245	1150	168	243	134
Cs	1.55	0.46	3.36	1.95	1.81	0.9	1.77	1.61
Ba	112.5	34	755	197.5	1470	120.5	59.5	106
V	300	241	263	288	22	320	250	264
Ta	0.2	0.1	0.1	0.1	0.1	0.1	0.2	0.1
Nb	2.6	1.9	1.4	1.9	2.1	1.8	2.3	1.4
Zr	52	29	33	44	126	52	46	40
Hf	1.4	0.9	1.1	1.4	3.8	1.6	1.4	1.2
Th	0.27	0.39	0.19	0.24	4.51	0.29	0.26	0.17
U	0.09	0.14	0.05	0.12	1.34	0.05	0.07	0.07
Y	19	15.1	14.8	19.6	2.1	22	16.7	16.9
La	3.3	6.4	2.4	3	27.7	3.4	3.3	2.6
Ce	9	14.5	6.1	7.7	58.6	8.5	8.7	6.4
Pr	1.38	1.89	0.92	1.17	7.1	1.35	1.28	1.01
Nd	7	8	4.6	5.9	27.1	6.8	6.4	5
Sm	2.21	2.06	1.6	1.99	4.41	2.2	2.09	1.8
Eu	0.86	0.69	0.65	0.75	0.97	0.78	0.76	0.63
Gd	2.69	2.37	2.05	2.52	2.92	2.88	2.44	2.12
Tb	0.51	0.4	0.37	0.49	0.21	0.54	0.44	0.4
Dy	3.39	2.69	2.67	3.51	0.59	3.82	3.14	2.93
Ho	0.72	0.55	0.54	0.75	0.07	0.83	0.64	0.61
Er	2.13	1.63	1.67	2.26	0.21	2.54	1.87	1.9
Tm	0.33	0.24	0.26	0.35		0.38	0.28	0.29
Yb	2.1	1.57	1.59	2.39	0.09	2.59	1.84	1.91
Lu	0.34	0.25	0.27	0.37	0.01	0.4	0.29	0.3
Cu	20	98	85	92	27	30	7	39
Zn	109	84	85	103	46	129	93	97
Mo	0	0	0	0	0	0	0	0
Ga	17.2	18.6	12.6	17.8	24.2	17.7	14.6	18.7
Ag	0	0	0	0	0	0	0	0
Tl	0	0	0	0	0	0	0	0
Pb	11	13	10	16	31	14	12	11
Sn	1	0	0	1	1	1	1	1
W	1	2	1	1	1	1	1	1
Au								

Sample	HE046	HE047	HE048	HE049	HE050	HE051	HE052	HE053
Easting	593353	593447	593612	593269	593231	593186	593141	593213
Northing	5388579	5388692	5388505	5388542	5388588	5388635	5388734	5388662
Description	Meta-sandstone	Foliated Metabasalt	Meta-sandstone	Meta-sandstone	Meta-siltstone	Meta-siltstone	Mafic Lapilli Tuff	Meta-greywacke
Staining Intensity	1	0	2	0.5	0	0.5	0	0
Staining Interpretatio	Primary		Primary	Primary		Primary		
SiO_2	69.6	52.4	69.3	67.1	72.7	71	48.5	75.9
TiO_2	0.39	0.95	0.34	0.38	0.32	0.27	0.96	0.39
Al_2O_3	15.2	17.1	15.4	16.55	14.9	15.6	16.9	13.5
Fe_2O_3	2.91	10.95	2.87	3.6	2.72	2.14	11.8	3.27
MnO	0.05	0.3	0.05	0.07	0.04	0.03	0.29	0.03
MgO	0.76	4.31	1.21	0.97	0.92	0.48	5.58	0.85
CaO	2.24	9.11	2.42	2.39	0.96	1.94	9.86	0.51
Na_2O	4.46	3.75	5.44	4.65	3.29	6.05	3.42	0.92
K_2O	2.78	0.56	1.93	3.21	2.67	0.96	0.74	2.46
P_2O_5	0.19	0.11	0.14	0.07	0.14	0.08	0.15	0.08
Cr_2O_3	0	0.05	0.01	0.01	0	0	0.04	0.01
SrO	0.06	0.03	0.09	0.05	0.04	0.08	0.04	0.02
BaO	0.11	0.02	0.09	0.08	0.08	0.03	0.03	0.04
LOI	0.39	0.3	0.39	0.99	1.23	1.58	1.58	2.07
Total	99.1	99.9	99.7	100	100	100	99.9	100
Cr	20	310	30	30	20	10	300	30
Co	5	58.1	6.9	6.3	4.6	4.6	51.2	6.6
Ni	0	159	11	5	7	0	108	5
Rb	227	20.1	56.3	94.4	83.1	25.1	17.5	53.5
Sr	500	262	707	390	338	635	292	166.5
Cs	28.4	4.94	2.5	20.8	5.58	3.72	1.99	4.97
Ba	948	172.5	810	644	631	256	298	352
V	30	287	45	60	40	29	286	52
Ta	0.9	0.2	0.2	0.3	0.3	0.2	0.2	0.3
Nb	10.5	2.3	2.7	3.7	3.5	2.4	2.3	3.6
Zr	167	51	118	140	128	93	52	117
Hf	4.5	1.6	3.5	3.9	3.5	2.6	1.6	3.3
Th	7.63	0.26	3.2	3.03	2.81	1.78	0.29	2.49
U	1	0.07	1.01	0.82	0.9	0.5	0.38	0.71
Y	9.3	21.3	4.6	3	5	4.1	19.6	6.1
La	27.4	2.9	19.6	4.9	12	13.7	2.9	17
Ce	56	7.7	41.3	9.1	26.8	28.2	7.6	32.9
Pr	5.87	1.24	5.16	0.98	3.05	3.38	1.22	3.78
Nd	20.5	6.3	20.5	3.7	11.2	12.8	6.2	14.2
Sm	3.47	2.14	3.54	0.79	2.08	2.11	2.26	2.4
Eu	1.05	0.99	0.9	0.44	0.6	0.71	0.84	0.53
Gd	3.23	3	2.71	0.67	1.64	1.78	2.71	2.07
Tb	0.39	0.56	0.28	0.1	0.22	0.2	0.52	0.24
Dy	1.82	3.75	1.06	0.46	1.05	0.94	3.52	1.23
Ho	0.34	0.81	0.17	0.11	0.18	0.16	0.75	0.24
Er	0.95	2.45	0.5	0.33	0.51	0.46	2.26	0.67
Tm	0.1	0.34	0.03	0.02	0.05	0.03	0.32	0.07
Yb	0.78	2.59	0.34	0.4	0.55	0.39	2.29	0.66
Lu	0.11	0.36	0.05	0.06	0.08	0.05	0.36	0.09
Cu	0	48	13	10	14	8	96	30
Zn	63	136	79	90	82	52	109	55
Mo	0	0	0	0	0	0	3	0
Ga	21.2	18.3	23.8	23.6	20.7	19.9	18.9	18.2
Ag	0	0	0	0	0	0	0	0
Tl	1	0	0	0.5	0	0	0	0
Pb	20	9	33	13	44	9	0	0
Sn	2	1	1	1	1	0	1	1
W	1	1	1	0	1	0	1	1
Au								

Sample	HE054	HE055	HE056	HE057	HE059	HE060	HE061	HE062
Easting	593374	592658	592549	592582	592564	592523	592631	593390
Northing	5388636	5388697	5388892	5388968	5388988	5389066	5388533	5387745
Description	Foliated Metawacke	Fragmental	Mafic Lapilli Tuff	Meta-sandstone	Meta-sandstone	Metawacke	Sericite Schist (Gouda)	Foliated Metabasalt
Staining Intensity	0	2	0	3	0	1.5	3	0
Staining Interpretation		Primary		Primary		Primary	Secondary	
SiO_2	63.3	62.9	49.5	69.8	68.4	61	70.5	48.3
TiO_2	0.75	0.59	0.73	0.32	0.3	0.61	0.19	1.02
Al_2O_3	16.65	14.75	14.8	13.45	14.9	14.65	15.4	14
Fe_2O_3	5.26	5	10.75	2.1	2.84	6.66	2.75	14.5
MnO	0.08	0.09	0.22	0.04	0.04	0.11	0.04	0.31
MgO	2.25	2.95	8.78	0.52	1.34	3.9	0.59	6.27
CaO	4.24	6.11	8.43	2.27	0.6	3.96	0.57	9.69
Na_2O	3.39	2.06	2.7	5.1	6	5.08	4.21	2.6
K_2O	2.04	2.74	1.03	2.63	2.26	1.68	3.68	0.89
P_2O_5	0.31	0.36	0.1	0.15	0.14	0.23	0.08	0.12
Cr_2O_3	0	0.02	0.05	0	0.01	0.02	0	0.02
SrO	0.13	0.14	0.04	0.03	0.01	0.07	0.06	0.02
BaO	0.13	0.11	0.08	0.09	0.06	0.08	0.11	0.02
LOI	1.47	2.28	2.11	1.89	1.94	0.98	1.39	2.17
Total	100	100	99.3	98.4	98.8	99	99.6	99.9
Cr	20	120	360	20	40	110	20	100
Co	7.5	11.4	58.2	7.9	9.9	22	6	56.9
Ni	0	53	256	18	34	38	0	79
Rb	106.5	66.9	44.5	64.4	69.1	53.6	116.5	40.4
Sr	1015	1150	346	252	110	559	465	177.5
Cs	189	2.99	2.56	2.17	2.13	1.26	5.72	2.45
Ba	1090	972	728	760	555	714	964	157
V	97	88	221	30	49	135	29	301
Ta	0.3	0.4	0.1	0.4	0.3	0.2	0.1	0.2
Nb	5.8	5.4	1.8	8.8	3.7	3.5	1.6	2.6
Zr	160	156	43	135	100	111	89	58
Hf	4.5	4.1	1.4	3.7	3	3.2	2.7	1.8
Th	3.45	11.9	0.55	4.18	3.89	4.32	2.31	0.36
U	0.75	2.51	0.13	5.35	0.95	1.04	1.23	0.11
Y	12.6	15.8	15.8	7.8	6.7	12.9	2.4	19.4
La	14.7	78	4.2	27.1	17.2	34.3	8.7	4
Ce	34	166	10.2	56.5	36.4	71.2	19.2	10.4
Pr	4.55	20.2	1.5	6.52	4.12	9.28	2.3	1.63
Nd	18.8	75.1	6.9	23.2	15.7	35.8	8.6	8.1
Sm	4.15	11.2	1.92	3.57	2.52	6.17	1.6	2.44
Eu	1.32	2.46	0.76	0.85	0.72	1.58	0.48	0.91
Gd	3.53	8.69	2.47	2.66	2.2	5.04	1.21	2.84
Tb	0.49	0.83	0.43	0.31	0.27	0.59	0.13	0.54
Dy	2.53	3.29	2.84	1.33	1.36	2.6	0.52	3.54
Ho	0.48	0.56	0.63	0.28	0.26	0.46	0.08	0.77
Er	1.21	1.71	1.81	0.86	0.75	1.42	0.26	2.3
Tm	0.12	0.21	0.25	0.1	0.08	0.16	0.01	0.29
Yb	0.99	1.39	1.83	0.79	0.69	1.24	0.25	2.2
Lu	0.13	0.21	0.27	0.12	0.1	0.17	0.03	0.33
Cu	7	59	61	40	90	41	67	81
Zn	99	55	103	3250	2840	93	1940	131
Mo	0	0	0	0	2	0	0	0
Ga	23.5	21.9	15.8	18.5	17.7	19	24	17.9
Ag	0	0	0	2	1	0	2	0
Tl	0.6	0	0	0	0	0	2.5	0
Pb	11	8	5	1355	1045	15	826	9
Sn	2	1	1	1	1	1	1	1
W	0	1	1	2	1	1	2	1
Au								

Sample	HE063	HE064	HE065	HE066	HE068	HE069	HE070
Easting	593560	593920	593995	593895	593824	593741	593820
Northing	5387761	5387824	5387920	5387909	5388815	5388768	5388730
Description	Foliated Metabasalt	Crenulated Metabasalt	Sericite Schist (Gouda)	Sericite Schist (Gouda)	Weakly Foliated Metabasalt	Weakly Foliated Metabasalt	Meta-sandstone
Staining Intensity	0	0	1	0	0	0	0
Staining Interpretation			Secondary				
SiO_2	49.3	49.3	72	76.4	50.5	52.2	56.1
TiO_2	1	0.98	0.2	0.06	0.93	0.91	0.56
Al_2O_3	13.75	13.8	14.65	13.2	16.7	15.75	15.6
Fe_2O_3	14.15	13.9	2.07	1.26	9.38	9.55	8.45
MnO	0.29	0.26	0.04	0.01	0.23	0.31	0.18
MgO	6.08	5.97	1.21	0.45	3.85	5.54	5.21
CaO	10.8	10.55	1.39	0.24	10.7	7.43	5.51
Na_2O	2.22	3.08	2.55	0.52	3.11	3.54	3.64
K_2O	1.05	0.85	2.73	3.76	0.7	1.77	1.51
P_2O_5	0.08	0.11	0.08	0.02	0.1	0.1	0.24
Cr_2O_3	0.02	0.02	0	0	0.04	0.04	0.02
SrO	0.02	0.02	0.03	0.01	0.02	0.05	0.05
BaO	0.03	0.01	0.06	0.09	0.04	0.04	0.06
LOI	1.66	1.77	3.31	2.08	1.8	2.05	2.77
Total	100.5	100.5	100.5	98.1	98.1	99.3	99.9
Cr	100	110	10	10	340	290	110
Co	55.4	53	3.9	0.5	42.8	50.6	28.7
Ni	78	84	0	0	91	155	13
Rb	53.1	24.6	87.3	89.8	28.3	164.5	87.5
Sr	183.5	145.5	221	58.3	217	418	421
Cs	1.77	1.03	4.3	4.83	2.06	3.66	2.04
Ba	299	93.3	485	775	351	386	524
V	301	283	21		312	278	214
Ta	0.2	0.2	0.2	0.3	0.2	0.2	0.2
Nb	2.8	3.6	2.5	3.6	2.4	2.3	4.1
Zr	58	60	87	42	56	50	106
Hf	1.8	1.7	2.7	2.2	1.7	1.5	3
Th	0.36	0.34	1.92	3.06	0.26	0.25	2.67
U	0.09	0.44	0.53	0.62	0.07	0.1	0.63
Y	19.9	19.1	3.4	4	21.1	20.5	16.4
La	4.1	3.9	8.8	8.5	3	3	22.6
Ce	10.3	9.8	19	17.9	8	7.8	47.5
Pr	1.63	1.53	2.07	2.17	1.3	1.22	5.93
Nd	8	7.3	7.4	8.1	6.5	6.3	23.3
Sm	2.35	2.26	1.31	1.75	2.21	2.11	4.52
Eu	0.89	0.89	0.45	0.22	0.87	0.8	1.11
Gd	2.95	2.92	1.22	1.44	2.94	2.72	3.95
Tb	0.55	0.54	0.14	0.18	0.55	0.51	0.55
Dy	3.58	3.36	0.67	0.79	3.71	3.54	2.99
Ho	0.75	0.74	0.12	0.14	0.84	0.78	0.6
Er	2.31	2.25	0.38	0.4	2.55	2.39	1.88
Tm	0.32	0.31	0.03	0.04	0.36	0.35	0.23
Yb	2.32	2.21	0.35	0.34	2.57	2.49	1.87
Lu	0.35	0.32	0.05	0.05	0.38	0.34	0.27
Cu	148	46	8	0	67	81	27
Zn	113	111	43	26	158	96	100
Mo	23	0	0	0	0	0	0
Ga	18.6	22.5	20.6	22.3	20.6	17.3	19.9
Ag	0	0	0	0	0	0	0
Tl	0	0	0	0	0	0.6	0
Pb	5	7	14	11	0	5	9
Sn	1	3	0	1	1	1	1
W	1	1	1	1	1	1	1
Au							

Sample	HE072	HE073	HE074
Easting	592553	593863	580320
Northing	5388990	5388693	5393727
Description	Meta-sandstone	Meta-sandstone	Sericite Schist (Hemlo Barren Sulphide Zone)
Staining Intensity	1	0	0
Staining Interpretatio	Secondary		
SiO_2	62.6	62.3	72.7
TiO_2	0.29	0.78	0.3
Al_2O_3	14.35	16.45	12.2
Fe_2O_3	2.49	3.75	2.81
MnO	0.07	0.07	0.01
MgO	1.15	2.08	0.47
CaO	4.11	4.09	0.91
Na_2O	5.63	4.58	4.55
K_2O	3.35	2.56	1.89
P_2O_5	0.09	0.31	0.06
Cr_2O_3	0.01	0	0.01
SrO	0.04	0.13	0.04
BaO	0.06	0.15	0.07
LOI	5.97	2.51	2.19
Total	100	99.8	98.2
Cr	50	10	50
Co	4.5	1.8	8.6
Ni	5	0	29
Rb	74.8	46.1	41.9
Sr	349	1110	370
Cs	1.06	1.34	3.91
Ba	550	1300	608
V	56	95	42
Ta	0.5	0.4	0.1
Nb	20.1	6.8	3.2
Zr	102	173	92
Hf	2.8	5	2.6
Th	6.53	3.48	3.99
U	4.38	0.72	1.14
Y	6.3	13.7	6.7
La	23.9	27.6	20.6
Ce	49.8	60.1	42.7
Pr	6.06	8.03	5.11
Nd	22.2	34	19.9
Sm	3.03	6.62	3.09
Eu	0.64	1.69	0.77
Gd	2.24	5.25	2.57
Tb	0.22	0.64	0.22
Dy	1.03	2.9	1.12
Ho	0.22	0.5	0.12
Er	0.74	1.36	0.45
Tm	0.11	0.14	0.06
Yb	0.89	1.02	0.44
Lu	0.13	0.14	0.02
Cu	131	0	9
Zn	1455	46	25
Mo	2	0	2
Ga	16.4	23.9	14.3
Ag	0	0	0
Tl	0	0	0
Pb	308	20	7
Sn	1	1	0
W	8	0	14
Au			0.038

Appendix C-3: 2009 Drill Core Samples Geochemistry

All Samples reported in this section were collected in the 2009 from archived diamond drill core and have been stained using the cobaltinitrite method. Drill hole locations reported in appendix A. Major elements as wt.%, trace elements as ppm.

Sample	WR001	WR002	WR003	WR004	WR005	WR006
Drill Hole	WR01-01	WR01-01	WR01-01	WR01-02	WR01-02	WR01-02
From	138.75	148.3	151.9	36.4	117.6	189.2
To	139.5	149.9	153.5	36.85	117.95	189.6
Description	Sericite Schist (Gouda)	Sericite Schist (Gouda)	Silicifed Sericite Schist (Gouda)	Foliated Metabasalt	Foliated Metabasalt, Poorly Developed Compositional Separation	Mafic Lapilli Tuff (Relatively Undeformed)
Staining Intensity	1	0	3	0	0	0
Staining Interpretation	Secondary		Secondary			
SiO_2	73.4	72.4	70.8	49	48.8	47.7
TiO_2	0.22	0.21	0.25	0.71	0.75	0.84
Al_2O_3	15.3	14.2	15.8	14.25	16.8	19.5
Fe_2O_3	1.84	3.83	1.04	12.45	11.7	11.25
MnO	0.02	0.01	0.02	0.21	0.25	0.16
MgO	0.78	0.45	0.29	7.89	4.4	4.89
CaO	0.73	0.5	2.52	10.85	12.25	11.45
Na_2O	0.63	1.25	5.19	2.25	2.4	3.1
K_2O	2.76	3.45	1.84	0.34	0.57	0.53
P_2O_5	0.06	0.08	0.05	0.05	0.06	0.07
Cr_2O_3	0	0	0	0.03	0.04	0.02
SrO	0.01	0.03	0.07	0.01	0.01	0.02
BaO	0.04	0.1	0.06	0.01	0.01	0.01
LOI	3.29	2.51	0.3	0.7	0.6	1.11
Total	99.1	99	98.2	98.8	98.6	100.5
Cr	10	10	20	230	290	170
Co	4.5	4.2	7.3	54.1	56.1	40.3
Ni	7	10	13	129	172	79
Rb	111	148	132.5	13.5	40.7	18.6
Sr	99.4	275	603	144.5	123	209
Cs	14.95	9.03	7.76	1.77	1.11	2.5
Ba	376	837	549	93	59	55.3
V	28	25	34	277	271	214
Ta	0.2	0.2	0.7	0.1	1	0.2
Nb	3	2.2	5.5	1.6	6.2	2.7
Zr	105	100	105	43	43	55
Hf	3	2.9	3.1	1.2	1.3	1.5
Th	3.33	2.26	2.05	0.24	0.22	0.29
U	0.48	0.7	0.6	0	0.27	0.08
Y	4.2	3	2.6	16.3	18.4	18.9
La	17.5	15.6	16.6	3	3.3	4.2
Ce	35.5	30.3	31.5	7.3	7.2	9.7
Pr	4.21	3.63	3.51	1.12	1.13	1.49
Nd	15.4	13.5	12.1	5.6	5.7	7.5
Sm	2.49	2.09	1.69	1.8	1.83	2.16
Eu	0.62	0.49	0.53	0.7	0.73	0.87
Gd	2.05	1.7	1.38	2.13	2.38	2.65
Tb	0.22	0.19	0.15	0.42	0.48	0.54
Dy	0.89	0.67	0.56	2.82	3.16	3.32
Ho	0.14	0.1	0.09	0.58	0.68	0.71
Er	0.41	0.32	0.28	1.79	2.04	2.15
Tm	0.04	0.02	0.02	0.25	0.3	0.3
Yb	0.32	0.28	0.24	1.82	2.14	2.1
Lu	0.05	0.04	0.03	0.29	0.33	0.33
Cu	6	409	20	145	75	78
Zn	55	278	47	90	118	90
Mo	2	6	5	0	0	0
Ga	21.5	20.8	23.1	15.9	24	18.9
Ag	0	4	0	0	0	0
Tl	0.5	0.9	0.6	0	0	0
Pb	14	21	15	0	11	0
Sn	1	1	1	1	5	1
W	2	2	1	0	0	0
Au	0.002	0.243	0.01			

Sample	WR007	WR008	WR009	WR010	WR011	WR012	WR013
Drill Hole	WR01-02	WR01-02	WR01-02	WR01-02	WR01-02	WR01-02	WR01-03
From	213.3	227.4	242.2	365	373.3	383.1	18.5
To	213.7	227.9	242.6	365.7	373.8	383.6	18.9
Description	Sheared Mafic Lapilli Tuff (Gouda)	Foliated Metabasalt	Foliated Metabasalt	Silicifed Sericite Schist (Gouda)	Quartz Eye Sericite Schist (Gouda)	Altered Felsic Schist (Gouda)	Sheared Mafic Lapilli Tuff
Staining Intensity	0	0	0	0	4	4	0
Staining Interpretation					Secondary	Secondary	
SiO_2	48.6	46.8	50.6	68.6	74.4	63.8	48.4
TiO_2	0.83	1.76	1.78	0.25	0.17	0.44	0.9
Al_2O_3	20.5	12.95	12.35	15.15	13.35	13.4	17.35
Fe_2O_3	8.43	17.65	18.05	2.62	1.25	6.45	12.2
MnO	0.17	0.28	0.28	0.03	0.01	0.08	0.21
MgO	2.74	4.79	5.13	0.79	0.17	2.07	5.65
CaO	11.85	9.2	6.53	1.48	1.9	2.8	9.69
Na_2O	2.76	2.27	3.29	5.5	4.89	4.45	2.62
K_2O	1.05	1.1	0.72	1.65	1.83	2.22	1.3
P_2O_5	0.07	0.15	0.14	0.05	0.03	0.19	0.09
Cr_2O_3	0.02	0.01	0	0	0	0.02	0.03
SrO	0.04	0.02	0.04	0.02	0.06	0.02	0.03
BaO	0.02	0.03	0.02	0.04	0.06	0.05	0.03
LOI	1.89	1.2	1	1.9	0.6	3.1	1.7
Total	99	98.2	99.9	98.1	98.7	99.1	100
Cr	170	30	30	30	10	110	210
Co	38.4	47.8	48.9	6.5	3.8	15.4	44.4
Ni	69	36	25	15	5	40	88
Rb	58.4	58.9	28.3	67.1	47.1	63.3	83.5
Sr	347	172	357	184	480	137	252
Cs	1.83	6.11	2.19	3.18	8.7	1.52	1.22
Ba	181	292	165.5	314	487	472	294
V	218	437	415	41	17	71	245
Ta	0.2	0.5	0.3	0.2	0.1	1	0.2
Nb	2.7	5.5	4.6	2.4	2.3	10.1	2.6
Zr	54	98	96	100	87	92	58
Hf	1.5	2.9	2.8	2.9	2.5	3	1.7
Th	0.32	0.55	0.46	1.74	1.33	5.28	0.37
U	0.07	0.25	0.13	0.56	1.04	2.61	0.08
Y	18.3	31.9	32.7	3.9	2.5	10.1	19.2
La	4	7.3	6.4	14.2	8.9	35.9	4.5
Ce	9.9	17.6	16.2	27.5	17.7	77.9	10.8
Pr	1.53	2.67	2.53	3.23	2.12	9.84	1.64
Nd	7.5	13.2	12.6	11.6	7.8	38	8
Sm	2.16	3.91	3.73	1.86	1.34	6.11	2.25
Eu	0.84	1.38	1.44	0.58	0.41	1.18	0.86
Gd	2.7	4.76	4.67	1.65	1.16	4.64	2.77
Tb	0.52	0.89	0.92	0.19	0.13	0.52	0.53
Dy	3.25	5.78	5.84	0.79	0.53	2.23	3.44
Ho	0.69	1.25	1.27	0.15	0.09	0.41	0.71
Er	2.13	3.64	3.7	0.45	0.29	1.23	2.17
Tm	0.28	0.52	0.55	0.05	0.02	0.16	0.31
Yb	2.02	3.69	3.77	0.4	0.28	1.11	2.15
Lu	0.3	0.55	0.59	0.06	0.03	0.17	0.33
Cu	83	135	128	38	5	8	85
Zn	85	189	148	37	60	56	125
Mo	0	2	0	0	3	5	0
Ga	19.1	24.6	20	20	18.4	14.3	17.9
Ag	0	0	0	0	0	0	0
Tl	0	0	0	0	0.6	0	0
Pb	0	8	0	9	19	0	13
Sn	1	3	1	1	4	1	1
W	1	2	1	1	1	1	0
Au				0	0	0.001	

Sample	WR014	WR015	WR016	WR017	WR018	WR019	WR020
Drill Hole	WR01-03	WR01-03	WR01-03	WR01-03	WR01-03	WR01-04	WR01-04
From	165.7	168.2	173.4	189.9	192.7	81.8	86.1
To	166.3	168.9	174	190.5	193.3	82.3	86.6
Description	Sericite Schist (Gouda)	Crenulated Muscovite Schist (Gouda)	Quartz Eye Sericite Schist (Gouda)	Foliated Metabasalt, Developed Compositional Separation	Foliated Metabasalt (Altered)	Quartz Eye Sericite Schist (Gouda)	Sericite Schist (Gouda)
Staining Intensity	0.5	0	0.5	0.5	1	3	3
Staining Interpretation	Secondary		Secondary	Secondary	Secondary	Secondary	econdary
SiO_2	72.2	72.9	70.9	48.4	45.4	73.5	68.8
TiO_2	0.22	0.2	0.2	1.06	1.22	0.16	0.2
Al_2O_3	15.35	15.2	15.85	14	8.78	13.2	16.25
Fe_2O_3	2.31	2.14	2.03	14.05	15.15	2.13	1.54
MnO	0.04	0.01	0.02	0.25	0.25	0.01	0.02
MgO	0.96	0.74	0.52	3.92	11.7	0.22	0.4
CaO	2.86	0.16	2.03	12.45	11.9	1.79	2.6
Na_2O	2.29	0.29	2.72	3.86	1.32	3.92	4.12
K_2O	2.28	3.03	2.49	0.57	0.76	2.08	2.79
P_2O_5	0.04	0.04	0.07	0.08	0.09	0.03	0.05
Cr_2O_3	0	0	0	0.01	0.2	0	0
SrO	0.04	0.01	0.06	0.05	0.02	0.05	0.07
BaO	0.05	0.05	0.05	0.01	0.01	0.05	0.04
LOI	1.5	4	1.8	0.6	1.2	1.39	1.49
Total	100	98.8	98.7	99.3	98	98.5	98.4
Cr	20	10	10	90	1340	10	10
Co	5.5	3.6	6.1	54	78.7	4	8.9
Ni	11	0	8	80	521	7	12
Rb	44.7	88.4	79.5	21	20	52.2	93.7
Sr	353	47.2	446	379	133.5	381	542
Cs	6.63	9.76	10	0.66	2.14	8.16	10.35
Ba	457	506	447	97.4	85.4	504	432
V	31	24	25	306	284	21	26
Ta	0.2	0.2	0.2	0.2	0.4	0.2	0.1
Nb	2.2	2	2.3	3.3	5.7	2.5	2
Zr	91	92	98	65	70	81	92
Hf	2.8	2.8	3	1.9	2	2.6	2.7
Th	1.77	1.5	1.63	0.4	0.82	1.44	1.67
U	0.63	0.49	0.57	0.16	0.46	0.56	0.59
Y	3.6	2.4	2.9	19.8	16.2	2.6	2.2
La	11.1	8.5	11	5.5	11	8.6	11.2
Ce	21.6	17.4	21.3	12.5	25.9	16.9	21.5
Pr	2.51	2.05	2.42	1.86	3.62	1.97	2.43
Nd	9.2	7.4	8.8	9.2	16.1	7.4	8.1
Sm	1.59	1.21	1.48	2.63	3.81	1.36	1.25
Eu	0.47	0.35	0.47	0.94	1.29	0.38	0.44
Gd	1.39	1.09	1.26	3.11	3.73	1.07	1.04
Tb	0.17	0.13	0.14	0.57	0.6	0.13	0.11
Dy	0.75	0.53	0.58	3.54	3.31	0.59	0.46
Ho	0.14	0.09	0.11	0.77	0.66	0.1	0.08
Er	0.38	0.3	0.31	2.25	1.74	0.27	0.25
Tm	0.04	0.02	0.03	0.33	0.22	0.03	0.02
Yb	0.33	0.27	0.28	2.16	1.62	0.24	0.23
Lu	0.06	0.05	0.05	0.34	0.23	0.04	0.03
Cu	26	0	15	146	133	26	14
Zn	52	47	77	103	156	287	75
Mo	0	0	0	2	0	8	8
Ga	18.9	19.7	19.6	18.4	17.2	16.7	19.9
Ag	1	0	1	0	0	1	0
Tl	0	0	0.6	0	0	0	0
Pb	8	9	20	10	6	72	14
Sn	1	1	1	1	1	1	0
W	1	2	2	1	0	1	1
Au	0.001	0.001	0.001			0.001	0

Sample	WR021	WR022	WR023	WR024	WR025	WR026
Drill Hole	WR01-04	WR01-04	WR01-04	WR01-05	WR01-05	WR01-05
From	86.8	100.4	108.6	11.3	43.6	175.7
To	87.35	101	109.1	11.7	47	176.3
Description	Sericite Schist (Gouda)	Foliated Metabasalt (Altered)	Crenulated Metabasalt, Moderately Developed Compositional Banding	Coarse Grained Porphyroblastic Metagabbro	Sheared Mafic Lapilli Tuff	Quartz Eye Sericite Schist (Gouda)
Staining Intensity	3	1	0	0	0	4
Staining Interpretation	Secondary	Secondary				Secondary
SiO_2	69.1	46.6	48.8	46.9	47.9	70.8
TiO_2	0.21	1.38	0.84	0.95	0.92	0.19
Al_2O_3	16.6	10.45	14.05	15.15	18.05	15.05
Fe_2O_3	2.11	15.4	12.95	14.15	11.65	1.76
MnO	0.02	0.27	0.25	0.21	0.16	0.04
MgO	0.38	9.48	7.3	7.43	5.78	1.47
CaO	3	12.35	11.05	10.45	10.95	2.36
Na_2O	4	2.23	2.28	2.34	2.97	2.68
K_2O	2.98	0.9	1.09	0.25	0.25	2.9
P_2O_5	0.04	0.09	0.09	0.08	0.06	0.03
Cr_2O_3	0	0.2	0.05	0.04	0.03	0
SrO	0.09	0.05	0.03	0.01	0.01	0.03
BaO	0.07	0.01	0.03	0	0.01	0.06
LOI	0.7	1	1.49	0.4	1	1.39
Total	99.3	100.5	100.5	98.4	99.7	98.8
Cr	10	1400	320	280	240	10
Co	16.6	84.3	57	56.4	43	4.4
Ni	27	468	119	136	94	7
Rb	97.7	24.8	64.9	8.1	10.5	181
Sr	728	379	265	99.9	132	277
Cs	9.56	0.56	1.71	1.59	2.52	22.9
Ba	678	107.5	271	26.1	51.4	595
V	28	315	281	270	255	24
Ta	0.2	0.4	0.1	0.2	0.2	0.2
Nb	2.4	6.1	2.4	2.9	2.4	2.5
Zr	98	79	52	59	55	91
Hf	2.8	2.2	1.5	1.8	1.6	2.8
Th	1.85	0.46	0.85	0.28	0.24	1.82
U	0.6	0.29	0.27	0.18	0.09	0.69
Y	2.2	20.3	17.1	21.3	18.8	3.2
La	11.9	7.1	6.6	4.2	3.7	10.5
Ce	22.4	17.4	14.6	9.9	8.9	20.2
Pr	2.49	2.71	2.09	1.57	1.41	2.31
Nd	8.5	13.1	9.6	8	7.1	8.5
Sm	1.3	3.51	2.58	2.37	2.11	1.45
Eu	0.4	1.21	0.9	0.92	0.84	0.41
Gd	1.07	3.95	2.81	2.98	2.73	1.28
Tb	0.11	0.68	0.49	0.58	0.53	0.14
Dy	0.48	4.09	3.15	3.73	3.4	0.6
Ho	0.08	0.82	0.66	0.82	0.73	0.11
Er	0.28	2.37	1.93	2.43	2.16	0.33
Tm	0.03	0.31	0.27	0.34	0.3	0.04
Yb	0.25	2.19	1.85	2.46	2.26	0.27
Lu	0.04	0.33	0.27	0.38	0.34	0.05
Cu	14	115	110	75	57	5
Zn	63	120	127	109	72	47
Mo	3	0	0	0	0	4
Ga	20	19.1	16.8	17.4	17.9	20.3
Ag	0	0	0	0	0	0
Tl	0	0	0	0	0	0.6
Pb	18	6	6	0	0	6
Sn	1	2	1	1	1	1
W	1	1	0	1	1	1
Au	0					0

Sample	WR027	WR028	WR029	WR030	WR031	WR032
Drill Hole	WR01-05	WR01-05	WR01-06	WR01-06	WR01-06	WR01-06
From	186	196.8	6	42.3	154.7	166.3
To	186.6	197.3	6.4	42.7	155.2	166.8
Description	Quartz Eye Sericite Schist (Gouda)	Coarse Grained Porphyroblastic Metagabbro	Coarse Grained Porphyroblastic Metagabbro	Strongly Sheared Mafic Lapilli Tuff, Flattened Lapilli	Sericite Schist (Gouda)	Quartz Eye Sericite Schist (Gouda)
Staining Intensity	4	0	0	0	2.5	3
Staining Interpretation	Secondary				Secondary	Secondary
SiO_2	75.5	48.8	47.5	47.9	70.5	74.7
TiO_2	0.16	0.74	0.85	0.85	0.24	0.18
Al_2O_3	12.9	13.9	18.2	18	15.5	13.5
Fe_2O_3	0.75	11.65	11.75	11.55	2.77	0.78
MnO	0.01	0.19	0.17	0.18	0.04	0.01
MgO	0.23	7.75	5.68	5.38	0.84	0.28
CaO	0.9	10.5	10.7	10.25	2.24	1.74
Na_2O	4.91	2.76	3.41	3.28	3.68	4.39
K_2O	2.16	1.22	0.61	1.01	2.62	2.35
P_2O_5	0.04	0.07	0.05	0.08	0.05	0.03
Cr_2O_3	0	0.03	0.03	0.03	0	0
SrO	0.03	0.03	0.02	0.04	0.05	0.05
BaO	0.05	0.02	0	0.02	0.04	0.06
LOI	0.4	1.6	0.7	1.99	1.69	0.7
Total	98	99.3	99.7	100.5	100.5	98.8
Cr	20	240	200	200	20	20
Co	2.5	51.2	45.7	43.3	6	3.3
Ni	9	127	93	82	11	6
Rb	80.8	112.5	38.4	51.2	66.6	52.3
Sr	267	246	162.5	321	401	431
Cs	5.55	5.35	9.51	5.09	10.4	8.01
Ba	506	169.5	33.9	157.5	447	601
V	17	252	248	239	33	21
Ta	0.2	0.2	0.2	0.2	0.4	0.2
Nb	3	3.3	2.6	2.7	4.4	2.1
Zr	84	44	50	54	96	86
Hf	2.4	1.3	1.6	1.6	2.8	2.6
Th	1.52	0.25	0.26	0.45	1.8	1.39
U	0.66	0.06	0.07	0.15	0.68	0.52
Y	2.6	14.6	17.8	19	4.2	2.1
La	9.5	3.6	4	6.8	11.9	7.1
Ce	18.8	8.4	8.8	14.3	23	14
Pr	2.16	1.29	1.36	1.99	2.7	1.66
Nd	7.9	6.3	6.9	9.1	9.8	6
Sm	1.23	1.78	2.02	2.43	1.72	1.11
Eu	0.36	0.72	0.8	0.91	0.52	0.38
Gd	1.05	2.31	2.59	3.01	1.54	0.9
Tb	0.13	0.44	0.51	0.56	0.17	0.1
Dy	0.5	2.74	3.22	3.42	0.81	0.45
Ho	0.09	0.59	0.68	0.73	0.16	0.08
Er	0.3	1.71	2.05	2.15	0.4	0.23
Tm	0.02	0.24	0.29	0.31	0.06	0.01
Yb	0.28	1.64	2.04	2.15	0.38	0.22
Lu	0.04	0.25	0.32	0.32	0.06	0.03
Cu	10	66	58	111	28	11
Zn	16	104	81	85	85	28
Mo	0	0	0	0	13	2
Ga	15	17.1	18.8	18.7	20.6	17.2
Ag	0	0	0	0	0	0
Tl	0	0	0	0	0	0
Pb	6	8	10	5	15	8
Sn	1	1	1	0	1	1
W	1	0	0	1	1	1
Au	0				0	0

Sample	WR034	WR035	WR036	WR037	WR038	WR039
Drill Hole	WR02-01	WR02-01	WR02-01	WR02-01	WR02-01	WR02-01
From	112	105.5	65.3	77	84.1	283.9
To	112.4	105.9	65.7	77.4	84.5	284.3
Description	Sheared Mafic Lapilli Tuff	Sheared Mafic Lapilli Tuff	Foliated Metabasalt	Coarse Grained Porphyroblastic Metagabbro	Coarse Grained Porphyroblastic Metagabbro	Sericite Schist (Gouda)
Staining Intensity	0	0	0	0	0	0
Staining Interpretation						
SiO_2	47.2	47.2	49	49	48.5	76.9
TiO_2	0.84	0.85	1.53	1	0.99	0.04
Al_2O_3	20.3	19.45	14.7	15.05	15.4	12.8
Fe_2O_3	10.4	11.2	16.5	13.1	13.8	1.35
MnO	0.16	0.17	0.22	0.2	0.2	0.01
MgO	3.89	4.9	5.07	6.46	6.57	0.42
CaO	11.45	11.9	9.49	10.55	10.65	0.72
Na_2O	3.07	2.22	1.46	2.61	1.91	0.75
K_2O	0.74	0.44	0.99	0.3	0.19	3.31
P_2O_5	0.08	0.08	0.12	0.07	0.08	0
Cr_2O_3	0.02	0.02	0.01	0.03	0.04	0
SrO	0.03	0.02	0.02	0.01	0.01	0.01
BaO	0.01	0.01	0.03	0	0.01	0.1
LOI	1.59	1.3	0.6	0.3	0.1	1.69
Total	99.8	99.8	99.7	98.7	98.5	98.1
Cr	170	170	70	160	270	10
Co	37.5	38.7	51.5	32.6	51.8	0.9
Ni	69	70	55	70	118	8
Rb	41.1	21	38.7	5.2	5	71.9
Sr	295	198	177	71.8	99.4	85.6
Cs	5.26	5.28	7.29	0.58	0.64	5.77
Ba	112.5	61.9	268	30.2	48.6	891
V	213	223	384	178	269	7
Ta	0.2	0.2	0.3	0.1	0.2	0.3
Nb	2.6	2.8	4.4	2	2.9	3.6
Zr	57	55	109	41	56	40
Hf	1.6	1.6	3.2	1.2	1.6	1.9
Th	0.65	0.3	0.58	0.25	0.29	3.17
U	0.35	0.14	0.13	0.17	0.1	1.11
Y	18.6	19.2	33.2	13.2	20.5	4.2
La	4.7	4.1	6.8	3.3	4.3	10.3
Ce	11.5	9.7	16.7	6.9	10	20.7
Pr	1.7	1.5	2.59	1.05	1.56	2.54
Nd	8.2	7.4	13	5.1	7.6	9.6
Sm	2.23	2.16	3.82	1.48	2.31	1.9
Eu	0.87	0.84	1.35	0.55	0.9	0.27
Gd	2.77	2.63	4.68	1.84	2.86	1.55
Tb	0.53	0.52	0.91	0.36	0.56	0.2
Dy	3.4	3.3	5.89	2.29	3.66	0.91
Ho	0.72	0.74	1.27	0.49	0.78	0.16
Er	2.17	2.19	3.76	1.45	2.32	0.43
Tm	0.3	0.31	0.56	0.22	0.33	0.05
Yb	2.12	2.18	3.85	1.44	2.29	0.34
Lu	0.33	0.33	0.57	0.23	0.34	0.05
Cu	61	95	106	63	100	0
Zn	83	88	152	65	96	87
Mo	0	0	0	0	0	0
Ga	18.9	18.9	21.1	11.3	17.5	19.8
Ag	0	0	0	0	0	0
Tl	0	0	0	0	0	0
Pb	0	0	0	0	0	9
Sn	1	1	1	0	1	1
W	0	0	1	1	0	1
Au						0.001

Sample	WR040	WR041	WR042	WR043	WR044	WR045	WR046
Drill Hole	WR02-01	WR02-02	WR02-02	WR02-02	WR02-02	R02-02	WR02-02
From	290.1	341.5	324.3	143.8	126	112.6	86.6
To	290.5	341.9	324.7	144.2	126.4	113	87
Description	Sericite Schist (Gouda)	Sericite Schist (Gouda)	Quartz Eye Sericite Schist (Gouda)	Sheared Mafic Lapilli Tuff	Coarse Grained Porphyroblastic Metagabbro	Biotite Schist	Foliated Metabasalt
Staining Intensity	1	0.5	3	0	0	0	0
Staining Interpretation	econdary	econdary	Secondary				
SiO_2	70.4	68.2	71.8	48.3	48.4	55.8	49.5
TiO_2	0.2	0.22	0.21	0.87	0.94	0.55	1.14
Al_2O_3	15.1	17.85	15.05	20.2	15.8	13.7	13.5
Fe_2O_3	2.17	1.49	2.17	10.65	13.5	7.45	15.55
MnO	0.04	0.02	0.04	0.16	0.21	0.13	0.23
MgO	1.88	0.71	1.58	3.98	6.79	8.39	6.19
CaO	1.64	4.02	2.16	12.6	10.95	6.58	9.39
Na_2O	1.11	3.68	2.09	2.3	1.99	3.75	3.01
K_2O	3.29	1.63	2.83	0.24	0.31	1.31	0.47
P_2O_5	0.05	0.04	0.06	0.08	0.08	0.32	0.09
Cr_2O_3	0	0	0	0.02	0.03	0.07	0.02
SrO	0.01	0.09	0.04	0.02	0.01	0.02	0.02
BaO	0.03	0.05	0.05	0.01	0.01	0.04	0.01
LOI	2.41	0.7	1.4	0.6	0.6	0.7	0
Total	98.3	98.7	99.5	100	99.6	98.8	99.1
Cr	20	10	20	180	240	480	140
Co	3.9	9	4.5	39.1	51	33.7	53.2
Ni	11	17	10	75	100	182	47
Rb	75.2	68.5	69.6	4.7	9.4	33.7	13.6
Sr	125.5	708	308	154.5	122	168.5	186.5
Cs	21.1	9.35	9.34	0.51	1.85	7.79	0.52
Ba	357	528	495	50.7	62.2	356	74.6
V	24	30	26	224	277	134	374
Ta	0.2	0.1	0.2	0.2	0.2	0.4	0.2
Nb	2.5	2.2	2.6	2.7	2.8	10	2.7
Zr	101	98	100	56	65	119	71
Hf	3	2.9	2.9	1.6	1.9	3	2.2
Th	2.09	1.82	2.1	0.32	0.3	8.3	0.4
U	0.63	0.57	0.7	0.07	0.07	1.41	0.08
Y	3.7	2.1	3.6	18.4	21.2	15.8	28.1
La	13.6	10.8	13.6	3.9	4.3	78.8	5
Ce	26.6	21.6	27.4	9.5	10.1	168.5	12.2
Pr	3.08	2.41	3.15	1.45	1.56	20.7	1.89
Nd	11.1	8.4	11.5	7.3	7.9	77.8	9.4
Sm	1.93	1.25	1.93	2.07	2.36	10.25	2.73
Eu	0.52	0.5	0.53	0.85	0.87	2.44	1.09
Gd	1.6	1.05	1.54	2.53	2.88	8.57	3.7
Tb	0.19	0.11	0.18	0.49	0.58	0.89	0.75
Dy	0.75	0.47	0.76	3.22	3.78	3.3	4.95
Ho	0.14	0.09	0.13	0.69	0.8	0.59	1.09
Er	0.39	0.25	0.4	2.08	2.4	1.85	3.19
Tm	0.04	0.02	0.04	0.29	0.34	0.21	0.47
Yb	0.33	0.22	0.32	2.12	2.41	1.46	3.25
Lu	0.05	0.03	0.05	0.31	0.37	0.21	0.51
Cu	0	24	8	81	98	31	113
Zn	42	52	60	88	100	78	118
Mo	0	0	0	0	0	0	0
Ga	19.6	22.3	19.5	19.8	17.7	16.6	19.1
Ag	0	1	0	0	0	0	0
Tl	0	2.5	0	0	0	0	0
Pb	7	82	11	0	0	5	0
Sn	0	1	1	0	0	1	1
W	1	2	1	0	0	0	1
Au	0.002	0.005	0.002				

Sample	WR047	WR048	WR049	WR050	WR051	WR052
Drill Hole	WR02-02	WR02-03	WR02-03	WR02-03	WR02-04	WR02-04
From	67.6	282.7	317.1	376.4	677.2	664.9
To	68	283.1	317.5	376.8	677.6	665.3
Description	Foliated Metabasalt	Foliated Metabasalt	Porphyroblastic Metagabbro	Foliated Metabasalt	Foliated Mafic Volcanic, Moderately Developed Compositional Banding	Foliated Metabasalt, Developed Compositional Separation
Staining Intensity	0	0	0	0	0	0.5
Staining Interpretation						Secondary
SiO_2	50.8	49	48.8	47	48.6	48.9
TiO_2	1.31	0.7	0.69	0.72	0.77	1.04
Al_2O_3	13.5	14.65	14.3	15.55	14.35	13.65
Fe_2O_3	15.45	12.3	12.5	12.45	12.15	14.95
MnO	0.25	0.23	0.21	0.2	0.22	0.26
MgO	4.71	7.76	8.31	8.55	7.04	5.93
CaO	9.26	11.7	11.25	10.9	12.15	10.25
Na_2O	3.03	2.6	2.29	2.49	2.41	2.69
K_2O	0.42	0.39	0.38	0.33	0.81	0.54
P_2O_5	0.11	0.06	0.04	0.06	0.05	0.08
Cr_2O_3	0.01	0.04	0.03	0.04	0.04	0.01
SrO	0.02	0.01	0.01	0.02	0.02	0.02
BaO	0.01	0.01	0	0	0	0
LOI	-0.8	0.6	0.5	0.6	1.1	-0.1
Total	98.1	100	99.3	98.9	99.7	98.2
Cr	50	260	220	270	250	80
Co	49.9	56.2	53.9	54.1	49.8	53.7
Ni	35	126	117	157	125	76
Rb	11.6	7.3	4.7	16	47.4	16.4
Sr	152.5	127.5	107.5	149	194	201
Cs	0.43	0.49	0.94	11.2	2.49	0.95
Ba	76.1	58.9	43.9	13.5	60.2	77.3
V	381	266	268	258	243	305
Ta	0.3	0.1	0.1	0.1	0.1	0.2
Nb	3.5	1.6	1.5	1.5	2.1	3
Zr	95	39	38	42	45	58
Hf	2.9	1.2	1.1	1.2	1.3	1.7
Th	0.77	0.17	0.15	0.15	0.34	0.38
U	0.17	0	0	0	0.14	0.09
Y	31.6	15.2	15.3	17.3	14.2	18.9
La	8.1	3	2.6	2.7	3.4	4.1
Ce	18.4	6.7	6.4	6.1	7.8	10.4
Pr	2.72	1.04	1.03	0.97	1.2	1.58
Nd	13.1	5.2	5.1	5.1	5.8	7.6
Sm	3.66	1.6	1.59	1.54	1.74	2.4
Eu	1.29	0.67	0.66	0.7	0.67	0.88
Gd	4.62	2.2	1.99	2.21	2.19	2.88
Tb	0.87	0.42	0.4	0.45	0.42	0.54
Dy	5.69	2.79	2.59	2.99	2.61	3.41
Ho	1.24	0.61	0.59	0.68	0.57	0.74
Er	3.68	1.78	1.75	1.96	1.69	2.2
Tm	0.53	0.23	0.23	0.29	0.25	0.32
Yb	3.74	1.65	1.74	2.04	1.66	2.14
Lu	0.58	0.26	0.27	0.32	0.23	0.33
Cu	127	90	109	126	85	55
Zn	135	88	91	92	107	110
Mo	0	0	0	0	0	0
Ga	19.8	15.7	15.4	16.4	15	17
Ag	0	0	0	0	0	0
Tl	0	0	0	0	0	0
Pb	0	0	0	0	8	0
Sn	1	0	0	0	1	1
W	0	0	0	0	0	0
Au						

Sample	WR053	WR054	WR055	WR056	WR057	WR058
Drill Hole	WR02-04	WR02-04	WR02-04	WR02-04	WR02-04	WR02-04
From	623.1	653.1	480.8	442	248.6	160
To	623.6	653.4	481.2	442.4	249	160.3
Description	Sericite Schist (Gouda)	Sericite Schist (Gouda)	Foliated Mafic Volcanic, Poorly Developed Compositional Banding	Foliated Metabasalt	Foliated Metabasalt, Poorly Developed Compositional Separation	Sheared Mafic Lapilli Tuff
Staining Intensity	0	2	0	0	0	0
Staining Interpretation		Secondary				
SiO_2	70.8	71.4	48.6	49.2	49.7	47.2
TiO_2	0.22	0.2	0.89	1.1	0.71	0.85
Al_2O_3	15.15	16.35	19.45	13.7	14.7	18.5
Fe_2O_3	2.07	1.45	10.05	15.3	12.15	10.7
MnO	0.04	0.02	0.18	0.24	0.23	0.17
MgO	1.56	0.45	3.98	6.16	6.49	4.79
CaO	3.23	3.58	11.4	9.34	11.6	10.55
Na_2O	1.96	2.92	2.76	3	1.58	3.14
K_2O	2.26	2.46	0.48	0.43	0.9	1.04
P_2O_5	0.05	0.04	0.06	0.1	0.04	0.06
Cr_2O_3	0	0	0.03	0.02	0.04	0.03
SrO	0.03	0.08	0.03	0.03	0.03	0.04
BaO	0.04	0.05	0	0	0	0.01
LOI	1.39	0.7	2.58	1.2	1.89	2.09
Total	98.8	99.7	100.5	99.8	100	99.2
Cr	10	10	170	140	260	170
Co	4.5	6.8	38.7	47.5	54.4	36.7
Ni	9	9	75	51	133	65
Rb	47.2	102	16.5	12.2	60.9	45.3
Sr	239	639	216	262	228	329
Cs	6.08	9.32	2.84	0.73	2.47	2.33
Ba	443	514	64.1	53.3	118	163
V	29	21	220	321	249	199
Ta	0.2	0.2	0.2	0.2	0.1	0.2
Nb	2.3	2.3	2.9	2.7	1.7	2.7
Zr	99	89	55	71	39	54
Hf	2.9	2.6	1.7	2.1	1.2	1.6
Th	2.26	1.71	0.35	0.83	0.23	0.34
U	0.65	0.52	0.08	0.16	0	0.1
Y	3.5	2	18.7	24.6	14.6	17.6
La	14.5	10.7	3.9	6.8	2.5	3.6
Ce	28.3	20.8	9.5	16	6.1	8.9
Pr	3.32	2.31	1.47	2.25	0.96	1.37
Nd	12.1	8	7.1	10.4	4.7	6.7
Sm	1.99	1.17	2.21	2.85	1.59	2.07
Eu	0.53	0.42	0.84	1.08	0.63	0.78
Gd	1.62	0.98	2.72	3.62	1.99	2.59
Tb	0.18	0.1	0.52	0.68	0.41	0.5
Dy	0.75	0.41	3.38	4.35	2.63	3.25
Ho	0.12	0.07	0.73	0.99	0.57	0.7
Er	0.38	0.22	2.19	3.08	1.74	2.08
Tm	0.03	0.01	0.33	0.42	0.22	0.29
Yb	0.31	0.19	2.17	2.95	1.56	2.01
Lu	0.04	0.03	0.33	0.45	0.24	0.3
Cu	6	10	79	105	104	72
Zn	33	65	90	120	84	83
Mo	0	0	0	0	0	0
Ga	19.5	19.6	17.7	18.3	15	16.2
Ag	1	0	0	0	0	0
Tl	0	0	0	0	0	0
Pb	8	7	0	0	0	0
Sn	1	0	1	1	0	1
W	2	1	0	0	0	1
Au	0.003	0				

Sample	WR059	WR060	WR061	WR062	WR063	WR064
Drill Hole	WR02-04	WR02-04	WR02-04	WR02-05	WR02-05	WR02-05
From	159.4	124.6	62.3	542.4	534.8	550.7
To	159.8	124.9	62.6	542.8	535.1	551
Description	Sheared Mafic Lapilli Tuff	Foliated Metabasalt, Poorly Developed Compositional Separation	Foliated Metabasalt	Silicified Biotite Quartz Feldspar Schist (Gouda)	Sericite Schist (Gouda)	Foliated Metabasalt
Staining Intensity	0	0	0	4	3	0
Staining Interpretation				Secondary	econdary	
SiO_2	47.9	49	49.8	70.1	69.3	49.9
TiO_2	0.82	1.42	0.75	0.2	0.29	1.06
Al_2O_3	19.65	14.05	14.95	14.95	15.6	14.05
Fe_2O_3	10.45	15.2	12.5	1.98	2.79	14.4
MnO	0.17	0.27	0.25	0.03	0.05	0.26
MgO	4.52	3.94	6.35	0.71	1.48	5.26
CaO	10.4	11.8	11.7	2.23	1.7	10.6
Na_2O	3.03	1.72	1.7	5.1	2.12	2.32
K_2O	1.28	0.56	0.37	2.3	3.76	0.64
P_2O_5	0.06	0.13	0.03	0.06	0.13	0.08
Cr_2O_3	0.02	0.01	0.03	0	0	0.01
SrO	0.04	0.03	0.01	0.12	0.07	0.02
BaO	0.01	0	0	0.09	0.19	0.01
LOI	1.69	0.7	1.39	0.3	2	1.29
Total	100	98.8	99.8	98.2	99.5	99.9
Cr	160	90	220	20	30	90
Co	35.3	47.4	53.9	3.9	5.7	55.1
Ni	68	52	111	7	14	79
Rb	53.6	12.6	12.1	72.1	126.5	28
Sr	330	231	121.5	965	602	186
Cs	2.49	0.39	1.8	4.64	4.7	0.64
Ba	206	120	65.5	832	1630	129.5
V	198	343	264	28	38	298
Ta	0.2	0.2	0.1	0.2	0.3	0.2
Nb	2.6	4	2.1	2.1	4.3	3.1
Zr	50	84	42	91	139	60
Hf	1.5	2.6	1.3	2.8	4.1	1.8
Th	0.32	0.5	0.27	2.8	5.91	0.38
U	0.07	0.12	0.06	1.35	2	0.17
Y	17.3	28.6	15.7	3.8	6.1	19.8
La	3.5	5.3	3.3	14	32.9	4.2
Ce	8.7	13.6	7.4	27.6	68.4	10.7
Pr	1.35	2.08	1.11	3.29	8.25	1.67
Nd	6.5	10.7	5.5	12.5	30.9	8.2
Sm	2.03	3.28	1.71	2.23	5.16	2.4
Eu	0.76	1.2	0.68	0.57	1.11	0.92
Gd	2.6	4.18	2.28	1.78	3.9	3
Tb	0.49	0.79	0.43	0.2	0.39	0.57
Dy	3.11	5.19	2.87	0.82	1.48	3.68
Ho	0.69	1.16	0.62	0.14	0.22	0.79
Er	2.01	3.31	1.91	0.39	0.67	2.41
Tm	0.29	0.5	0.26	0.03	0.05	0.32
Yb	1.96	3.42	1.78	0.29	0.43	2.25
Lu	0.31	0.51	0.29	0.05	0.07	0.34
Cu	81	113	108	6	0	155
Zn	85	128	95	57	37	111
Mo	0	0	2	0	7	7
Ga	17.5	18.7	15	21.3	21	17.2
Ag	0	0	0	0	0	0
Tl	0	0	0	0	0	0
Pb	0	0	0	20	10	0
Sn	1	1	0	1	1	1
W	3	1	0	0	1	1
Au				0.002	0.002	

Sample	WR065	WR066	WR067	WR068	WR069	WR070
Drill Hole	WR02-05	WR02-05	WR02-05	WR02-05	WR02-06a	WR02-06a
From	411.8	395.4	348.8	281.4	492.2	505.2
To	412.1	395.8	395.3	281.8	492.6	505.5
Description	Weakly Sheared Mafic Lapilli Tuff	Sheared Mafic Lapilli Tuff	Foliated Metabasalt, Poorly Developed Compositional Separation	Foliated Metabasalt	Quartz Eye Sericite Schist (Gouda)	Sericite Schist (Gouda)
Staining Intensity	0	0	0	0	0	3
Staining Interpretation						Secondary
SiO_2	49.6	48.6	48.7	49.6	74.6	71
TiO_2	0.86	0.89	0.85	0.69	0.19	0.23
Al_2O_3	20.2	18.6	14.65	14.45	14.95	16.2
Fe_2O_3	9.7	11.55	13.5	12.5	0.77	0.99
MnO	0.17	0.16	0.22	0.22	0.01	0.01
MgO	3.02	5.24	7.84	7.31	0.16	0.3
CaO	11.6	11.8	11.05	12.1	1.47	3.15
Na_2O	3.28	2.6	2.69	2.36	3.27	5.15
K_2O	0.76	0.24	0.31	0.41	1.92	1.7
P_2O_5	0.07	0.06	0.05	0.03	0.02	0.04
Cr_2O_3	0.03	0.03	0.04	0.04	0	0
SrO	0.03	0.02	0.02	0.02	0.03	0.1
BaO	0.01	0	0	0	0.06	0.06
LOI	0.9	0.3	0.7	0.8	1.1	0.1
Total	100	100	100.5	100.5	98.6	99
Cr	170	170	270	260	10	10
Co	36.9	39	52.6	53.1	3.7	7.2
Ni	67	70	122	127	9	14
Rb	22	7.2	9.2	23	33.8	49.4
Sr	269	139	151	189	257	807
Cs	3.26	0.92	1.9	2.09	1.59	6.33
Ba	142.5	11.8	16.7	22.3	624	595
V	211	218	270	244	23	28
Ta	0.2	0.2	0.1	0.1	0.1	0.1
Nb	2.9	2.9	1.8	2	1.8	2.2
Zr	57	55	48	36	91	111
Hf	1.8	1.7	1.5	1.1	2.8	3.2
Th	0.41	0.34	0.25	0.22	1.43	2
U	0.1	0.08	0.06	0.06	0.5	0.6
Y	18.5	18.7	19	14.1	3.5	2.3
La	4.3	3.7	3.1	2.6	10.7	14.9
Ce	10.3	9.1	7.2	6.2	21.3	28.6
Pr	1.55	1.41	1.14	0.95	2.46	3.09
Nd	7.6	7	5.7	4.8	8.8	10.6
Sm	2.23	2.19	1.91	1.54	1.51	1.54
Eu	0.86	0.81	0.77	0.65	0.4	0.47
Gd	2.75	2.7	2.62	2.05	1.22	1.17
Tb	0.5	0.51	0.52	0.4	0.14	0.13
Dy	3.4	3.4	3.42	2.55	0.67	0.51
Ho	0.72	0.75	0.76	0.58	0.14	0.08
Er	2.18	2.23	2.34	1.66	0.39	0.26
Tm	0.31	0.33	0.34	0.23	0.05	0.03
Yb	2.13	2.16	2.26	1.63	0.33	0.23
Lu	0.32	0.33	0.36	0.25	0.06	0.04
Cu	88	83	87	110	10	13
Zn	89	89	99	93	117	78
Mo	0	0	0	0	3	17
Ga	18.8	17.3	15.6	15.3	20.1	21.6
Ag	0	0	0	0	0	0
Tl	0	0	0	0	0	0
Pb	5	0	0	6	9	12
Sn	1	1	0	1	1	1
W	0	1	1	0	0	1
Au					0	0.003

Sample	WR071	WR072	WR073	WR074	WR075
Drill Hole	WR02-06a	WR02-06a	WR02-06a	WR02-06a	WR02-06a
From	517.4	367.9	359.2	338.5	240.8
To	517.7	368.3	359.5	338.8	241.2
Description	Foliated Metabasalt, Poorly Developed Compositional Separation	Sheared Mafic Lapilli Tuff	Sheared Mafic Lapilli Tuff	Foliated Metabasalt, Poorly Developed Compositional Separation	Foliated Metabasalt
Staining Intensity	0	0	0	0	0
Staining Interpretation					
SiO_2	50.4	49.5	49.6	51.7	49.7
TiO_2	0.99	0.9	0.91	1.18	0.7
Al_2O_3	14.05	19.7	19.65	13.55	14.25
Fe_2O_3	13.45	9.95	10.45	14.45	12.3
MnO	0.27	0.18	0.19	0.28	0.21
MgO	6.13	3.59	3	5.08	7.33
CaO	10.95	10.8	13.25	9.98	12.4
Na_2O	2.23	3.29	2.03	2.68	1.91
K_2O	0.56	0.24	0.49	0.38	0.18
P_2O_5	0.08	0.07	0.08	0.1	0.06
Cr_2O_3	0.02	0.02	0.02	0.02	0.04
SrO	0.02	0.02	0.02	0.02	0.02
BaO	0.01	0	0.01	0.01	0
LOI	0.5	1	0.7	0.2	1.08
Total	99.7	99.3	100.5	99.6	100
Cr	140	170	170	130	260
Co	55.5	38.4	39.2	53.3	55.3
Ni	96	72	70	47	132
Rb	21.4	7.7	10	7	4.1
Sr	162.5	163.5	195	159.5	163.5
Cs	1.11	2.25	2.21	0.25	0.58
Ba	87.4	14.5	47.6	64.4	33.3
V	292	217	226	364	255
Ta	0.2	0.2	0.2	0.2	0.1
Nb	2.7	2.8	3	2.6	1.6
Zr	53	53	55	69	35
Hf	1.6	1.6	1.6	2.1	1.1
Th	0.36	0.37	0.38	0.37	0.21
U	0.16	0.09	0.11	0.1	0.06
Y	18.4	18.4	19.8	26.8	14.4
La	3.8	3.6	4	4.1	2.6
Ce	9.7	9.2	9.9	10.4	5.9
Pr	1.5	1.45	1.51	1.64	0.91
Nd	7.4	7	7.4	8.2	4.7
Sm	2.26	2.17	2.23	2.78	1.57
Eu	0.86	0.82	0.92	1.01	0.65
Gd	2.74	2.63	2.86	3.63	2
Tb	0.52	0.51	0.54	0.69	0.41
Dy	3.32	3.26	3.47	4.56	2.56
Ho	0.72	0.7	0.75	1.01	0.56
Er	2.15	2.13	2.31	3.08	1.68
Tm	0.34	0.35	0.38	0.52	0.25
Yb	2.06	2.06	2.22	3.08	1.55
Lu	0.31	0.32	0.34	0.48	0.24
Cu	139	100	73	120	111
Zn	106	90	101	129	86
Mo	0	0	0	0	0
Ga	17	17.9	19.4	19	15.4
Ag	0	0	0	0	0
Tl	0	0	0	0	0
Pb	0	0	0	0	0
Sn	1	0	1	1	0
W	1	1	1	1	1
Au					

Sample	WR076	WR077	WR078	WR079	WR080	WR081
Drill Hole	WR02-09	WR02-09	WR02-09	WR02-09	WR01-07	WR01-07
From	228.6	241.2	264.8	12.3	24.7	64.2
To	229	241.5	265.2	12.7	25	64.5
Description	Quartz Eye Sericite Schist (Gouda)	Sericite Schist (Gouda)	Quartz Eye Sericite Schist (Gouda)	Sheared Mafic Lapilli Tuff	Medium Grained, Sheared Porphyroblastic Metagabbro	Foliated Metabasalt
Staining Intensity	3	0.5	3	1.5	0	0
Staining Interpretation	Secondary	econdary	Secondary	Secondary		
SiO_2	77.2	73	75.7	48.3	48.3	50.5
TiO_2	0.13	0.26	0.2	0.86	0.72	1.13
Al_2O_3	12.05	16.5	12.95	18.1	15.05	13.75
Fe_2O_3	1.11	1.46	0.68	10.9	12.15	14.8
MnO	0.02	0.01	0.01	0.17	0.2	0.27
MgO	0.29	0.17	0.13	4.94	8.34	5.46
CaO	1.2	0.11	1.61	9.82	9.38	10.5
Na_2O	4.53	0.73	5.12	3.44	3.04	2.51
K_2O	2.01	3.39	1.49	1.24	0.84	0.4
P_2O_5	0.01	0.01	0.03	0.07	0.04	0.13
Cr_2O_3	0	0	0	0.02	0.04	0.02
SrO	0.03	0.02	0.07	0.06	0.03	0.03
BaO	0.06	0.04	0.07	0.01	0.01	0.01
LOI	0.5	2.48	0.7	1.4	0.89	0.5
Total	99.1	98.2	98.8	99.3	99	100
Cr	10	10	20	170	260	140
Co	7.2	4.8	6.2	38	53.1	52.2
Ni	0	7	5	71	160	48
Rb	163.5	133.5	80.4	69.8	113	18.3
Sr	211	148	564	513	215	218
Cs	4.69	10.1	4.1	12.8	20.2	0.68
Ba	503	308	556	85.7	83.2	106.5
V	12	35	10	223	238	348
Ta	0.5	0.4	0.1	0.2	0.2	0.2
Nb	12.2	7	1.9	2.5	2.7	2.8
Zr	61	112	91	51	37	69
Hf	2.1	3.2	2.6	1.5	1.2	2.1
Th	2.04	2.39	1.9	0.34	0.19	0.6
U	1.43	0.69	0.58	0.14	0.14	0.17
Y	4.4	3.3	2.1	17.3	16.1	26
La	7.7	16.7	13.3	3.9	2	6.1
Ce	15.9	32.5	26.5	9.4	5.4	14.8
Pr	1.93	3.66	3	1.41	0.85	2.17
Nd	7.1	12.3	10.9	7	4.7	10.2
Sm	1.46	1.87	1.72	2.13	1.7	3.12
Eu	0.31	0.57	0.49	0.78	0.65	1.1
Gd	1.19	1.67	1.34	2.57	2.14	3.7
Tb	0.15	0.16	0.14	0.47	0.42	0.71
Dy	0.74	0.65	0.52	3.03	2.76	4.58
Ho	0.13	0.11	0.08	0.66	0.63	1
Er	0.41	0.32	0.23	1.97	1.88	3.01
Tm	0.04	0.05	0.03	0.41	0.32	0.49
Yb	0.34	0.24	0.18	1.86	1.87	3
Lu	0.06	0.04	0.03	0.3	0.3	0.47
Cu	13	20	11	48	136	170
Zn	52	44	27	101	90	128
Mo	0	0	2	0	15	0
Ga	21.9	27.1	18.8	20.2	17.2	18.8
Ag	0	0	0	0	0	0
Tl	0	0	0	0	0	0
Pb	39	62	25	6	6	0
Sn	2	1	1	0	1	1
W	2	2	2	1	1	1
Au	0	0	0.001	0	0	

Sample	WR082	WR083	WR084	WR085	WR086	WR087
Drill Hole	WR01-07	WR01-07	WR01-07	WR01-07	WR01-07	WR01-08
From	96	123.8	151.9	252.3	258.5	12.8
To	96.4	124.2	152.4	252.6	258.9	13.2
Description	Sheared Porphyroblastic Mafic Lapilli Tuff	Weakly Sheared Mafic Lapilli Tuff	Foliated Metabasalt	Quartz Eye Sericite Schist (Gouda)	Quartz Eye Sericite Schist (Gouda)	Feldspathic Schist
Staining Intensity	0	0	0	4	3	0
Staining Interpretation				Secondary	Secondary	
SiO_2	47.5	47.8	51.9	76	79.7	61.9
TiO_2	0.95	0.85	1.07	0.18	0.17	0.57
Al_2O_3	17.85	19.6	16.15	12.9	11.4	14.95
Fe_2O_3	11.8	9.89	11.75	0.89	0.82	5.71
MnO	0.17	0.17	0.21	0.01	0.02	0.08
MgO	5.34	4.18	3.92	0.23	0.41	3.18
CaO	10.4	11.75	9.38	2.13	2.15	4.72
Na_2O	2.98	2.24	3.26	4.63	3.6	4.68
K_2O	0.7	1.23	0.61	1.42	1.24	1.71
P_2O_5	0.07	0.07	0.08	0.05	0.03	0.17
Cr_2O_3	0.03	0.02	0.04	0	0	0.01
SrO	0.02	0.03	0.03	0.06	0.05	0.09
BaO	0.01	0.02	0.01	0.06	0.06	0.09
LOI	1.6	2.1	1.7	0.3	0.88	1.07
Total	99.4	100	100	98.9	100.5	98.9
Cr	180	170	260	20	20	100
Co	41.8	37.6	54.2	6.3	2.3	18.2
Ni	75	69	113	11	7	40
Rb	58.3	85	32.6	32.6	75.7	45.1
Sr	183	267	225	518	394	731
Cs	1.54	2.18	1.16	4.1	7.19	1.92
Ba	115	177.5	90	534	521	744
V	230	206	286	16	15	107
Ta	0.2	0.2	0.2	0.2	0.2	0.2
Nb	2.7	2.6	3.3	4.8	2.6	4.2
Zr	47	54	63	79	74	111
Hf	1.4	1.6	1.9	2.3	2.1	3
Th	0.32	0.32	0.4	1.42	1.25	3.64
U	0.07	0.08	0.11	0.58	0.56	0.98
Y	17.4	17.9	22.6	3	2.6	9.9
La	3.4	3.7	4.3	7.8	7.7	26.3
Ce	8.5	9.2	10.7	16.3	15.2	54.6
Pr	1.32	1.41	1.63	1.94	1.75	6.78
Nd	6.5	6.8	8.1	7.4	6.6	26.8
Sm	2.02	2.11	2.53	1.32	1.1	4.63
Eu	0.81	0.8	0.98	0.43	0.32	1.21
Gd	2.54	2.59	3.14	1.07	0.92	3.65
Tb	0.48	0.5	0.63	0.13	0.11	0.43
Dy	3.1	3.19	3.97	0.56	0.52	2.01
Ho	0.66	0.68	0.87	0.11	0.1	0.37
Er	2.01	2.04	2.6	0.32	0.28	1.09
Tm	0.32	0.33	0.43	0.04	0.03	0.16
Yb	1.97	1.98	2.41	0.29	0.24	0.94
Lu	0.31	0.32	0.39	0.04	0.05	0.14
Cu	71	140	124	9	8	29
Zn	91	83	121	29	116	87
Mo	5	0	0	3	0	0
Ga	17.6	18.3	18.3	18.1	15.9	21.2
Ag	0	0	0	0	0	0
Tl	0	0	0	0	0	0
Pb	0	0	0	11	11	9
Sn	0	0	1	1	1	1
W	1	1	1	1	1	2
Au				0.001	0	

Sample	WR088	WR089	WR090	WR091	WR092	WR093
Drill Hole	WR01-08	WR01-07	WR01-09	WR01-09	WR01-09	WR01-09
From	29.5	291	24.8	107.1	147.8	288.9
To	29.9	291.3	25.2	107.5	148.2	289.3
Description	Feldspathic Schist	Foliated Metabasalt, Poorly Developed Compositional Separation	Foliated Metabasalt	Foliated Mafic Volcanic, Poorly Developed Compositional Banding	Sheared Mafic Lapilli Tuff	Quartz Eye Sericite Schist (Gouda)
Staining Intensity	0	0	0	0	0	0
Staining Interpretation						
SiO_2	64.5	49.4	49.1	47.8	49	75.6
TiO_2	0.45	0.82	0.74	1.13	0.88	0.21
Al_2O_3	15.15	14.05	14.3	14.55	18.95	14.15
Fe_2O_3	4.55	12.25	12.4	15.25	10.1	0.88
MnO	0.07	0.2	0.2	0.23	0.19	0.01
MgO	2.45	7.55	7.83	6.09	4.01	0.22
CaO	4.49	11.25	10.9	9.75	10.35	1.68
Na_2O	4.27	2.65	2.5	2.82	3.48	3.69
K_2O	2.05	0.75	0.57	0.31	0.62	1.62
P_2O_5	0.14	0.06	0.05	0.09	0.07	0.03
Cr_2O_3	0.01	0.04	0.03	0.02	0.02	0
SrO	0.11	0.03	0.02	0.02	0.03	0.03
BaO	0.09	0.01	0.01	0	0.02	0.05
LOI	-0.3	1.05	0.8	0.79	0.7	0.1
Total	98	100	99.5	98.9	98.4	98.3
Cr	80	250	230	120	170	10
Co	14.1	51.1	51.5	53.5	39.2	4.1
Ni	34	122	114	68	68	9
Rb	48.1	52.8	33.7	24.8	32.6	28.8
Sr	902	216	137	197	237	238
Cs	1.87	2.32	2.54	1.54	3.81	2.06
Ba	726	68.7	97.2	33.6	134.5	409
V	81	255	262	328	216	18
Ta	0.3	0.2	0.1	0.2	0.2	0.2
Nb	3.6	2.4	1.6	2.7	3	2.3
Zr	114	45	39	66	54	97
Hf	3.1	1.4	1.2	2	1.7	2.8
Th	4.16	0.34	0.21	0.39	0.4	1.78
U	1.2	0.25	0.06	0.1	0.11	0.64
Y	9.5	15.7	15.3	25.8	18.7	3.2
La	28.1	3.3	2.4	4.3	4.2	11.7
Ce	57.1	8.2	6.3	11	10.3	22.5
Pr	6.96	1.24	1.01	1.71	1.54	2.6
Nd	26.5	6.3	5	8.5	7.4	9.1
Sm	4.42	1.91	1.66	2.58	2.24	1.46
Eu	1.14	0.7	0.63	0.98	0.85	0.39
Gd	3.6	2.31	2.07	3.25	2.71	1.25
Tb	0.4	0.43	0.42	0.64	0.5	0.14
Dy	1.89	2.86	2.64	4.29	3.39	0.61
Ho	0.35	0.6	0.58	0.95	0.71	0.12
Er	1.02	1.75	1.69	2.91	2.14	0.34
Tm	0.15	0.28	0.29	0.44	0.35	0.07
Yb	0.91	1.65	1.77	2.84	2.06	0.29
Lu	0.14	0.27	0.27	0.46	0.32	0.05
Cu	25	116	134	175	75	19
Zn	73	90	87	126	89	38
Mo	0	0	0	0	0	7
Ga	21.3	16.3	15.4	19	18.1	19.4
Ag	0	0	0	0	0	0
Tl	0	0	0	0	0	0
Pb	10	0	0	0	0	5
Sn	1	1	0	1	1	0
W	1	1	1	2	1	2
Au						0

Sample	WR094	WR095	WR096	WR097	WR098	WR099
Drill Hole	WR01-09	WR01-09	WR01-10	WR01-10	WR01-10	WR01-10
From	295.9	322.8	62	78	96.6	116.7
To	296.3	323.9	62.4	78.3	97	117.1
Description	Silicified Sericite Schist (Gouda)	Foliated Mafic Volcanic, Moderately Developed Compositional Banding	Foliated Mafic Volcanic, Poorly Developed Compositional Banding	Quartz Eye Sericite Schist	Sericite Schist (Gouda)	Fine Grained Weakly Foliated Porphyroblastic Metagabbro
Staining Intensity	3	0	0	4	0	0
Staining Interpretation	Secondary			Secondary		
SiO_2	74.4	49.4	50.1	75.1	69.5	49.7
TiO_2	0.07	1.05	0.76	0.26	0.28	1.02
Al_2O_3	13.8	13.7	16.1	14.35	17.6	13.6
Fe_2O_3	1.24	14.15	11.25	0.97	2.36	14.35
MnO	0.04	0.27	0.21	0.01	0.01	0.22
MgO	0.97	5.1	5.31	0.46	0.52	6.92
CaO	1.45	11.85	10.65	1.44	0.15	9.97
Na_2O	0.96	2.42	2.6	3.56	0.42	2.61
K_2O	4.71	0.6	0.56	2.45	2.95	0.37
P_2O_5	0.01	0.08	0.04	0.03	0.06	0.07
Cr_2O_3	0	0.01	0.04	0	0	0.01
SrO	0.02	0.02	0.02	0.04	0.02	0.01
BaO	0.12	0.01	0.02	0.05	0.06	0.01
LOI	1.19	0	0.8	1.2	4.6	0.5
Total	99	98.7	98.5	99.9	98.5	99.4
Cr	10	90	300	30	10	100
Co	1.1	56.6	52.6	4.9	5	54.1
Ni	0	83	145	21	10	81
Rb	123.5	26.4	17.7	39	67.4	7.9
Sr	135.5	191.5	128.5	337	124	112
Cs	6.16	0.6	4.17	13.55	11.4	0.88
Ba	1015	103.5	197	449	501	46.9
V	5	317	254	27	26	298
Ta	0.3	0.2	0.1	0.1	0.2	0.2
Nb	4.1	3.3	1.7	2.1	2.2	2.8
Zr	43	62	41	99	122	56
Hf	2.2	1.8	1.3	2.7	3.4	1.6
Th	3.29	0.41	0.21	3.57	2.37	0.32
U	1.47	0.14	0.08	0.6	0.67	0.08
Y	5	20.1	18.4	3	2.6	18.9
La	10.3	4.4	2.6	19.6	17.8	3.7
Ce	21.5	10.8	6.2	39.2	34.5	9.7
Pr	2.65	1.69	1.01	4.57	3.89	1.55
Nd	9.8	8.5	5.3	16	13.4	7.5
Sm	2.11	2.52	1.79	2.34	1.99	2.26
Eu	0.28	0.94	0.68	0.64	0.47	0.88
Gd	1.67	3.03	2.33	1.84	1.53	2.82
Tb	0.23	0.57	0.46	0.18	0.16	0.52
Dy	0.98	3.52	3.15	0.67	0.59	3.28
Ho	0.18	0.76	0.71	0.12	0.1	0.72
Er	0.48	2.3	2.17	0.34	0.3	2.08
Tm	0.06	0.36	0.35	0.04	0.04	0.33
Yb	0.39	2.25	2.12	0.26	0.26	1.99
Lu	0.06	0.35	0.34	0.04	0.04	0.31
Cu	7	167	118	9	14	146
Zn	55	128	96	76	145	107
Mo	0	0	0	0	0	0
Ga	22.7	18.2	17.3	20.6	24.5	17.1
Ag	0	0	0	0	0	0
Tl	0	0	0	0	0	0
Pb	19	5	0	8	29	0
Sn	1	1	0	0	0	0
W	2	1	1	1	2	1
Au	0				0.002	

Sample	WR100	WR101	WR102	WR103	WR104	WR105
Drill Hole	WR01-10	WR00-01	WR00-01	WR00-01	WR00-01	WR00-01
From	139	33	65.6	94.8	131	139
To	139.4	33.4	66	95.1	131.4	139.3
Description	Foliated Mafic Volcanic, Moderately Developed Compositional Banding	Sheared Mafic Lapilli Tuff	Massive Metabasalt	Foliated Mafic Volcanic, Poorly Developed Compositional Banding	Quartz Eye Sericite Schist (Gouda)	Quartz Eye Sericite Schist (Gouda)
Staining Intensity	0	0	0	0	4	4
Staining Interpretation					Secondary	Secondary
SiO_2	51.5	50.4	50.8	49.6	75.7	73.2
TiO_2	0.74	1.06	0.82	0.87	0.15	0.23
Al_2O_3	15.65	16.3	13.8	14.2	13.15	15.2
Fe_2O_3	11.5	11.95	12.6	16.55	0.57	0.6
MnO	0.25	0.25	0.19	0.44	0.01	0.02
MgO	5.56	3.93	6.83	4.23	0.13	0.21
CaO	12.45	9.84	9.76	10.1	1.12	1.68
Na_2O	2.12	4.09	3.12	2.29	3.26	4.71
K_2O	0.23	0.9	0.8	0.43	5.23	2.11
P_2O_5	0.05	0.08	0.12	0.06	0.04	0
Cr_2O_3	0.04	0.03	0.04	0.04	0	0.01
SrO	0.01	0.02	0.03	0.01	0.02	0.05
BaO	0.01	0.04	0.03	0.01	0.1	0.07
LOI	0.1	1.6	0.7	1.09	0.4	0.69
Total	100	100.5	99.6	99.9	99.9	98.8
Cr	280	180	250	260	10	10
Co	54.5	52	45.8	52.8	1.6	1.4
Ni	147	91	95	112	0	0
Rb	7.2	55.5	54.5	9.5	92.9	119.5
Sr	110	137	213	103.5	211	432
Cs	0.92	2.28	8.51	0.77	14.3	7.57
Ba	55.7	297	223	83.1	818	599
V	258	308	265	287	14	21
Ta	0.1	0.2	0.1	0.1	0.3	0.2
Nb	1.6	3.1	2.3	1.8	3	2.2
Zr	39	63	57	49	69	94
Hf	1.2	1.9	1.7	1.5	2.3	2.8
Th	0.19	0.37	0.94	0.3	2.13	1.92
U	0.06	1.34	0.39	0.09	1.28	0.85
Y	15.4	22.4	18.8	22.2	3.8	2.9
La	2.5	4	7.1	3.6	9.5	12.6
Ce	6.3	9.8	15.8	8.7	19.4	24.4
Pr	0.99	1.53	2.2	1.35	2.29	2.96
Nd	5.2	7.5	9.8	6.9	8.7	10.3
Sm	1.67	2.38	2.64	2.15	1.55	1.65
Eu	0.63	0.92	0.9	0.83	0.34	0.51
Gd	2.04	2.96	2.97	2.87	1.21	1.43
Tb	0.39	0.58	0.52	0.58	0.16	0.16
Dy	2.67	3.71	3.22	3.74	0.65	0.65
Ho	0.58	0.8	0.7	0.82	0.13	0.12
Er	1.72	2.39	2.07	2.48	0.35	0.31
Tm	0.27	0.42	0.32	0.41	0.08	0.03
Yb	1.67	2.41	2.05	2.51	0.32	0.28
Lu	0.27	0.39	0.33	0.4	0.05	0.04
Cu	127	118	82	103	0	0
Zn	89	131	88	109	35	13
Mo	0	0	0	9	2	0
Ga	16.1	19.7	16.7	16.6	19.3	18.9
Ag	0	0	0	0	0	0
Tl	0	0	0	0	0	0
Pb	0	11	5	0	14	5
Sn	0	1	1	0	1	0
W	1	1	1	1	1	1
Au					0.004	0

Sample	WR106	WR107	WR108	WR109	WR110
Drill Hole	WR00-02	WR00-02	WR00-02	WR00-03	WR00-03
From	48.6	72.6	89.3	339.3	362.9
To	49	73	89.7	339.7	363.3
Description	Foliated Mafic Volcanic, Developed Compositional Separation	Quartz Eye Sericite Schist (Gouda)	Quartz Eye Sericite Schist (Gouda)	Foliated Mafic Volcanic, Poorly Developed Compositional Banding	Foliated Mafic Volcanic, Poorly Developed Compositional Banding
Staining Intensity	1	3	0.5	0	0
Staining Interpretation	Secondary	Secondary	Secondary		
SiO_2	46.1	75.6	72.9	49	49.5
TiO_2	0.75	0.14	0.21	0.67	0.67
Al_2O_3	15.85	12.2	14.75	14.1	13.95
Fe_2O_3	12.65	1	1.01	12.35	12
MnO	0.2	0.02	0.02	0.21	0.2
MgO	6.73	0.24	0.45	7.63	7.27
CaO	11.1	1.65	2.08	10.85	10.8
Na_2O	2.63	3.8	2.73	2.8	2.4
K_2O	1.27	2.67	2.24	0.29	0.3
P_2O_5	0.07	0.03	0.02	0.03	0.03
Cr_2O_3	0.05	0.02	0.01	0.04	0.04
SrO	0.02	0.03	0.03	0.02	0.02
BaO	0.05	0.08	0.05	0	0.01
LOI	1.79	0.69	1.59	0.6	1
Total	99.3	98.2	98.1	98.6	98.2
Cr	260	10	20	280	260
Co	52.9	1.8	2	53.4	53
Ni	154	0	0	121	120
Rb	78.7	83.7	108	4.8	9.7
Sr	205	275	297	192.5	156
Cs	16.7	7.29	8.26	1.23	2.64
Ba	472	765	429	43.1	67.2
V	244	12	27	254	252
Ta	0.1	0.2	1.2	0	0
Nb	1.6	2.6	4.7	1.5	1.5
Zr	42	60	91	39	34
Hf	1.3	2.1	2.9	1.3	1.1
Th	0.23	1.81	2.27	0.14	0.2
U	0.06	0.96	0.91	0	0
Y	17.5	3.7	4.2	14.8	15.1
La	2.5	9	13.1	2.9	2.7
Ce	6.5	18	25.7	6.4	6
Pr	1.08	2.26	2.8	0.78	0.74
Nd	5.3	8.2	10.9	4.5	4.6
Sm	1.74	1.46	1.65	1.33	1.26
Eu	0.78	0.4	0.27	0.4	0.42
Gd	2.36	1.39	1.37	1.72	1.8
Tb	0.47	0.16	0.1	0.32	0.32
Dy	3.32	0.78	0.53	2.38	2.43
Ho	0.74	0.14	0.03	0.48	0.42
Er	2.26	0.38	0.19	1.53	1.45
Tm	0.32	0.05	0.04	0.23	0.24
Yb	2.09	0.33	0.16	1.44	1.36
Lu	0.33	0.05		0.18	0.18
Cu	53	8	5	107	94
Zn	94	29	39	83	78
Mo	0	0	0	0	0
Ga	16.7	17.8	19.7	14.7	13.8
Ag	0	0	0	0	0
Tl	0	0	0	0	0
Pb	0	0	23	0	0
Sn	0	0	0	0	0
W	1	1	0	0	0
Au			0		

Sample	WR111	WR112	WR113	WR114	WR115	WR116
Drill Hole	WR00-04	WR00-04	WR00-04	WR00-04	WR00-04	WR00-07
From	16.4	50.4	82.7	93	131.1	111.5
To	16.9	50.8	83.2	93.4	131.5	111.9
Description	Foliated Mafic Volcanic, Poorly Developed Compositional Banding	Foliated Mafic Volcanic, Moderately Developed Compositional Banding	Quartz Eye Sericite Schist (Gouda)	Quartz Eye Sericite Schist (Gouda)	Foliated Mafic Volcanic, Poorly Developed Compositional Banding	Silicified Felsic Schist (Frank Lake)
Staining Intensity	0.5	0.5	3	3	0	1.5
Staining Interpretation	Secondary	Secondary	Secondary	Secondary		Secondary
SiO_2	48	50	70	77.6	50.7	67.1
TiO_2	0.68	0.85	0.15	0.13	1.14	0.32
Al_2O_3	15.25	14.05	13.95	11.45	13.8	14.3
Fe_2O_3	11.95	12.5	3.03	1.05	14.05	3.19
MnO	0.19	0.29	0.08	0.02	0.2	0.05
MgO	7.83	5.53	0.81	0.25	4.57	1.21
CaO	10.45	10.05	1.8	1.23	9.36	3.07
Na_2O	3.21	3.7	4.7	4.58	3.17	2.94
K_2O	0.6	0.47	2.01	1.94	0.43	2.52
P_2O_5	0.03	0.05	0	0.06	0.05	0.09
Cr_2O_3	0.04	0.04	0.03	0.01	0.01	0.01
SrO	0.01	0.02	0.04	0.03	0.02	0.03
BaO	0.01	0.01	0.07	0.08	0.01	0.03
LOI	1.5	0.6	1.39	0.69	0.59	3.97
Total	99.8	98.2	98.1	99.1	98.1	98.8
Cr	290	270	160	30	30	40
Co	51.4	49.2	2.7	1.6	45.7	7.7
Ni	148	95	0	6	31	25
Rb	10.1	8.6	76.9	42.9	15.8	146
Sr	112	157.5	373	314	204	305
Cs	0.68	0.2	2.83	1.2	1.08	11.7
Ba	62.1	104.5	639	668	62	302
V	234	297	27	21	324	53
Ta	0	0.1	0.1	0.1	0.1	0.2
Nb	1.3	1.7	2.5	1.8	2.9	3.4
Zr	44	50	70	60	63	131
Hf	1.4	1.6	2.6	2.1	1.9	3.7
Th	0.13	0.2	2.29	1.8	0.33	5.95
U	0	0	0.87	0.6	0	1.42
Y	17.1	20.8	5.4	3.1	22.4	7.6
La	3.2	3.6	10.1	9.5	5.3	34.1
Ce	6.1	8.3	20.7	18.3	12.3	68.7
Pr	0.73	1.04	2.23	1.97	1.67	7.75
Nd	4.6	6.2	9.1	7.7	8.9	28.3
Sm	1.36	1.85	1.5	1.24	2.53	4.09
Eu	0.45	0.59	0.18	0.14	0.81	0.8
Gd	2.05	2.52	1.36	1.02	3.17	3.33
Tb	0.34	0.42	0.15	0.08	0.51	0.28
Dy	2.74	3.18	0.83	0.44	3.8	1.34
Ho	0.54	0.67	0.11	0.01	0.74	0.16
Er	1.83	2.22	0.48	0.14	2.46	0.65
Tm	0.27	0.35	0.09	0.06	0.38	0.06
Yb	1.78	2.16	0.45	0.12	2.26	0.46
Lu	0.24	0.31	0.03		0.3	0.04
Cu	94	92	9	7	57	24
Zn	82	100	41	14	82	58
Mo	0	0	0	0	4	0
Ga	14.8	16.3	19.7	15.7	18.2	19.2
Ag	0	0	0	0	0	0
Tl	0	0	0	0	0	0
Pb	5	5	6	7	0	5
Sn	0	0	0	0	0	0
W	2	1	0	0	0	0
Au			0	0.059		0.001

Sample	WR117	WR118	WR119	WR120	WR121	WR122
Drill Hole	WR00-07	WR00-07	WR00-07	WR00-08	WR00-08	WR01-08
From	132.9	203.3	231.6	130	156.9	98.5
To	133.3	203.8	232	130.5	157.4	98.9
Description	Silicified Felsic Schist (Frank Lake)	Quartz Eye Sericite Schist (Frank Lake)	Silicified Felsic Schist (Frank Lake)	Silicified Felsic Schist (Frank Lake)	Silicified Felsic Schist (Frank Lake)	Foliated Metabasalt, Strongly Developed Compositional Layering
Staining Intensity	1	3	0	0	3	0
Staining Interpretation	Secondary	Secondary	Secondary		Secondary	
SiO_2	64.5	74.6	62.6	65.6	68.1	49.2
TiO_2	0.36	0.3	0.38	0.38	0.36	0.79
Al_2O_3	14.4	12.25	14.65	15.2	13.95	15.15
Fe_2O_3	2.45	2.61	3.59	3.88	3.56	10.8
MnO	0.05	0.05	0.07	0.07	0.06	0.29
MgO	1.23	0.57	1.2	1.42	1.34	7.31
CaO	4.31	1.36	4.29	3.26	2.6	9.96
Na_2O	3.52	3.63	2.62	3.4	3.48	3.22
K_2O	2.29	1.78	3.02	2	2.19	1.06
P_2O_5	0.2	0.05	0.15	0.09	0.14	0.04
Cr_2O_3	0.01	0.01	0.01	0.01	0.01	0.05
SrO	0.02	0.02	0.01	0.05	0.04	0.02
BaO	0.02	0.04	0.02	0.07	0.04	0.06
LOI	4.75	0.8	5.48	2.68	2.99	1.2
Total	98.1	98.1	98.1	98.1	98.9	99.2
Cr	70	40	50	60	60	290
Co	7.7	7.2	8.5	12.5	11.1	57.4
Ni	17	16	13	32	36	202
Rb	140.5	50.6	230	51.5	108	41.3
Sr	182.5	216	104	415	388	242
Cs	8.47	3.31	14.7	3.8	14.35	35.7
Ba	168.5	356	214	580	382	545
V	55	47	69	69	73	237
Ta	0.2	0.2	0.6	0.2	0.2	0.1
Nb	3.3	2.7	9.7	3.5	3.2	2.1
Zr	122	103	161	120	115	44
Hf	3.4	2.7	4.3	3.4	3	1.3
Th	9.65	2.38	4.38	3.91	2.95	0.17
U	1.9	0.82	0.98	0.89	0.66	0.13
Y	9.6	5.4	11.6	8	7.3	18.2
La	67.4	19.5	28.3	25.1	25	3.2
Ce	136.5	37.6	59	50.7	48	7.7
Pr	15.75	4.11	7.02	5.82	5.48	0.92
Nd	57.5	15.8	26	21.7	20.8	5.6
Sm	7.93	2.4	3.8	3.24	3.01	1.64
Eu	1.05	0.46	0.58	0.65	0.6	0.55
Gd	5.72	1.85	3.2	2.54	2.55	2.27
Tb	0.46	0.17	0.27	0.24	0.24	0.39
Dy	1.79	0.93	1.54	1.4	1.13	3.01
Ho	0.27	0.1	0.21	0.2	0.16	0.58
Er	0.89	0.43	0.77	0.63	0.61	1.9
Tm	0.11	0.06	0.09	0.1	0.07	0.33
Yb	0.66	0.32	0.66	0.6	0.43	1.81
Lu	0.08	0.03	0.08	0.05	0.05	0.25
Cu	52	21	14	32	37	82
Zn	30	786	73	105	80	98
Mo	0	0	0	0	16	0
Ga	18.3	16.6	22.7	20.9	18.6	16.3
Ag	0	0	0	0	0	0
Tl	0	0	0.5	0	0	0
Pb	0	53	11	11	0	0
Sn	0	0	1	0	1	0
W	0	0	0	0	1	1
Au	0.001	0.003	0	0	0	0

Appendix D

Geochronology Compilation

Appendix D-1: Geochronology Compilation

Sample	Location (unit)	Rock Type	UTM_E	UTM_N	Age (Ma)	Error
		This Study				
FRL	Frank Lake Felsic Horizon	Metasedimentary	587700	5389490	2720.8	1
HEZ01	Gouda Lake	Volcanic	593540	5387887	2704.8	1.1
HEZ03	Thor Lake	Volcanic	592629	5388535	2705.6	1
HEZ02	DC Lake	Volcanic	592553	5388990	2694.5	1
UAZ	Upper Anomalous Zone	Metasedimentary	586774	5391632	2691.6	1.1
MooseLake_ET	Moose Lake Porphyry (hemlo)	Volcanic	586563	5398027	2693.1	1
CLP	Cedar Lake Pluton	Intrusive	591505	5389744	2683.4	1.7
WRS	White River Stock	Intrusive	591505	5389744	2686.5	1.3
		Davis and Lin (2003)				
DD95-38	Moose Lake Porphyry, highway 17	Volcanic	580658	5393497	2694	2
DD96-25	Fragmental Moose Lake Porphyry, south zone outcrop	Volcanic	578474	5394067	inconclusive	
DD95-41	Moose Lake Porphyry, barren sulphide zone, highway 17	Volcanic	581270	5393503	2688	2
DD95-44	Quartz Porphyry South of Hemlo Fault	Intrusive	580908	5392075	2722	1
DD95-43(a)	Lower Graywacke, Highway 17	Metasedimentary	582123	5393912	2690.5	0.8
DD95-43(b)	Lower Graywacke, Highway 17	Metasedimentary	582123	5393912	2697.7	1.1
DD95-39	Upper Graywacke, Highway 17	Metasedimentary	580493	5393496	2690.5	0.9
DD95-26	Reworked felsic volcaniclastic rock, north wall of the north zone pit	Metasedimentary	578198	5394419	2693.3	1.9
DD95-37(a)	Hanging-wall sediments (metawacke), entrance to A zone pit	Metasedimentary	580157	5393738	2693.5	0.8
DD95-37(b)	Hanging-wall sediments (metawacke), entrance to A zone pit	Metasedimentary	580157	5393738	2685.4	4.1
DD95-42	Heterolithic Conglomerate, Highway 17	Metasedimentary	581602	5393627	<2689	2
LIN97-1	Feldspar porphyry dike intruding ore, hanging wall contact, david bell mine	Intrusive	David Bell Mine		2677.5	1.3
DD96-23,25	Kusin's porphyry intruding sericitic ore, golden giant mine	Intrusive	Golden Giant Mine		2692.6	1.9
LIN97-2	Mineralized Aplite dike	Intrusive	David Bell Mine		2677.2	1.5
DD98-2	Cedar Lake Pluton, Highway 17	Intrusive	585041	5395434	2680.2	1.1

Sample	Location (unit)	Rock Type	UTM_E	UTM_N	Age (Ma)	Error
	Beakhouse and Davis (2005)					
96GPB7271	Biotite tonalite gneiss, Pukaskwa Batholith	Intrusive	554025	5379067	2718.1	1.4
DD97-19	Biotite tonalite gneiss, Black-Pic batholith	Intrusive	580954	5416976	2720	
95GPB7079	Biotite leucogranodiorite, Dotted Lake pluton	Intrusive	592154	5413829	2697.1	1.1
95GPB7066	Biotite granodiorite, Botham Lake stock	Intrusive	577209	5393772	2683	3
DD97-16,26	Hornblende-biotite granodiorite, Heron Bay pluton, northeast lobe	Intrusive	572697	5393603	2682	2
DD97-9	Hornblende-biotite granodiorite, Musher Lake pluton	Intrusive	588370	5409210	2678.6	1.5
96GPB7241	Hornblende-biotite-clinopyroxene quartz monzodiorite, Fourbay Lake pluton	Intrusive	570452	5424542	2677.7	1.1
96GPB7115	Hornblende Granodiorite dike	Intrusive	584592	5400046	2676	1
96GPB7114	Aplite dike	Intrusive	584592	5400046	2675	1
	Corfu and Muir (1989 a,b)					
GSv	Quartz Porphyry Complex near Hemlo	Intrusive			2772	2
HBv	Heron Bay volcanic complex	Volcanic			2695	2
PCm	Pukaskwa Gneissic Complex Margin	Intrusive			2719	+ 6 / -4
Pci	Pukaskwa Gneissic Complex Interior	Intrusive			2688	3
CLi	Cedar Lake Pluton Interior	Intrusive			2688	3
CLm	Cedar Lake Pluton Margin	Intrusive			2687	3
CLp	Porphyritic dike intruding metasedimentary rocks marginal to the Cedar Lake Pluton	Intrusive			2687	3
CC	Cedar Creek Stock	Intrusive			2684	+ 4 / -3
HBm-i	Heron Bay Pluton	Intrusive			2688	5
PWd	Altered diorite dike, A zone, Williams Mine	Intrusive			2690-2680	
GL	Gowan Lake Pluton	Intrusive			2678	2

Sample	Location (unit)	Rock Type	UTM_E	UTM_N	Age (Ma)	Error
		Daviset al., (1998)				
DD97-11	Petrant Lake Felsic fragmental	Intrusive			2698	
DD97-13	Petrant Lake Sandstone in conglomerate	Metasedimentary			2717-2693	
DD97-17	Pic River Sandstone in Basalt	Metasedimentary			2749-2693	
DD97-10	Musher Lake Quartz porphyry	Intrusive			2692	
DD97-14	Pinegrove Volcanics Intermediate Fragmental	Volcanic			2689	
DD97-19	Black-Pic Batholith	Intrusive			2720	
96GPB7271	Pukaskwa Batholith	Intrusive			2718	
96GPB7079	Dotted Lake Batholith	Intrusive			2697	
DD97-16	Heron Bay pluton Rous Lake	Intrusive			2693-2686	
DD97-26	Heron Bay pluton West lobe	Intrusive			2690	
95GPB7004B	Cedar Lake pluton	Intrusive			inconclusive	
DD97-9	Musher Lake pluton	Intrusive			2679	
96GPB7241	Fourbay Lake pluton	Intrusive			2677	
95GPB7066	Botham Stock	Intrusive			2690	
95SLJ244C	Bremner Lake pluton	Intrusive			2677	
96GPB7115	DikeB Hwy north of Cedar Lake pluton	Intrusive			inconclusive	
DD97-7	Syn-folding dike Roger Lake area	Intrusive			2688	
DD97-8	Post-folding dike Roger Lake area	Intrusive			2697	
DD97-12	Feldspar porphyry dike cutting conglomerate Petrant Lake	Intrusive			2679	
DD97-15	Leucogranite dike Cache Lake	Intrusive			2691, 2676	

Appendiz D-2: Geochronology Data

Notes: (a) A, B etc. are labels for fractions composed of single zircon grains or fragments; all fractions annealed and chemically abraded after Mattinson (2005) and Scoates and Friedman (2008).

(b) Nominal fraction weights estimated from photomicrographic grain dimensions, adjusted for partial dissolution during chemical abrasion.

(c) Nominal U and total Pb concentrations subject to uncertainty in photomicrographic estimation of weight and partial dissolution during chemical abrasion.

(d) Model Th/U ratio calculated from radiogenic 208Pb/206Pb ratio and 207Pb/235U age.

(e) Pb* and Pbc represent radiogenic and common Pb, respectively; mol % 206Pb* with respect to radiogenic, blank and initial common Pb.

(f) Measured ratio corrected for spike and fractionation only. Mass discrimination of 0.23%/amu based on analysis of NBS-982; all Daly analyses.

(g) Corrected for fractionation, spike, and common Pb; up to 4 pg of common Pb was assumed to be procedural blank: 206Pb/204Pb = 18.50 ± 1.0%; 207Pb/204Pb = 15.20 ± 1.0%;

208Pb/204Pb = 38.40 ± 1.0% (all uncertainties 1-sigma). Excess over blank was assigned to initial common Pb with S-K model Pb composition at 2721Ma.

(h) Errors are 2-sigma, propagated using the algorithms of Schmitz and Schoene (2007) and Crowley et al. (2007).

(i) Calculations are based on the decay constants of Jaffey et al. (1971). 206Pb/238U and 207Pb/206Pb ages corrected for initial disequilibrium in 230Th/238U using Th/U [magma] = 3.

(j) Corrected for fractionation, spike, and blank Pb only.

		Compositional Parameters								Radiogenic Isotope Ratios								Isotopic Ages						
Sample	Wt. mg	U ppm	Th/U	Pb ppm	$^{206}Pb^*$ x10^{-13} mol	mol % $^{206}Pb^*$	Pb^*/Pb_c	Pb_c (pg)	$^{206}Pb/^{204}Pb$	$^{208}Pb/^{206}Pb$	$^{207}Pb/^{206}Pb$	% err	$^{207}Pb/^{235}U$	% err	$^{206}Pb/^{238}U$	% err	corr. coef.	$^{207}Pb/^{206}Pb$	±	$^{207}Pb/^{235}U$	±	$^{206}Pb/^{238}U$	±	% disc
(a)	(b)	(c)	(d)	(c)	(e)	(e)	(e)	(e)	(f)	(g)	(g)	(h)	(g)	(h)	(g)	(h)		(i)	(h)	(i)	(h)	(i)	(h)	
CLP (Cedar Lake Pluton)																								
A	0.006	87	0.314	49.2	11.2109	99.82%	174	1.69	9898	0.087	0.183381	0.105	13.035571	0.248	0.515555	0.185	0.925	2683.69	1.73	2682.23	2.34	2680.30	4.05	0.13
B	0.004	26	0.501	15.6	2.2275	99.12%	37	1.65	2034	0.139	0.184390	0.125	13.133908	0.348	0.516602	0.296	0.937	2692.75	2.07	2689.32	3.28	2684.75	6.50	0.30
C	0.004	121	0.414	70.3	10.4132	99.75%	123	2.28	6597	0.115	0.183431	0.097	13.064004	0.226	0.516538	0.156	0.936	2684.14	1.60	2684.29	2.13	2684.48	3.43	-0.01
D	0.003	80	0.302	45.9	5.1699	99.42%	51	2.64	2788	0.084	0.183139	0.133	13.042875	0.242	0.516524	0.156	0.865	2681.51	2.20	2682.76	2.29	2684.42	3.43	-0.11
F	0.003	60	0.236	33.3	3.8385	99.69%	102	0.97	6051	0.066	0.182797	0.108	12.981640	0.254	0.515062	0.188	0.922	2678.41	1.79	2678.32	2.39	2678.21	4.13	0.01
G	0.002	50	0.324	29.0	2.1474	99.15%	37	1.52	2169	0.090	0.183372	0.123	13.045641	0.287	0.515979	0.222	0.914	2683.60	2.04	2682.96	2.71	2682.11	4.88	0.06
FRL (Frank Lake)																								
A	0.008	29	0.389	17.3	5.1121	99.54%	71	1.92	4060	0.108	0.186914	0.114	13.498423	0.272	0.523769	0.210	0.921	2715.20	1.87	2715.17	2.57	2715.15	4.65	0.00
B	0.007	37	0.521	22.8	5.7237	99.52%	70	2.25	3880	0.144	0.187640	0.105	13.589967	0.227	0.525282	0.152	0.922	2721.58	1.73	2721.57	2.15	2721.54	3.38	0.00
C	0.010	32	0.384	18.6	6.8574	99.42%	55	3.31	3173	0.107	0.184729	0.109	13.166899	0.235	0.516949	0.160	0.916	2695.79	1.81	2691.69	2.22	2686.23	3.52	0.35
D	0.005	48	0.704	30.3	5.2391	99.51%	70	2.14	3748	0.195	0.187412	0.105	13.547799	0.226	0.524288	0.150	0.922	2719.58	1.73	2718.63	2.14	2717.34	3.33	0.08
E	0.003	28	0.426	17.0	1.8356	98.96%	31	1.59	1771	0.118	0.186870	0.091	13.455522	0.281	0.522228	0.222	0.962	2714.81	1.50	2712.17	2.65	2708.62	4.91	0.23
F	0.008	12	0.454	7.6	2.1213	97.92%	15	3.71	888	0.126	0.187517	0.195	13.583146	0.411	0.525361	0.341	0.882	2720.51	3.21	2721.09	3.89	2721.88	7.57	-0.05
G	0.008	23	0.387	13.9	4.0988	99.46%	60	1.83	3428	0.107	0.187611	0.108	13.610511	0.233	0.526157	0.158	0.918	2721.33	1.77	2722.99	2.20	2725.24	3.52	-0.14
HEZ01 (Gouda)																								
F	0.0030	55	0.402	32.9	3.5873	99.13%	37	2.59	2129	0.111	0.185758	0.122	13.333488	0.331	0.520590	0.273	0.937	2704.96	2.01	2703.56	3.13	2701.68	6.02	0.12
G	0.0015	35	0.401	20.5	1.1273	99.31%	47	0.64	2682	0.111	0.185667	0.118	13.323293	0.319	0.520447	0.261	0.937	2704.15	1.95	2702.84	3.01	2701.07	5.76	0.11
H	0.0015	40	0.426	27.2	1.3096	95.13%	6	5.52	380	0.118	0.185809	0.406	13.382361	0.594	0.522355	0.286	0.793	2705.41	6.70	2707.01	5.61	2709.16	6.33	-0.14
I	0.0015	32	0.432	19.2	1.0423	99.23%	42	0.67	2387	0.119	0.185747	0.122	13.362022	0.323	0.521734	0.262	0.934	2704.86	2.02	2705.58	3.05	2706.53	5.79	-0.06
J	0.0010	36	0.393	23.2	0.7848	96.60%	9	2.27	544	0.109	0.186040	0.336	13.401491	0.583	0.522452	0.402	0.829	2707.46	5.55	2708.36	5.51	2709.57	8.88	-0.08
HEZ02 (DC Lake)																								
A	0.003	88	0.606	52.9	5.6792	99.96%	763	0.21	41559	0.168	0.184831	0.225	13.191491	0.411	0.517628	0.337	0.837	2696.70	3.72	2693.45	3.88	2689.11	7.40	0.28
C	0.003	85	0.385	49.4	5.4881	99.54%	69	2.11	3936	0.107	0.184512	0.104	13.164826	0.215	0.517474	0.133	0.926	2693.85	1.72	2691.54	2.03	2688.46	2.93	0.20
D	0.003	51	0.405	29.8	3.3168	99.77%	140	0.63	7984	0.112	0.184534	0.116	13.182036	0.227	0.518088	0.148	0.893	2694.05	1.91	2692.77	2.14	2691.07	3.26	0.11
E	0.003	57	0.760	35.7	3.6718	99.56%	79	1.34	4187	0.211	0.184717	0.118	13.177704	0.243	0.517405	0.169	0.898	2695.69	1.95	2692.46	2.29	2688.17	3.70	0.28
F	0.002	45	0.466	27.2	1.9399	98.83%	28	1.88	1586	0.129	0.184466	0.152	13.147264	0.321	0.516912	0.252	0.887	2693.44	2.51	2690.28	3.03	2686.07	5.53	0.27

		Compositional Parameters								Radiogenic Isotope Ratios								Isotopic Ages						
Sample	Wt. mg	U ppm	Th/U	Pb ppm	$^{206}Pb^*$ x10^{-13} mol	mol % $^{206}Pb^*$	Pb^*/Pb_c	Pb_c (pg)	$^{206}Pb/^{204}Pb$	$^{208}Pb/^{206}Pb$	$^{207}Pb/^{206}Pb$	% err	$^{207}Pb/^{235}U$	% err	$^{206}Pb/^{238}U$	% err	corr. coef.	$^{207}Pb/^{206}Pb$	±	$^{207}Pb/^{235}U$	±	$^{206}Pb/^{238}U$	±	% disc
(a)	(b)	(c)	(d)	(c)	(e)	(e)	(e)	(e)	(f)	(g)	(g)	(h)	(g)	(h)	(g)	(h)		(i)	(h)	(i)	(h)	(i)	(h)	
HEZ03 (Thor)																								
F	0.021	96	0.300	54.7	43.6526	99.84%	194	5.89	11287	0.083	0.185858	0.095	13.308443	0.332	0.519331	0.290	0.962	2705.85	1.57	2701.78	3.14	2696.34	6.40	0.35
G	0.010	34	0.356	20.6	7.6879	99.83%	188	1.09	10698	0.098	0.196444	0.102	14.692849	0.349	0.542459	0.307	0.960	2796.87	1.66	2795.56	3.32	2793.73	6.95	0.11
H	0.010	34	0.360	20.1	7.4569	99.42%	56	3.55	3213	0.100	0.185896	0.113	13.383643	0.275	0.522159	0.213	0.923	2706.19	1.87	2707.10	2.60	2708.33	4.70	-0.08
I	0.007	25	0.317	15.5	3.8896	98.05%	16	6.35	949	0.088	0.185762	0.189	13.393331	0.426	0.522914	0.362	0.898	2705.00	3.11	2707.79	4.03	2711.53	8.01	-0.24
J	0.009	34	0.323	19.9	6.6261	99.19%	39	4.44	2287	0.089	0.185744	0.119	13.400826	0.254	0.523258	0.180	0.905	2704.84	1.96	2708.32	2.40	2712.98	4.00	-0.30
Moose Lake																								
A	0.006	60	0.470	35.0	7.7372	99.94%	575	0.36	32285	0.130	0.182521	0.087	12.907657	0.217	0.512901	0.150	0.954	2675.91	1.44	2672.93	2.05	2669.00	3.27	0.26
B	0.007	30	0.913	19.0	4.4670	99.83%	207	0.64	10624	0.253	0.183753	0.101	13.116394	0.214	0.517700	0.136	0.927	2687.04	1.67	2688.06	2.02	2689.42	2.99	-0.09
C	0.008	8	0.467	4.7	1.3655	99.50%	65	0.57	3671	0.129	0.184305	0.131	13.197208	0.318	0.519331	0.255	0.918	2691.99	2.17	2693.86	3.00	2696.34	5.62	-0.16
D	0.006	32	0.347	18.3	4.1413	99.85%	207	0.53	11964	0.096	0.184469	0.084	13.201821	0.219	0.519050	0.152	0.961	2693.47	1.39	2694.19	2.06	2695.15	3.35	-0.06
E	0.003	28	0.838	17.8	1.8083	99.72%	127	0.42	6634	0.232	0.184444	0.103	13.153652	0.366	0.517226	0.320	0.964	2693.24	1.70	2690.74	3.45	2687.40	7.04	0.22
UAZ (Upper Anomalous Zone)																								
A	0.005	40	0.474	23.9	4.3315	99.50%	66	1.79	3706	0.131	0.184223	0.108	13.160654	0.223	0.518121	0.138	0.930	2691.26	1.78	2691.24	2.11	2691.21	3.04	0.00
B	0.005	37	0.451	22.5	4.0363	98.95%	31	3.52	1758	0.125	0.184377	0.128	13.197919	0.315	0.519155	0.238	0.930	2692.64	2.12	2693.91	2.97	2695.60	5.24	-0.11
C	0.005	38	0.576	22.9	4.0667	99.52%	70	1.60	3884	0.160	0.184250	0.118	13.110407	0.243	0.516069	0.161	0.908	2691.50	1.95	2687.63	2.29	2682.49	3.54	0.33
D	0.005	33	0.416	19.2	3.5078	99.27%	45	2.11	2551	0.115	0.183912	0.113	13.105952	0.271	0.516840	0.197	0.932	2688.47	1.87	2687.31	2.56	2685.77	4.34	0.10
E	0.005	27	0.522	16.5	2.9165	99.00%	33	2.43	1848	0.145	0.184110	0.208	13.146822	0.338	0.517897	0.226	0.800	2690.24	3.43	2690.25	3.19	2690.25	4.97	0.00
WRS-01 (White River Stock)																								
A	0.008	39	0.560	23.6	6.6575	99.12%	38	4.88	2093	0.155	0.183724	0.123	13.108626	0.266	0.517476	0.195	0.903	2686.78	2.03	2687.50	2.51	2688.47	4.29	-0.06
B	0.007	25	0.462	14.1	3.5237	99.01%	33	2.91	1862	0.134	0.182349	0.127	11.979823	0.263	0.476480	0.187	0.894	2674.36	2.11	2602.83	2.47	2511.91	3.89	6.07
C	0.008	28	0.544	16.9	4.8173	99.39%	55	2.42	3052	0.151	0.183697	0.108	13.105204	0.235	0.517418	0.161	0.918	2686.53	1.78	2687.26	2.21	2688.22	3.53	-0.06
D	0.007	29	0.662	17.7	4.2967	99.26%	46	2.62	2516	0.184	0.182984	0.116	12.927074	0.241	0.512372	0.162	0.905	2680.10	1.92	2674.35	2.27	2666.75	3.55	0.50
E	0.008	18	0.487	12.3	3.1091	94.81%	6	14.15	348	0.135	0.183377	0.415	12.989093	0.803	0.513728	0.692	0.856	2683.65	6.86	2678.86	7.57	2672.52	15.14	0.41